

# Solid-Phase Synthesis for the Construction of Biologically Interesting Molecules and the Total Synthesis of Trioxacarcin DC-45-A2

**Mikkelsen, Remi Jacob Thomsen**

*Publication date:*
2015

*Document Version*
Publisher's PDF, also known as Version of record

# Solid-Phase Synthesis for the Construction of Biologically Interesting Molecules and the Total Synthesis of Trioxacarcin DC-45-A2

Remi Mikkelsen

PhD Thesis


Technical University of Denmark

# Solid-Phase Synthesis for the Construction of Biologically Interesting Molecules and the Total Synthesis of Trioxacarcin DC-45-A2

Remi Mikkelsen

PhD Thesis
carried out at
Department of Chemistry
Technical University of Denmark
Kemitorvet, building 201
2800 Kgs. Lyngby

PhD supervisors:
Director Thomas Eiland Nielsen, Novo Nordisk
Professor David Tanner, Technical University of Denmark

December 2015

**Abstract**

This thesis covers three research projects in addition to a literature survey on solid-phase organic synthesis and photolabile linkers.

**Synthesis of Doxorubicin Derivatives on Photolabile Solid Support.** The synthesis of doxorubicin derivatives on photolabile solid support, compatible with bead-based screening, was investigated. Two different strategies for the synthesis of doxorubicin derivatives were developed leading to the synthesis of doxorubicin derivatives with both amino acids and peptide fragments attached in good to excellent crude purities.

**Total Synthesis of Trioxacarcin DC-45-A2.** In efforts towards the total synthesis of trioxacarcin DC-45-A2 by the Nicolaou group a new and efficient route for a key fragment was optimized. The new route featured distinct and high yielding steps and thus provided superior access to this key building block in terms of overall yield, step count and scalability. Furthermore a route to another key building block was developed featuring a Stille cross-coupling.

**Synthesis of Poly-fused Heterocycles.** In the search for new biologically active compounds a methodology for the synthesis of poly-fused heterocycles was investigated. This led to the development and optimization of a key aldol condensation/conjugate addition sequence for the synthesis of poly-fused heterocycles.

**Resumé**

Denne afhandling dækker tre forskningsprojekter udover et litteraturstudie omhandlende fast-fase syntese i organisk kemi og fotolabile linkere.

**Syntese af doxorubicin derivater på fotolabil fast-fase.** Syntesen af doxorubicin derivater på fotolabil fast-fase, kompatibelt med bead-baseret screening, er blevet undersøgt. To forskellige strategier for syntese af doxorubicin derivater blev udviklet og førte til syntesen af doxorubicin derivater med både aminosyrer og peptidfragmenter fastgjort, i gode til fremragende renheder uden oprensning.

**Totalsyntese af trioxacarcin DC-45-A2.** En ny og effektiv rute til en central byggeblok til brug i totalsyntesen af trioxacarcin DC-45-A2 i Nicolaou gruppen er blevet optimeret. Den nye rute indeholder trin med højt udbytte og giver forbedret adgang til denne byggeblok hvad angår overordnet udbytte, antal af trin og skalérbarhed. Ydermere er en rute til en anden central byggeblok blevet udviklet indeholdende en Stille krydskobling.

**Syntese af poly-forbundne heterocykler.** I jagten på nye biologisk aktive kemiske stoffer er en metode til syntese af poly-forbundne heterocykler blevet undersøgt. Dette førte til udvikling og optimering af en central aldolkondensation/konjugeret additions sekvens til brug i syntesen af poly-forbundne heterocykler.

# Contents

# Preface

The work presented in this thesis was mainly carried out at the Department of Chemistry at the Technical University of Denmark (DTU) in the period 2011–2015 under the supervision of former Professor Thomas E. Nielsen (director at Novo Nordisk since September 1, 2014) and Professor David Tanner (since September 1, 2014) as part of my PhD studies. A six months external stay was conducted at the BioScience Research Collaborative at Rice University, Houston, Texas, in the laboratory of Professor K. C. Nicolaou.

The thesis covers three projects. The first details efforts to develop a bead-based platform integrating solid-phase synthesis of doxorubicin derivatives and cell-based screening via the use of photolabile linkers. The second project was carried out during my stay in the Nicolaou laboratories and describes the endeavour towards the total synthesis of the anticancer natural product trioxacarcin DC-45-A2. The last project deals with a method for the synthesis of structurally diverse poly-fused heterocycles.

The project regarding solid-phase synthesis of doxorubicin derivatives was initiated during my Master's project and a brief overview of some of these initial experiments (mainly the work described in §2.4.1) have been presented in this thesis.

First and foremost I would like to thank Thomas E. Nielsen for accepting me as a PhD student in his research group, it has been a privilege to be part of such an ambitious and inspiring environment. Thomas has been an inexhaustive source of great ideas and his always encouraging engagement, enthusiasm and support have made the experience something truly special.

David Tanner is thanked for accepting to become my primary supervisor when Thomas left DTU and his guidance and support during the final part of my PhD studies are gratefully acknowledged. David is furthermore thanked for providing invaluable chemical insight during the years and for being the best and most inspiring lecturer I have had the pleasure of experiencing during my studies at DTU.

Katrine Qvortrup and Sebastian T. Le Quement are thanked for valuable

guidance in practical as well as theoretical matters.

Mette Terp Petersen, Ragnhild G. Ohm and Sanne Mygind are gratefully acknowledged for the time and effort they have put into proof-reading this thesis, it has been much appreciated!

Members of the former Nielsen group are thanked for creating a great work environment and especially lab 255 for all the great discussions and many hours we spend together.

Special thanks go to Mette Terp Petersen, Mette Ishøy, Thomas Flagstad and Casper L. Hansen for being great friends and colleagues throughout our entire education at DTU.

Tina Gustafsson is greatly thanked for keeping the technical equipment running, much of the research presented in this thesis would not have been possible without her persistent effort to assure that the instruments behave the way they should. Anne Hector is thanked for being ever helpful and Brian Ekman-Gregersen and Janne B. Rasmussen for help with ordering chemicals. Mette Lange is thanked for help with administrative tasks.

Past and present members of DTU ScienceShow are thanked for providing me with endless fun and explosions over the years!

Professor K. C. Nicolaou is thanked for inviting me to join his research group at Rice University. It has been an outstanding experience and a great honor to work in his laboratories and has provided me with valuable knowledge and skills. Frants Alling's Scholarship, Knud Højgaard's Foundation, the Augustinus Foundation, Jorck's Foundation, the Oticon Foundation, Otto Mønsted's Foundation, the Rudolph Als Foundation and the Danish Tennis Foundation are thanked for financially supporting my external stay.

Remi Mikkelsen
Kgs. Lyngby, December 2015

# Publications

## Publications included in the thesis

1. Nicolaou, K. C.; Cai, Q.; Qin, B.; Petersen, M. T.; Mikkelsen, R. J. T.; Heretsch, P. Total Synthesis of Trioxacarcin DC-45-A2, *Angew. Chem. Int. Ed.* **2015**, *54*, 1–6.

## Publications in preparation

2. Mikkelsen, R. J. T.; Qvortrup, K. and Nielsen, T. E. Photolabile Linkers for Solid-Phase Organic Synthesis. *Manuscript in preparation for Tetrahedron included in the appendix.*

3. Mikkelsen, R. J. T.; Qvortrup, K.; Le Quement, S. T. and Nielsen, T. E. Solid-Phase Synthesis of Doxorubicin Derivatives: Towards Cell-Based On-Bead Screening. *Manuscript in preparation.*

## Publications not included in the thesis

4. Le Quement, S. T.; Flagstad, T; Mikkelsen, R. J. T.; Hansen, M. R.; Givskov, M. C.; Nielsen. T. E., Petasis Three-Component Coupling Reactions of Hydrazides for the Synthesis of Oxadiazolones and Oxazolidinones, *Org. Lett.* **2012**, *14*, 640–643.

# Conference Proceedings

1. Mikkelsen, R. J. T.; Qvortrup, K; Le Quement, S. T.; Nielsen, T. E., Synthesis of Doxorubicin Derivatives on Photolabile Solid Support, January **2012**, 27th Organic Chemistry Winter Meeting, Skeikampen, Norway. *Oral and poster presentation.*

2. Mikkelsen, R. J. T.; Qvortrup, K; Le Quement, S. T.; Nielsen, T. E., Synthesis of Doxorubicin Derivatives on Photolabile Solid Support, January **2013**, 28th Organic Chemistry Winter Meeting, Skeikampen, Norway. *Oral and poster presentation.*

3. Mikkelsen, R. J. T.; Qvortrup, K; Le Quement, S. T.; Nielsen, T. E., Solid-Phase Synthesis of Doxorubicin Derivatives: Towards Cell-based On-Bead Screening, June **2013**, Komppa Symposium, Espoo, Finland. *Poster presentation.*

4. Mikkelsen, R. J. T.; Qvortrup, K; Le Quement, S. T.; Nielsen, T. E., Synthesis of Doxorubicin Derivatives on Photolabile Solid Support, September **2013**, 246th American Chemical Society National Meeting & Exposition, Indianapolis, IN, USA. *Poster presentation.*

5. Mikkelsen, R. J. T.; Qvortrup, K; Le Quement, S. T.; Nielsen, T. E., Solid-Phase Synthesis of Doxorubicin Derivatives: Towards Cell-based On-Bead Screening, July **2014**, 14th Belgian Organic Synthesis Symposium, Louvain-la-Neuve, Belgium. *Poster presentation.*

6. Mikkelsen, R. J. T.; Qvortrup, K; Le Quement, S. T.; Nielsen, T. E., Solid-Phase Synthesis of Doxorubicin Derivatives: Towards Cell-based On-Bead Screening, August **2014**, 248th American Chemical Society National Meeting & Exposition, San Francisco, CA, USA. *Poster presentation.*

# Abbreviations

| | |
|---|---|
| AA | amino acid |
| Ac | acetyl |
| AIBN | azobisisobutyronitrile |
| All | allyl |
| Alloc | allyloxycarbonyl |
| BHA | benzhydrylamine |
| Bn | benzyl |
| Boc | *tert*-butyloxycarbonyl |
| BOP | benzotriazole-1-yl-oxy-tris-(dimehtlamino)-phosphonium hexafluorophosphate |
| BQ | 1,4-benzoquinone |
| BTC | bis(trichloromethyl) carbonate |
| Bu | butyl |
| calcd | calculated |
| Cbz | benzyloxycarbonyl |
| CDI | carbonyldiimidazole |
| Cy | cyclohexyl |
| DABCO | 1,4-diazabicyclo[2.2.2]octane |
| DBU | 1,8-Diazabicyclo[5.4.0]undec-7-ene |
| DCC | *N*,*N*'-dicyclohexylcarbodiimide |
| DCE | dichloroethane |
| Dde | 1-(4,4-dimethyl-2,6-dioxacyclohexylidene)ethyl |
| DDQ | 2,3-dichloro-5,6-dicyano-1,4-benzoquinone |
| DEAD | diethyl azodicarboxylate |
| DIC | *N*,*N*'-diisopropylcarbodiimide |
| DIPEA | *N*,*N*-diisopropylethylamine |
| DMAP | 4-dimethylaminopyridine |
| DMDO | dimethyldioxirane |
| DMF | *N*,*N*-dimethylformamide |

| | |
|---|---|
| DMP | Dess-Martin periodinane |
| DMSO | dimethylsulfoxide |
| DMT | bis-(4-methoxyphenyl)phenylmethyl |
| DOX | doxorubicin |
| d.r. | diastereomeric ratio |
| Dts | dithiasuccinoyl |
| EDCI | 1-ethyl-3-(3-dimethylaminopropyl) carbodiimide |
| *ee* | enantiomeric excess |
| equiv | equivalent(s) |
| Et | ethyl |
| Fmoc | 9-fluorenylmethyloxycarbonyl |
| h | hour(s) |
| HATU | 1-[bis(dimethylamino)methylene]-1*N*-1,2,3-triazolo[4,5-*b*]pyridinium 3-oxid hexafluorophosphate |
| HBTU | 3-[bis(dimethylamino)methyliumyl]-3-*H*-benzotriazol-1-oxide hexafluorophosphate |
| HMBA | hydroxymethylbenzoic acid |
| HMPA | hexamethylphosphoramide |
| HOAt | 1-hydroxy-7-azabenzotriazole |
| HOBt | 1-hydroxybenzotriazole |
| HPLC | high-performance liquid chromatography |
| HTS | high-throughput screening |
| *i* | *iso* |
| Im | imidazole |
| LCAA-CPG | long chain alkyl amine controlled pore glass |
| LCMS | liquid chromatography mass spectrometry |
| *m* | *meta* |
| MBHA | 4-methylbenzhydrylamine |
| *m*CBPA | *meta*-chloroperoxybenzoic acid |
| Me | methyl |
| MOM | methoxymethyl |
| m.p. | melting point |
| MSNT | 1-(mesitylene-2-sulfonyl)-3-nitro-1,2,4-triazole |
| MW | microwave |
| *n* | *normal* |
| NEM | *N*-ethylmorpholine |
| NIS | *N*-iodosuccinimide |
| NMM | *N*-methylmorpholine |
| NMP | *N*-methyl-2-pyrrolidone |
| NMR | nuclear magnetic resonance |
| Nu | nucleophile |
| Nvoc | 6-nitroveratryloxycarbonyl |
| *o* | *ortho* |
| OBOC | one-bead-one-compound |

| | |
|---|---|
| *p* | *para* |
| PDMA | polydimethylacrylamide |
| PEG | polyethylene glycol |
| PEGA | polyethylene glycol dimethyl acrylamide |
| PG | protecting group |
| Ph | phenyl |
| PIDA | iodobenzene diacetate |
| pip. | piperidine |
| PMB | *para*-methoxybenzyl |
| Pr | propyl |
| PyBOP | benzotriazole-1-yl-oxy-tripyrrolidinophosphonium hexafluorophosphate |
| PyBroP | bromotripyrrolidinophosphonium hexafluorophosphate |
| RP | reversed-phase |
| rt | room temperature |
| sat. | saturated |
| SPPS | solid phase peptide synthesis |
| Su | *N*-succinimidyl |
| *t* | *tert* |
| TBAF | tetrabutylammonium fluoride |
| TBS | *tert*-butyldimethylsilyl |
| TBTU | *N*-[(1H-benzotriazol-1-yl)(dimethylamino)methylene]-*N*-methyl methanaminium tetrafluoroborate |
| TC | thiophene-2-carboxylate |
| TCA | 2,2,2-trichloroacetimidate |
| TEMPO | 2,2,6,6-tetramethyl-1-piperidinyloxy |
| TES | triethylsilyl ether |
| Tf | triflate |
| TFA | trifluoroacetic acid |
| TFAA | trifluoroacetic acid anhydride |
| THF | tetrahydrofuran |
| TLC | thin layer chromatography |
| TMEDA | *N*,*N*,*N*,'*N*'-tetramethylethylenediamine |
| TMS | trimethylsilyl |
| TPAP | tetrapropylammonium perruthenate |
| Tr | trityl |
| Trt | triphenylmethyl |
| Ts | tosyl |

# Canonical Amino Acids

| | | |
|---|---|---|
| A | Ala | alanine |
| R | Arg | arginine |
| N | Asn | asparagine |
| D | Asp | aspartic acid |
| C | Cys | cysteine |
| Q | Gln | glutamine |
| E | Glu | glutamic acid |
| G | Gly | glycine |
| H | His | histidine |
| I | Ile | isoleucine |
| L | Leu | leucine |
| K | Lys | lysine |
| M | Met | methionine |
| F | Phe | phenylalanine |
| P | Pro | proline |
| S | Ser | serine |
| T | Thr | threonine |
| W | Trp | tryptophan |
| Y | Tyr | tyrosine |
| V | Val | valine |

Chapter 1

# Solid-Phase Synthesis and Photolabile Linkers

## 1.1 Solid-Phase Organic Synthesis

Originally developed by Nobel Prize winning chemist Robert Bruce Merrifield for the synthesis of peptides [1], solid-phase organic synthesis is an attractive synthetic technique that offers unique advantages over conventional solution phase chemistry, both in terms of purification and experimental simplicity. The technique introduced by Merrifield revolutionized the field of peptide synthesis and greatly increased the effectiveness and ease with which peptides can be synthesized. Merrifield's method relies on the anchoring of the growing peptide onto a functionalized solid support, cf. scheme 1.1. Firstly, a linker, linking the substrate to the solid support is attached leading to construct **1.2**, cf. scheme 1.1. Then the first $N^{\alpha}$-protected amino acid is attached followed by deprotection of the temporary $N^{\alpha}$-protection group furnishing construct **1.4**. From this point on iterative cycles of amino acid coupling and deprotection builds the desired peptide from *C*- to *N*-terminus. Finally, any amino acid side-chain protection groups (positioned to mask the reactivity of side-chain functional groups during the synthesis) are deprotected and the substrate is released from the solid support by cleavage of the linker providing the desired peptide **1.6**.

Since its introduction half a century ago, many laboratories have focused on the development of technologies and chemistry suitable for solid-phase organic synthesis, which has resulted in a remarkable outburst of chemical transformations that can be applied for the routine synthesis of organic molecules on solid support [2–6]. This has led to the application of solid phase synthesis in the generation of combinatorial libraries both in academia and industry, ultimately leading to the identification of new drugs and catalysts [7, 8].

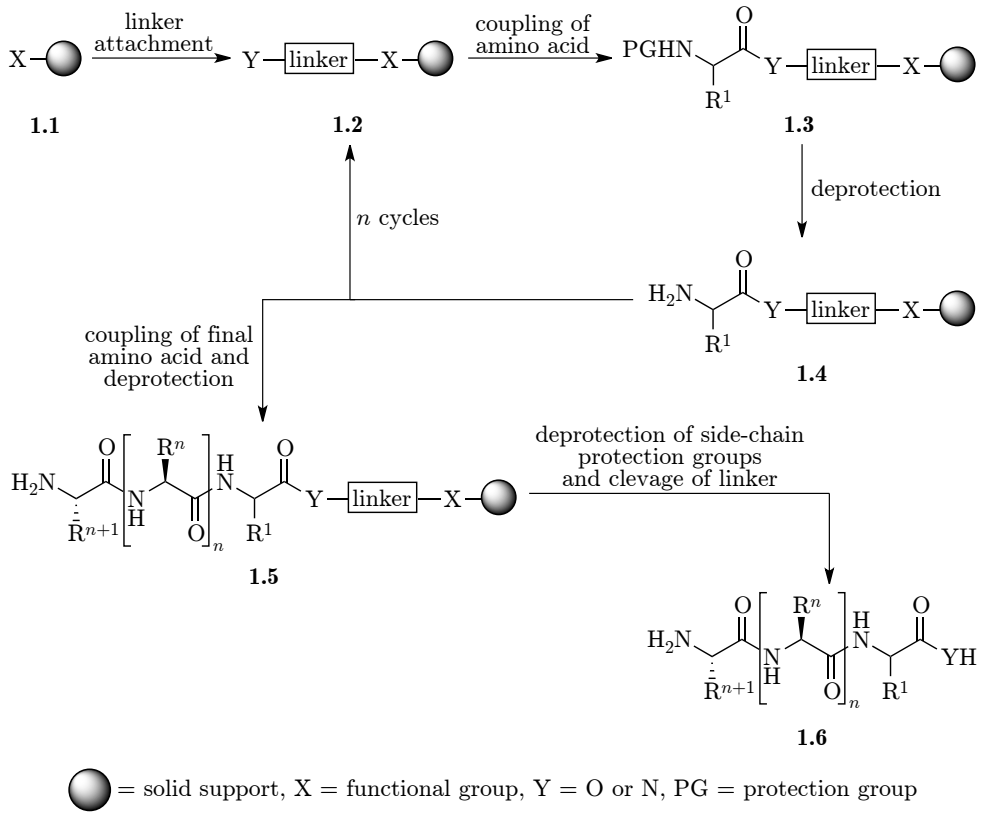


**Scheme 1.1:** Illustration of the principles of solid-phase peptide synthesis.

Below follows a brief introduction to the supports, linkers, coupling reagents and protection group strategies used in solid-phase synthesis.

### 1.1.1 Supports

The solid support used in solid-phase synthesis must be chemically inert and mechanically stable under the conditions used and furthermore completely insoluble in the chosen solvents. Additionally it is important that the solid supports exhibit good swelling characteristics in the used solvents thus allowing for diffusion of reagents and solvent molecules into the beads. A variety of resins are available for use in solid-phase synthesis, and a few selected examples are provided below.

The first resin used by Merrifield for peptide synthesis, a chloromethylated polystyrene resin cross-linked with divinylbenzene known as the Merrifield resin (**1.7**), is still used today [9], cf. figure 1.1. Polystyrene resins show good swelling properties in DMF and $CH_2Cl_2$ but they, however, display low compatibility with polar solvents, such as water and alcohols, commonly used in the handling of peptides.

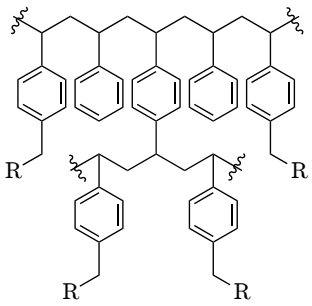

Merrifield resin (**1.7**): R = Cl
TentaGel (**1.8**): R = $(OCH_2CH_2O)_nCH_2OH$ or $(OCH_2CH_2O)_nCH_2NH_2$

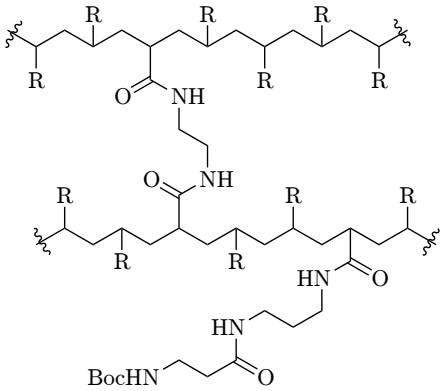

PDMA (**1.9**): R = $CON(Me)_2$

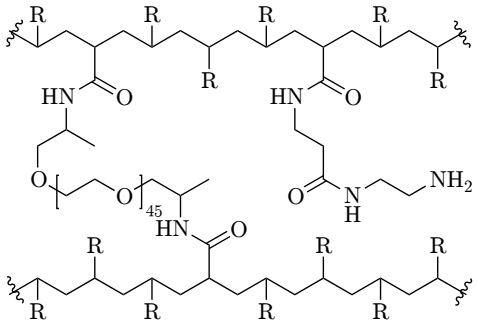

PEGA (**1.10**): R = $CON(Me)_2$

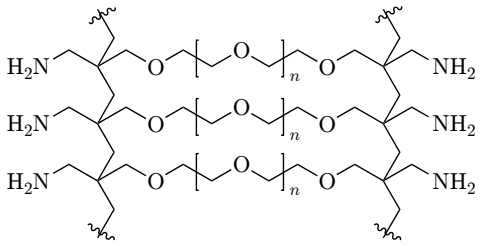

ChemMatrix (**1.11**)

**Figure 1.1:** Selected resins for solid-phase synthesis.

Sheppard later introduced a polydimethylacrylamide (PDMA) resin (**1.9**), cf. figure 1.1, that overcame the low compatibility with polar solvents and displayed excellent swelling properties in solvents such as DMF, AcOH and water [10, 11]. The resin however displayed decreased swelling in apolar solvents such as $CH_2Cl_2$, thus possessing reverse properties compared to those of the Merrifield resin.

A graft copolymer of polystyrene and polyethylene glycol (PEG) was later developed independently by Barany and Bayer [12, 13]. This resin exhibited good swelling properties in polar solvents such as MeCN, MeOH and water, improved mechanical stability as well as lower glass adherence. A typical example of this type of resin is the TentaGel resin (**1.8**), cf. figure 1.1, with PEG chains grafted to a matrix of polystyrene through ether bonds [9]. Furthermore TentaGel resin shows stability at high pressures which, combined with its high mechanical stability, makes it ideal for continuous flow synthesis [13].

Meldal introduced a copolymer of polyacrylamide and PEG, the PEGA resin (**1.10**), cf. figure 1.1 [14, 15]. With the good hydrophilic properties of the PEG-grafted polymers in mind Meldal developed a resin mainly consisting

of PEG. This resin displayed a high degree of swelling under standard peptide synthesis conditions in a broad range of solvents [16] and was furthermore stable under continuous flow conditions thus allowing for automated synthesis [15]. The resin furthermore had the ability to allow large proteins to enter the polymeric matrix thus making the resin highly interesting for use in the area of chemical biology [16]. The PEGA resin, however, has a drawback in that it is unsuitable for harsh reaction conditions due to the amide backbone in the polymer matrix [17, 18].

More recently, Albericio introduced an entirely PEG-based resin, termed ChemMatrix (**1.11**) [19], cf. figure 1.1. The resin showed good swelling properties in most common solvents (e.g. MeCN, DMF, $CH_2Cl_2$, DMSO, MeOH and water) and was even compatible with aqueous buffers [19]. The ChemMatrix resin additionally displayed good chemical stability being compatible with strong acids and bases, with the exception of strong Lewis acids [19]. The resin furthermore had good mechanical stability and allowed for relatively high loading levels.

### 1.1.2 Linkers

The use of solid supports in organic synthesis relies on the ability to link the substrate to the resin while retaining the ability to selectively cleave off some or all of the product from the solid support during synthesis for the analysis of reactions, and ultimately to release the target molecule of interest. Thus, the linker used in solid-phase synthesis serve as temporary immobilization of the substrate and as protection group for the attached functional group. The linkers must be stable to all chemical transformations used during the synthesis, and the final cleavage of the substrate from the resin has to be high yielding under conditions where the substrate is stable.

Two types of linkers are used in solid-phase synthesis, integral linkers and non-integral linkers [20]. Integral linkers where developed first and are synthesized directly on the resin, an example is the chloromethylated linker **1.7** used by Merrifield, cf. figure 1.1, where the first amino acid is attached via a benzyl ester linkage. Other examples of integral linkers are the BHA (**1.12**) and MBHA (**1.13**) linkers, which are cleaved by HF [21, 22], the trityl linker **1.14** (cleaved by dilute HCl) [23–25] and the oxime linker **1.15** (cleaved by nucleophiles) [26, 27], cf. figure 1.2.

The integral linkers however give rise to several disadvantages due the fact that they are synthesized directly on the resin which can lead to uncontrollable loading and functionalization [20]. Thus the majority of linkers used in solid-phase synthesis are non-integral linkers where the linker is attached to the resin after being prepared in solution. A wide variety of non-integral linkers have been developed and many are inspired by classical protection group strategies. Examples of this are the base-labile HMBA linker **1.16** [11] and the acid labile Rink-amide linker **1.17** [28], cf. figure 1.3, which are still widely used today.

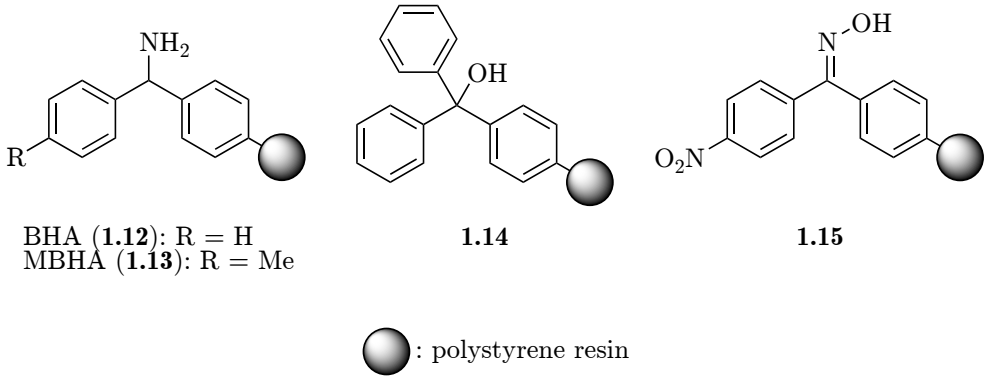


**Figure 1.2:** Selected integral linkers for solid-phase synthesis.

Other examples of linkers include safety-catch linkers **1.18** [29] and photolabile linkers[1] **1.19** [30], cf. figure 1.3.

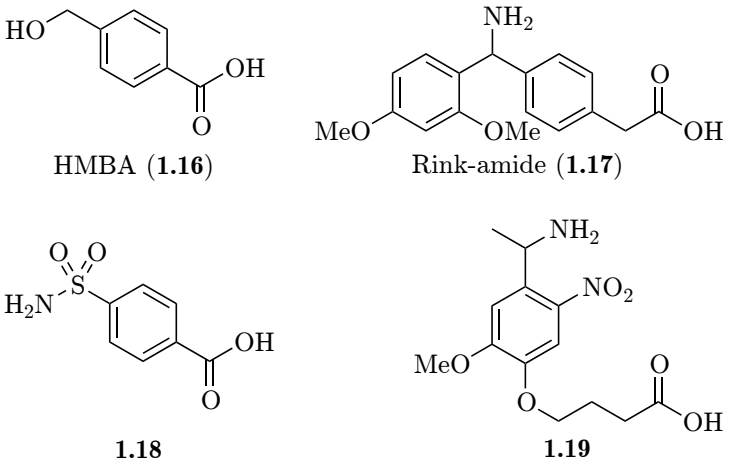


**Figure 1.3:** Selected non-integral linkers for solid-phase synthesis.

### 1.1.3 Coupling reagents

Solid-phase peptide synthesis requires repetitive and efficient amide bond formation by the coupling of protected amino acid building blocks to an amino functionalized resin. For this to proceed in a quantitative manner without detrimental side reactions a coupling reagent or an activated amino acid is used to drive the reaction to completion. One of the first coupling reagents used was the carbodiimide DCC (**1.20**) [31], cf. figure 1.4. However, DCC is not compatible with peptide synthesis using the Fmoc protection group strategy due to solubility issues and has thus been replaced by the carbodiimides

[1] For a brief account of the photolabile linkers available for solid-phase synthesis cf. §1.2.

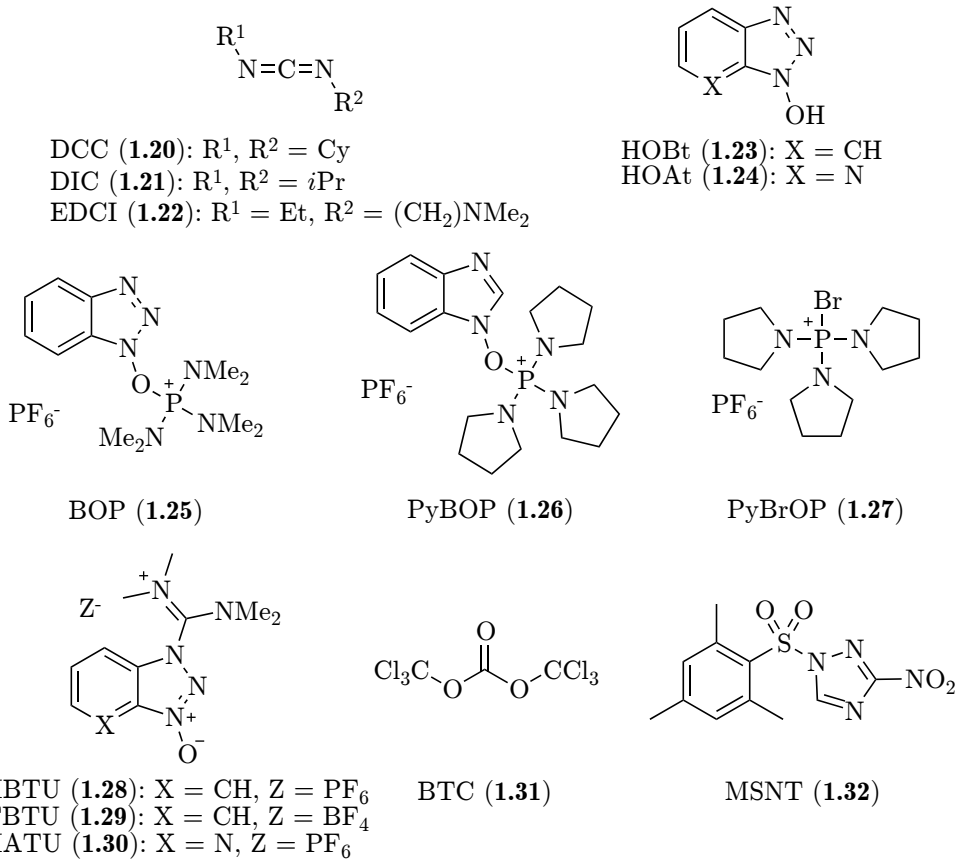


**Figure 1.4:** Selected coupling reagents used in solid-phase synthesis.

DIC (**1.21**) and EDCI (**1.22**) [31], cf. figure 1.4. A drawback with the use of the carbodiimides is however that they are prone to cause racemization of the amino acid stereogenic center. Racemization can occur by direct enolization, cf. scheme 1.2. However, another important contributor to racemization is

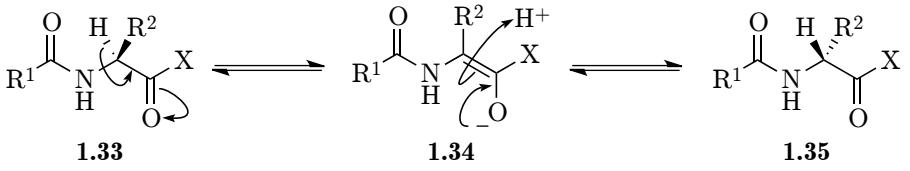


$R^2$ = amino acid side-chain

**Scheme 1.2:** Epimerization by direct enolization.

the formation of oxazolones **1.36** [32–34], cf. scheme 1.3.

Using carbodiimides in combination with the benzotriazole-based additives HOBt (**1.23**) and HOAt (**1.24**), cf. figure 1.4, has been shown to suppress

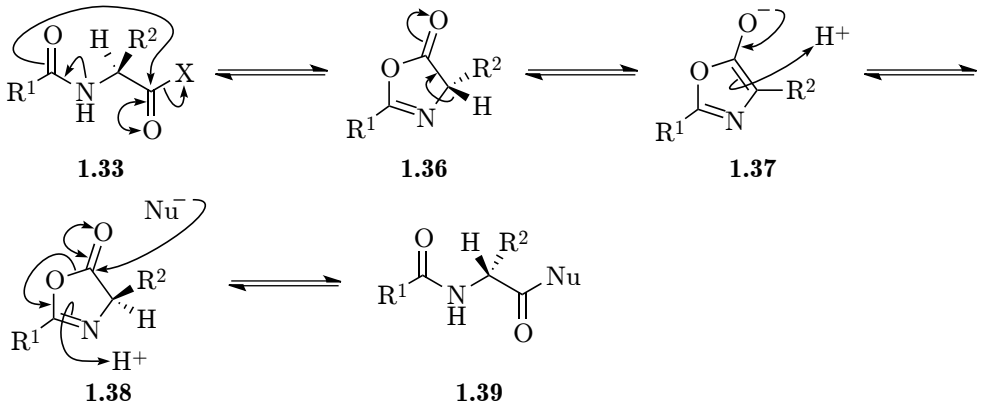

**1.33** **1.36** **1.37**

**1.38** **1.39**

$R^2$ = amino acid side-chain

**Scheme 1.3:** Epimerization by oxazolone formation.

racemization and accelerate the reactions of the activated esters [35].

Another coupling reagent is the phosphonium salt BOP (**1.25**) [36], cf. figure 1.4. BOP is based on the HOBt structure and is a very efficient coupling reagent, however, the very toxic byproduct hexamethylphosphoramide (HMPA) is generated when BOP is used. To avoid this detrimental side product the equally effective reagent PyBOP (**1.26**), cf. figure 1.4, was introduced [37]. Later the more reactive reagent PyBrOP (**1.27**), cf. figure 1.4, was introduced, which has been shown to be very effective in sterically demanding situations [38, 39].

Another type of HOBt-based coupling reagents are the aminium salts HBTU (**1.28**) [40] and TBTU (**1.29**) [41], cf. figure 1.4. These coupling reagents were shown to be very efficient and resulted in practically no racemization. A more reactive variant, termed HATU (**1.30**), cf. figure 1.4, based on the structure of HOAt was later introduced by Carpino [35]. These salts were originally assigned a uronium-type structure based on the corresponding phosphonium salts. It was, however, later shown that the salts have an aminium-type structure [42].

Later Gilon used BTC (**1.31**) as an even more reactive peptide coupling reagent, generating acid chlorides *in situ* [43], cf. figure 1.4. BTC was proven to be very efficient for difficult couplings and in most cases caused no racemization.

Another approach is the use of activated amino acids. Thus, the use of the corresponding pentafluorophenyl esters of the commonly used amino acids removes the necessity of adding a coupling reagent [44, 45]. These ester are furthermore shelf stable.

Finally, the coupling reagent MSNT (**1.32**), cf. figure 1.4, can be used for coupling of amino acids to hydroxyl functionalized resins or linkers [46].

### 1.1.4 Protection group strategies

With every cycle of deprotection of the $N^{\alpha}$-protection group and subsequent amino acid coupling it is vital that the conditions used for deprotection do not in any way cause premature cleavage from the resin or removal of side-chain protection groups. Two protection group strategies are widely used, the Boc/Bn- [47] and Fmoc/*t*Bu-protection group schemes [48, 49]. Both rely on orthogonal removal of the $N^{\alpha}$-protection group without affecting side-chain protection groups.

The Boc/Bn-protection group scheme utilizes the acid labile Boc protection group (**1.40**), cf. figure 1.5, as the temporary $N^{\alpha}$-protection group and protection groups of the benzyl type **1.41** as side-chain protection groups and relies on graded acid lability of the temporary protection group and the side-chain protection groups. Boc can usually be removed with a mixture of TFA

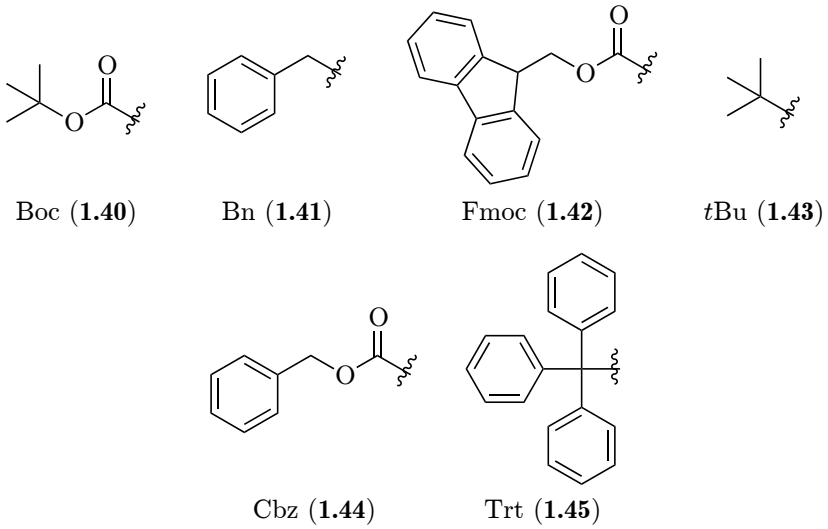


**Figure 1.5:** Selected acid and base labile protection groups used in solid-phase synthesis.

and $CH_2Cl_2$ whereas the benzyl type side-chain protection groups usually require more hash acidic conditions such as HF. If a linker that has the same lability as the side-chain protection groups (e.g. stable to TFA and labile to HF) is chosen, such as the BHA (**1.12**) or MBHA (**1.13**) linker, cf. figure 1.2, both the linker and the side-chain protection groups can be cleaved simultaneously on completion of the synthesis.

The Fmoc/*t*Bu-protection group scheme makes use of the base labile Fmoc protection group (**1.42**), cf. figure 1.5, as the temporary $N^{\alpha}$-protection group and acid labile protection groups of the *t*Bu type **1.43** as side-chain protection groups. The Fmoc group is cleaved by 20 (v/v)% piperidine in DMF while the *t*Bu type side-chain protection groups usually can be removed under relatively

mild acidic conditions with TFA. The Fmoc/*t*Bu-protection group scheme is thus an example of a more truly orthogonal protection group strategy relying on the base lability of the Fmoc group and the acid lability of the *t*Bu group instead of graded acid lability of the $N^{\alpha}$- and side-chain protection groups as seen with the Boc/Bn-protection group scheme.

Other commonly used protection groups are the Cbz group (**1.44**) [50], which can be removed by e.g. HBr, HF and catalytic hydrogenation, and the Trt group (**1.45**) [51–53], removable by mild acidic conditions, cf. figure 1.5.

Alternatively, protection groups that offer another dimension of orthogonality exist, relying on deprotection conditions completely orthogonal to common acid- and base labile protection groups. Among these are the Alloc (**1.46**) and All (**1.47**) protection groups [54], cf. figure 1.6, which can be cleaved by a Pd catalyst. Other examples are the Dde (**1.48**) [55–57] and Dts (**1.49**) [58–60] groups removable by hydrazinolysis and thiolysis, respectively, and the photolabile Nvoc protection group (**1.50**) [61].

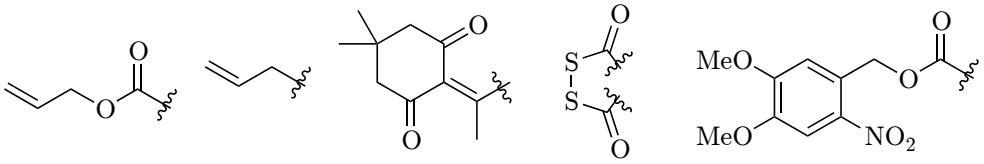


Alloc (**1.46**) All (**1.47**) Dde (**1.48**) Dts (**1.49**) Nvoc (**1.50**)

**Figure 1.6:** Selected protection groups orthogonal to acid and base labile protection groups.

## 1.2 Photolabile Linkers

In solid phase organic synthesis the desired molecule is bound through a linker inserted between the solid support and the molecule in question. Often harsh cleavage conditions such as strong acids/bases or nucleophiles, are needed, which can pose compatibility problems with acid- and base-labile compounds as well as commonly used protecting groups. Furthermore, the range of chemical transformations available for the synthesis of compounds is restricted by the cleavage conditions of the linker in order to avoid premature cleavage. Thus, to provide an additional dimension for the introduction of chemical diversity, linkers relying on alternative cleavage principles are needed.

Photolysis offers a method of cleavage, which is fully orthogonal to conventional chemical methods. Photolabile linkers are particularly interesting since they do not need acidic, basic or metal-assisted activation for cleavage. Indeed photochemical substrate release often occurs without additional reagents and under mild conditions that renders the process environmentally friendly and especially appealing in the context of green chemistry. The mild condi-

tions are, furthermore, attractive for direct applications in biological screening where contamination with cleavage reagents is undesired. Additionally, recent advances in LED lighting have significantly increased the ease with which photochemical transformations can be achieved.

Below follows an overview of some of the commonly used photolabile linkers in solid phase organic synthesis, with a focus on *o*-nitrobenzyl and *o*-nitroveratryl linkers, and their applications.

### 1.2.1 Mechanism of photolysis

The mechanism for photochemical cleavage of *o*-nitrobenzyl and *o*-nitroveratryl linkers is a Norrish type II [62] mechanism and a likely path is depicted in scheme 1.4 [61, 63–66]. An initial hydrogen abstraction leading to the *o*-

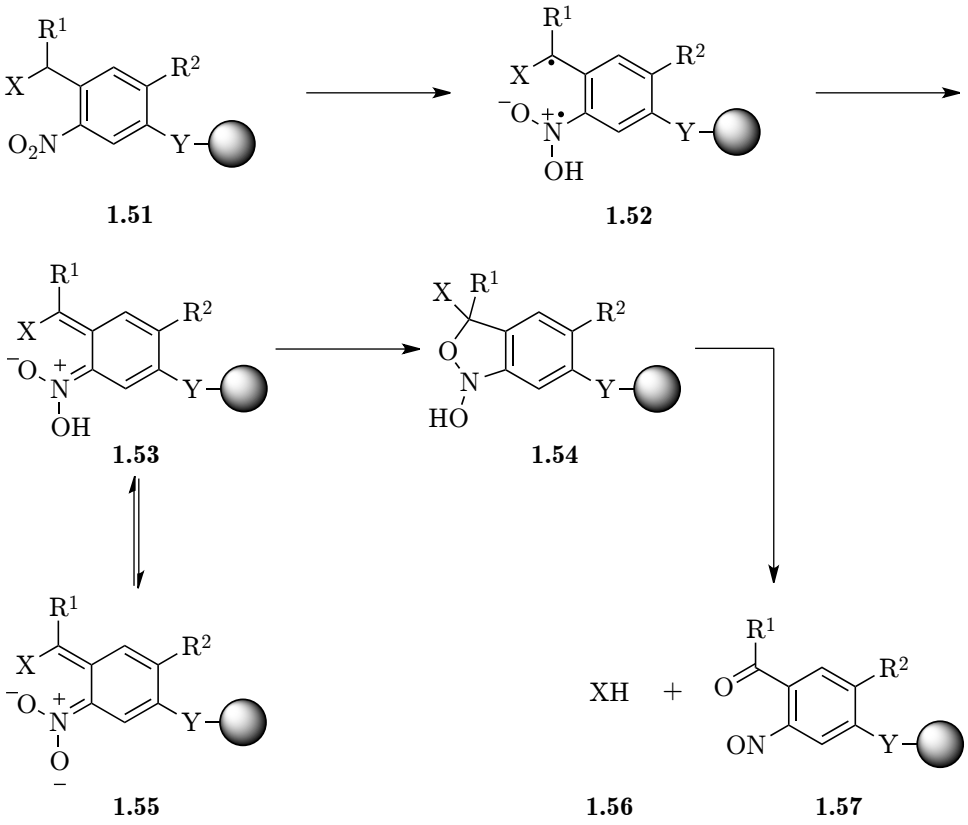


$R^1$ = H or Me, $R^2$ = H or OMe, X = OR or $NR^3R^4$, Y = O or $CH_2$

**Scheme 1.4:** Mechanism for the photolysis of *o*-nitrobenzyl and *o*-nitroveratryl linkers.

quinonoid intermediate **1.53** followed by cyclization provides the intermediate **1.54**. The cyclization leading to **1.54** was originally thought to proceed via

the anion species **1.55** [66] this was, however, later revised [61, 65]. Finally a rearrangement results in the formation of *o*-nitroso species **1.57** and release of the attached molecule **1.56**.

### 1.2.2 *o*-nitrobenzyl linkers

The first account of a photolabile linker was the *o*-nitrobenzyloxy based linker pioneered by Rich and Gurwara in 1973 [67]. The linker (in this case an integral linker) **1.58** was set up for attachment of the first amino acid at the *C*-terminus via substitution affording the construct **1.59**, cf. scheme 1.5. After standard SPPS and photolysis the first peptide ever constructed on a

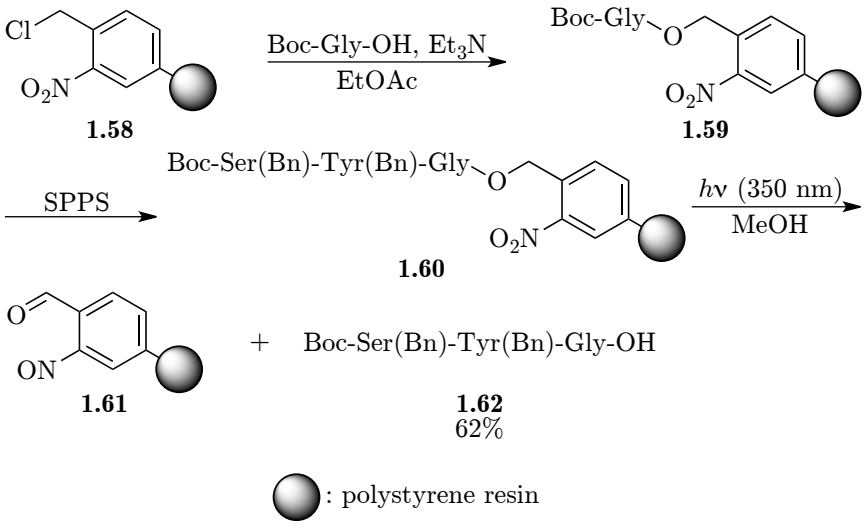


**Scheme 1.5:** The first photolabile linker based on the *o*-nitrobenzyloxy moiety.

photolabile linker was released in an overall yield of 62%.

However, due to over-nitration during the synthesis of the integral linker **1.58**, which made it unsuitable for peptides longer than four amino acids due to reduced swelling capacity [68], Rich and Gurwara developed a new non-integral linker **1.63**, cf. scheme 1.6. The linker **1.63** was prepared in solution and then coupled to the resin leading to construct **1.64** [68]. Attachment of the first amino acid followed by standard SPPS and final photolysis led to the decapeptide **1.66** in a yield of 64%.

The linker has been used by Merrifield for the preparation of multi detachable resins [69, 70] and by Barany and co-workers to achieve three dimensional orthogonal protection in solid-phase organic synthesis [59]. Different variations of the connection of the linker unit to the resin have been explored, e.g. adding a phenyl group in the benzylic position [71, 72] or inserting a glycine unit acting as an internal standard [73].

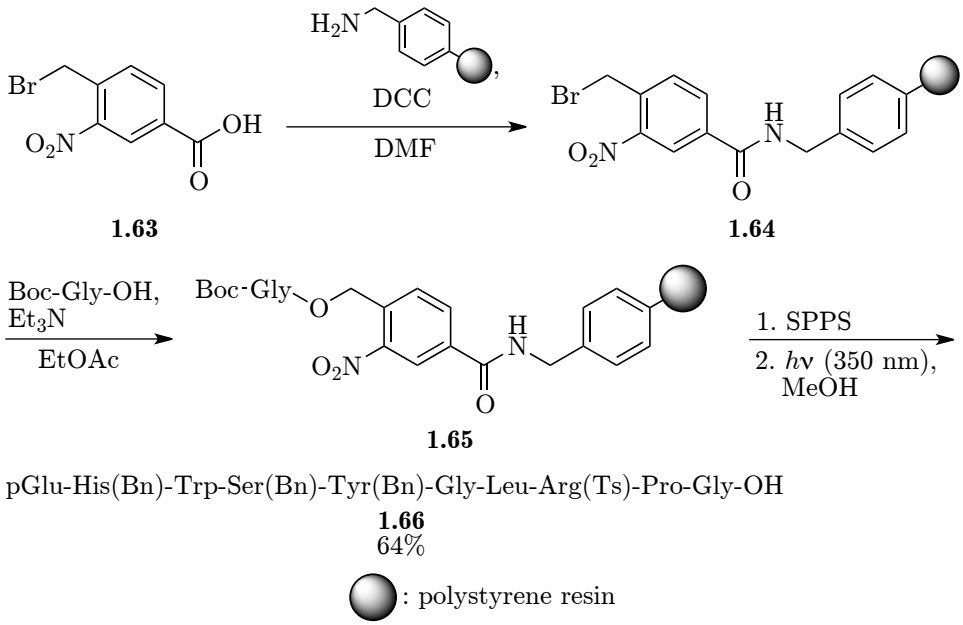


**Scheme 1.6:** Non-integral *o*-nitrobenzyloxy photolabile linker used for the synthesis of a decapeptide.

In a study focusing on the synthesis of combinatorial libraries Ohlmeyer used the *o*-nitrobenzyloxy linker, which facilitated easy release of the synthesized ligands under conditions optimal for subsequent use in biological assays [74].

The linker has furthermore been used for oligonucleotide synthesis by Green [75–77] and oligosaccharide synthesis by Zehavi [78], Nicolaou [79, 80] and Parquette [81].

To take into account the fact that many biologically active peptides possess a terminal primary amide, Rich and Gurwara also developed an *o*-nitrobenzylamino variation of the *o*-nitrobenzyl-based linker that upon photolysis releases an amide [82]. Pillai and co-workers documented the possibility of releasing secondary amides using this linker [83–85]. An *o*-nitrobenzylamino linker was used by Gerace and Auer in their on-bead screening of a one-bead one-compound library in the search for nuclear import inhibitors [86]. Recently Seeberger developed an approach for automated oligosaccharide synthesis using this type of linker [87–89].

### 1.2.3 $\alpha$-substituted *o*-nitrobenzyl linkers

The *o*-nitrobenzyl-based linkers presented so far have the disadvantage that the side product of their photolysis is an *o*-nitrosobenzaldehyde, cf. construct **1.61**, scheme 1.5. This is a very reactive species that is prone to polymerization, generating a highly colored side product, which acts as an internal light

filter. This has a detrimental effect on the photolytic cleavage of the desired compounds due to limited access of light to the reaction site [90].

To solve this issue Pillai prepared the integral linker **1.67**, featuring a methyl group in the $\alpha$-position [90], cf. scheme 1.7. Using this linker the

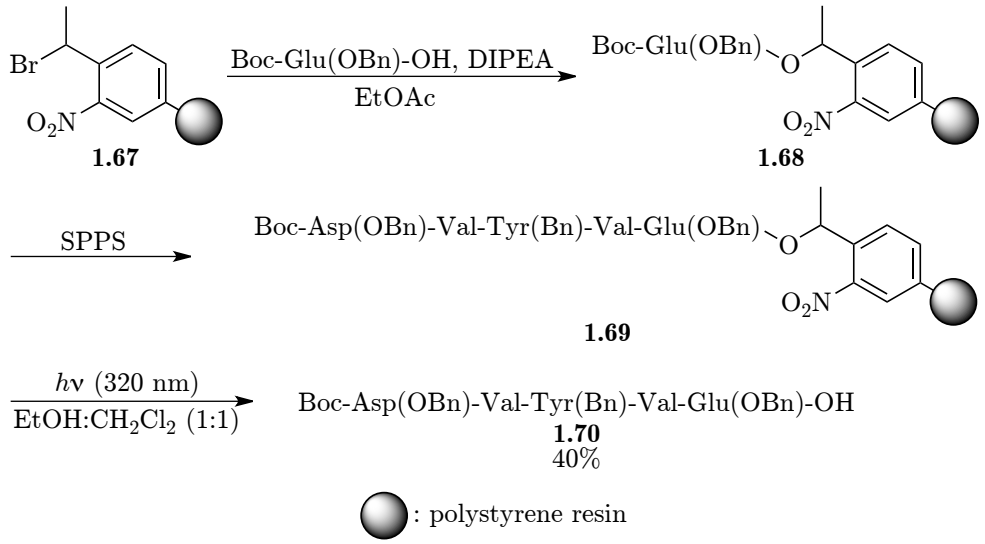


**Scheme 1.7:** Integral $\alpha$-substituted nitrobenzyl-derived photolabile linker used for the synthesis of pentapeptide **1.70**.

pentapeptide **1.70** was synthesized in a yield of 40%.

This resin however suffered from the same problems as seen with Rich and Gurwara's original $o$-nitrobenzyloxy linker, cf. scheme 1.5, in that over-nitration degraded the swelling properties of the resin and prevented the synthesis of longer peptides.

A solution to this issue was to introduce the nitrated moiety in a more controlled manner via a nitrated building block instead of performing a nitration directly on the resin [91], cf. scheme 1.8. Thus, the resin **1.71** underwent Friedel-Crafts acylation followed by reduction leading to $o$-nitrobenzhydryl resin **1.72**. With this resin in hand Pillai synthesized both peptides **1.76** [91] and, after transformation to the amine-functionalized resin **1.74** [92], amidopeptides **1.75**. Peptides with up to 10 amino acids were synthesized in good yields.

Geysen used a related non-integral linker, the 3-amino-3-(2-nitrophenyl)propionyl (ANP) linker **1.77**, for the synthesis of amidopeptides [93], cf. scheme 1.9. A more acid stable variant was proposed by Schreiber with two methyl groups in the $\alpha$-position of the amide [94]. An alcohol-based variant of linker **1.77** was used for oligosaccharide synthesis by Geysen [95]. It also incorporated a longer spacer between the support and the photosensitive part to avoid problems with $\beta$-elimination and lactonization of the alcohol [95].

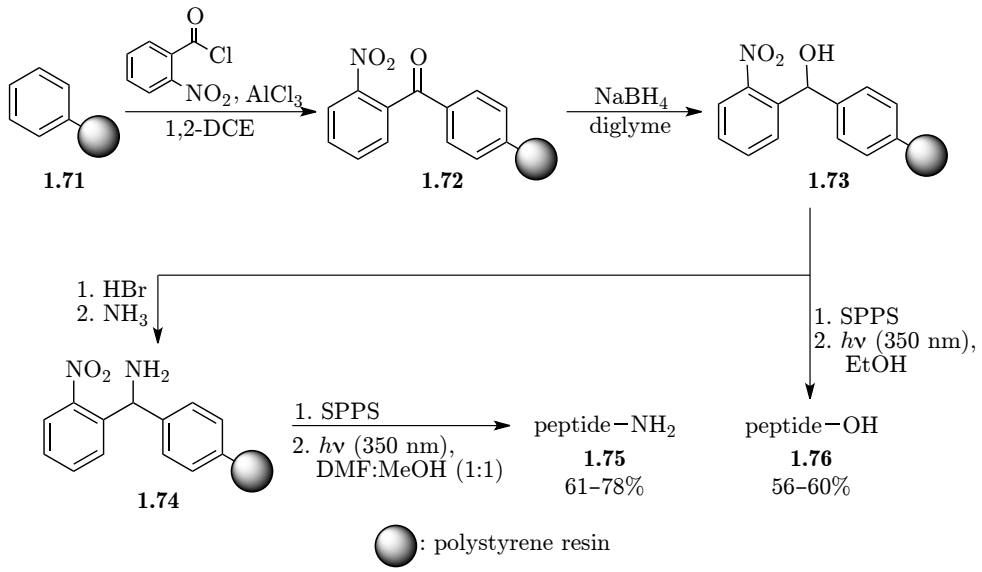


**Scheme 1.8:** Integral photolabile *o*-nitrobenzhydryl linker providing access to both peptides and amidopeptides.

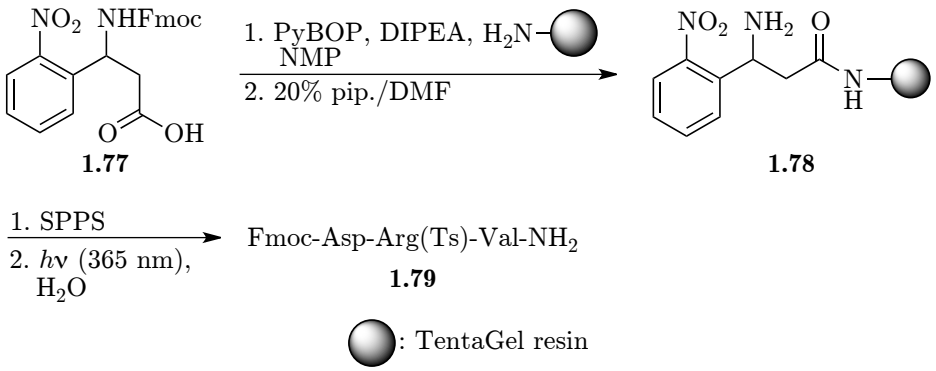


**Scheme 1.9:** Non-integral photolabile ANP linker used for the synthesis of tripeptide **1.79**.

### 1.2.4 *o*-nitroveratryl linkers

Initially introduced by Patchornik as a photolabile linker in 1973 [96], the use of the *o*-nitroveratryl group (4,5-dimethoxy-2-nitrobenzyl) in photolabile linkers was popularized in the mid-1990s by Greenberg [97] and Holmes [30].

Greenberg utilized this type of linker to circumvent some of the issues observed with the original unsubstituted *o*-nitrobenzyl linkers, namely long photolysis times and low yields of liberation [97]. It was theorized that the introduction of the alkoxy substituents would improve the aforementioned issues.

The linker **1.80** was prepared in solution and then bound to a long chain alkyl amine controlled pore glass (LCAA-CPG) support leading to construct **1.81** which was then used for the synthesis of oligonucleotides in good yields [97], cf. scheme 1.10. Later it was shown that a more efficient photolysis

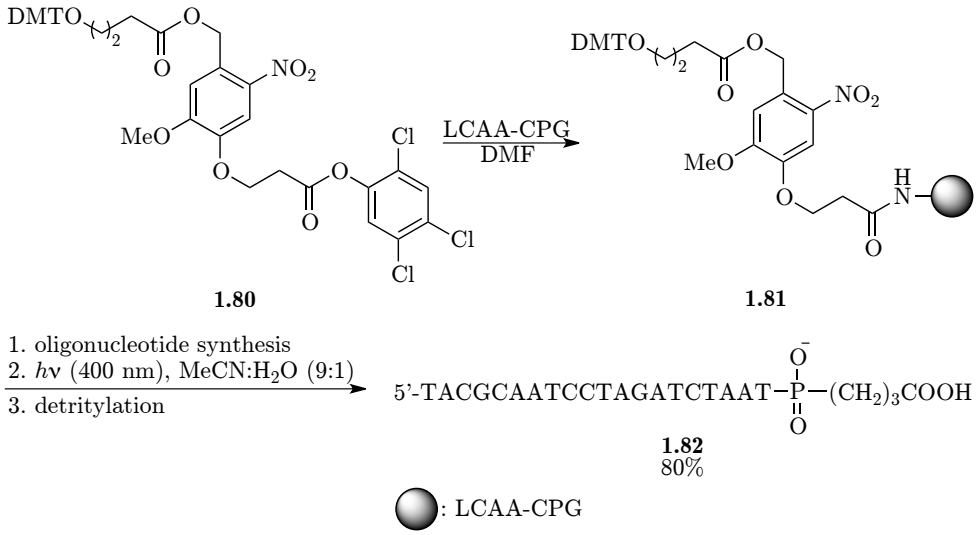


**Scheme 1.10:** Use of photolabile *o*-nitroveratryl-based linker for the synthesis of oligonucleotides.

could be achieved by linking the hydroxyl group of the nucleotide directly to the linker via a carbonate functionality [98]. This modified linker was later used for oligonucleotide synthesis by other groups [99].

Nearly simultaneously with the work of Greenberg, Holmes introduced an *o*-nitroveratryl-based amine linker with a methyl group in the $\alpha$-position and used it for the synthesis of a hexapeptide [30], cf. scheme 1.11. This linker, producing amides upon photolysis, also solved the problem with formation of a reactive nitroso aldehyde upon photolysis as described earlier.

In 1997, Holmes published a systematic study of the effect of nitroveratryl substituents on the photolysis efficiency [100]. It was shown that the rate of cleavage was 7 to 20 times higher when the *o*-nitrobenzyl ring was sub-

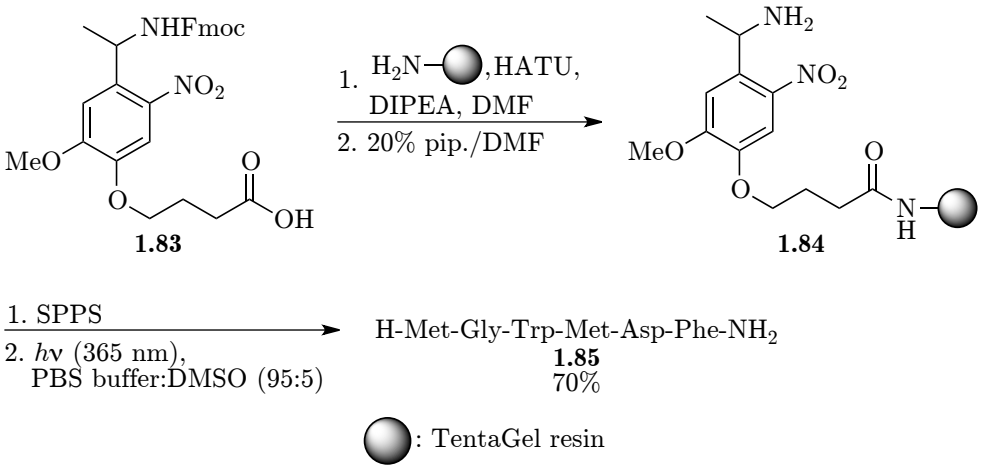


**Scheme 1.11:** Use of photolabile amine-containing $\alpha$-methylated nitroveratryl linker for the synthesis of a hexapeptide by Holmes.

stituted with electron-donating alkoxy substituents. It was also shown that an alkyl group in the $\alpha$-position to the amine increased the rate of cleavage by a factor of 3. The length of the spacer chain also had an influence with a slightly increased rate for longer chains. It was concluded that both the alkoxy substituents on the aromatic ring and the alkyl group in the $\alpha$-position were significantly beneficial for the photochemical reactivity.

Holmes also developed an alcohol-based version of the linker **1.83** [100], cf. figure 1.7.

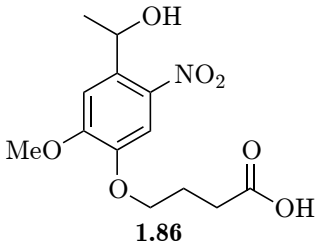


**Figure 1.7:** Photolabile alcohol-containing $\alpha$-methylated nitroveratryl linker by Holmes.

The linkers **1.83** and **1.86** have found numerous applications and it has also been shown that this linker type could be coupled to a hydroxy based resin without effect on the efficiency of the photolytic cleavage [101]. An *o*-nitroveratryl linker was used by McKeown to develop methods for easing the analysis of solid phase synthesis reactions by mass spectrometric techniques [102]. Another example is the use of linker **1.83** by Madder for the preparation of serine protease mimics [103]. Blackwell likewise used this linker for the

synthesis of a diketopiperazine library using the Ugi multicomponent reaction [104], cf. scheme 1.12. The linker **1.83** was attached to the solid support and

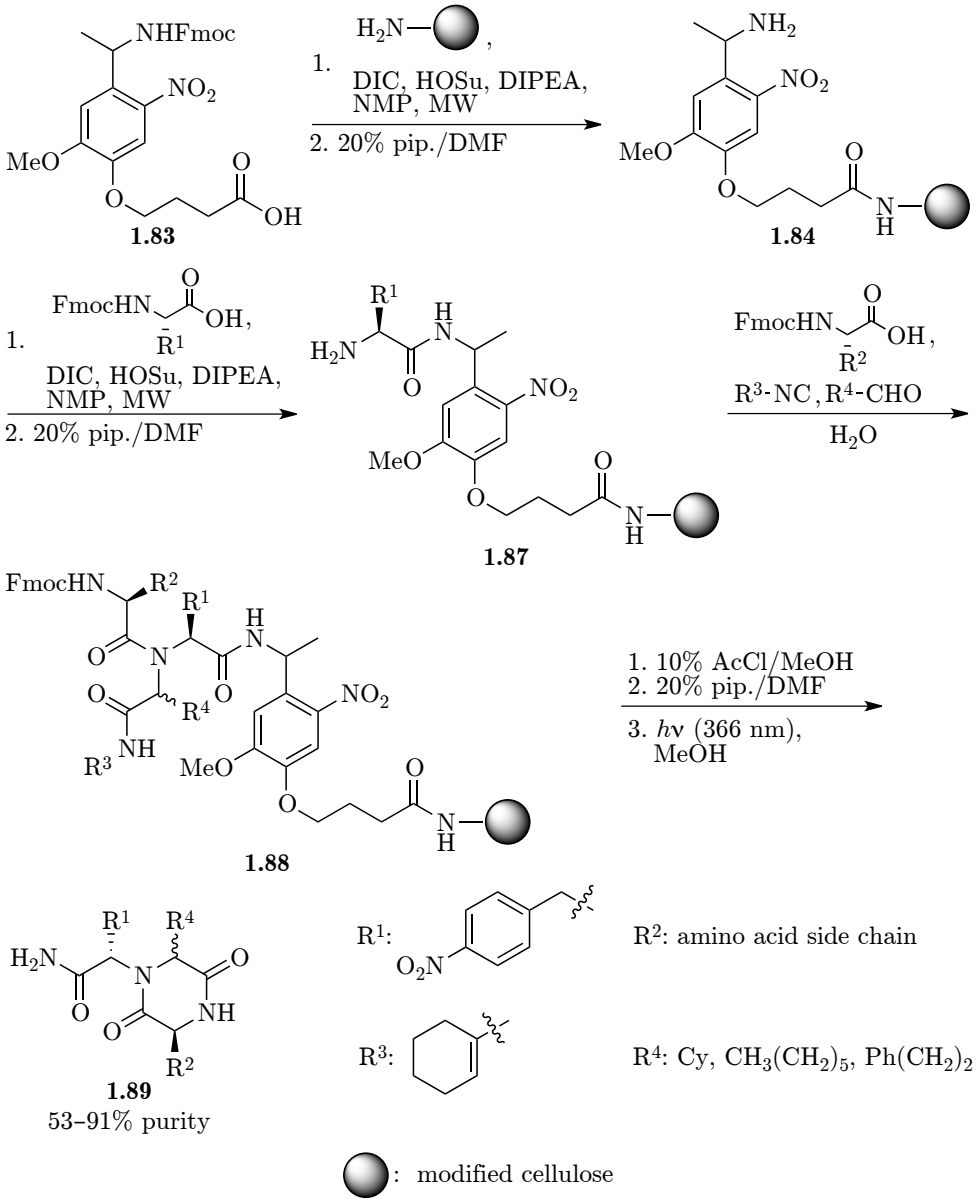


**Scheme 1.12:** *o*-nitroveratryl linker used in multicomponent reactions by Blackwell.

subsequent coupling of Fmoc-Phe(4-$NO_2$)-OH by standard methods led to the construct **1.87**. Subjection to Ugi conditions and subsequent methanolysis and photochemical release afforded diketopiperazines **1.89** in moderate to good purities.

The linker **1.83** was again used by Gennari for the synthesis of combi-

natorial libraries of vinylogous sulfonamidopeptides [105]. Furthermore, this study confirmed the trends Holmes had encountered [100], namely that *o*-nitroveratryl-based linkers are superior to *o*-nitrobenzyl linkers due to the beneficial effects of alkoxy substituents and the presence of $\alpha$-methyl group.

Another example is the synthesis of 3,4-disubstituted $\beta$-lactams proposed by Gallop [106], cf. scheme 1.13. The construct **1.90** was deprotected and condensed with an aldehyde producing imine **1.91** which then underwent a $[2+2]$ cycloaddition with a ketene providing **1.92**. Final photolysis led to

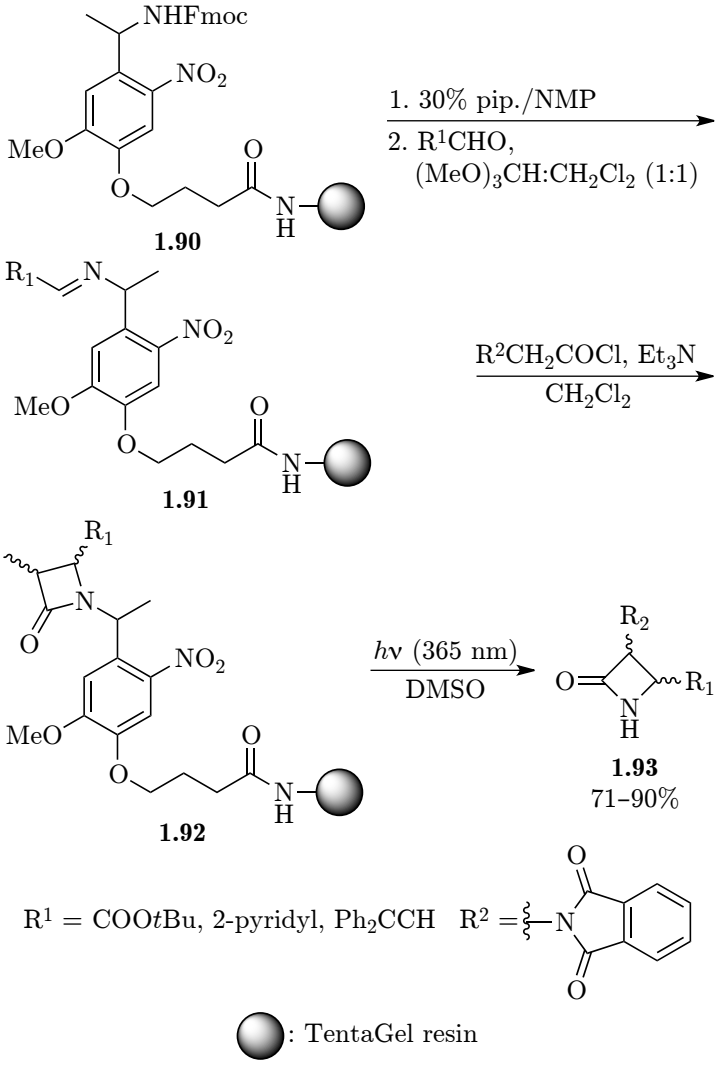


**Scheme 1.13:** $\alpha$-methylated nitroveratryl linker used in the synthesis of $\beta$-lactams.

$\beta$-lactams **1.93** in good yields [106], cf. scheme 1.13.

Meldal used an aldehyde linker closely related to **1.86**, for the synthesis of a small library of arylpiperazine melanocortin subtype-4 agonists [107].

Recently, a new azido-linker based on the *o*-nitroveratryl group was introduced by Nielsen for the synthesis of 1,2,3-trizoles [108], cf. scheme 1.14. The

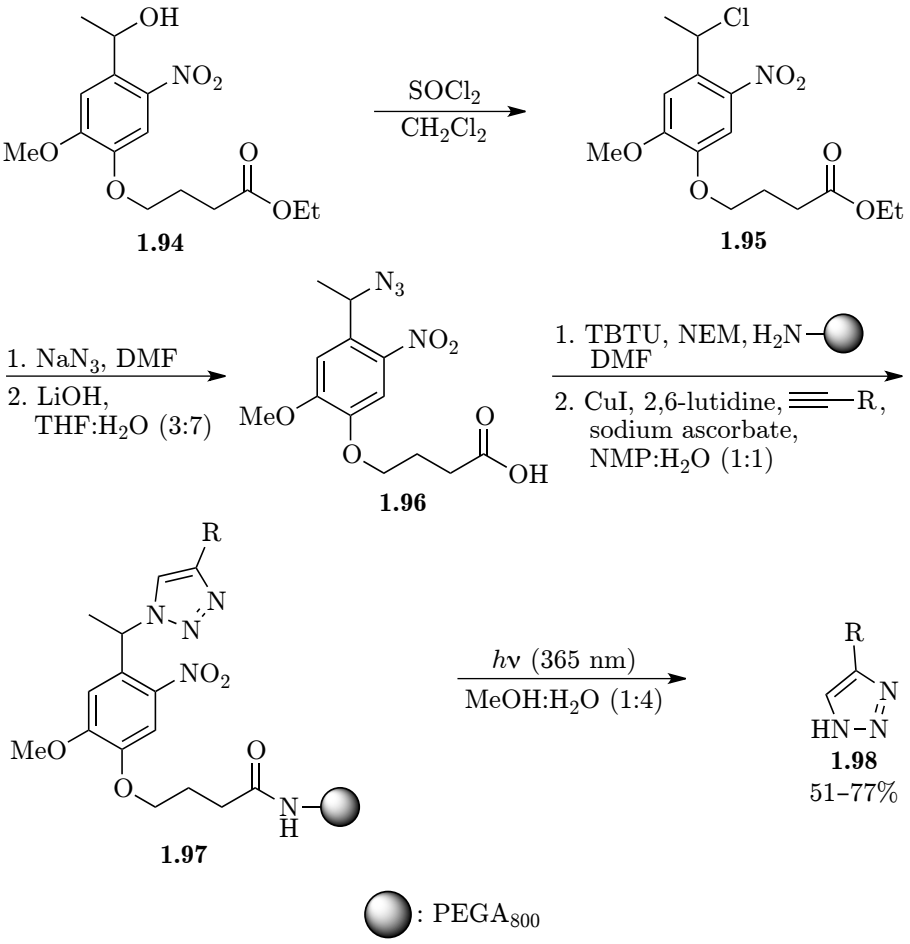


**Scheme 1.14:** Photolabile nitroveratryl-based azido-linker for the synthesis of 1,2,3-triazoles.

alcohol **1.94** was subjected to $SOCl_2$ followed by substitution with $NaN_3$ and ester hydrolysis with LiOH leading to the azido linker **1.96**. Attachment to the solid support and subsequent copper(I)-catalyzed azide-alkyne cycloaddition led to the construct **1.97**, which after photolytic cleavage provided 1,2,3-triazoles **1.98** in good yields.

Later Nielsen introduced a hydrazine linker also based on the alcohol **1.94** used in the synthesis of peptide hydrazides in yields of 21–83% [109]. This methodology also allowed for the solid-phase synthesis of dihydropyrano[2,3-c]pyrazoles [109].

Another recent example is the linker developed by Lee [110]. This linker has the tether to the solid support positioned in the $\alpha$-position, cf. scheme 1.15.

After attachment to the solid support, standard SPPS and photolytic cleavage, Leu-enkephalin (**1.100**) was liberated as an amide in a yield of 50%.

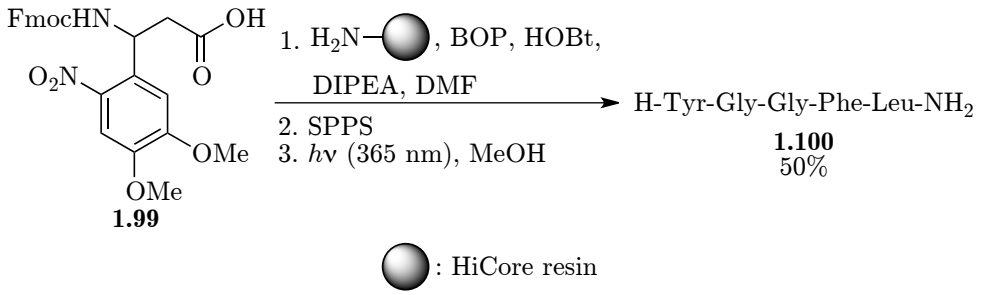


**Scheme 1.15:** Synthesis of Leu-enkephalin as an amide using the photolabile linker **1.99** developed by Lee.

Chapter 2

# Synthesis of Doxorubicin Derivatives on Photolabile Solid Support

Screening of chemical compounds is an essential part of identifying leads for drug development. However, much HTS-based chemical biology research is a time-consuming and costly process, and as such preserved for very few researchers. Thus efficient and less costly screening-technologies of compound libraries are sought to complement current drug discovery approaches.

Bead-based screening assays where compounds are synthesized on solid support and screened while still attached to the resin (so-called *on-bead screening*) or after cleavage from the resin (*off-bead screening*) provides an efficient and rapid method for the synthesis and biological evaluation of libraries of thousands of compounds [111–113]. On-bead assays are however not always predictive of the activity of a compound as a free molecule in solution e.g. because of interference from the bead matrix [114–116]. Off-bead assays are not hampered by this limitation and thus provide a method more akin to classic solution based assays. Off-bead screening furthermore provides the advantage of being able to screen targets where it is of importance that the compounds are in solution e.g. enzymes with binding sites that are not readily accessible and cells [117, 118]. Such methods include the use of microtiter plates to keep beads spatially separated [119, 120] and the immobilization of beads in a thin layer of soft agar to reduce compound diffusion [118, 121]. However, the use of microtiter plates is hampered by the difficulties of homogenous filling of wells with beads, while the use of gels is limited by the fact that the assay environment is determined by the nature of the gel.

Two major challenges are given when establishing a bead-based platform for the synthesis and off-bead screening of compounds. Firstly, the library

compounds must be synthesized and released under conditions that are compatible with the structural complexity and sensitivity of a given compound to reaction conditions often employed in automated and parallel synthesis efforts, including common bases and acids. Secondly, the library compounds must be released under neutral, biocompatible conditions into an aqueous buffer.

The aim of this study was to develop a methodology for the synthesis of biologically interesting compounds compatible with a bead-based platform integrating solid-phase synthesis and cell-based screening (cf. figure 2.1 for principle). It was envisioned that a library of biologically interesting drug

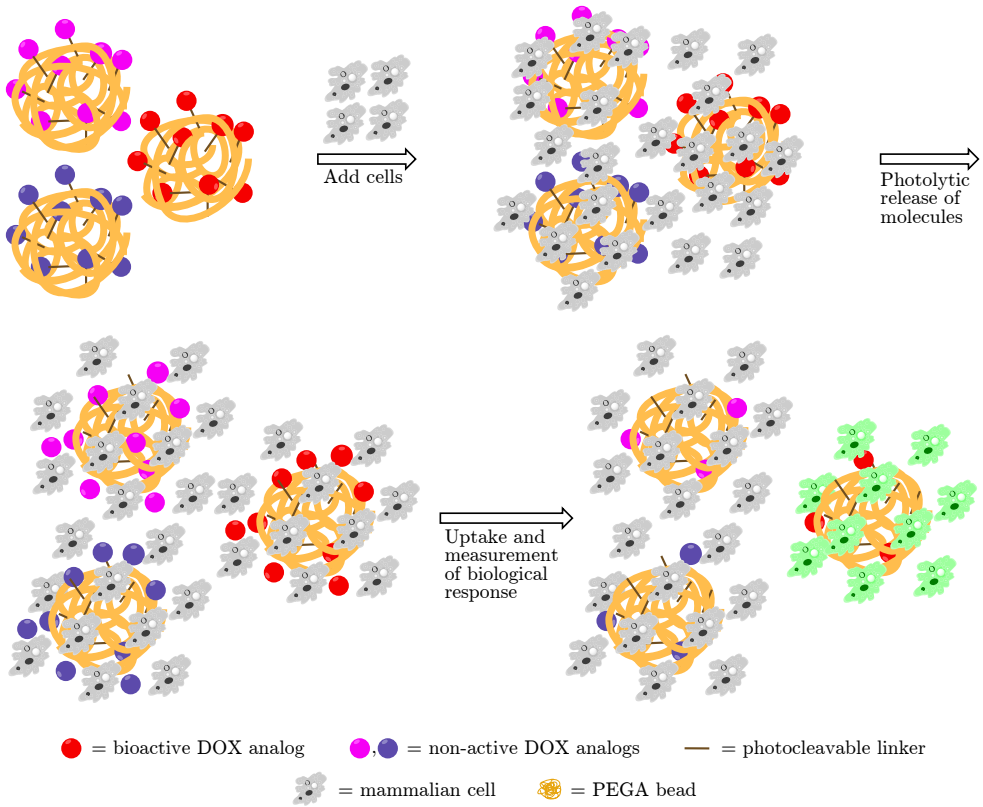


**Figure 2.1:** Illustration of bead-based platform integrating solid-phase synthesis and cell-based screening.

analogs prepared on solid support upon mixing with cells and subsequent photolytic release of the prepared analogs [114,115,118,119,122] would interact with the cells and thus lead to identification of bioactive drug analogs by measurement of the biological response, cf. figure 2.1.

To serve as a model substrate for the methodology, doxorubicin (DOX, **2.1**), cf. figure 2.2, a renowned cytotoxic agent, was chosen. DOX is a highly potent anticancer agent and was isolated from cultures of a mutant of *Streptomyces peucetius* for the first time in 1969 [123]. DOX is an anthracycline

and among the most utilized antitumor drugs in the world. The mechanism of action of DOX and other anthracyclines remains a matter of controversy but intercalation of DNA and inhibition of topoisomerase II are likely to be events of importance for the antitumor activity of DOX [124–126]. Most patients receiving systemic cancer treatment receive DOX or another anthracycline at some time during treatment [127]. DOX is the most commonly used anthracycline and is widely used against a wide range of malignancies, especially solid tumors [126, 128]. DOX is commonly used as part of combination chemotherapy regimens for the treatment of lymphomas and is one of the most active drugs in the treatment of breast cancer and soft tissue sarcomas where it is used both by itself as the primary treatment and in combination with other drugs as adjuvant chemotherapy [129].

However, its application is limited by significant side effects, the most serious being severe cardiotoxicity [130]. Considerable work has therefore been undertaken to chemically modify DOX with the goal of reducing its systemic toxicity. More than five DOX analogs are marketed in other countries, and two, daunorubicin (**2.2**) and idarubicin (**2.4**), are available in the United States [131], cf. figure 2.2.

Daunorubicine (**2.2**) was the first anthracycline found to have antineoplastic activity [129], cf. figure 2.2. It is marketed worldwide [131] and is only used in leukemia treatment being an important drug in the treatment of acute lymphocytic leukemia. It exhibits similar side effects to those associated with DOX [129].

Epirubicin (**2.3**) is marketed worldwide (except the United States) [131] and differs from DOX only in the the orientation of a single hydroxyl group (changing from an axial to an equatorial orientation) [125], cf. figure 2.2. It has similar antitumor activity to DOX, however, it is less potent. Even though it causes slightly less cardiac toxicity it has no major advantage over DOX [129].

Idarubicin (**2.4**) is marketed worldwide [131] and is structurally similar to daunorubicin (**2.2**) differing only in the removal of a methoxy group, cf. figure 2.2. Idarubicin is used for the treatment of myelogenous leukemia [129] and also shows activity against multiple myeloma, non-Hodgkins's lymphoma and breast cancer and can furthermore be administered orally [125]. It is not agreed upon whether idarubicin (**2.4**) offers advantages over DOX and daunorubicin (**2.2**) (also with regard to cardiac toxicity) [125].

Pirarubicin (**2.5**), a 4-tetrahydropyranyl doxorubicin analog, and Aclarubicin (**2.6**), a trisaccharide anthracycline, cf. figure 2.2, are both marketed in Japan and France [131]. They show no real advantage over either DOX or daunorubicin (**2.2**) [125, 129].

In an effort to either expand the antitumor spectrum of DOX or reduce cardiotoxicity a wide range of newer DOX analogs have been prepared. Below follows a few selected examples.

Van der Vijgh tested a new DOX prodrug with the aim of lowering the

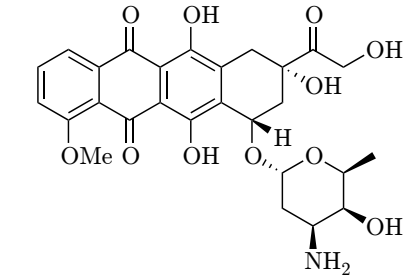

doxorubicin (**2.1**)

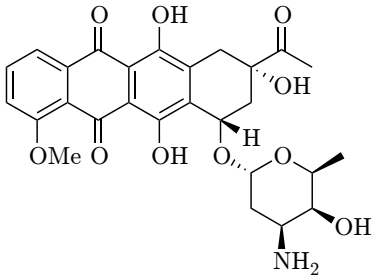

daunorubicin (**2.2**)

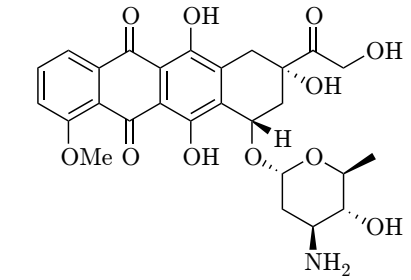

epirubicin (**2.3**)

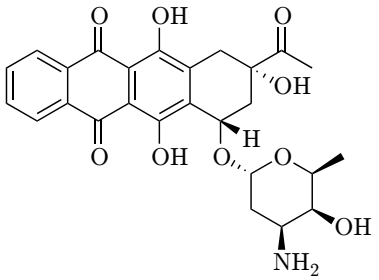

idarubicin (**2.4**)

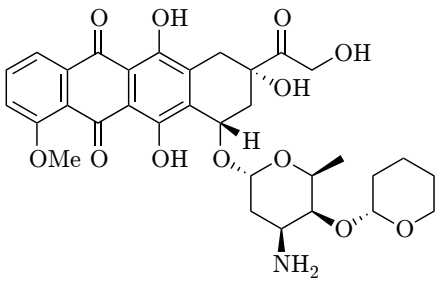

pirarubicin (**2.5**)

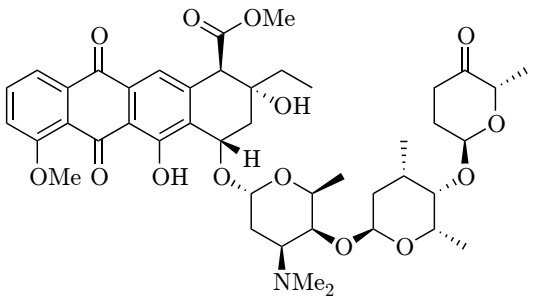

aclarubicin (**2.6**)

**Figure 2.2:** DOX analogs marketed around the world.

cardiotoxicity and improving the therapeutic index produced by DOX [132]. The prodrug was a leucine-doxorubicin analog (Leu-DOX, **2.7**) , originally developed by Trouet (but as a daunorubicin analog) in 1980 [133], cf. figure 2.3. Leu-DOX (**2.7**) rapidly formed DOX upon intravenous administration and showed diminished cardiotoxicity [132].

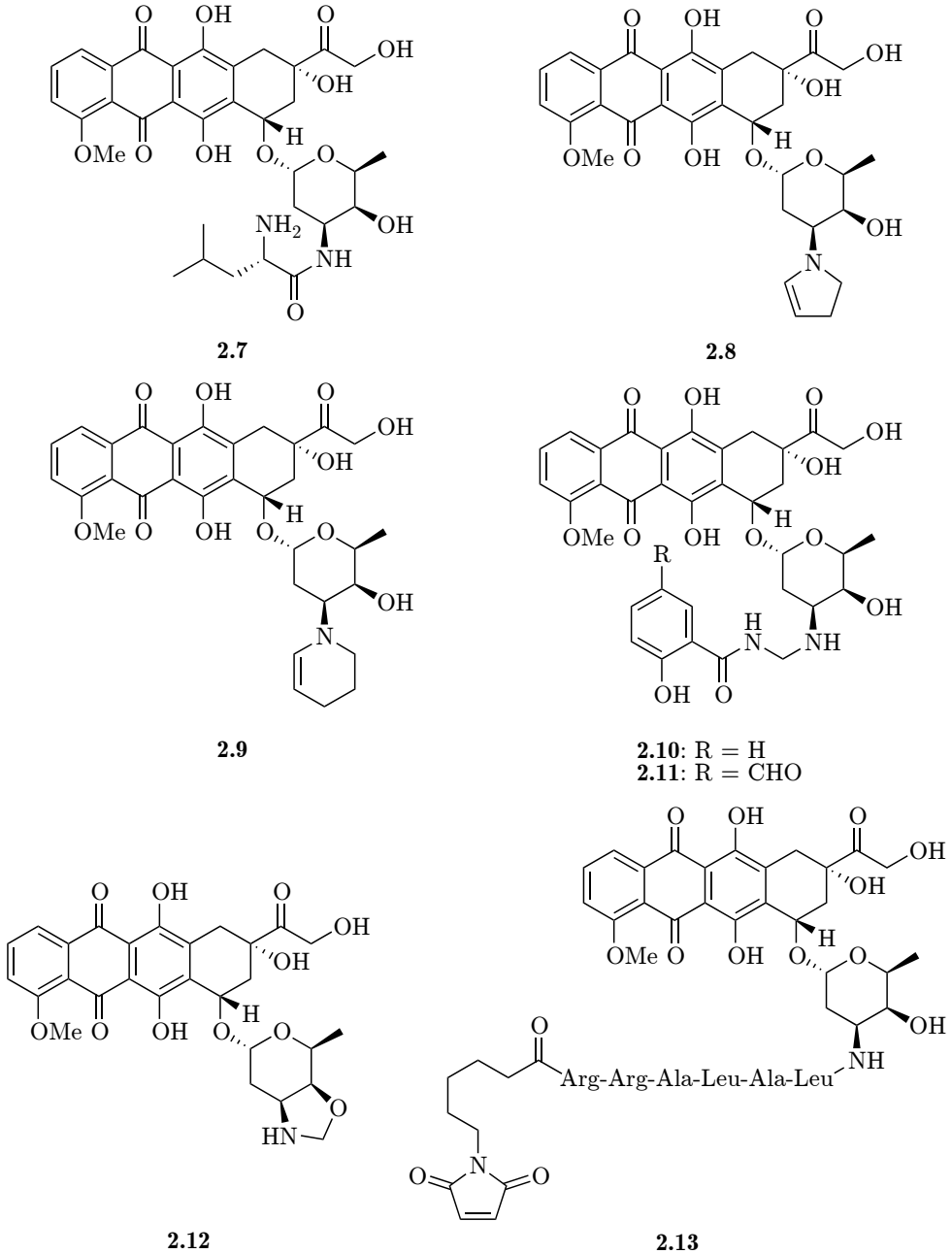


**Figure 2.3:** New DOX analogs.

Schally introduced the DOX analogs 2-pyrrolinodoxorubicin **2.8** and 1,3-tetrahydropyridinodoxorubicin **2.9** in 1996 [134], cf. figure 2.3, obtained from DOX by reaction with 4-iodobutyraldehyde and 5-iodovaleraldehyde. 2-pyrrolinodoxorubicin **2.8** was 500–1000 times more potent than DOX and 30–50 times more potent than 1,3-tetrahydropyridinodoxorubicin **2.9** [134]. This was explained by an increased steric hindrance caused by the 6-membered ring in **2.9** as compared to the 5-membered ring of **2.8**, which is more planar [134]. Carditoxicity of the analogs was not commented upon in the study.

Koch developed a DOX-formaldehyde conjugate **2.10**, cf. figure 2.3, targeted against breast cancer cells in 2004 [130]. The conjugate, also called doxsaliform, was 4–10-fold more cytotoxic than DOX. The aromatic ring can be functionalized as seen with DOX-5-formylsaliform **2.11**, cf. figure 2.3, which may be utilized for the attachment to a targeting molecule [130]. A year later, Koch introduced the new DOX-formaldehyde conjugate Doxaz **2.12** [135], cf. figure 2.3. This cyclic conjugate is more reactive than **2.11** and shows a reduced cytotoxicity [135].

Kratz developed a peptide prodrug of DOX **2.13** in 2007 [136], cf. figure 2.3. A peptide sequence which can be specifically cleaved by the cysteine protease cathepsin B, which has been observed overexpressed in malignant tumors, was incorporated into the prodrug thus making specific drug delivery to the tumor possible [136].

Methods have been fashioned to keep the plasma level of DOX muted to minimize cardiotoxicity, but the only apparently effective methods available so far are slow infusion and the use of iron chelators [125]. Continuous infusion of DOX over 96 h has been shown to maintain therapeutic efficacy while reducing cardiotoxicity compared to bolus administration [131]. This technique is however cumbersome and costly and requires prolonged hospitalization of the patients every three weeks [131]. Infusion of dexrazoxane, an iron chelator, before DOX has been shown to reduce cardiotoxicity [125]. However, there have been reports showing reduced response rates in women receiving DOX for the treatment of breast cancer when used in combination with dexrazoxane [125].

Synthetic efforts in the context of preparing DOX analogs are hampered by the structural complexity and sensitivity of DOX to the often harsh reaction conditions used in solid-phase synthesis for the deprotection of protection groups or linker cleavage such as strong acids and bases [137–141]. At acidic pH (pH $< 4$) the major degradation product is the aglycone **2.14** resulting from hydrolysis and loss of the amino sugar [139], cf. scheme 2.1. At higher pH (pH $> 4$) the major degradation product is the aromatized aglycone **2.15** [139], cf. scheme 2.1. For the structurally related daunorubicin (**2.2**) the main degradation product at alkaline pH (pH 8) is the aromatized aglycone **2.16** [138, 139], cf. scheme 2.2. The corresponding degradation product is, however, not observed for DOX (it can however be obtained upon subjecting DOX to severe acidic conditions) [139]. At highly alkaline conditions both DOX and daunorubicin (**2.2**) degrade in to a complex mixture of degradation

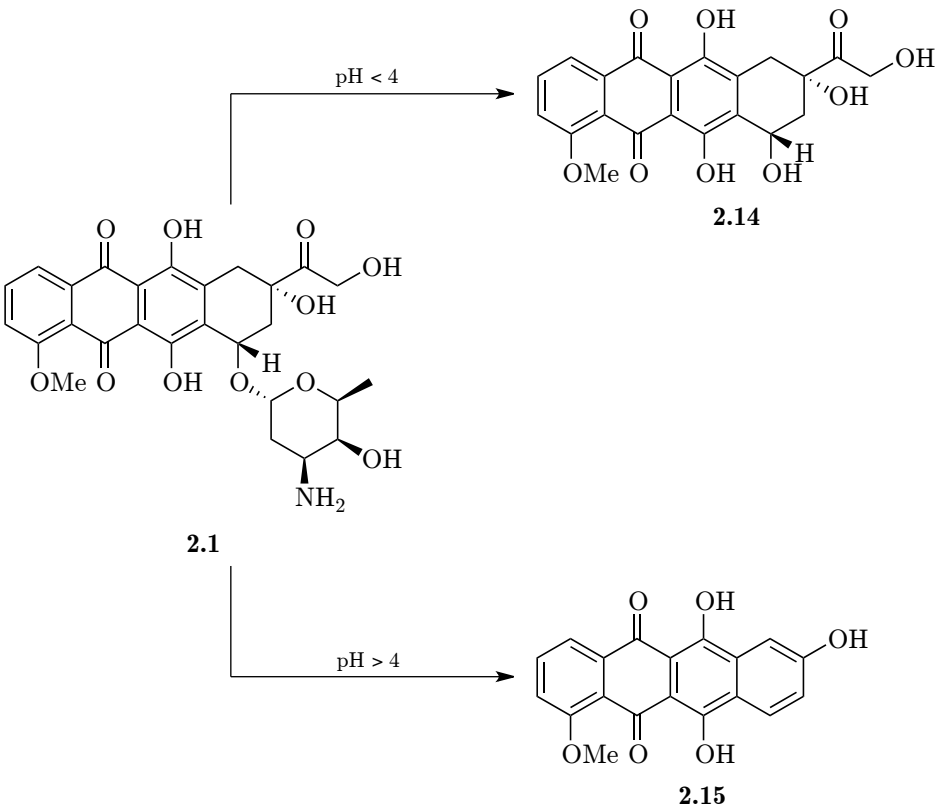


**Scheme 2.1:** Degradation of doxorubicin at pH $< 4$ and pH $> 4$.

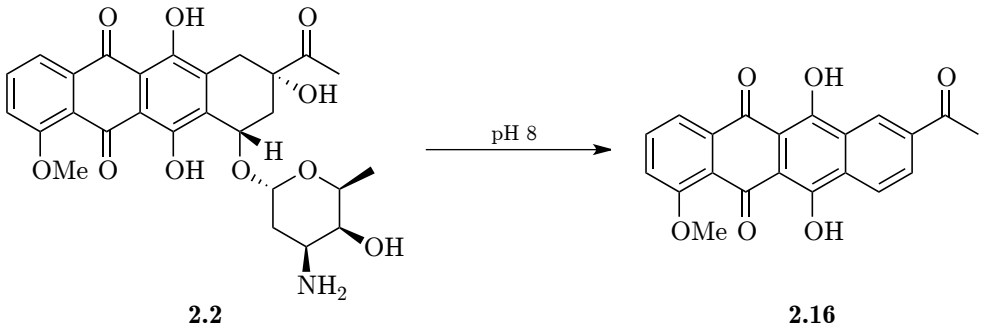


**Scheme 2.2:** Degradation of daunorubicin at pH 8.

products [138, 140].

DOX would thus provide a challenging case study showcasing the mild conditions of the aforementioned methodology and its applicability in the synthesis and release of structurally complex compound derivatives, conditions that would furthermore be ideal for direct screening efforts.

## 2.1 Synthetic Strategy

The goal was thus to develop a synthetic methodology compatible with the aforementioned screening platform. Two different strategies for the synthesis of DOX derivatives were envisioned, utilizing either the primary amine or the primary alcohol in DOX as the functional handle for derivatization, cf. scheme 2.3. In both cases, the photolabile linker will initially be attached

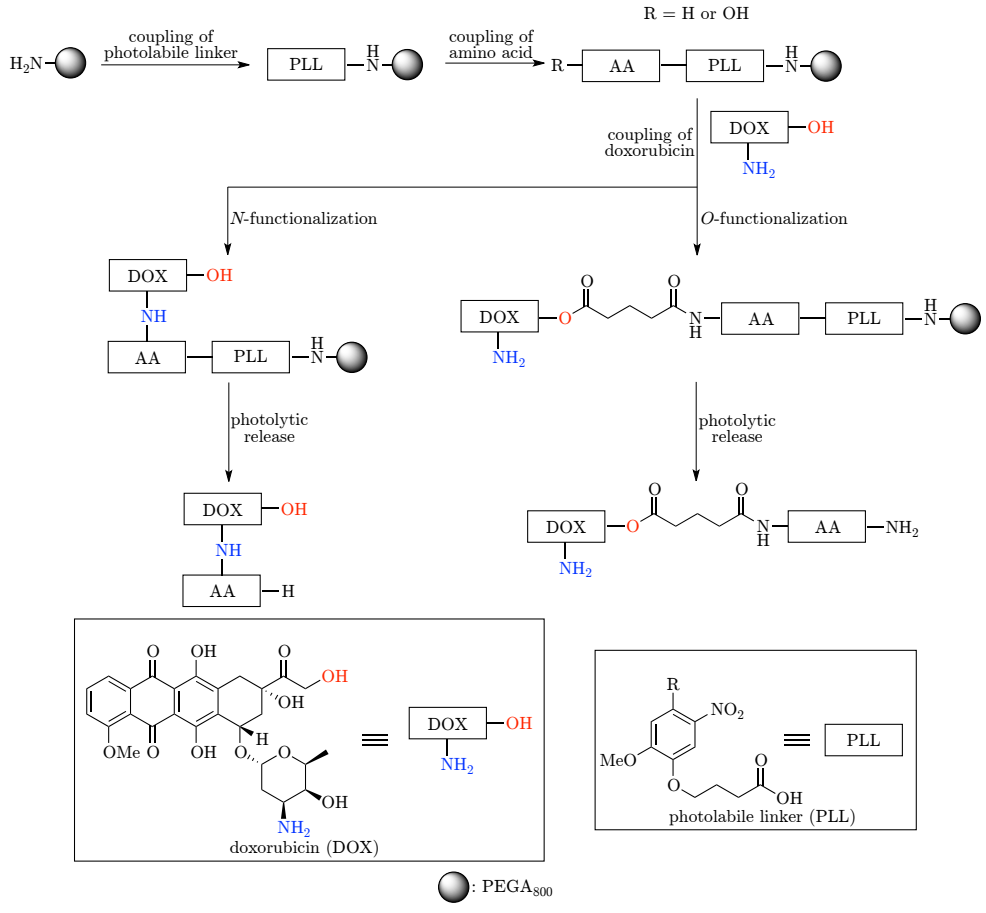


**Scheme 2.3:** Synthetic strategy for the synthesis of DOX derivatives.

to the solid support followed by amino acid coupling. DOX is then attached either via its primary amine (*N*-functionalization) or its primary alcohol (*O*-

functionalization) leading to DOX amino acid/peptide derivatives. Finally, the DOX derivative will be photolytically released from the resin.

## 2.2 Acid- and Base Stability of Doxorubicin

Aware of the limited stability of DOX towards acidic and basic conditions [137], chemical investigations were initiated with studying the stability of DOX towards some of the standard reaction conditions used in SPPS, TFA in $H_2O$ and piperidine in DMF.[1] The results showed that DOX is stable in 10% TFA for an extended period of time, while a concentration of 5% piperidine is allowed for 20 min, cf. figure 2.4.

## 2.3 Photolabile Linker Synthesis

The photolabile linker intermediates **2.20**, **1.94** and **1.95**, cf. scheme 2.4 (originally prepared by Nielsen for the synthesis of azido linker **1.96**, cf. scheme 1.14), were thought to be a good starting point for the development of the photolabile handle needed. Thus, large scale synthesis of chloride **1.95** was initiated. The first step leading to ketone **2.19** was performed in approx. the same scale as originally reported with a comparable yield. The following nitration could easily be scaled to a 40 g scale (four times what was originally reported) without any effect on the yield. Likewise, the reduction affording alcohol **1.94** proved to be very scalable and provided in a 40 g scale (10 times what was originally reported) a yield only slightly lower than reported by Nielsen (87% vs. quant.). Scale-up of the last step leading to chloride **1.95** was however associated with a drop in yield (from 79% to 52%) in a 35 g scale (nine times what was originally reported) due to elimination leading to alkene formation.

Furthermore, the *o*-nitroveratryl linker **1.83**, cf. figure 2.5, was prepared according to the original procedure by Holmes [30], as this linker was needed for the *O*-functionalization approach, cf. scheme 2.3.

## 2.4 *N*-functionalization of Doxorubicin

After the successful synthesis of linker intermediates **2.20**, **1.94** and **1.95**, the development of a method for *N*-functionalization of DOX was initiated.

[1] These experiments were done in collaboration with former Senior Scientist Sebastian T. Le Quement during my Master's project.

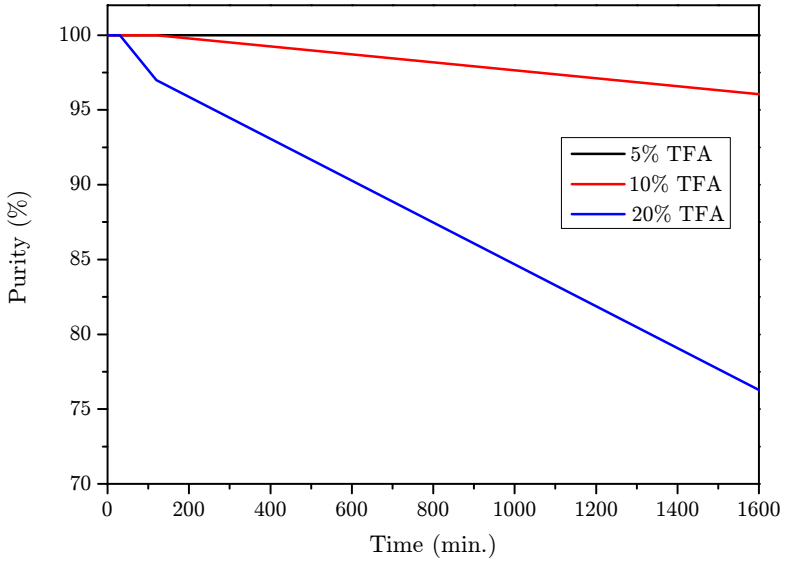


**(a)** Stability of DOX in TFA (aq).

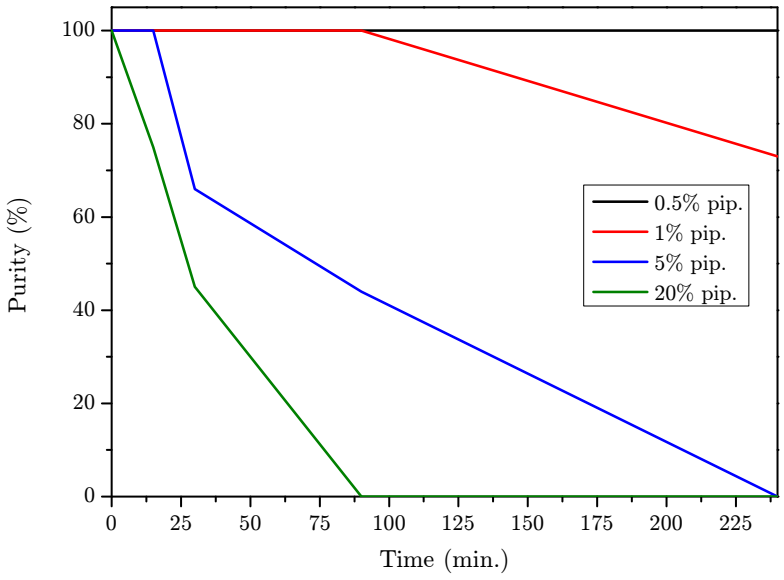


**(b)** Stability of DOX in piperidine.

**Figure 2.4:** Investigation of the acid and base stability of DOX in (a) TFA (aq) and (b) piperidine in DMF. Determined by LCMS.

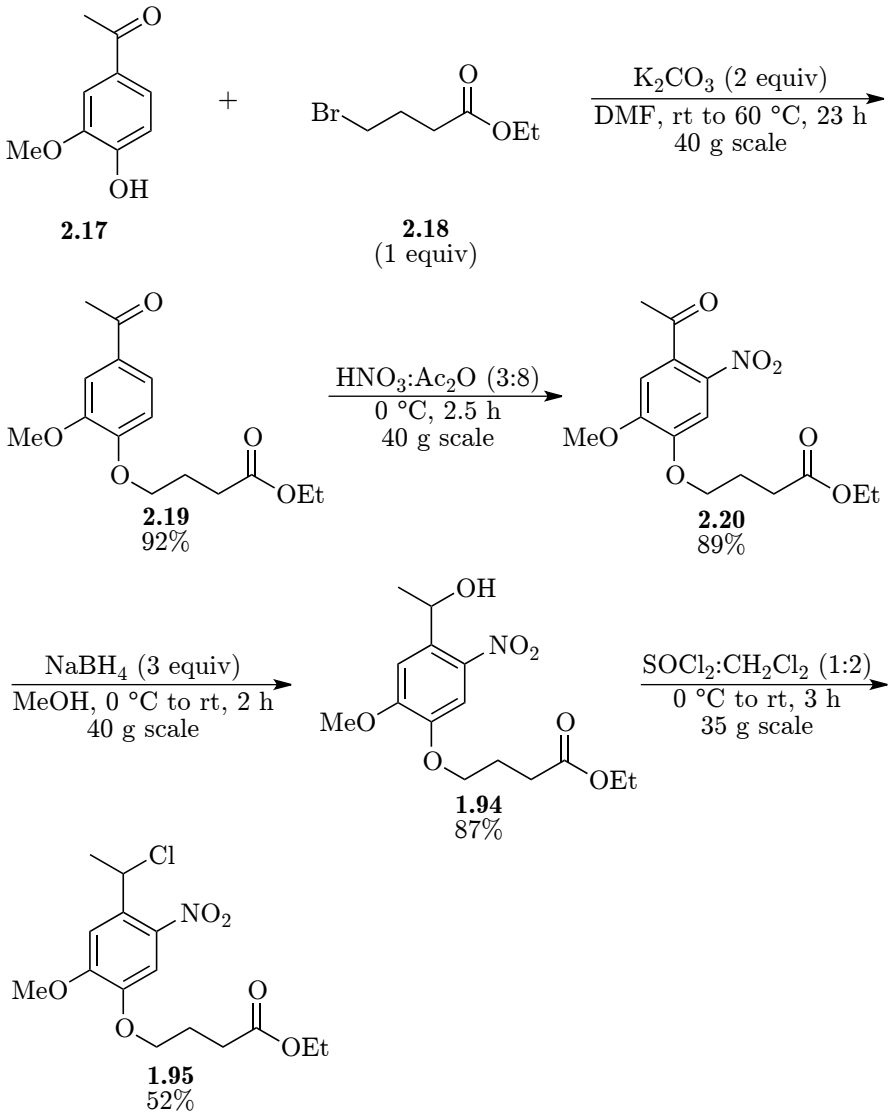


**Scheme 2.4:** Large scale synthesis of photolabile linker intermediate **1.95**.

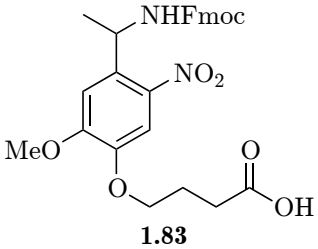


**Figure 2.5:** Photolabile *o*-nitroveratryl linker **1.83**.

### 2.4.1 Solid-phase approach for the synthesis of *N*-functionalized DOX derivatives

To investigate[2] the use of the primary amine in DOX as the functional handle for derivatization and attachment to the solid support the linker intermediates **2.20** and **1.94** were, after ester hydrolysis, coupled to the solid support already functionalized with a HMBA linker to ease analysis, cf. scheme 2.5. Following attachment of H-Ala-O*t*Bu · HCl either via reductive amination or

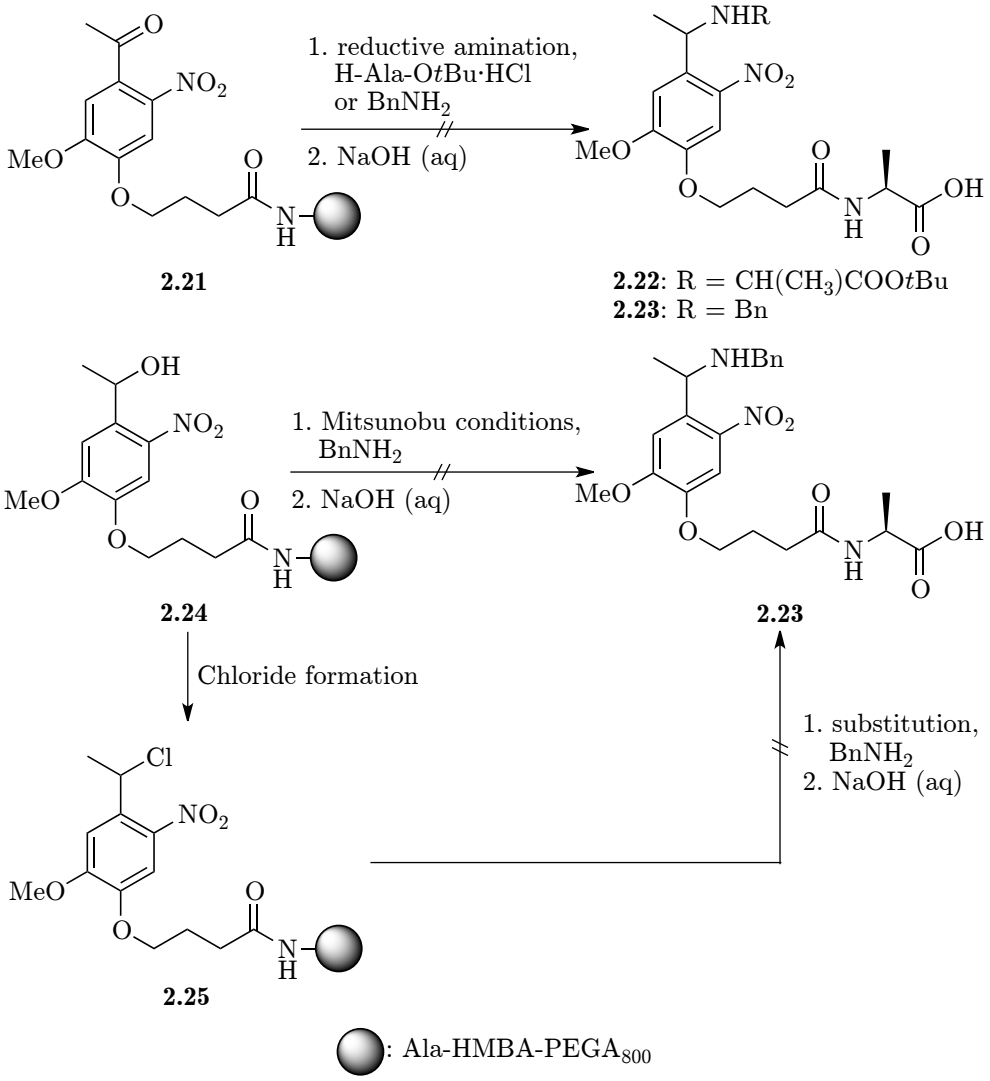


**Scheme 2.5:** Attempts at installation of H-Ala-O*t*Bu or $BnNH_2$ on constructs **2.21** and **2.24**.

Mitsunobu/substitution conditions would then, after *t*Bu deprotection pro-

[2]The experiments described in this section were performed during my Master's project.

vide the carboxylic acid handle needed for attachment of DOX via its primary amine. Thus construct **2.21** was subjected to reductive amination conditions, cf. scheme 2.5. However, even though a wide variety of reductive amination conditions were tested, both with H-Ala-O*t*Bu · HCl and with the more nucleophilic model substrate $BnNH_2$, the photolinker substrates **2.22** and **2.23** were not observed after HMBA linker cleavage in any of the performed experiments.

Construct **2.24** was likewise subjected to either Mitsunobu conditions with $BnNH_2$ or several different methods for chloride formation followed by substitution with $BnNH_2$, however, this did not lead to the wanted substrate **2.23** after HMBA linker cleavage either, cf. scheme 2.5.

As no successful method for the attachment of neither H-Ala-O*t*Bu · HCl nor $BnNH_2$ had been found the pure solid-phase approach was abandoned.

### 2.4.2 Combined solution and solid-phase approach for the synthesis of *N*-functionalized DOX derivatives

Instead it was rationalized that an amino acid could be attached to one of the photolabile linker intermediates in solution, before being coupled to the solid support, thus leading to photolabile linker building blocks of the general structure **2.26**, cf. figure 2.6. This would thus eliminate the need to perform

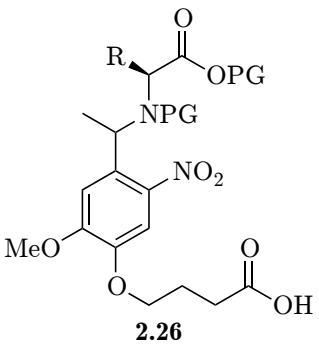


**2.26**

**Figure 2.6:** General structure of proposed amino acid photolabile linker building block.

the difficult coupling of the first amino acid on solid-phase.

Initially, a reductive amination approach utilizing photolabile linker intermediate **2.20** was attempted, cf. table 2.1. The use of $NaCNBH_3$ and $Na(OAc)_3BH$ in different solvents (MeOH, THF and $CH_2Cl_2$) did not lead to any formation of the product or the corresponding imine (table 2.1, entry 1–3). The addition of a Lewis acid to aid imine formation (this time without adding any reducing agent) did not improve the outcome and these conditions did not lead to any imine formation either. As no successful conditions leading to the

**Table 2.1:** Attempts at synthesis of photolabile Gly linker intermediate **2.27** via reductive amination.

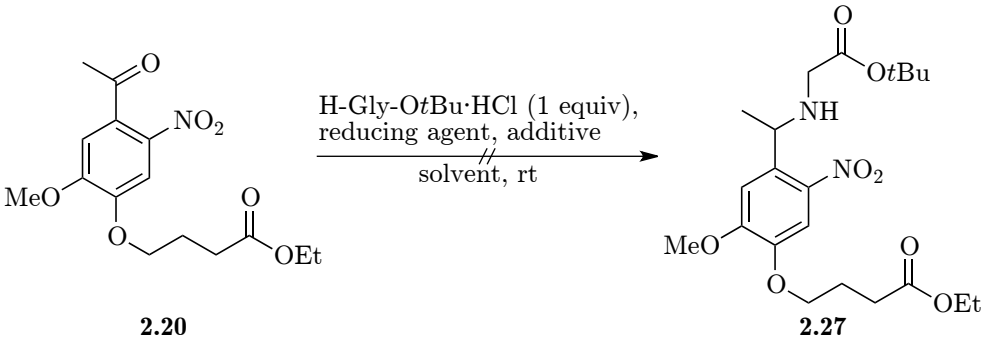


**2.20** **2.27**

| Entry | Reducing agent (equiv) | Additive (equiv) | Solvent |
|---|---|---|---|
| 1 | $NaCNBH_3$ (1) | AcOH (1) | MeOH |
| 2[a] | $Na(OAc)_3BH$ (1.5) | $Et_3N$ (1) | THF |
| 3[a] | $Na(OAc)_3BH$ (1.5) | $Et_3N$ (1) | $CH_2Cl_2$ |
| 4 | - | $TiCl_4$ (0.5), $Et_3N$ (1) | $CH_2Cl_2$ |
| 5 | - | $TiCl_4$ (0.5), $Et_3N$ (3) | $CH_2Cl_2$ |

[a] 4 Å molecular sieves added.

desired photolabile Gly linker intermediate **2.27** (or even the corresponding imine) had been found the reductive amination approach was abandoned.

A new strategy was devised relying on the chloride photolabile linker intermediate **1.95**, cf. scheme 2.4. It was thus envisioned that subjecting chloride **1.95** to substitution conditions with H-Gly-O*t*Bu would lead to the desired photolabile Gly linker intermediate **2.27**. Initial attempts suffered from low yields and severe side product formation (mainly the alcohol **1.94**). Thorough optimization[3] varying base ($K_2CO_3$, DBU, $Et_3N$, DIPEA, DMAP), additives ($Ag_2O$, KI) and reaction mixture concentration identified the conditions shown in scheme 2.6 as the most optimal. It was furthermore discovered that dry conditions and extensive degassing were essential for obtaining a high yield and that running the reaction relatively concentrated ($\sim 0.5$M) was beneficial. Thus the subjection of chloride **1.95** to H-Gly-O*t*Bu · HCl, $Et_3N$ and KI led to the formation of the wanted photolabile Gly linker intermediate **2.27** in a yield of 74%, cf. scheme 2.6.

Fmoc protection of **2.27** followed. The secondary amine of photolabile Gly linker intermediate **2.27** proved to be quite unreactive (likely due to steric factors) and extended reaction time under standard Fmoc protection conditions furnished photolabile Fmoc-Gly intermediate **2.28** in a yield of 67%, cf. scheme 2.7. To avoid deprotection of the base-labile Fmoc group, **2.28** was then subjected to enzymatic ester hydrolysis, instead of more conventional

[3]Some of these experiments were performed during my Master's project.

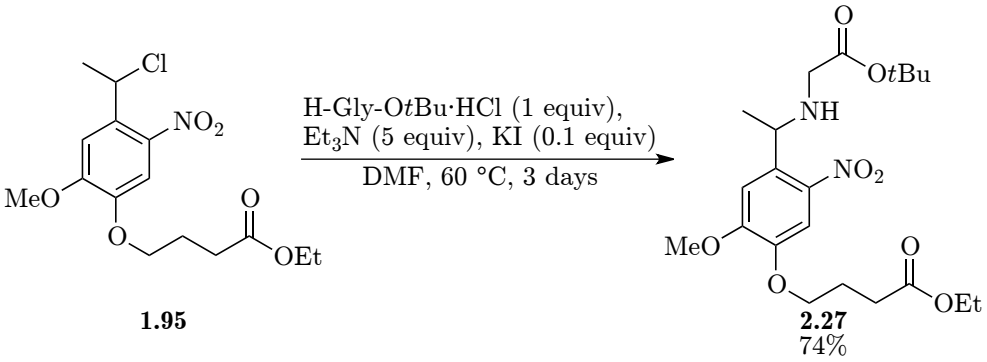


**Scheme 2.6:** Substitution reaction between chloride **1.95** and H-Gly-O*t*Bu · HCl.

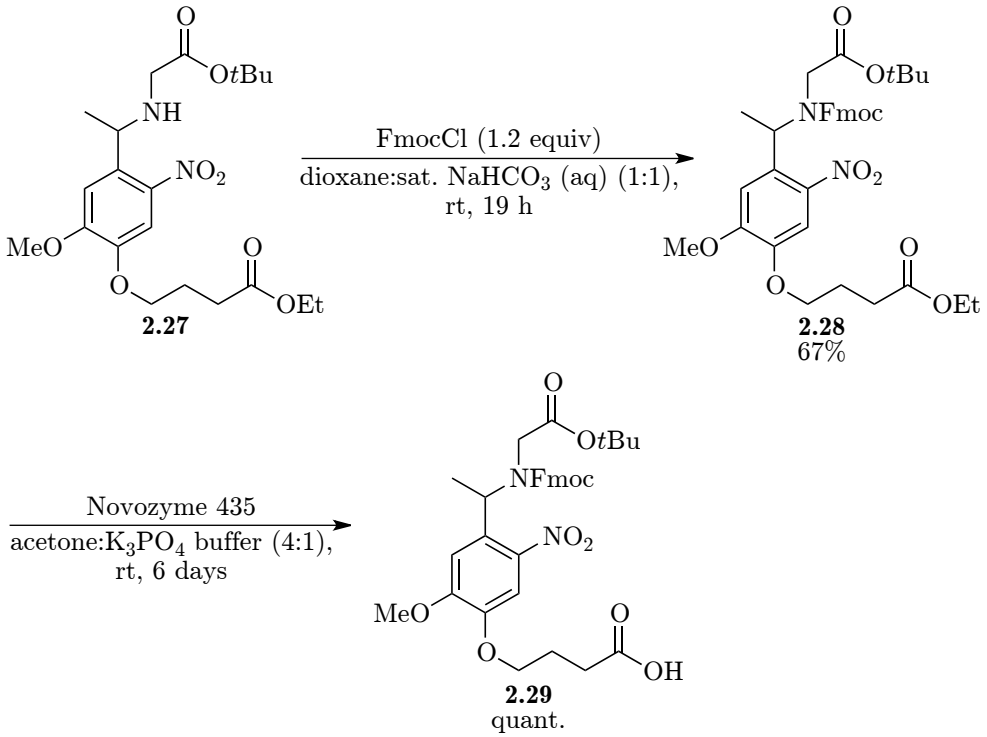


**Scheme 2.7:** Fmoc-protection of **2.27** followed by enzymatic ester hydrolysis leading to photolabile Gly linker **2.29**.

methods (e.g. LiOH or NaOH), affording the photolabile Gly linker **2.29** in a quantitative yield (up to a 5 g scale), cf. scheme 2.7.

With linker **2.29** in hand the investigation into using it as a linker for the synthesis of DOX derivatives was commenced. HATU-mediated coupling of **2.29** to an Ala-HMBA functionalized PEGA resin provided the *t*Bu-protected Gly-functionalized photolabile support **2.30**, cf. scheme 2.8. The *t*Bu-protection group was then removed with TFA:$CH_2Cl_2$ (1:1) to expose a carboxylic acid handle, which was then reacted with DOX under standard HATU-mediated coupling conditions to afford the Fmoc-protected photolabile construct **2.31**, cf. scheme 2.8.

In order to establish the conditions that accomplished removal of the Fmoc-protection group without affecting the DOX moiety the Fmoc-Gly-DOX construct **2.31** was subjected to piperidine in DMF[4] at different concentrations, cf. figure 2.7. These results indicated that 0.5% piperidine in DMF would be the optimal conditions to remove the Fmoc group without causing unwanted decomposition. Construct **2.31** was thus exposed to these conditions. Gratifyingly, subsequent photolytic release led to the release of Gly-DOX **2.32** in a high crude purity of 87%.

Expanding on the successful initial synthesis of Gly-DOX the next step was the synthesis of other photolabile amino acid linkers. Thus chloride **1.95** was subjected to the earlier developed conditions together with either H-Leu-O*t*Bu · HCl, H-Ala-O*t*Bu · HCl or H-Phe-O*t*Bu · HCl, cf. table 2.2. How-

**Table 2.2:** Synthesis of photolabile amino acid linker intermediates **2.33a–c**.

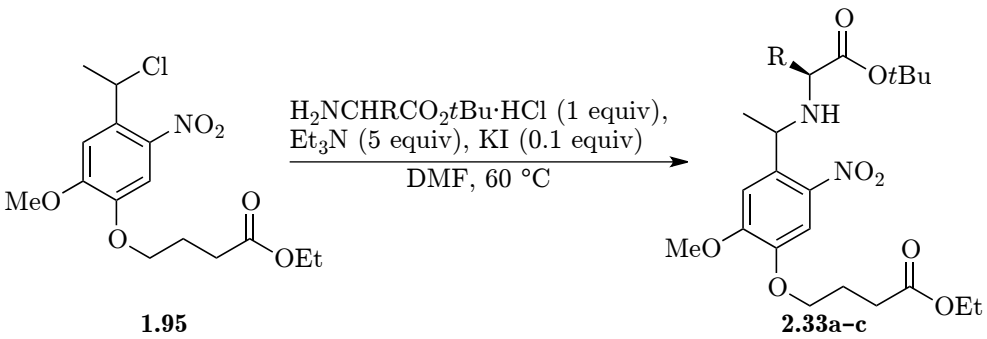


**1.95** **2.33a–c**

| Entry | R | Reaction time (days) | Product, yield (%)[a] |
|---|---|---|---|
| 1 | $CH_2CH(CH_3)_2$ | 7 | **2.33a**, 42 |
| 2 | Me | 6 | **2.33b**, 50 |
| 3 | $CH_2Ph$ | 6 | **2.33c**, 34 |

[a] Isolated yield after flash column chromatography

ever, these amino acids proved to be less reactive than H-Gly-O*t*Bu · HCl and

[4]These experiments were performed by Senior Research Scientist Katrine Qvortrup.

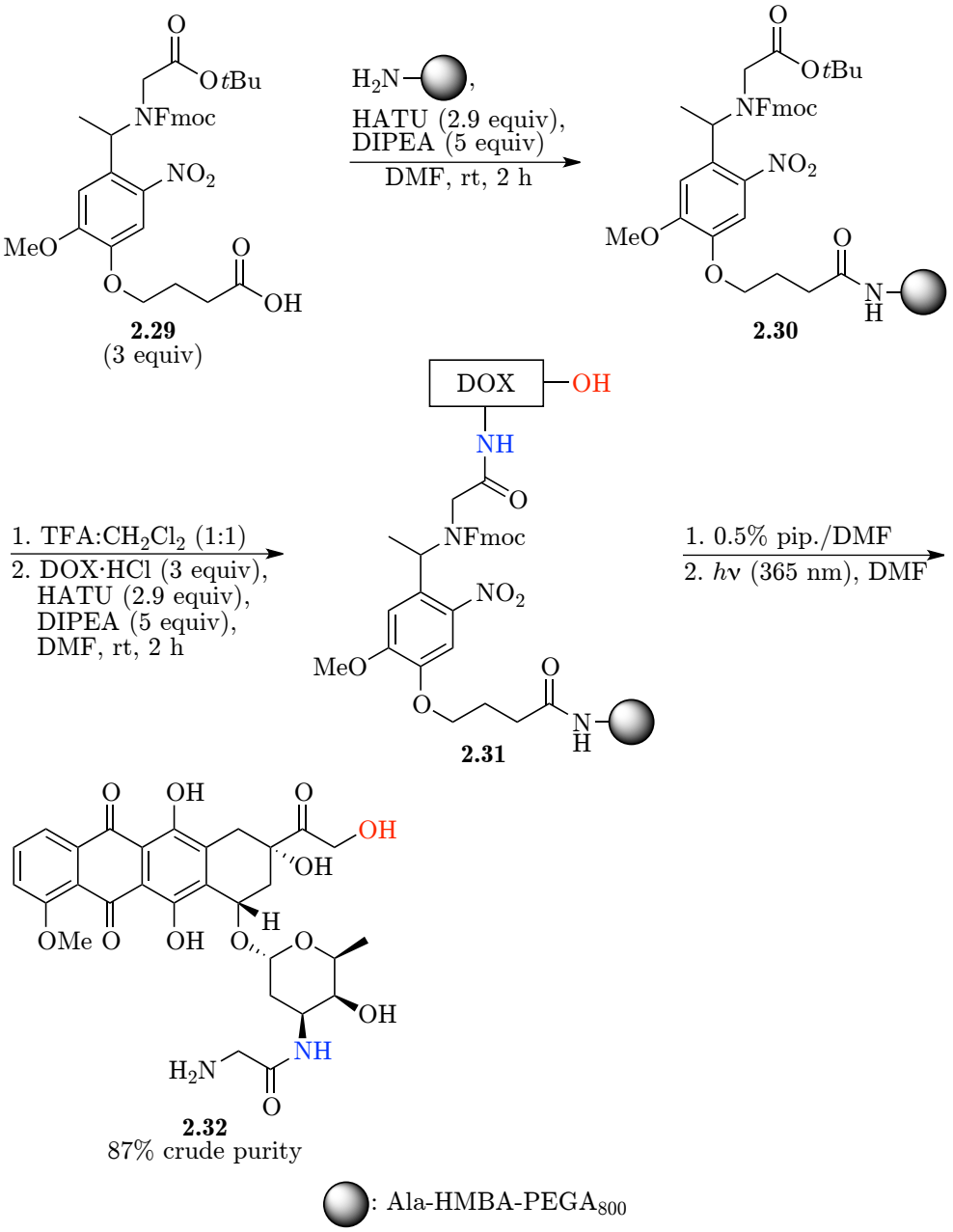


**Scheme 2.8:** Attachment of photolabile Gly linker **2.29** to the solid support followed by coupling of DOX and photolytic release of Gly-DOX **2.32**.

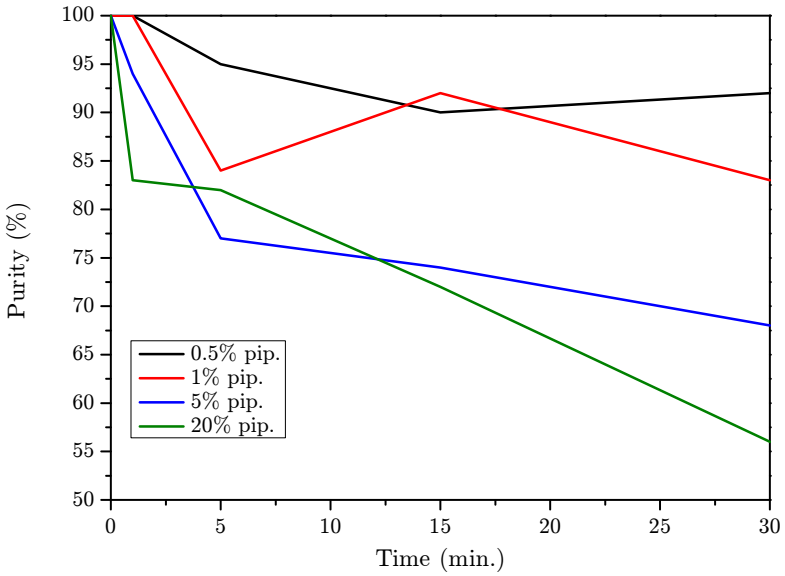


**(a)** Stability of Fmoc-Gly-DOX construct **2.31**.

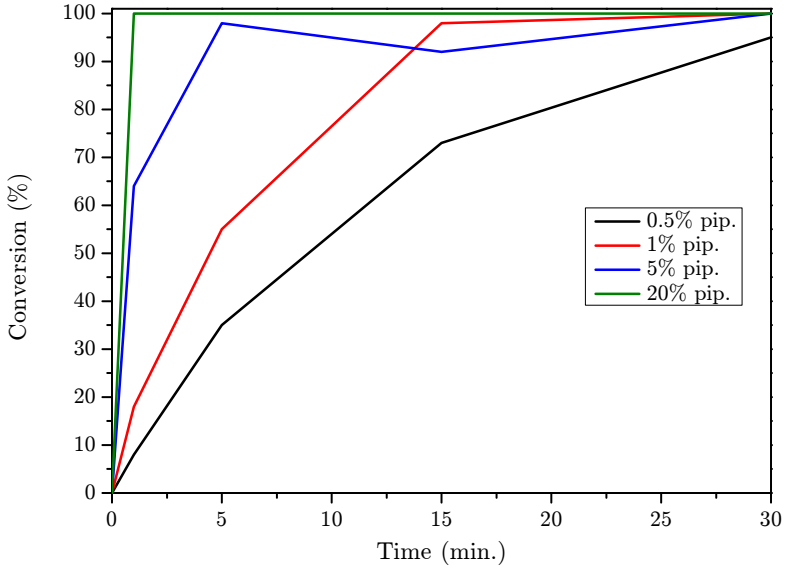


**(b)** Deprotection of Fmoc-Gly-DOX construct **2.31**.

**Figure 2.7:** Investigation of (a) the stability of and (b) the deprotection rate of Fmoc-Gly-DOX photolabile construct **2.31** in piperidine in DMF. Determined by LCMS.

furthermore the products **2.33a–c** were very difficult to purify leading to the desired photolabile amino acid linker intermediates in yields of 34–50%, cf. table 2.2.

With photolabile amino acid linker intermediates **2.33a–c** in hand the next step was Fmoc protection of the secondary amine moieties, cf. table 2.3. However, in none of the performed experiments were the desired photolabile

**Table 2.3:** Attempts at Fmoc protection of photolabile amino acid linker intermediates **2.33a–c**.

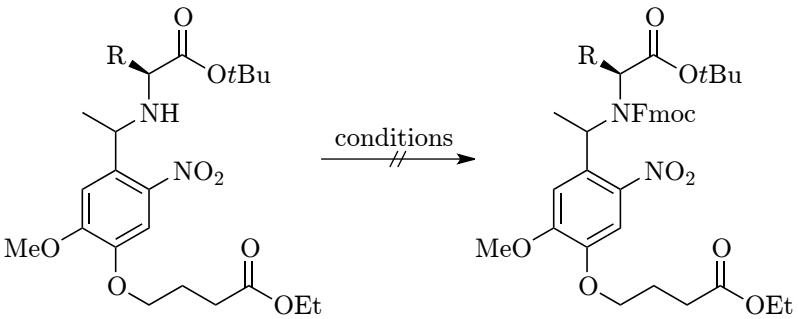


**2.33a–c** **2.34a–c**

| Entry | R | Fmoc reagent | base | Solvent |
|---|---|---|---|---|
| 1 | $CH_2CH(CH_3)_2$ | FmocCl | - | dioxane:10% $NaHCO_3$ (aq) (1:1) |
| 2 | $CH_2CH(CH_3)_2$ | FmocOSu | $Et_3N$ | MeCN:$H_2O$ (1:1) |
| 3 | Me | FmocCl | - | dioxane:10% $NaHCO_3$ (aq) (1:1) |
| 4 | Me | FmocOSu | $Et_3N$ | MeCN:$H_2O$ (1:1) |
| 5 | $CH_2Ph$ | FmocCl | - | dioxane:10% $NaHCO_3$ (aq) (1:1) |
| 6 | $CH_2Ph$ | FmocOSu | $Et_3N$ | MeCN:$H_2O$ (1:1) |

Fmoc-amino acid intermediates **2.34a–c** observed.

With the very low reactivity of the secondary amines **2.33a–c** in mind it was theorized that these photolabile amino acid linker intermediates could, after ester hydrolysis, be coupled to the solid support without any polymerization occurring if a less reactive coupling reagent was used. To test the hypothesis intermediates **2.33a–c** were subjected to ester hydrolysis, cf. table 2.4. As the Fmoc group present on the original photolabile Gly linker was not present this time, a more conventional ester hydrolysis method was used. Thus linker intermediates **2.33a–c** were exposed to LiOH affording photolabile amino acid linkers **2.35a–c** in excellent yields (85% to quant.) with the non-quantitative yield in the hydrolysis of **2.33b** being due to slight hydrolysis of the *t*Bu-ester, cf. table 2.4.

The photolabile amino acid linkers **2.35a–c** were now attached to the solid support, cf. scheme 2.9. The Gly-DOX linker was attached using a HATU mediated protocol, cf. scheme 2.8, but the linkers **2.35a–c** were coupled with the less reactive coupling reagent TBTU instead to avoid polymerization due to the free, but very unreactive, secondary amine. Gratifyingly, the linkers

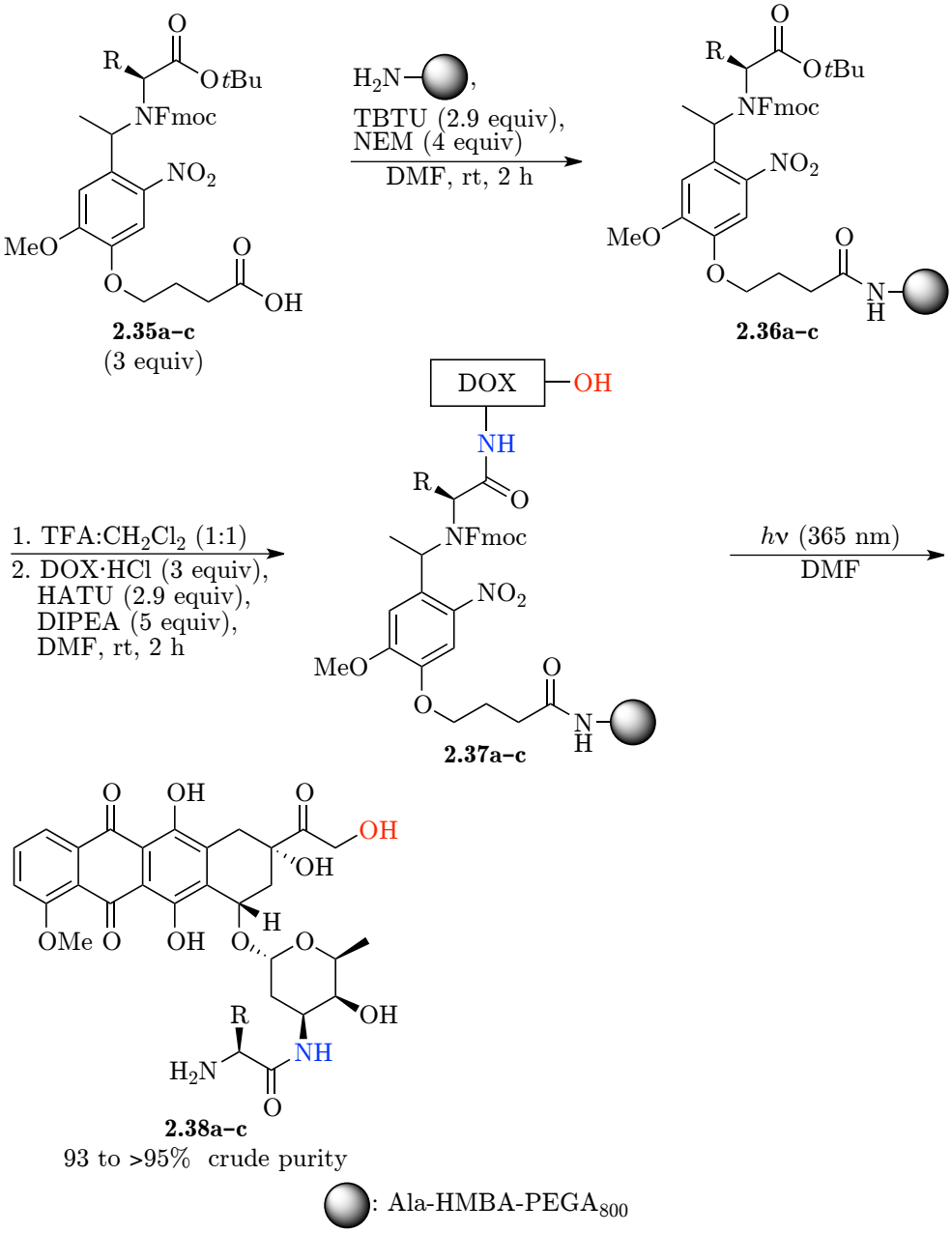


**Scheme 2.9:** Attachment of photolabile amino acid linkers **2.35a–c** to the solid support followed by coupling of DOX and photolytic release of Leu-DOX **2.38a**, Ala-DOX **2.38b** and Phe-DOX **2.38c**.

**Table 2.4:** Ester hydrolysis of **2.33a–c** leading to photolabile amino acid linkers **2.35a–c**.

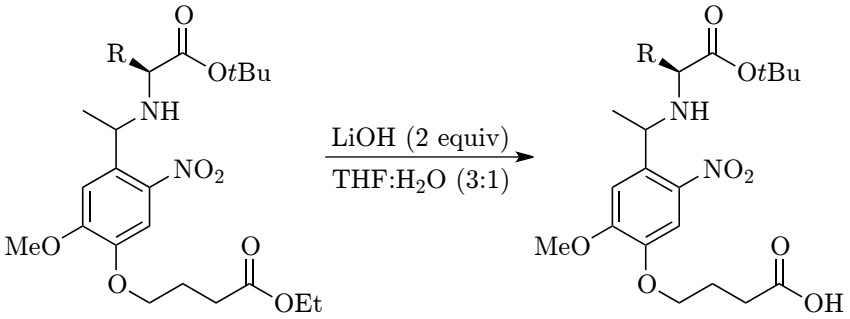


**2.33a–c** **2.35a–c**

| Entry | R | Reaction time (h) | Product, yield (%)[a] |
|---|---|---|---|
| 1 | $CH_2CH(CH_3)_2$ | 25 | **2.35a**, quant. |
| 2 | Me | 26 | **2.35b**, 85 |
| 3 | $CH_2Ph$ | 26 | **2.35c**, quant. |

[a] Isolated yield after aqueous work-up.

were coupled to the solid support without any indication of polymerization taking place leading to constructs **2.36a–c**, cf. scheme 2.9. Deprotection of the *t*Bu-protection group, attachment of DOX and photolytic release then furnished, in excellent crude purities, Leu-DOX **2.38a** (>95%), Ala-DOX **2.38b** (94%) and Phe-DOX **2.38c** (93%).

After the successful synthesis of four amino acid DOX derivatives the next goal was the construction of more elaborate DOX derivatives. In the attempt to attach small peptides to DOX, the photolabile construct **2.30** was subjected to Fmoc deprotection and subsequent coupling of Fmoc-Gly-OH using either HATU or PyBrOP as coupling reagent, cf. table 2.5.

However, in both cases **2.39** was isolated after HMBA linker cleavage indicating that the coupling procedure had not been successful, likely due to the very low reactivity of the secondary amine as seen earlier. These results turned the focus to finding an even more reactive coupling reagent. BTC had been reported by Gilon to be very effective for the use in difficult peptide couplings [43]. The use of these conditions led to successful coupling of Fmoc-Gly-OH and a subsequent Fmoc deprotection and HATU-mediated coupling of Fmoc-Ala-OH provided the photolabile peptide construct **2.41**, cf. scheme 2.10. Finally, *t*Bu deprotection, HATU-mediated coupling of DOX and photolysis provided Ala-Gly-Gly-DOX tripeptide **2.43** in a remarkable crude purity of >95%.

In an attempt to expand on this satisfying result, amino acid coupling was likewise attempted on the photolabile amino acid constructs **2.36a–c**, cf. table 2.6. As seen with the photolabile Gly construct **2.30**, HATU and

**Table 2.5:** Attempts at amino acid coupling onto photolabile Gly construct **2.30**.

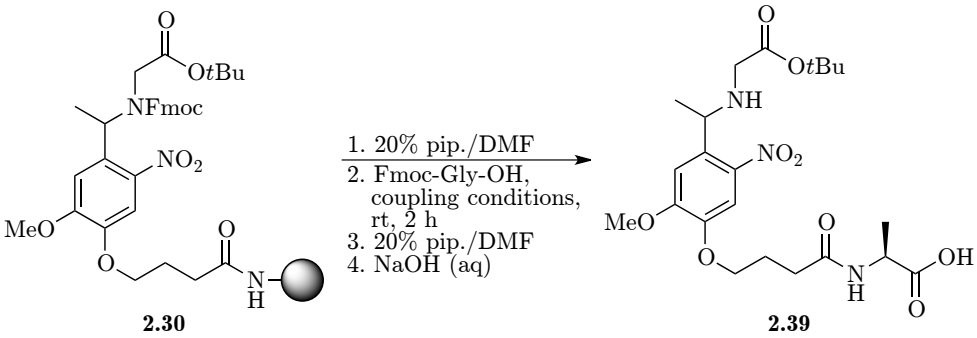


**2.30** **2.39**

: Ala-HMBA-PEGA$_{800}$

| Entry | Equiv of Fmoc-Gly-OH | Coupling reagent (equiv) | Base (equiv) |
|---|---|---|---|
| 1 | 3 | HATU (2.9) | DIPEA (5) |
| 2 | 3 | PyBrOP (4) | DIPEA (6) |

**Table 2.6:** Attempts at amino acid coupling onto the secondary amines **2.36a–c**.


**2.36a–c** **2.44a–c**

: Ala-HMBA-PEGA$_{800}$

| Entry | R | Coupling reagent | Base | Temp. (°C) |
|---|---|---|---|---|
| 1 | $CH_2CH(CH_3)_2$ | HATU | DIPEA | rt |
| 2[a] | $CH_2CH(CH_3)_2$ | BTC | 2,4,6-collidine | rt |
| 3 | $CH_2CH(CH_3)_2$ | BTC | 2,4,6-collidine | 50 |
| 4 | Me | HATU | DIPEA | rt |
| 5 | Me | BTC | 2,4,6-collidine | 50 |
| 6 | $CH_2Ph$ | PyBroP | DIPEA | rt |

[a] Beads preswelled in THF:DIPEA (1:1).

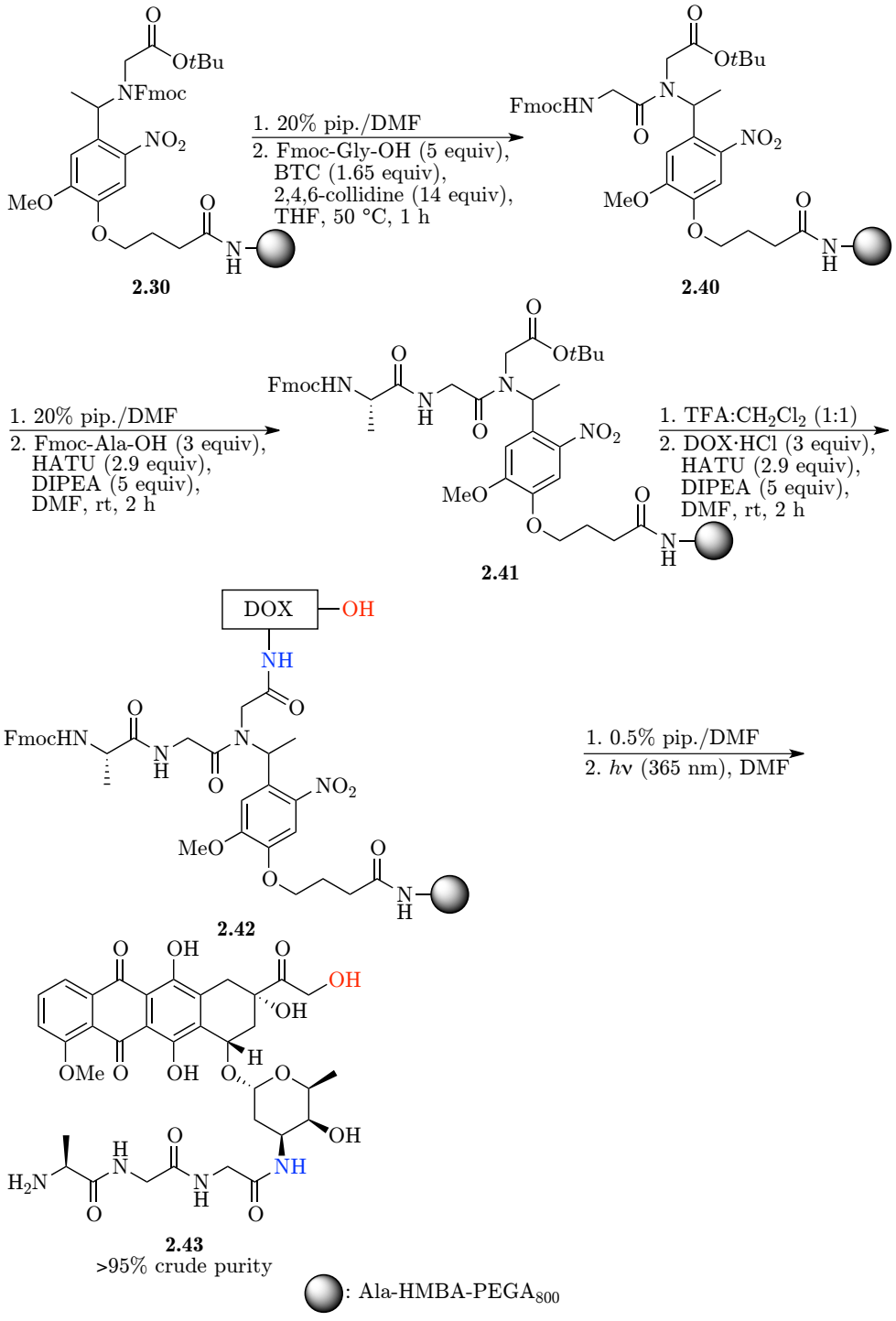


**Scheme 2.10:** Synthesis of *N*-functionalized Ala-Gly-Gly-DOX tripeptide **2.43**.

PyBrOP were unable to effect the coupling of Fmoc-Gly-OH, only leading to **2.44a–c** (entries 1, 4 and 6). However, with the photolabile constructs **2.36a–c** not even the use of BTC as a coupling reagent furnished the desired products and again only **2.44a** and **2.44b** were observed, (entries 3 and 5). Another procedure for amino acid coupling using BTC [142], relying on pretreatment of the resin with DIPEA, was also investigated but did not accomplish the coupling either (entry 2). The secondary amine in the constructs **2.36a–c** thus proved to be very unreactive, likely due to steric factors, and in fact not even acetylation of this moiety could be accomplished using common acetylating reagents (e.g. AcCl, $Ac_2O$).

## 2.5 *O*- and *N*-functionalization of Doxorubicin

To explore different sites of structural modification with regard to the synthesis of DOX derivatives focus was turned towards the primary alcohol of DOX as this would be an obvious site for modification, cf. figure 2.11. It was further-

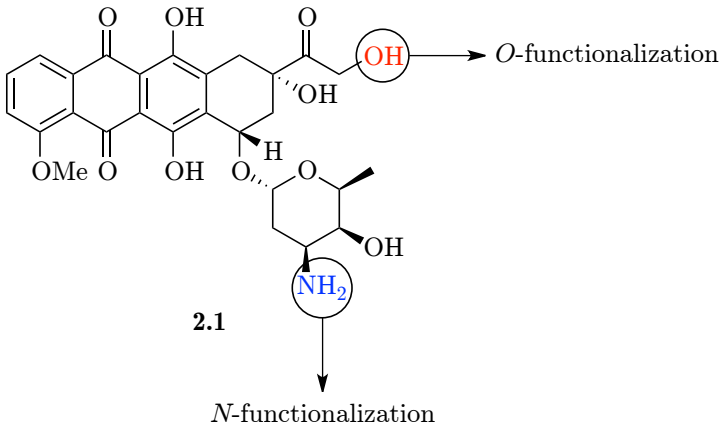


**Scheme 2.11:** Sites for structural modification of DOX.

more envisioned that this site, after modification, could serve as a handle for attachment to the solid support thus also allowing for *N*-functionalization via standard SPPS methods, which had proved to be difficult with the methods developed in §2.4.

To fuel these investigations the DOX ester building block **2.48**, known from the literature [143], was deemed essential and its synthesis thus became a starting point, cf. scheme 2.12. The original procedure was reported to provide **2.48** in an overall yield of 70%. This procedure however performed poorly in our laboratory and gave rise to complex reaction mixtures with only small amounts of product formed.[5] With the high price of DOX in mind a new

[5]These initial experiments were performed by former Senior Scientist Sebastian T. Le Quement.

and improved route to DOX ester building block **2.48** was thus developed, cf. scheme 2.12. DOX was Fmoc protected with FmocCl providing Fmoc-DOX

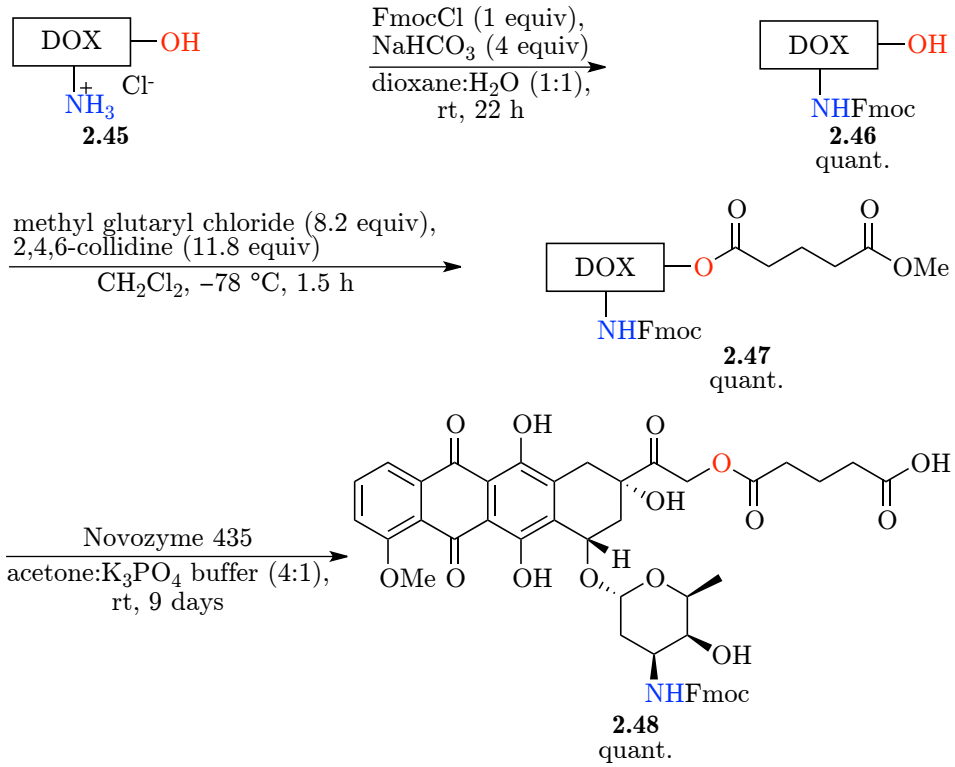


**Scheme 2.12:** Synthesis of DOX ester building block **2.48**.

**2.46** in quantitative yield. Then Fmoc-DOX **2.46** was reacted with methyl glutaryl chloride with 2,4,6-collidine as base furnishing the DOX diester **2.47** again in a quantitative yield, cf. scheme 2.12. Both steps proceeded without the need for any chromatographic purification. Finally, enzymatic ester hydrolysis with Novozyme 435 selectively hydrolyzed the methyl ester, without affecting the internal ester, affording the DOX ester building block **2.48** in a quantitative yield (in up to a 1 g-scale).

With DOX ester building block **2.48** in hand an initial experiment were performed where **2.48** was coupled to the solid support in a HATU-mediated coupling, this time functionalized with the *o*-nitroveratryl linker **1.83** [30], cf. scheme 2.13. Rewardingly, the resulting DOX construct **2.50** was readily Fmoc-deprotected (using the previously established conditions, cf. §2.4.2) and released by photolysis providing DOX amide derivative **2.51** in a crude purity of 64%.

The release of **2.51** confirmed the possibility of anchoring DOX to the solid support via its primary alcohol and then functionalizing the primary amine (*N*-functionalization) via standard SPPS. Thus Fmoc deprotection of

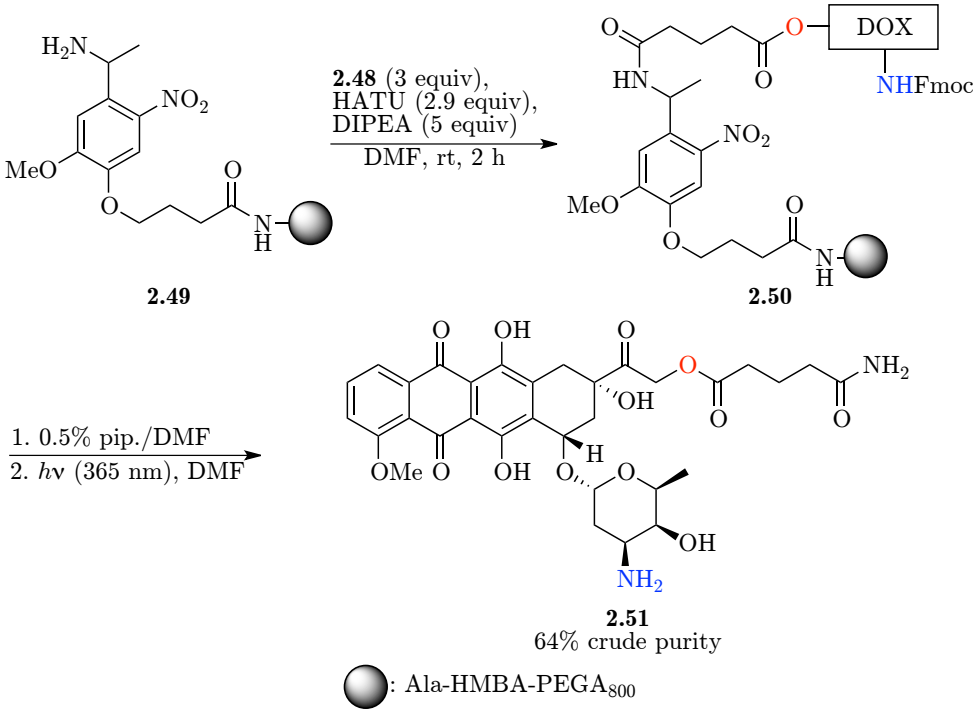


**Scheme 2.13:** Synthesis of *O*-functionalized DOX amide derivative **2.51**.

the primary amine on DOX construct **2.50** and subsequent HATU-mediated coupling of Fmoc-Ala-OH was attempted. This however led to unclean coupling and the generation of an unidentified side product. It was speculated that the use of a less reactive coupling reagent such as TBTU would suppress side product formation. Gratifyingly, Fmoc deprotection of construct **2.50** followed by a TBTU-mediated coupling of Fmoc-Ala-OH provided a clean coupling and led to the release of Ala-Dox amide **2.52** in a good crude purity of 70%, cf. scheme 2.14.

After the successful release of **2.52** a test of the developed methodology in a more complex setting was attempted. Thus a tripeptide (Gly-Lys-Ala) was synthesized on the *o*-nitroveratryl linker using HATU-mediated couplings followed by attachment of DOX ester building block **2.48** leading to the photolabile DOX construct **2.54** cf. scheme 2.15. Fmoc deprotection of the primary amine on DOX and subsequent TBTU-mediated coupling of Fmoc-Ala-OH followed by further HATU-mediated SPPS afforded, after photolysis, the DOX dipeptide derivative **2.55** in a crude purity of 48%.

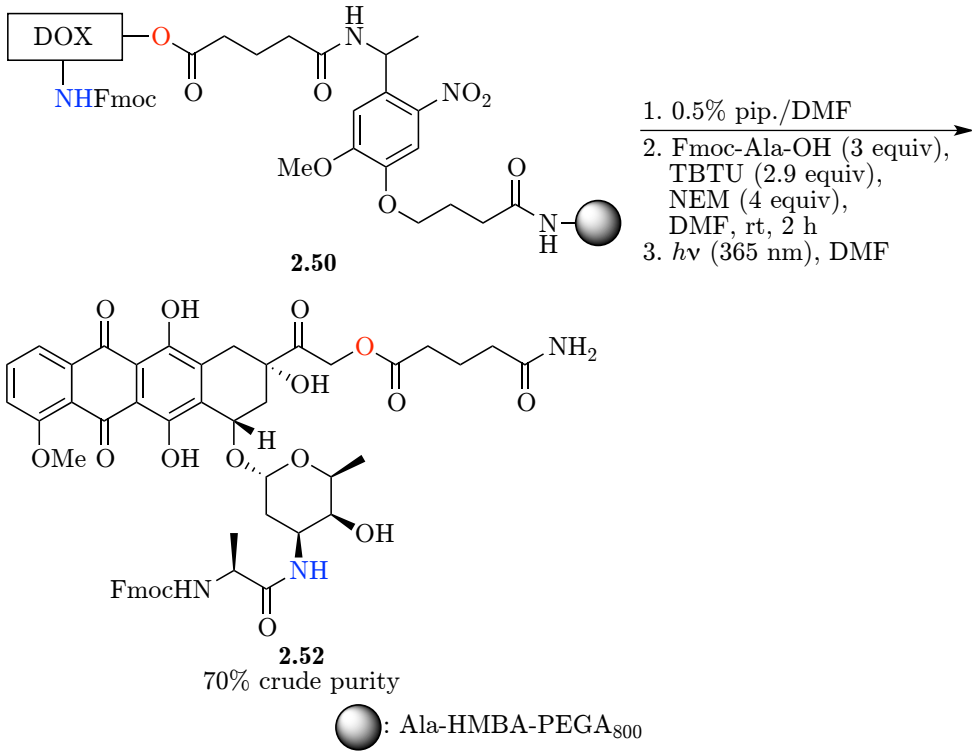


**Scheme 2.14:** *N*-functionalization of construct **2.50** and subsequent photolytic release.

## 2.6 Conclusion

In the present project the synthesis of DOX derivatives on photolabile solid support, compatible with bead-based screening, has been investigated. Two different strategies for the synthesis of DOX derivatives have been explored where both the primary amine and the primary alcohol of DOX were utilized as sites for structural modification.

Four amino acid photolabile linkers have been synthesized allowing for the photolytic release of DOX amino acid derivatives (*N*-functionalization) in excellent crude purities (87 to >95%). Furthermore, the photolabile Gly linker **2.29** has been used to construct Ala-Gly-Gly-DOX tripeptide **2.43** in a remarkable crude purity of >95%. This methodology was however not compatible with the other amino acid photolabile linkers likely due to steric factors.

Another methodology allowing for both *N*- and *O*-functionalization was also developed. The DOX ester building block **2.48** was synthesized in three steps, all of which proceeded with a quantitative yield. This allowed for the tethering of DOX to the solid support through its primary alcohol and subsequent *N*-functionalization via standard SPPS methods. It was furthermore possible to construct peptides on the solid support before the attachment

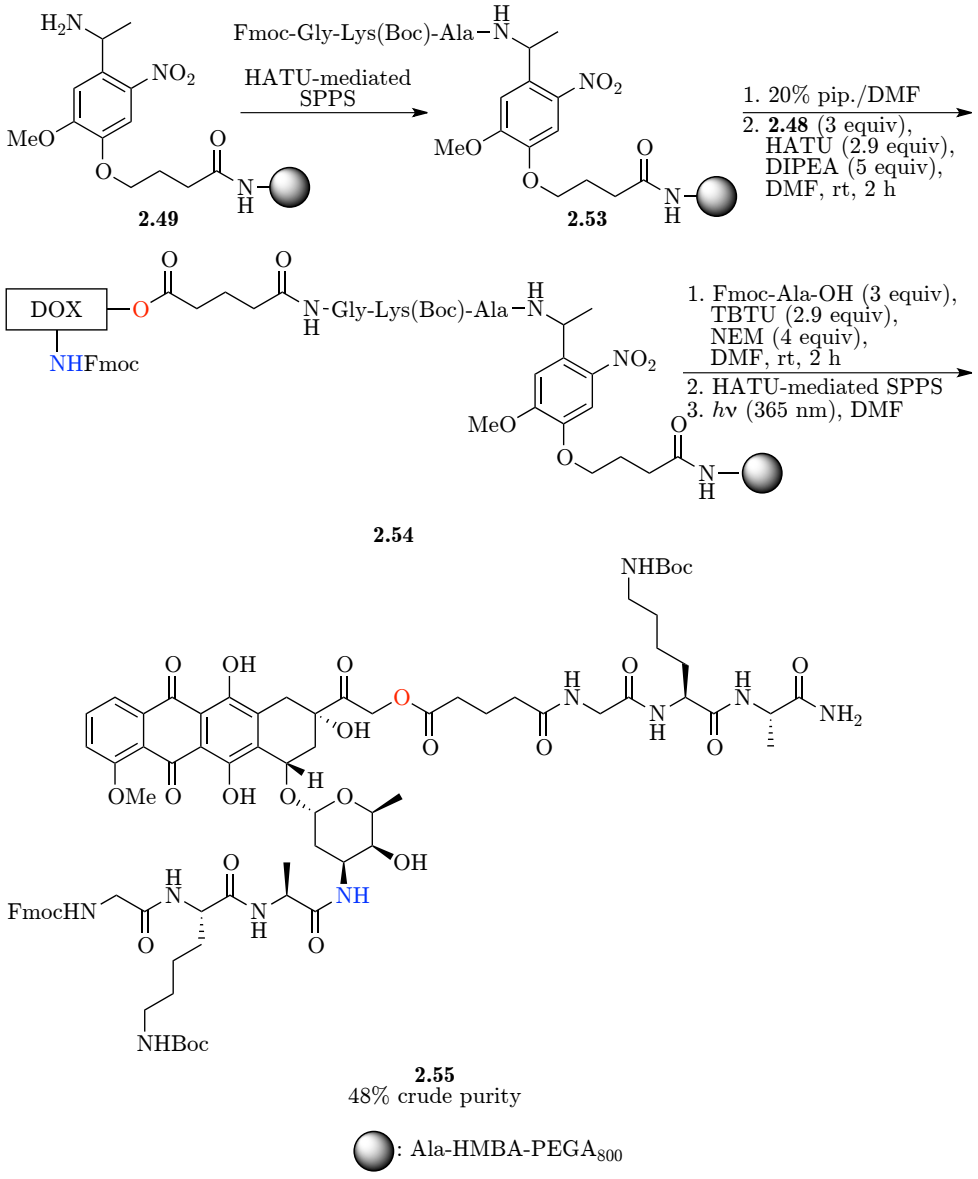


**Scheme 2.15:** Synthesis of DOX dipeptide derivative **2.55**.

of DOX ester building block **2.48** thus allowing for *O*-functionalized DOX peptide derivatives. This culminated in the synthesis of the *O*- and *N*-functionalized DOX dipeptide **2.55** in a crude purity of 48% thus leaving room for further optimization.

## 2.7 Experimental

### 2.7.1 General methods

Reagents were purchased at the highest commercial quality and used without further purification, unless otherwise noted. All reactions were carried out under an argon atmosphere with dry solvent under anhydrous conditions, unless otherwise noted. Dry solvents were obtained by passing commercially available pre-dried, oxygen-free formulations through activated alumina columns. Yields refer to chromatographically and spectroscopically ($^1$H NMR) homogeneous material, unless otherwise stated.

Reactions were monitored by thin-layer chromatography (TLC) carried out on Merck aluminium sheets covered with silica (C60) using UV light as visualizing agent or an aqueous solution of phosphomolybdic acid and cerium sulfate or a basic aqueous solution of potassium permanganate and heat as developing agents. Matrex silica gel (60, particle size 0.035–0.070 mm) was used for flash column chromatography.

Solid-phase synthesis was carried out using plastic-syringe techniques. Flat-bottomed polyethylene syringes were fitted with polypropylene filters and were attached to Teflon® tubing and valves, allowing vacuum to be applied to the syringes.

NMR spectra were recorded on a Bruker Ascend 400 MHz instrument equipped with a Prodigy cryoprobe, a Varian Unity Inova 500 MHz instrument or a Bruker Avance 800 MHz instrument equipped with a TCI cryoprobe.The chemical shifts ($\delta$) are reported in parts per million (ppm) and the coupling constants ($J$) in Hz. For spectra recorded in DMSO-$d_6$, signal positions were measured relative to the signal for DMSO ($\delta$ 2.50 ppm for $^1$H NMR and $\delta$ 39.43 ppm for $^{13}$C NMR). For spectra recorded in $CDCl_3$, signal positions were measured relative to the signal for $CHCl_3$ ($\delta$ 7.26 ppm for $^1$H NMR and $\delta$ 77.0 ppm for $^{13}$C NMR).

Infrared (IR) spectra were recorded on a Bruker Alpha FT-IR spectrometer. Analytical RP-UPLC-MS (ESI) analysis was performed on a Waters AQUITY RP-UPLC system equipped with a diode array detector using an AQUITY UPLC BEH C18 column ($d$ 1.7 mm, 2.1 × 50 mm; column temp: 65 °C; flow: 0.6 mL/min.). Eluents A (0.1% $HCO_2H$ in $H_2O$) and B (0.1% $HCO_2H$ in MeCN) were used in a linear gradient (5% B to 100% B) in a total run time of 2.6 min. The LC system was coupled to a SQD mass spectrometer. Analytical LC-HRMS (ESI) analysis was performed on an Agilent 1100 RP-LC system equipped with a diode array detector using a Phenomenex Luna C18 column ($d$ 3 mm, 2.1 × 50 mm; column temp: 40 °C; flow: 0.4 mL/min.). Eluents A (0.1% $HCO_2H$ in $H_2O$) and B (0.1% $HCO_2H$ in MeCN) were used in a linear gradient (20% B to 100% B) in a total run time of 15 min. The LC system was coupled to a Micromass LCT orthogonal time-of-flight mass spectrometer equipped with a Lock Mass probe operating in positive electrospray mode.

### 2.7.2 Synthesis of photolabile linkers

**Ketone 2.19**. Acetovanillone **2.17** (36.00g, 216.6mmol), ethyl 4-bromobutyrate **2.18** (43.04 g, 220.7 mmol) and $K_2CO_3$ (62.38 g, 451.4 mmol) were dissolved in DMF (200 mL). The reaction mixture was stirred at rt for 20 h. The reaction mixture was then heated to 60 °C for 3 h whereupon water (500 mL) was added. The resulting mixture was extracted with EtOAc (3 × 250 mL) and the combined organic phases were washed with water (7 × 500 mL) and brine (4 × 500 mL), dried over $Na_2SO_4$ and the solvent was removed *in vacuo* to give the title compound as an off-white solid (56.09 g, 92%). $^1$H NMR ($CDCl_3$, 400 MHz) $\delta$ 7.56–7.50 (m, 2H), 6.89 (d, $J$ = 8.3 Hz, 1H), 4.18–4.10 (m, 4H), 3.90 (s, 3H), 2.55 (s, 3H), 2.52 (d, $J$ = 7.2 Hz, 2H), 2.18 (p, $J$ = 6.8 Hz, 2H), 1.25 (t, $J$ = 7.1 Hz, 3H). $^1$H NMR spectroscopic data were consistent with those in the literature [108].

**Nitro ketone 2.20**. Solutions of ketone **2.19** (2 × 20.00 g, 2 × 71.35 mmol) in $Ac_2O$ (2 × 70 mL) were added to solutions of $HNO_3$ (2 × 400 mL) and $Ac_2O$ (2 × 80 mL) at 0 °C in two flasks. The reaction mixtures were stirred at 0 °C for 2h 30 min. and were then poured into ice water (6 L). The solution was filtered and the solid was dissolved in EtOAc (1 L) and washed with sat. $K_2CO_3$ (aq) (1 L), water (2 × 1 L) and brine (1 L), dried over $MgSO_4$ and the solvent was removed *in vacuo* to give the title compound as a yellow solid (41.47 g, 89%). $^1$H NMR ($CDCl_3$, 400 MHz) $\delta$ 7.60 (s, 1H), 6.74 (s, 1H), 4.19–4.12 (m, 4H), 3.95 (s, 3H), 2.54 (t, $J$ = 7.2 Hz, 2H), 2.49 (s, 3H), 2.19 (p, $J$ = 6.7 Hz, 2H), 1.26 (t, $J$ = 7.1 Hz, 3H). $^1$H NMR spectroscopic data were consistent with those in the literature [108].

**Nitro alcohol 1.94**. Nitro ketone **2.20** (2 × 19.50 g, 2 × 59.94 mmol) was dispersed in MeOH (2 × 1.2 L) in two flasks and the solutions were cooled to 0 °C. $NaBH_4$ (2 × 6.850 g, 2 × 181.1 mmol) was added in portions whereupon the solutions were allowed to reach rt. The reaction mixtures were stirred for 2 h and then sat. $NH_4Cl$ (aq) (2 × 600 mL) was added. The solutions were concentrated *in vacuo* to 2 × 600 mL, combined and extracted with EtOAc (4 × 500 mL). The combined organic phases were washed with water (2 × 500 mL) and brine (500 mL), dried over $MgSO_4$ and the solvent was removed *in vacuo* to give the title compound as a yellow solid (33.98 g, 87%). $^1$H NMR ($CDCl_3$, 400 MHz) $\delta$ 7.55 (s, 1H), 7.29 (s, 1H), 5.55 (q, $J$ = 6.3 Hz, 1H), 4.17–4.08 (m, 4H), 3.96 (s, 3H), 2.53 (t, $J$ = 7.2 Hz, 2H), 2.22–2.13 (m, 2H), 1.54 (d, $J$ = 6.3 Hz, 3H), 1.26 (t, $J$ = 7.1 Hz, 3H). $^1$H NMR spectroscopic data were consistent with those in the literature [108].

**Chloride 1.95**. Nitro alcohol **1.94** (33.99 g, 103.8 mmol) was dissolved in $CH_2Cl_2$ (680 mL) and the resulting solution was cooled to 0 °C whereupon $SOCl_2$ (340 mL) was added. The reaction mixture was allowed to reach rt and was then stirred for 3 h. The reaction mixture was concentrated *in vacuo* and then co-evaporated with toluene (6 × 300 mL). The residue was then purified by flash column chromatography on silica gel (EtOAc:heptane (2:3))

to give the title compound as a yellow solid (18.59 g, 52%). $^1$H NMR ($CDCl_3$, 400 MHz) $\delta$ 7.48 (s, 1H), 7.27 (s, 1H), 5.91 (q, $J = 6.6$ Hz, 1H), 4.18–4.06 (m, 4H), 3.97 (s, 3H), 2.52 (t, $J = 7.2$ Hz, 2H), 2.17 (p, $J = 6.7$ Hz, 2H), 1.86 (d, $J = 6.7$ Hz, 3H), 1.24 (t, $J = 7.1$ Hz, 3H). $^1$H NMR spectroscopic data were consistent with those in the literature [108].

**Gly photolabile linker intermediate 2.27**. Chloride **1.95** (5.000 g, 14.46mmol), H-Gly-O*t*-Bu·HCl (2.908g, 17.35mmol) and KI (0.288g, 1.73mmol) were dissolved in DMF (29 mL). $Et_3N$ (10.09 mL, 72.34 mmol) was added and then the reaction mixture was heated to 60 °C. The reaction mixture was stirred at 60 °C for 3 days whereupon water (100 mL) was added. The resulting mixture was extracted with EtOAc ($3 \times 100$ mL) and the combined organic phases were washed with water ($2 \times 200$ mL) and brine (200 mL), dried over $Na_2SO_4$ and the solvent was removed *in vacuo*. The residue was then purified by flash column chromatography on silica gel (EtOAc:heptane:$Et_3N$ (40:59:1)) to give the title compound as a yellow amorphous solid (4.717 g, 74%). $R_f$ = 0.11 (EtOAc:heptane:$Et_3N$ (30:69:1)); $^1$H NMR ($CDCl_3$, 400 MHz) $\delta$ 7.45 (s, 1H), 7.40 (s, 1H), 4.54 (q, $J = 6.4$ Hz, 1H), 4.14 (q, $J = 7.1$ Hz, 2H), 4.09 (t, $J = 6.3$ Hz, 2H), 3.95 (s, 3H), 3.19–3.04 (m, 2H), 2.52 (t, $J = 7.3$ Hz, 2H), 2.21–2.13 (m, 2H), 1.46 (d, $J = 6.4$ Hz, 3H), 1.42 (s, 9H), 1.25 (t, $J = 7.1$ Hz, 3H); $^{13}$C NMR ($CDCl_3$, 101 MHz) $\delta$ 173.0, 170.9, 154.1, 147.1, 141.7, 134.2, 109.7, 109.1, 82.0, 68.4, 60.7, 56.7, 52.7, 49.5, 30.7, 28.2, 24.4, 23.7, 14.3; IR (neat) cm$^{-1}$: 2977, 2935, 1729, 1578, 1515, 1368, 1335, 1269, 1212, 1150, 1056, 1031, 846; HRMS (ESI) calcd for $C_{21}H_{33}N_2O_8^+$ $[M + H]^+$ 441.2231, found 441.2266.

**Fmoc-Gly photolabile linker intermediate 2.28**. Gly photolabile linker intermediate **2.27** (4.539g, 10.30mmol) was dissolved in dioxane (16mL) and then sat. $NaHCO_3$ (aq) (26mL) was added. A solution of FmocCl (3.199g, 12.37 mmol) in dioxane (10 mL) was then added and the reaction mixture was stirred at rt for 19 h whereupon water (400 mL) was added. The resulting mixture was extracted with EtOAc ($3 \times 400$ mL) and the combined organic phases were washed with water ($2 \times 400$ mL) and brine (400 mL), dried over $MgSO_4$ and the solvent was removed *in vacuo*. The residue was then purified by flash column chromatography on silica gel (EtOAc:heptane (1:3)) to give the title compound as a yellow amorphous solid (4.598 g, 67%). $R_f$ = 0.46 (EtOAc:heptane (1:1)); $^1$H NMR ($CDCl_3$, 400 MHz)[6] $\delta$ 7.80–7.69 (m, 1H), 7.69–7.60 (m, 1H), 7.59–7.48 (m, 2H), 7.43–6.89 (m, 6H), 6.06–5.73 (m, 1H), 4.55–4.23 (m, 2H), 4.23–4.00 (m, 6H), 3.95–3.84 (m, 4H), 2.59–2.48 (m, 2H), 2.26–2.12 (m, 2H), 1.73–1.55 (m, 2H), 1.50–1.36 (m, 10H), 1.26 (t, $J = 7.1$ Hz, 3H); $^{13}$C NMR ($CDCl_3$, 101 MHz)[7] $\delta$ 173.0, 169.2, 156.6/155.8, 153.9/153.4, 147.1/146.9, 143.9/143.7, 141.3/141.2, 139.9, 134.7/132.7, 127.7, 127.1, 125.2/124.8, 120.0/119.9, 110.4/109.0, 110.0/109.5, 82.02, 68.3, 67.8,

[6]Due to the presence of rotamers the NMR data was difficult to analyze.
[7]Due to the presence of rotamers some carbon signals were present twice.

60.7, 56.5, 52.9/51.9, 48.0/46.9, 47.3, 30.7, 28.1, 24.4, 19.5/18.9, 14.4; IR (neat) $cm^{-1}$: 2978, 2940, 1731, 1703, 1579, 1520, 1450, 1333, 1270, 1152, 1040, 740; HRMS (ESI) calcd for $C_{36}H_{42}N_2NaO_{10}^+$ $[M + H]^+$ 685.2732, found 685.2734.

**Gly photolabile linker 2.29**. Fmoc-Gly photolabile linker intermediate **2.28** (4.255 g, 6.420 mmol) was dissolved in acetone (96 mL) and buffer (0.1 M $KH_2PO_4$/0.1 M NaOH, 24 mL) was added. Novozyme 435 beads were added and the resulting mixture was shaken gently at rt for 6 days. The reaction mixture was filtered through a plug of Celite and the solvent was removed *in vacuo*. The residue was dissolved in $CH_2Cl_2$ and filtered and the solution was then concentrated and co-evaporated with MeCN several times to give the title compound as a yellow amorphous solid (4.723 g, quant). $^1$H NMR ($CDCl_3$, 799 MHz)[8] $\delta$ 7.79–7.69 (m, 1H), 7.67–7.58 (m, 1H), 7.58–7.49 (m, 2H), 7.48–6.89 (m, 6H), 6.03–5.77 (m, 1H), 4.57–4.27 (m, 2H), 4.21–3.97 (m, 4H), 3.95–3.85 (m, 4H), 2.70–2.53 (m, 2H), 2.26–2.11 (m, 2H), 1.67–1.59 (m, 2H), 1.48–1.39 (m, 10H); $^{13}$C NMR ($CDCl_3$, 201 MHz)[9] $\delta$ 178.5, 169.2/169.1, 156.6/155.8, 153.8/153.3, 147.0/146.8, 143.8, 141.2, 139.8, 134.5/132.6, 127.6, 127.0, 125.1/124.7, 120.0/119.8, 110.3/108.9, 109.9/109.5, 82.1/82.0, 68.0, 67.9/67.8, 56.4, 52.7/51.8, 47.8/46.8, 47.3/47.11, 30.4, 28.0, 24.1, 19.4/18.7; IR (neat) $cm^{-1}$: 3290, 2940, 1702, 1521, 1450, 1332, 1270, 1215, 1151, 1040, 740; HRMS (ESI) calcd for $C_{34}H_{39}N_2O_{10}^+$ $[M + H]^+$ 635.2599, found 635.2598.

**Leu photolabile linker intermediate 2.33a**. Chloride **1.95** (1.00 g, 2.89 mmol), H-Leu-O*t*Bu·HCl (0.776 g, 3.47 mmol) and KI (0.058 g, 0.35 mmol) were dissolved in DMF (5.8 mL). $Et_3N$ (2.02 mL, 14.5 mmol) was added and then the reaction mixture was heated to 60 °C. The reaction mixture was stirred at 60 °C for 7 days whereupon water (20 mL) was added. The resulting mixture was extracted with EtOAc (3 × 20 mL) and the combined organic phases were washed with water (2 × 40 mL) and brine (2 × 40 mL), dried over $Na_2SO_4$ and the solvent was removed *in vacuo*. The residue was then purified by flash column chromatography on silica gel (EtOAc:heptane:$Et_3N$ (20:78:2)) to give the title compound as a yellow amorphous solid (0.610 g, 42%). $R_f = 0.42$ (EtOAc:heptane (2:3)); $^1$H NMR ($CDCl_3$, 400 MHz) $\delta$ 7.75–7.42 (m, 2H), 4.75–4.52 (m, 1H), 4.19–4.05 (m, 4H), 3.97 (s, 3H), 3.30–2.76 (m, 1H), 2.53 (dd, $J$ = 13.4, 7.1 Hz, 2H), 2.22–2.12 (m, 2H), 1.84–1.65 (m, 1H), 1.65–1.37 (m, 11H), 1.36 (s, 3H), 1.25 (t, $J$ = 7.1 Hz, 3H), 0.92–0.70 (m, 6H); $^{13}$C NMR ($CDCl_3$, 101 MHz)[10] $\delta$ 173.1, 173.0, 154.0, 147.1, 141.8/141.0, 134.2, 110.1, 109.0/109.0, 82.3, 68.4/68.3, 60.7, 58.6/58.5, 56.7, 51.6, 42.4, 30.7, 28.1, 28.1, 25.2/25.0, 24.4/24.4, 22.9/22.5, 14.4; IR (neat) $cm^{-1}$: 2958, 2871, 1726, 1515, 1469, 1368, 1336, 1269, 1211, 1147, 1058, 1028; HRMS (ESI) calcd for $C_{25}H_{41}N_2O_8^+$ $[M + H]^+$ 497.2857, found 497.2862.

[8]Due to the presence of rotamers the NMR data was difficult to analyze.

[9]Due to the presence of rotamers some carbon signals were present twice.

[10]Due to the presence of diastereomers some carbon signals were present twice.

**Ala photolabile linker intermediate 2.33b**. Chloride **1.95** (1.009 g, 2.918mmol), H-Ala-O*t*Bu·HCl (0.636g, 3.50mmol) and KI (0.058g, 0.35mmol) were dissolved in DMF (5.8 mL). $Et_3N$ (2.03 mL, 14.6 mmol) was added and then the reaction mixture was heated to 60 °C. The reaction mixture was stirred at 60 °C for 6 days whereupon water (20 mL) was added. The resulting mixture was extracted with EtOAc (3 × 20 mL) and the combined organic phases were washed with water (2 × 50 mL) and brine (2 × 50 mL), dried over $Na_2SO_4$ and the solvent was removed *in vacuo*. The residue was then purified by flash column chromatography on silica gel (EtOAc:heptane:$Et_3N$ (25:73:2)) to give the title compound as a yellow amorphous solid (0.660 g, 50%). $R_f = 0.28$ (EtOAc:heptane (2:3)); $^1$H NMR ($CDCl_3$, 400 MHz) $\delta$ 7.92–7.34 (m, 2H), 4.95–4.59 (m, 1H), 4.19–4.05 (m, 4H), 4.04–3.91 (m, 3H), 3.33–2.89 (m, 1H), 2.58–2.45 (m, 2H), 2.24–2.10 (m, 2H), 1.91–1.30 (m, 15H), 1.26 (t, $J$ = 7.1 Hz, 3H); $^{13}$C NMR ($CDCl_3$, 101 MHz)[11] $\delta$ 173.1, 169.2, 154.2, 147.3, 141.9/141.2, 133.8, 110.1, 109.1/109.0, 82.4/81.8, 68.4, 60.7, 57.1/56.6, 55.2, 51.6/50.9, 30.7, 28.0, 24.4, 23.5/23.3, 18.5, 14.4; IR (neat) cm$^{-1}$: 2977, 2935, 1726, 1514, 1368, 1335, 1267, 1212, 1147, 1054, 1034; HRMS (ESI) calcd for $C_{22}H_{35}N_2O_8^+$ $[M + H]^+$ 455.2388, found 455.2394.

**Phe photolabile linker intermediate 2.33c**. Chloride **1.95** (0.721 g, 2.09mmol), H-Phe-O*t*Bu·HCl (0.653g, 2.53mmol) and KI (0.042g, 0.25mmol) were dissolved in DMF (4.2 mL). $Et_3N$ (1.47 mL, 10.5 mmol) was added and then the reaction mixture was heated to 60 °C. The reaction mixture was stirred at 60 °C for 6 days whereupon water (20 mL) was added. The resulting mixture was extracted with EtOAc (3 × 20 mL) and the combined organic phases were washed with water (2 × 50 mL) and brine (2 × 50 mL), dried over $Na_2SO_4$ and the solvent was removed *in vacuo*. The residue was then purified by flash column chromatography on silica gel (acetone:toluene:$Et_3N$ (1.5:97.5:1)) to give the title compound as a yellow amorphous solid (0.372 g, 74%). $R_f = 0.42$ (EtOAc:heptane (2:3)); $^1$H NMR ($CDCl_3$, 400 MHz) $\delta$ 7.46–7.06 (m, 7H), 4.51–4.41 (m, 1H), 4.15 (q, $J$ = 7.1 Hz, 2H), 4.11–4.03 (m, 2H), 3.93–3.50 (m, 3H), 3.35–2.95 (m, 1H), 2.94–2.65 (m, 2H), 2.52 (t, $J$ = 7.3 Hz, 2H), 2.17 (p, $J$ = 6.7 Hz, 2H), 1.43–1.23 (m, 15H); $^{13}$C NMR ($CDCl_3$, 101 MHz)[12] $\delta$ 174.7/173.5, 173.1/173.1, 153.9/153.8, 146.7/146.7, 141.6/141.1, 138.1/137.5, 136.4/135.7, 129.7/129.5, 128.4/128.3, 126.7/126.6, 109.9/109.6, 109.1/108.9, 81.8/81.4, 68.4/68.3, 61.6/61.0, 60.7, 56.4/56.1, 51.1/51.0, 40.2/39.6, 30.8/30.8, 28.1/28.0, 24.8/23.6, 24.5/24.4, 14.36; IR (neat) cm$^{-1}$: 2977, 2933, 1726, 1514, 1368, 1335, 1268, 1211, 1149, 1057, 1029; HRMS (ESI) calcd for $C_{28}H_{39}N_2O_8^+$ $[M + H]^+$ 531.2701, found 531.2706.

**Leu photolabile linker 2.35a**. Leu photolabile linker intermediate **2.33a** (0.572g, 1.15mmol) was dissolved in THF (11.5mL) and water (1.5mL). Then 1 M LiOH (aq) (2.30 mL, 2.30 mmol) was added and the reaction mixture was

[11] Due to the presence of diastereomers some carbon signals were present twice.
[12] Due to the presence of diastereomers most carbon signals were present twice.

stirred at rt for 25 h whereupon 1 M HCl (aq) (3.15 mL) and water (40 mL) were added. The resulting mixture was extracted with EtOAc (3 × 50 mL). The combined organic phases were washed with brine (50 mL), dried over $Na_2SO_4$ and the solvent was removed *in vacuo* to give the title compound as a yellow amorphous solid (0.543 g, quant.). $^1$H NMR ($CDCl_3$, 400 MHz) $\delta$ 7.53–7.34 (m, 2H), 4.60–4.42 (m, 1H), 4.16–4.06 (m, 2H), 3.94 (d, $J$ = 7.6 Hz, 3H), 3.20–2.72 (m, 1H), 2.61 (q, $J$ = 7.0 Hz, 2H), 2.24–2.13 (m, 2H), 1.87–1.65 (m, 1H), 1.53–1.32 (m, 14H), 0.92–0.73 (m, 6H); $^{13}$C NMR ($CDCl_3$, 101 MHz)[13] $\delta$ 178.1, 178.1, 153.9/153.8, 146.8, 141.8/141.0, 135.6, 110.2/109.8, 109.1/109.0, 81.7, 68.2/68.1, 58.5, 56.5/56.3, 51.1, 43.1/42.8, 30.4/30.4, 28.2, 28.1, 25.2/24.9, 24.2/24.2, 23.2/22.9, 22.5/22.4; IR (neat) cm$^{-1}$: 2975, 2933, 2874, 1722, 1514, 1334, 1268, 1212, 1147, 1052; HRMS (ESI) calcd for $C_{23}H_{37}N_2O_8^+$ $[M + H]^+$ 469.2544, found 469.2548.

**Ala photolabile linker 2.35b**. Ala photolabile linker intermediate **2.33b** (0.627 g, 1.38 mmol) was dissolved in THF (13.8 mL) and water (2 mL). Then 1 M LiOH (aq) (2.75 mL, 2.75 mmol) was added and the reaction mixture was stirred at rt for 26 h whereupon 1 M HCl (aq) (3.81 mL) and water (40 mL) were added. The resulting mixture was extracted with EtOAc (3 × 50 mL). The combined organic phases were washed with brine (50 mL), dried over $Na_2SO_4$ and the solvent was removed *in vacuo* to give the title compound as a yellow amorphous solid (0.497 g, 85%). $^1$H NMR ($CDCl_3$, 400 MHz) $\delta$ 7.53–7.29 (m, 2H), 4.66–4.46 (m, 1H), 4.17–4.04 (m, 2H), 3.95 (s, 3H), 3.21–2.81 (m, 1H), 2.64–2.57 (m, 2H), 2.24–2.13 (m, 2H), 1.55–1.28 (m, 12H), 1.28–1.16 (m, 3H); $^{13}$C NMR ($CDCl_3$, 101 MHz)[14] $\delta$ 178.1, 178.1, 154.0, 146.8, 141.8/141.2, 135.3, 109.8, 109.2/109.1, 81.8/81.6, 68.2, 56.5, 55.3/55.0, 51.4/50.7, 30.4/30.4, 28.1/28.1, 24.3/23.4, 24.2, 19.5/18.6; IR (neat) cm$^{-1}$: 2975, 2932, 2873, 1722, 1514, 1368, 1334, 1212, 1147, 1052; HRMS (ESI) calcd for $C_{20}H_{31}N_2O_8^+$ $[M + H]^+$ 427.2075, found 427.2071.

**Phe photolabile linker 2.35c**. Phe photolabile linker intermediate **2.33c** (0.353 g, 0.665 mmol) was dissolved in THF (6.7 mL) and water (1 mL). Then 1 M LiOH (aq) (1.35 mL, 1.35 mmol) was added and the reaction mixture was stirred at rt for 26 h whereupon 1 M HCl (aq) (1.93 mL) and water (20 mL) were added. The resulting mixture was extracted with EtOAc (3 × 20 mL). The combined organic phases were washed with brine (20 mL), dried over $Na_2SO_4$ and the solvent was removed *in vacuo* to give the title compound as a yellow amorphous solid (0.333 g, quant.). $^1$H NMR ($CDCl_3$, 400 MHz) $\delta$ 7.47–7.10 (m, 7H), 4.60–4.44 (m, 1H), 4.21–4.00 (m, 2H), 3.95–3.52 (m, 3H), 3.46–2.99 (m, 1H), 2.99–2.65 (m, 2H), 2.61 (t, $J$ = 7.2 Hz, 2H), 2.18 (p, $J$ = 6.7 Hz, 2H), 1.42–1.24 (m, 12H); $^{13}$C NMR ($CDCl_3$, 101 MHz)[15] $\delta$ 178.1, 178.0, 154.0/153.9, 146.8/146.7, 141.6/141.1, 137.9, 135.3, 129.7/129.5, 128.5/128.3, 126.9/126.6,

[13] Due to the presence of diastereomers some carbon signals were present twice.
[14] Due to the presence of diastereomers some carbon signals were present twice.
[15] Due to the presence of diastereomers most carbon signals were present twice.

110.2/109.7, 109.2/109.0, 82.04, 68.2/68.1, 61.5/61.1, 56.5/56.3, 51.4/51.1, 40.0/39.3, 30.4/30.3, 28.1/28.0, 24.58, 24.16; IR (neat) $cm^{-1}$: 2973, 2932, 1719, 1514, 1334, 1268, 1211, 1149, 1056; HRMS (ESI) calcd for $C_{26}H_{35}N_2O_8^+$ $[M + H]^+$ 503.2388, found 503.2388.

### 2.7.3 Synthesis of DOX ester building block 2.48

**FmocDOX 2.46**. DOX · HCl **2.45** (0.101 g, 0.174 mmol) was dissolved in $H_2O$ (1 mL) and dioxane (0.6 mL) and then $NaHCO_3$ (0.058 g, 0.69 mmol) was added. FmocCl (0.045 g, 0.17 mmol) was added dropwise as a solution in dioxane (0.4 mL). The reaction mixture was stirred at rt for 22 h whereupon 0.2% TFA (aq) (20 mL) was added and the resulting mixture was put in the fridge for 10 min. The reaction mixture was then filtered and the solid was washed with 0.2% TFA and then $Et_2O$ to give the title compound as red amorphous solid (0.131 g, quant.). $^1$H NMR (DMSO, 500 MHz) $\delta$ 14.05 (s, 1H), 13.28 (s, 1H), 7.94–7.89 (m, 2H), 7.88–7.83 (m, 2H), 7.70–7.63 (m, 3H), 7.42–7.34 (m, 2H), 7.33–7.26 (m, 3H), 6.97 (d, $J$ = 7.9 Hz, 1H), 5.45 (s, 1H), 5.25–5.20 (m, 1H), 4.99–4.91 (m, 1H), 4.75–4.68 (m, 1H), 4.63–4.59 (m, 1H), 4.56 (s, 2H), 4.28–4.20 (m, 2H), 4.19–4.12 (m, 3H), 3.99 (s, 3H), 3.77–3.67 (m, 1H), 3.48–3.40 (m, 1H), 3.03–2.93 (m, 2H), 2.23–2.11 (m, 2H), 1.91–1.81 (m, 1H), 1.53–1.45 (m, 1H), 1.13 (d, $J$ = 6.4 Hz, 3H); $^{13}$C NMR (DMSO, 125 MHz) $\delta$ 212.3, 186.7, 186.6, 159.4, 154.8, 154.0, 153.1, 142.4, 139.3, 135.0, 134.1, 133.2, 132.5, 126.2, 125.6, 123.9, 118.9, 118.6, 118.4, 117.7, 109.4, 109.2, 99.2, 73.5, 68.7, 66.7, 64.5, 64.0, 62.0, 55.1, 45.8, 44.9, 35.2, 30.7, 28.3, 15.5; IR (neat) $cm^{-1}$: 3435, 2935, 1716, 1615, 1578, 1409, 1283, 1207, 1118, 1075, 1015, 983, 760, 739; HRMS (ESI) calcd for $C_{42}H_{39}NNaO_{13}^+$ $[M + Na]^+$ 788.2314, found 788.2313.

**DOX ester building block intermediate 2.47**. FmocDOX **2.46** (0.822g, 1.07mmol) was dissolved in $CH_2Cl_2$ (280mL) and then 2,4,6-collidine (1.66mL, 12.6 mmol) was added. The reaction mixture was cooled to −78 °C and then a solution of methyl glutaryl chloride (1.440 g, 8.749 mmol) in $CH_2Cl_2$ (13.9 mL) was added dropwise. The reaction was stirred at −78 °C for 90 min whereupon the reaction mixture was concentrated *in vacuo* and then co-evaporated with EtOH (2 × 400 mL). 2% TFA (aq) (280 mL) was added and the resulting mixture was put in the fridge for 15 min. The reaction mixture was then filtered and the solid was washed with cold heptane. The solid was dissolved in $CH_2Cl_2$ (350 mL), concentrated *in vacuo* and then co-evaporated with EtOH (450 mL) to give the title compound as red amorphous solid (0.937 g, quant.). $^1$H NMR (DMSO, 500 MHz) $\delta$ 14.03 (s, 1H), 13.26 (s, 1H), 7.94–7.87 (m, 2H), 7.87–7.80 (m, 2H), 7.70–7.62 (m, 3H), 7.42–7.34 (m, 2H), 7.32–7.26 (m, 2H), 6.97 (d, $J$ = 7.8 Hz, 1H), 5.62 (s, 1H), 5.28–5.13 (m, 3H), 4.97–4.91 (m, 1H), 4.71 (s, 1H), 4.26–4.19 (m, 2H), 4.18–4.13 (m, 2H), 3.98 (s, 3H), 3.77–3.71 (m, 1H), 3.59 (s, 3H), 3.47–3.41 (m, 1H), 3.09–2.86 (m, 2H), 2.48–2.38 (m, 4H), 2.36–2.00 (m, 2H), 1.83–1.78 (m, 2H), 1.93–1.46 (m, 2H), 1.14 (d, $J$ = 5.9 Hz,

3H); $^{13}$C NMR (DMSO, 125 MHz)[16] $\delta$ 207.7, 186.3, 172.7, 171.7, 160.5, 155.8, 155.1, 154.2, 143.6, 140.4, 136.5, 135.1, 134.5, 133.5, 127.8, 127.2, 125.5, 120.1, 119.8, 119.1, 118.8, 110.5, 110.4, 100.7, 75.1, 69.9, 68.1, 66.5, 65.9, 65.4, 56.4, 51.0, 47.0, 46.4, 36.1, 32.0, 32.0, 31.5, 29.7, 19.5, 16.6; IR (neat) cm$^{-1}$: 3434, 2945, 1727, 1615, 1578, 1409, 1283, 1205, 1117, 1068, 1012, 982, 761, 739; HRMS (ESI) calcd for $C_{48}H_{47}NNaO_{16}^{+}$ $[M + Na]^+$ 916.2787, found 916.2784.

**DOX ester building block 2.48**. DOX ester building block intermediate **2.47** (0.937 g, 1.05 mmol) was dissolved in acetone (125 mL) and buffer (0.1 M $KH_2PO_4$/0.1 M NaOH, 20 mL) was added. Novozyme 435 beads were added and the resulting mixture was shaken gently at rt for 9 days. Then EtOAc (1 L) was added and the resulting mixture was filtered. The solution was then washed with 2% TFA (aq) (500 mL) and water (9 × 500 mL), dried over $MgSO_4$ and the solvent was removed *in vacuo* to give the title compound as a red amorphous solid (0.9407 g, quant). $^1$H NMR (DMSO, 500 MHz) $\delta$ 14.03 (s, 1H), 13.26 (s, 1H), 12.09 (s, 1H), 7.93–7.88 (m, 2H), 7.88–7.83 (m, 2H), 7.70–7.62 (m, 3H), 7.42–7.35 (m, 2H), 7.33–7.27 (m, 2H), 6.97 (d, $J$ = 8.0 Hz, 1H), 5.61 (s, 1H), 5.27–5.13 (m, 3H), 4.98–4.91 (m, 1H), 4.71 (d, $J$ = 5.5 Hz, 1H), 4.27–4.19 (m, 2H), 4.18–4.13 (m, 2H), 3.98 (s, 3H), 3.73–3.66 (m, 1H), 3.48–3.43 (m, 1H), 3.09–2.85 (m, 2H), 2.44 (t, $J$ = 7.1 Hz, 2H), 2.31 (t, $J$ = 7.2 Hz, 2H), 2.24–1.96 (m, 2H), 1.83–1.74 (m, 2H), 1.93–1.45 (m, 2H), 1.14 (d, $J$ = 6.2 Hz, 3H); $^{13}$C NMR (DMSO, 125 MHz)[17] $\delta$ 207.2, 185.9, 173.4, 171.4, 160.1, 155.4, 154.6, 153.8, 143.2, 140.0, 135.7, 134.8, 134.0, 133.1, 126.7, 126.3, 124.7, 119.5, 119.5, 118.9, 118.3, 110.1, 109.9, 100.1, 74.7, 69.7, 67.7, 65.9, 65.6, 65.2, 56.2, 46.9, 46.3, 35.9, 32.1, 32.0, 31.5, 29.6, 19.6, 16.7; IR (neat) cm$^{-1}$: 3400, 2935, 1721, 1615, 1578, 1409, 1282, 1206, 1116, 1069, 1014, 982, 760, 739; HRMS (ESI) calcd for $C_{47}H_{45}NNaO_{16}^{+}$ $[M + Na]^+$ 902.2631, found 902.2622.

### 2.7.4 Solid-phase synthesis

#### General solid-phase procedures

Prior to usage, the amino-functionalized $PEGA_{800}$ resin was washed with $H_2O$ (×6), EtOH (×6), DMF (×6), MeOH (×6) and $CH_2Cl_2$ (×6) before being lyophilized.

**MSNT coupling.** Acid (3 equiv) was dissolved in $CH_2Cl_2$ at rt, then MeIm (2.25 equiv) and MSNT (3 equiv) were added. After 5 min. the mixture was added to the resin and the mixture was occasionally stirred over the next 1 h. The resin was then washed with $CH_2Cl_2$ (×1), DMF (×1) and $CH_2Cl_2$ (×1) and the coupling was repeated once whereupon the resin was washed

[16] Signal from one of the carbonyl carbons in the anthracycline ring system could not be observed.

[17] Signal from one of the carbonyl carbons in the anthracycline ring system could not be observed.

with $CH_2Cl_2$ (×6), DMF (×6), $CH_2Cl_2$ (×6), DMF (×6) and $CH_2Cl_2$ (×6) before being lyophilized.

**TBTU coupling.** Acid (3 equiv) was dissolved in DMF at rt and then NEM (4 equiv) and TBTU (2.9 equiv) were added. After 5 min. the mixture was added to the resin and the mixture was occasionally stirred over 2 h. The resin was then washed with DMF (×6), $CH_2Cl_2$ (×6), DMF (×6) and $CH_2Cl_2$ (×6) before being lyophilized.

**HATU coupling.** Acid (3 equiv) was dissolved in DMF at rt and then DIPEA (5 equiv) and HATU (2.9 equiv) were added. After 5 min. the mixture was added to the resin and the mixture was occasionally stirred over 2 h. The resin was then washed with DMF (×6), $CH_2Cl_2$ (×6), DMF (×6) and $CH_2Cl_2$ (×6) before being lyophilized.

**BTC coupling.** Acid (5 equiv) was dissolved in THF at rt and then BTC (1.65 equiv) was added followed by slow addition of 2,4,6-collidine (14 equiv). After 1 min. the mixture was added to the resin and the mixture was heated to 50 °C and shaken for 1 h. The resin was the washed with DMF (×6), $CH_2Cl_2$ (×6), DMF (×6) and $CH_2Cl_2$ (×6) and the coupling was repeated once whereupon the resin was washed with THF (×6), DMF (×6), $CH_2Cl_2$ (×6), DMF (×6) and $CH_2Cl_2$ (×6) before being lyophilized.

**20% Fmoc deprotection.** The resin was swelled in 20 (v/v)% piperidine in DMF for 2 min. and then washed with DMF (×6). Then the resin was again swelled in 20 (v/v)% piperidine in DMF for 18 min. whereupon the resin was washed with DMF (×6), $CH_2Cl_2$ (×6), DMF (×6) and $CH_2Cl_2$ (×6).

**0.5% Fmoc deprotection.** The resin was swelled in 0.5(v/v)% piperidine in DMF for 45min.. The resin was then washed with DMF (×6), $CH_2Cl_2$ (×6), DMF (×6) and $CH_2Cl_2$ (×6). For difficult deprotections the procedure was repeated once or twice.

***t*Bu deprotection.** The resin was swelled in $CH_2Cl_2$:TFA (1:1) and the mixture was occasionally stirred over 2 h. The resin was then washed with $CH_2Cl_2$ (×6), DMF (×6), $CH_2Cl_2$ (×6), DMF (×6) and $CH_2Cl_2$ (×6).

**Release from HMBA linker.** 5–10 mg of resin was treated with 0.1 M NaOH (aq) for 2 h followed by neutralization with 0.1 M HCl (aq).

**Photolytic release.** 10–20 mg of resin was swelled in DMF in a petri dish with a custom-made quartz cover and irradiated at 365 nm for 1–2 h.

### DOX derivatives

Cf. appendix A for RP-HPLC-UV chromatograms of these products.

**Gly-DOX 2.32.** Prepared according to the general solid-phase procedures followed by photolytic release. RP-HPLC purity: 87%, $R_t = 5.38$ min.; HRMS (ESI) calcd for $C_{29}H_{33}N_2O_{12}^+$ $[M + Na]^+$ 601.2033, found 601.2029.

**Leu-DOX 2.38a.** Prepared according to the general solid-phase procedures followed by photolytic release. RP-HPLC purity: >95%, $R_t = 5.65$min.; HRMS (ESI) calcd for $C_{33}H_{41}N_2O_{12}^+$ $[M + Na]^+$ 657.2659, found 657.2655.

**Ala-DOX 2.38b.** Prepared according to the general solid-phase procedures followed by photolytic release. RP-HPLC purity: 94%, $R_t = 5.75$ min.; HRMS (ESI) calcd for $C_{30}H_{35}N_2O_{12}^+$ $[M + Na]^+$ 615.2190, found 615.2184.

**Phe-DOX 2.38c.** Prepared according to the general solid-phase procedures followed by photolytic release. RP-HPLC purity: 93%, $R_t = 5.78$ min.; HRMS (ESI) calcd for $C_{36}H_{39}N_2O_{12}^+$ $[M + Na]^+$ 691.2503, found 691.2499.

**Ala-Gly-Gly-DOX tripeptide 2.43.** Prepared according to the general solid-phase procedures followed by photolytic release. RP-HPLC purity: >95%, $R_t = 5.71$ min.; HRMS (ESI) calcd for $C_{34}H_{41}N_4O_{14}^+$ $[M + Na]^+$ 729.2619, found 729.2613.

**DOX amide 2.51.** Prepared according to the general solid-phase procedures followed by photolytic release. RP-HPLC purity: 64%, $R_t = 8.12$ min.; MS (ESI) calcd for $C_{32}H_{37}N_2O_{13}^+$ $[M + H]^+$ 657.2, found 657.5.

**Ala-Dox amide 2.52.** Prepared according to the general solid-phase procedures followed by photolytic release. RP-HPLC purity: 70%, $R_t = 7.80$min.; MS (ESI) calcd for $C_{50}H_{52}N_3O_{16}^+$ $[M + H]^+$ 950.3, found 950.4.

**DOX dipeptide 2.55.** Prepared according to the general solid-phase procedures followed by photolytic release. RP-HPLC purity: 48%, $R_t = 8.00$min.; MS (ESI) calcd for $C_{79}H_{103}N_{10}O_{25}^+$ $[M + H]^+$ 1591.7, found 1591.7.

Chapter 3

# Total Synthesis of Trioxacarcin DC-45-A2

The stereoselective synthesis of biologically active natural products via total synthesis provides a unique opportunity to access structural analogs and, in some cases, provides a more efficient access to large quantities of the natural product, both of which are crucial in drug discovery efforts. It furthermore serves as the true test of power for existing synthetic methodologies and is thus the driving force for refinement of existing synthetic methods and the discovery of new chemical reactivity. It also provides final proof and confirmation of the structure of complex natural products or, in many cases, results in revision and discovery of the true structure [144].

In the following the work performed during a research stay in the group of Professor K.C. Nicolaou at Rice University on the total synthesis of trioxacarcin DC-45-A2 will be described.[1]

## 3.1 The Trioxacarcin Class of Antitumor Antibiotics

The trioxacarcins are a class of antitumor antibiotics isolated from various *Streptomyces* strains in 1981 and 2004 [146–148]. Several members of the class inhibit different cancer cell lines and furthermore show antibacterial properties.

Naturally occurring trioxacarcins share the structural core DC-45-A2 **3.1** and obtain their structural diversity mainly by glycosylation with various

[1] The work described in this chapter contributed to the completion and publication of the total synthesis of trioxacarcin DC-45-A2 [145].

saccharides on two of the hydroxy functionalities, exemplified by trioxacarcin A **3.2**, cf. figure 3.1.

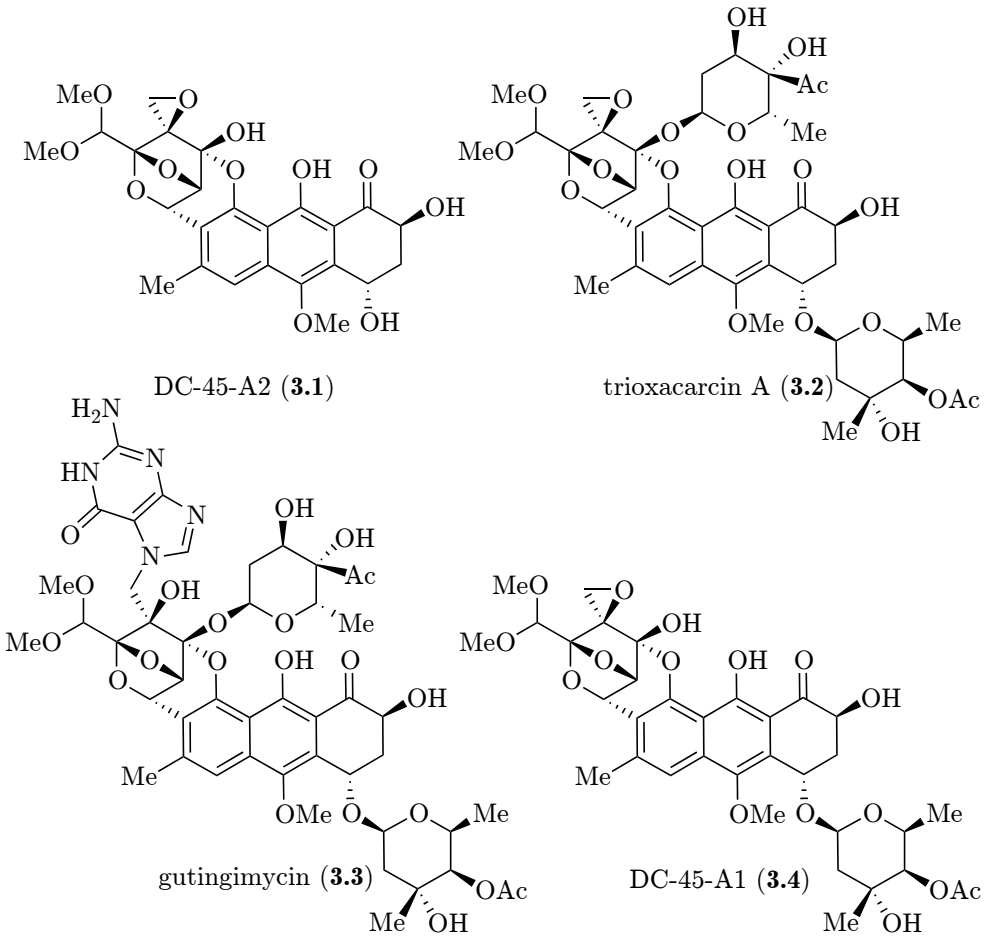


**Figure 3.1:** The molecular structure of trioxacarcin DC-45-A2 **3.1**, trioxacarcin A **3.2**, gutingimycin **3.3** and the monoglycosylated trioxacarcin DC-45-A1 **3.4**.

The mode of action of the trioxacarcins is believed to be alkylation of DNA by attack of a guanosine residue on the trioxacarcin spiro epoxide. For trioxacarcin A **3.2** this has been supported by a crystal structure of the natural product covalently bound to DNA [149] and furthermore by isolation of the trioxcarcin A guanine conjugate gutingimycin **3.3** [150]. It is furthermore believed that the planar trioxacarcin ring system can intercalate DNA analogous to the anthracycline cancer drugs, e.g. doxorubicin [150], cf. chapter 2.

The first total synthesis of trioxacarcin DC-45-A2 **3.1** was published by Andrew Myers in 2011 [151]. Myers furthermore published routes to the monosaccharides trioxacarcinoside A [152] and B [153] and these efforts ultimately led to the total synthesis of trioxacarcin A **3.2** [154]. Myers' synthesis

commenced with a Hauser-Kraus annulation [155–157] of advanced building blocks **3.5** and **3.6**, cf. scheme 3.1. A few chemical manipulations followed to

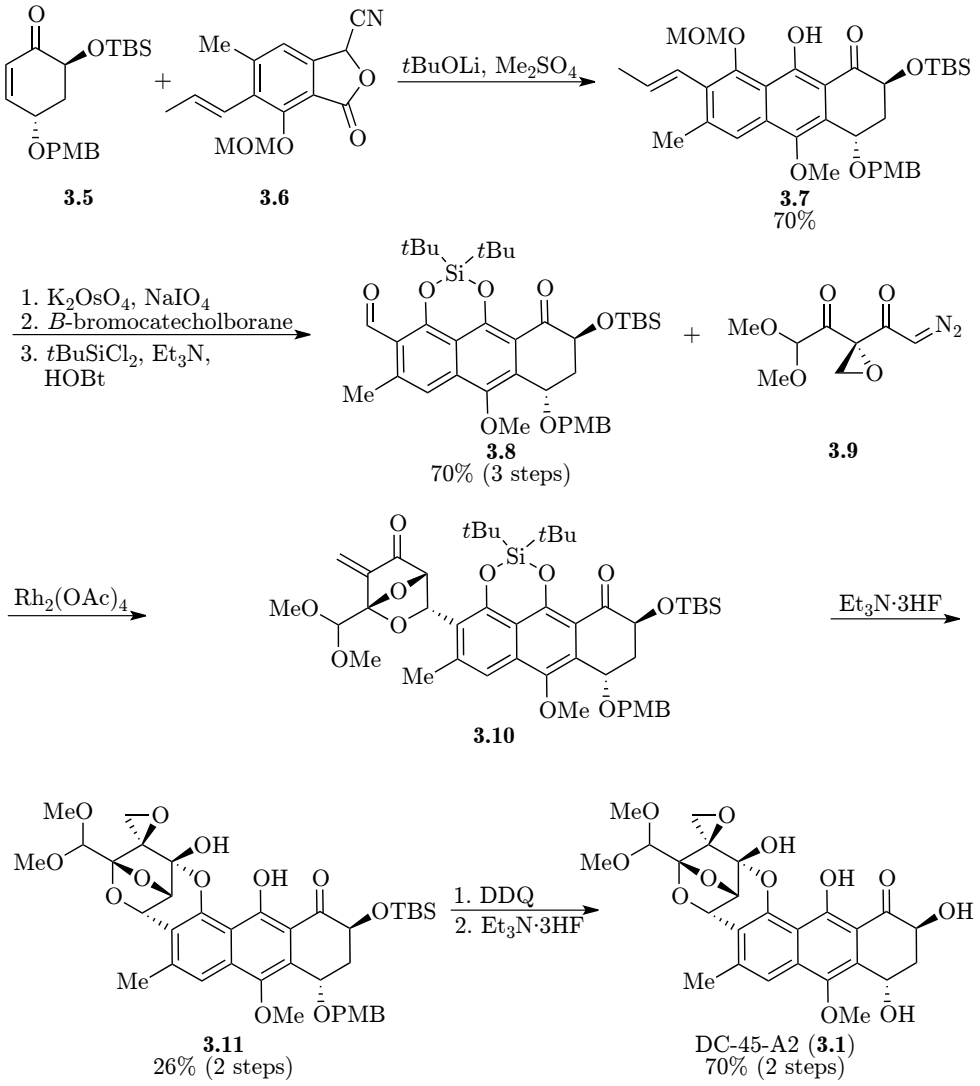


**Scheme 3.1:** Myers' total synthesis of trioxacarcin DC-45-A2 **3.1**.

give aldehyde **3.8** set up for the key step; a rhodium-mediated 1,3-dipolar cycloaddition employing diazo ketone **3.9** leading to the bicyclic polyoxygenated system present in **3.10** which after a final series of deprotections was transformed to trioxacarcin DC-45-A2 **3.1**. Even though Myers' total synthesis is highly convergent, the key step was hampered by low diastereoselectivity leading to a mixture of diastereomers comprised of all four possible outcomes so difficult to separate that it was subjected to the next step without purification. This resulted in a low yield of 26% of the wanted diastereomer and

thus led to the loss of valuable late-stage material.

With room for improvement evident, the group of K. C. Nicolaou commenced an effort to develop an enantioselective route to trioxacarcin DC-45-A2 **3.1** with an improved strategy for the construction of the tricyclic polyoxygenated system based on a stereo- and regioselective epoxide rearrangement, cf. scheme 3.2. For the synthetic plan to succeed, large amounts of the cyclo-

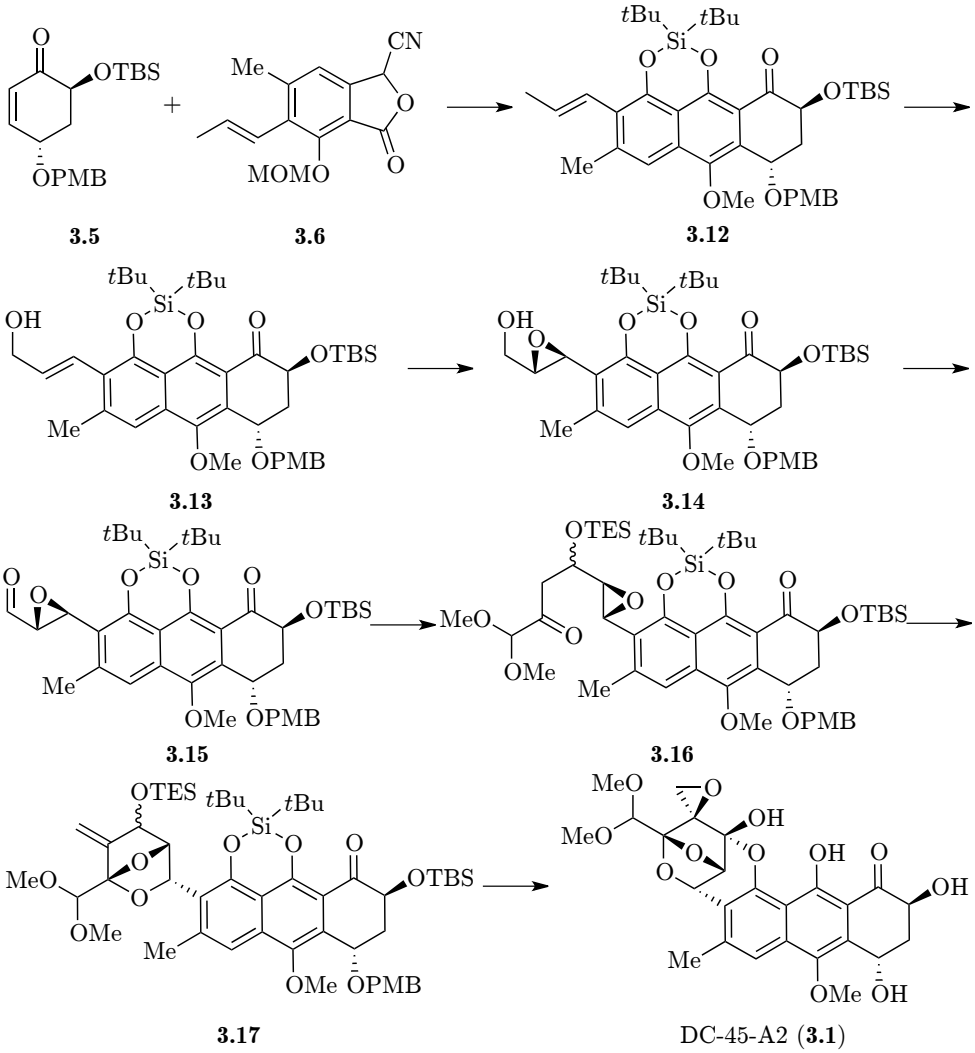


**Scheme 3.2:** Synthetic strategy for the synthesis of trioxacarcin DC-45-A2 **3.1** by the Nicolaou group.

hexenone **3.5** were needed. A new route for this building block had just been developed in the Nicolaou group and one of the goals of the project described herein was the optimization and scale-up of this route. Furthermore, the allylic oxidation of **3.12** to **3.13** gave low yields due to poor chemoselectivity

resulting in oxidation of the benzylic methyl group when subjected to common allylic oxidation methods. Thus another goal was to find an alternative way of installing the allylic hydroxy group possibly before the Hauser-Kraus annulation. For this purpose the intermediates on the way to cyanophthalide **3.6** would likely prove interesting and as **3.6** was furthermore needed to fuel front-line investigations of the key step, large amounts of this building block was likewise needed.

## 3.2 Optimization and Scale-up of New Route to Cyclohexenone 3.5

Before the K. C. Nicolaou group started their investigation into an optimized route for cyclohexenone **3.5** four routes were already known. Myers' group had developed three distinct routes as part of their trioxacarcin program [151, 158] and Ueda had published a fourth route in connection with development of new fluorescence-labelled probes [159, 160].

### 3.2.1 Literature reports on synthetic routes to cyclohexenone 3.5

Myers' first (and preferred) route started from L-malic acid **3.18** [151], cf. scheme 3.3. A four step procedure, known from the literature [161, 162], led to lactone **3.21**, which after Weinreb amide formation, oxidation, chemoselective vinyl addition and PMB-protection was converted to the Weinreb amide **3.23**. Final addition of another vinyl group and following RCM gave cyclohexenone **3.5** in an overall yield of 19% over 10 steps [151]. 1.3 g was produced whereby the route seemed to be somewhat scalable, but was, with 10 steps, rather lengthy.

The second route from the Myers group commenced from TBS-protected resorcinol[2] **3.25** [151], cf. scheme 3.4, which was transformed into *trans*-diol **3.27** in three steps by a known procedure [163]. DMP oxidation followed by elimination led to cyclohexenone **3.28**, which after a protection group shuffle comprising a low yielding mono TBS deprotection and a subsequent PMB protection provided cyclohexenone **3.5** in an overall yield of 12% over seven steps [151]. However, only 0.3 g of cyclohexenone **3.5** was produced calling into question the scalability of the route.

The last route published by Myers started from quinic acid **3.30** [158], cf. scheme 3.5, and was then transformed to PMB-protected cyclohexenone **3.37** in seven steps by a previously reported procedure [164, 165]. Silyl enol ether formation followed by a Rubottom oxidation [166] led to the hydroxy

[2] It is not stated in the references cited in Myers' paper whether TBS-protected resorcinol **3.25** was prepared in their lab or acquired from commercial sources. It appears to be very expensive to obtain commercially in the amounts used.

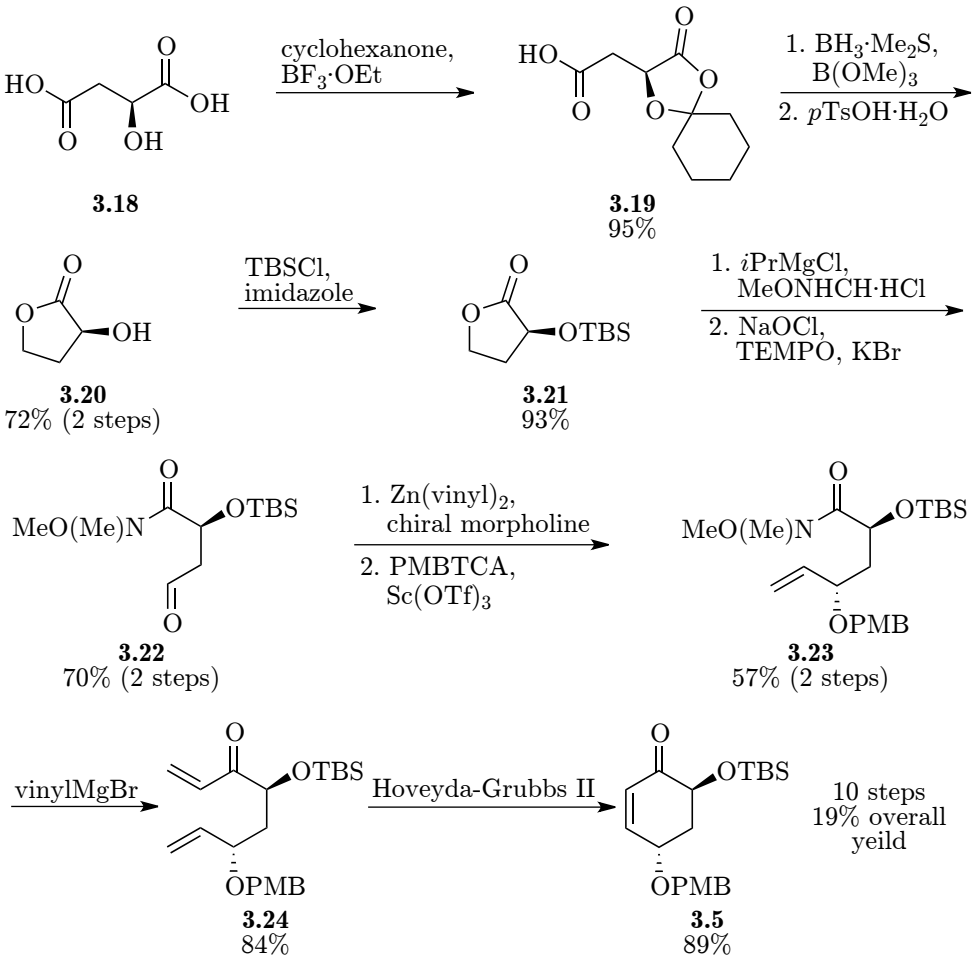


**Scheme 3.3:** Myers' route to cyclohexenone **3.5** starting from L-malic acid **3.18**.

ketone **3.39**, which after a final TBS-protection provided cyclohexenone **3.5** in an overall yield of 6% over 10 steps [158]. In addition to being rather low yielding and lengthy, the route was only reported in a very small scale (30 mg of product).

The fourth route was published by the group of Minuro Ueda as part of investigations into new fluorescence-labelled probes [159,160]. The route commenced from D-glucose **3.40**, which was transformed into iodide **3.44** by an eight step procedure [159], cf. scheme 3.6. A TBS-protection followed by an elimination afforded alkene **3.45**. A Ferrier carbocyclization [167], with simultaneous demethylation of the methoxy group, followed by a final elimination step provided cyclohexenone **3.5** in an overall yield of 14% over 12 steps [160]. Even though the overall yield was satisfactory the route was very lengthy (12 steps) and only a very small amount of product was synthesized (5.5 mg) seriously calling into question the scalability of the route.

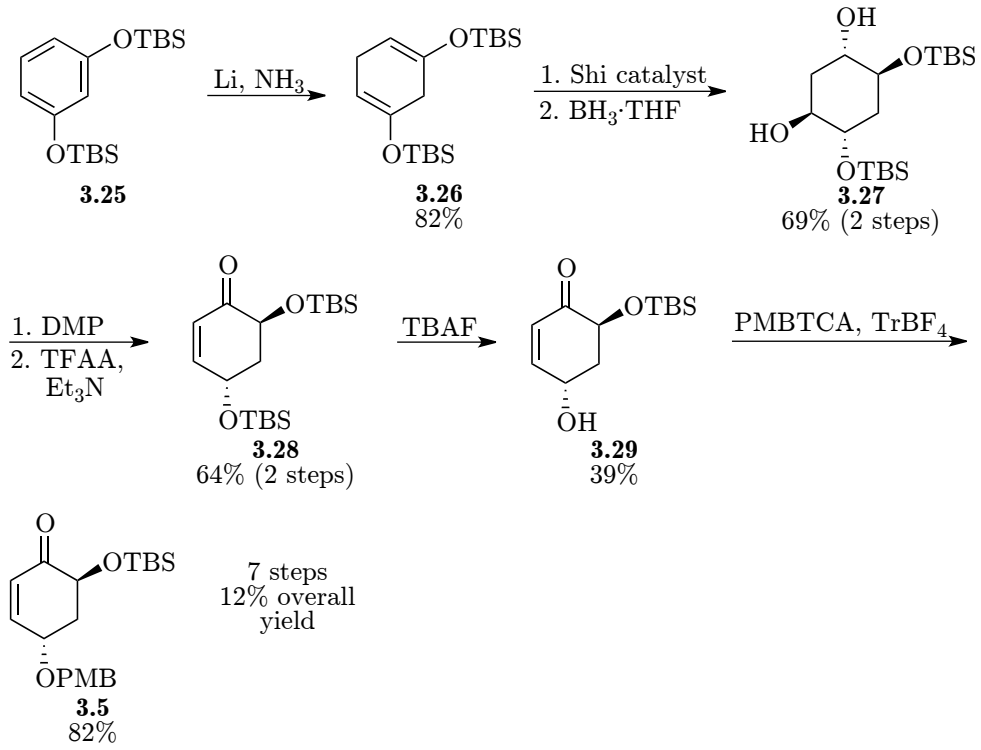


**Scheme 3.4:** Myers' route to cyclohexenone **3.5** starting from TBS-protected resorcinol **3.25**.

As none of the previous routes to cyclohexenone **3.5** seemed optimal and furthermore had not been reported in a large scale the Nicolaou group set out to develop an improved, scalable synthetic strategy.

### 3.2.2 New route to cyclohexenone 3.5

The new route developed in the Nicolaou group[3] relied upon access to allylic alcohol **3.51** as reported by the O'Brien group [168, 169]. The route started from 1,4-cyclohexadiene **3.46**, which was converted into the *meso*-diol **3.47** by the Upjohn method ($OsO_4$/NMO) [170,171] in a yield of 50%, cf. scheme 3.7. The O'Brien group used modified Woodward conditions ($KIO_3$, $I_2$, KOAc) [172], however, the basic Amberlite resin used for the acetate hydrolysis was not available in the Nicolaou lab so an alternate method was used. The next step was a double TBS-protection leading to the bis-TBS ether **3.48** in an excellent yield of 93%. Bis-TBS ether **3.48** was then diastereoselectively epoxidized with *m*CPBA. O'Brien reported that the use of cyclohexane as solvent was crucial for the facial selectivity [169] and these conditions led to the formation of the wanted *trans*-epoxide **3.49** in a good yield of 89%. The

[3]This route was developed by former visiting PhD student Mette Terp Petersen.

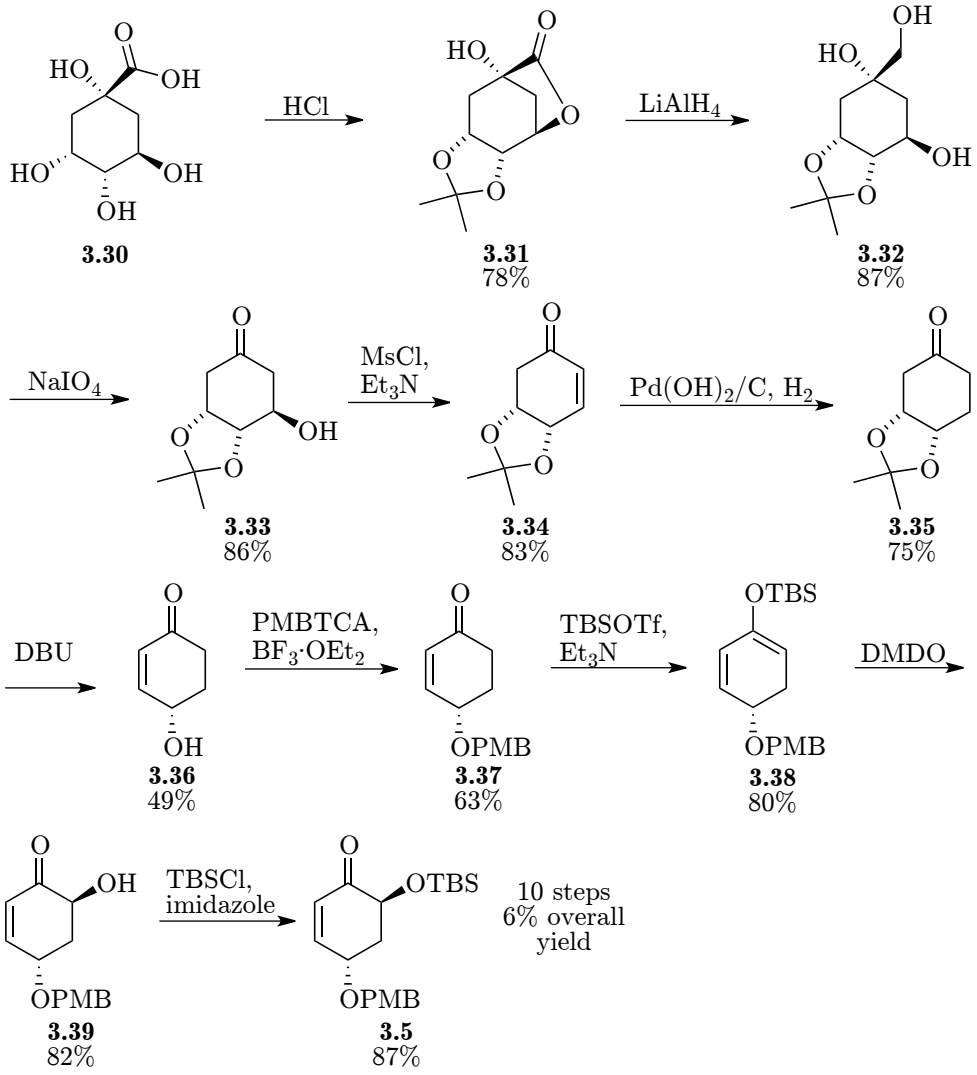


**Scheme 3.5:** Myers' route to cyclohexenone **3.5** starting from quinic acid **3.30**.

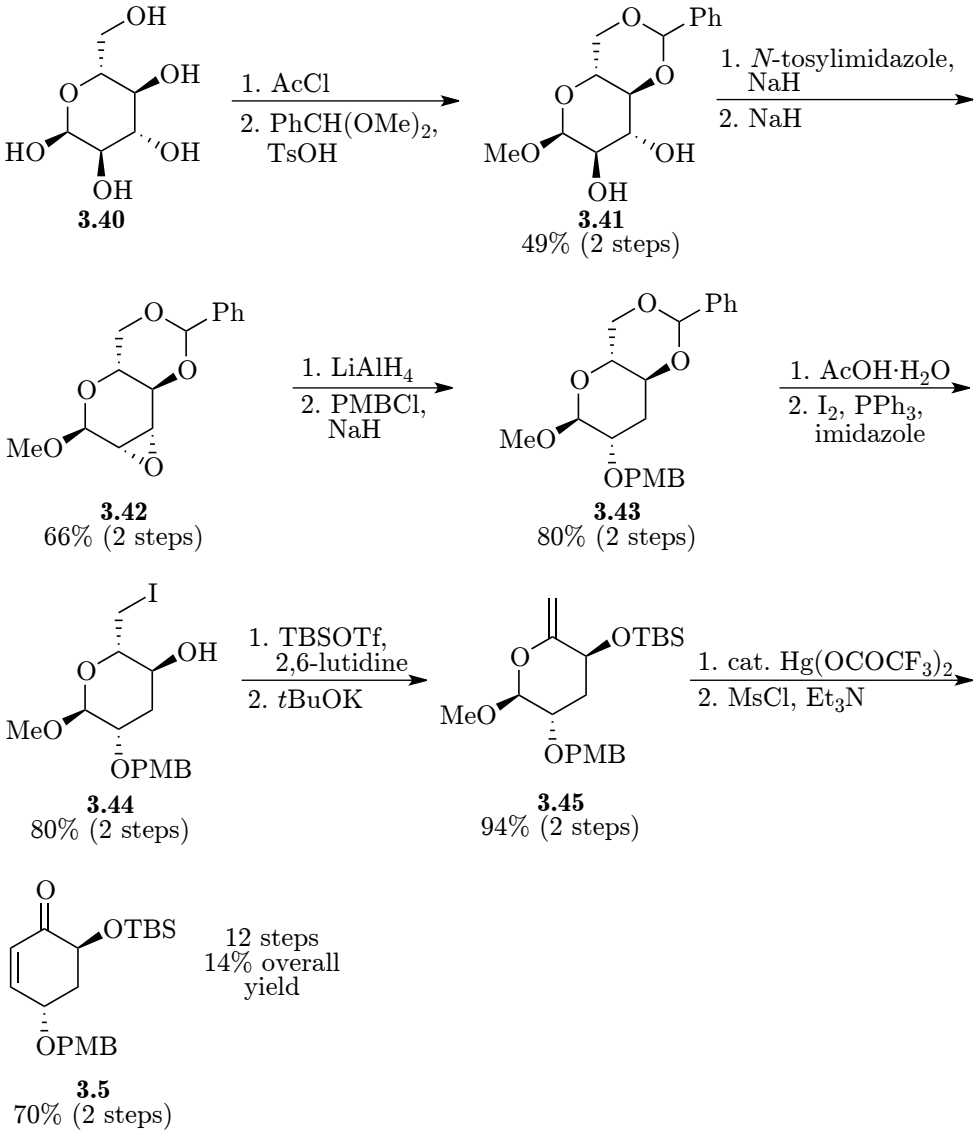


**Scheme 3.6:** Ueda's route to cyclohexenone **3.5** starting from D-glucose **3.40**.

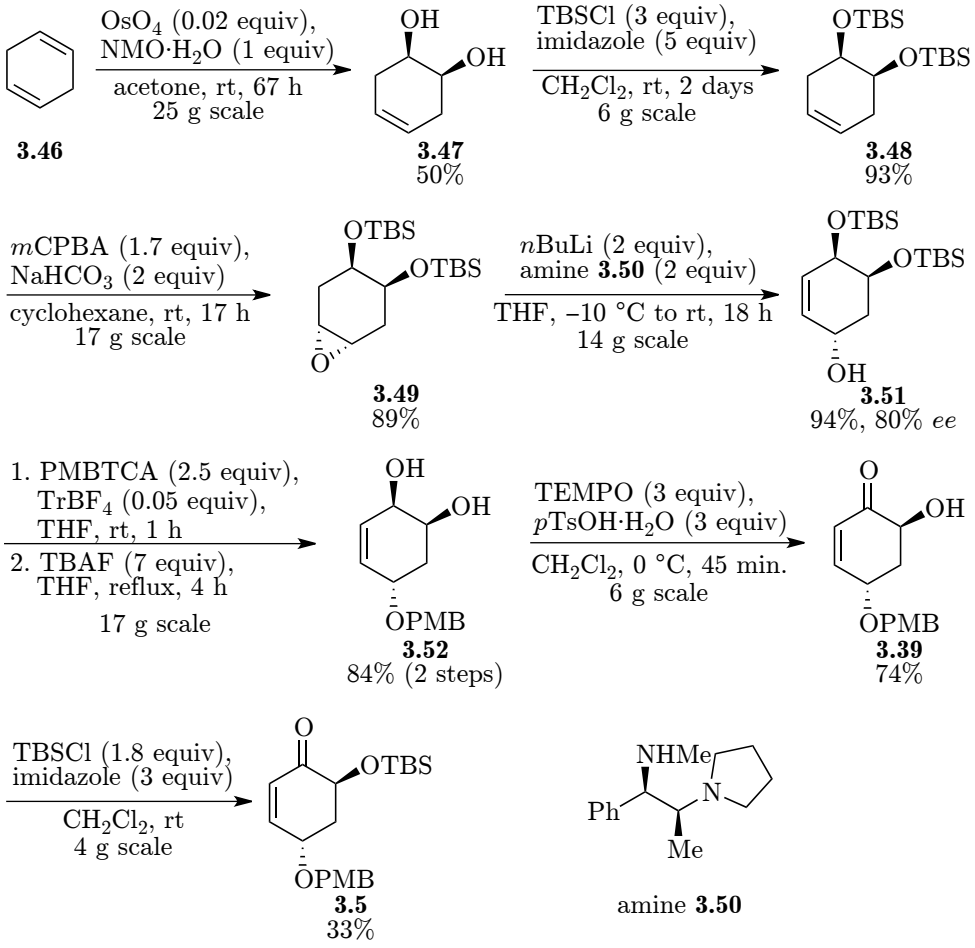


**Scheme 3.7:** The new route developed in the K. C. Nicolaou lab for the synthesis of cyclohexenone **3.5**.

following enantioselective epoxide rearrangement was mediated by the (+)-norephedrine derived chiral amine **3.50** and provided allylic alcohol **3.51** in a high yield of 94%. The enantioselectivity was however significantly lower than what was originally reported by O'Brien (80% *ee* vs. 94% *ee*) leaving room for optimization. The next step was a one-pot PMB-protection, effected by PMBTCA and catalytic $TrBF_4$, and double TBS-deprotection with TBAF. Initially, a two step procedure was attempted but the intermediate PMB-protected bis-TBS ether was very difficult to purify due to the presence of several decomposition products from the PMBTCA. Deprotection of the two TBS-protected alcohols significantly changed the polarity of the product and thus greatly eased the purification resulting in isolation of the PMB-protected diol **3.52** in a good yield of 84%. The PMB-protected diol **3.52** was then subjected to allylic oxidation effected by TEMPO and *p*TsOH [173] leading

to the hydroxy ketone **3.39** in a good yield of 84%. The final TBS-protection however proceeded in disappointingly low yields and only provided the desired cyclohexenone **3.5** in a yield of 33% on a 4 g scale again leaving room for optimization.

The newly developed route to cyclohexenone **3.5** seemed very promising but the scalability still needed to be tested and the enantioselective epoxide rearrangement and final TBS-protection to be optimized. The dihydroxylation of 1,4-cyclohexadiene **3.46** under Upjohn conditions could be run on a 51 g scale without the yield dropping and actually provided diol **3.47** in a slightly higher yield of 61% on this scale, cf. scheme 3.8. The double TBS-protection of

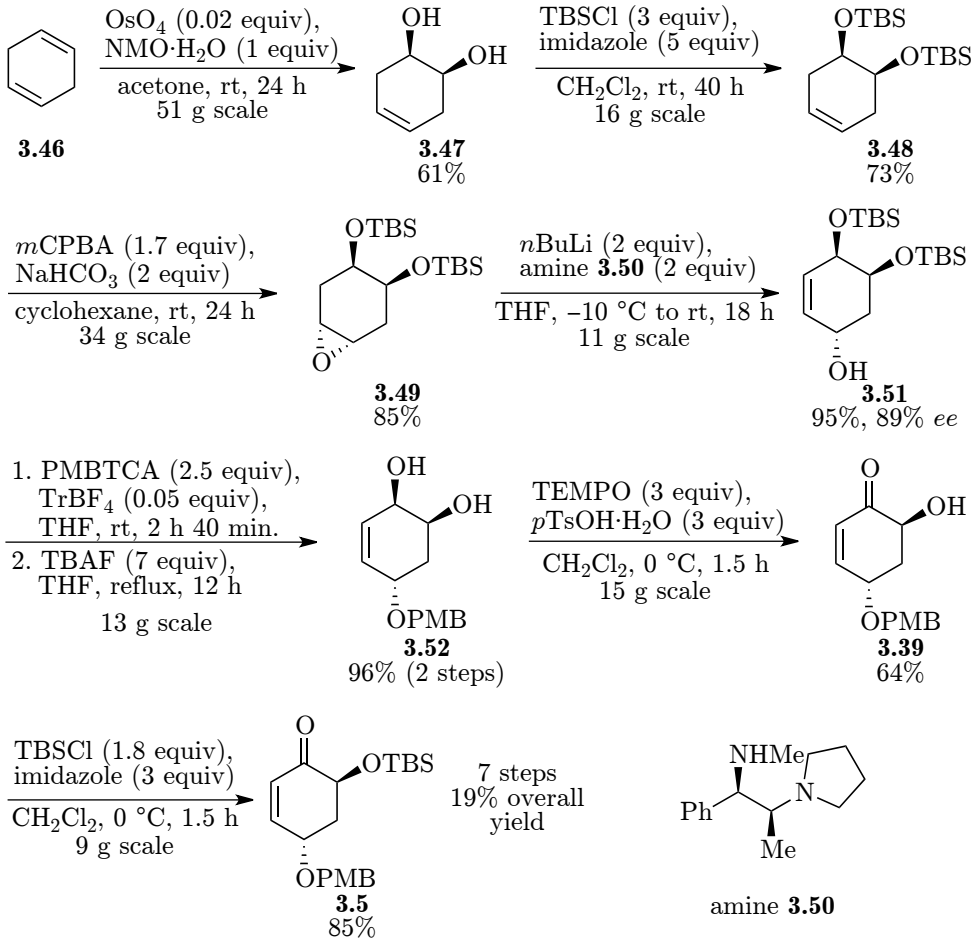


**Scheme 3.8:** Optimized conditions for the new route developed in the K. C. Nicolaou lab for the synthesis of cyclohexenone **3.5**.

diol **3.47** on a 16g scale (approx. three times the original scale) was associated with a slightly lower yield of 73%. This could, however, also be caused by a slightly higher amount of impurities left over from the dihydroxylation step

as the combined yield over the first two steps was comparable with what had originally been observed in the Nicolaou group (45% vs. 47%). The diastereoselective epoxidation effected by *m*CPBA could be run on a 34g scale, without decrease of either diastereoselectivity or yield, resulting in formation of epoxide **3.49** in a yield of 85% and thus confirming the scalability of the first three steps of the route.

The enantioselectivity of the epoxide rearrangement, leading to allylic alcohol **3.51**, as reported by O'Brien had been difficult to reproduce, so an investigation into this step was needed. It was found that a very high purity of the (+)-norephedrine derived chiral amine **3.50** was paramount for a high *ee* and extensive and tedious purification was necessary.[4] It was furthermore found that the scale of the reaction impacted the *ee*, cf. table 3.1. The yields

**Table 3.1:** Scale dependence of the enantioselectivity in the epoxide rearrangement of epoxide **3.49**.

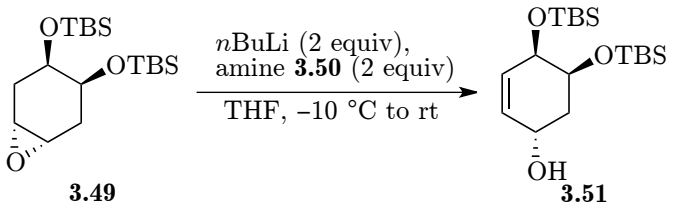


**3.49** **3.51**

| Entry | Scale | Yield (%)[a, b] | *ee* (%)[b] |
|---|---|---|---|
| 1 | 3.8 g | 95 | 89 |
| 2 | 5.4 g | 95 | 88 |
| 3 | 7.0 g | 92 | 85 |

[a] Isolated yield after flash column chromatography.
[b] Average of at least two reactions.

remained consistently high, but the *ee* decreased as the scale increased with the highest *ee* of 89% being obtained on a 3.8 g scale (entry 1). The reaction could however be run in several flasks simultaneously, and the reaction mixtures could be combined and worked-up together thus easing the throughput of material.

The one-pot PMB-protection/double TBS-deprotection was found to give a slightly higher yield at a scale a little smaller than originally reported in the Nicolaou group with reaction on a 13 g scale resulting in a high yield of 96% of PMB-protected diol **3.52** vs. the original 84% on a 17 g scale. The allylic oxidation leading to hydroxy ketone **3.39** was found to proceed in slightly lower yields on a larger scale with reaction on a 15 g scale (approx. three times the scale originally reported) proceeding with a yield of 64%.

[4] Usually 4–5 successive distillations of the (+)-norephedrine derived chiral amine **3.50** was necessary.

The final TBS-protection had been found to proceed in low yields under the conditions originally used by the Nicolaou group. Reproduction of these results with $CH_2Cl_2$ as the solvent confirmed this and led to yields around 50% at the most. It was however found that a change of solvent to DMF and performing the chromatographic purification as fast as possible greatly increased the yield leading to formation of the desired cyclohexenone building block **3.5** in a yield of 85% on a 9 g scale. Thus the synthesis was completed in an overall yield of 19% over seven steps and provided 11.6 g of product.

The optimized route to cyclohexenone **3.5**, proceeding in an overall yield of 19% in only seven steps and with 11.6 g of product produced was thus superior to the existing routes with regard to overall yield, step count and scalability, cf. table 3.2.

**Table 3.2:** Comparison of different routes to cyclohexenone **3.5**.

| Route | Starting material | No. of steps | Scale[a] | Overall yield |
|---|---|---|---|---|
| Myers 1 | L-malic acid | 10 | 1.3 g | 19% |
| Myers 2 | TBS-protected resorcinol | 7 | 0.3 g | 12% |
| Myers 3 | quinic acid | 10 | 30 mg | 6% |
| Ueda | D-glucose | 12 | 5.5 mg | 14% |
| Nicolaou | 1,4-cyclohexadiene | 7 | 11.6 g | 19% |

[a] Amount of cyclohexenone **3.5** produced.

## 3.3 Scale-Up of Cyanophthalide Building Block 3.6

The cyanophthalide building block **3.6** was needed for further investigations into the key step leading to the bicyclic polyoxygenated system present in **3.17**, cf. scheme 3.2. Furthermore, several intermediates on the way to **3.6** could possibly prove useful for later investigations into the installation of the allylic alcohol in **3.13** before the Hauser-Kraus annulation.

The route to cyanophthalide **3.6** was reproduced in large scale according to the literature procedure [151]. Thus 4-methylsalicylic acid **3.53** was subjected to MeI on a 74 g scale leading to ester **3.54**, cf. scheme 3.9. Substitution with AllBr and subsequent amidation through activation with $Al(Me)_3$ and reaction with $Et_2NH$ provided amide **3.56**, which was subjected to a neat Claisen rearrangement [174] leading to terminal olefin **3.57**, which after isomerization of the double bond provided phenol **3.58** in a yield of 66% over five steps without purification of intermediates. A MOM-protection on a 65 g scale followed affording the MOM ether **3.59** in a quantitative yield. The subsequent *ortho*-lithiation was performed on a smaller scale of 23 g due to safety considerations and provided aldehyde **3.60** in a yield of 91% upon quenching with DMF. Finally, treating the aldehyde **3.60** with TMSCN, catalytic amounts of

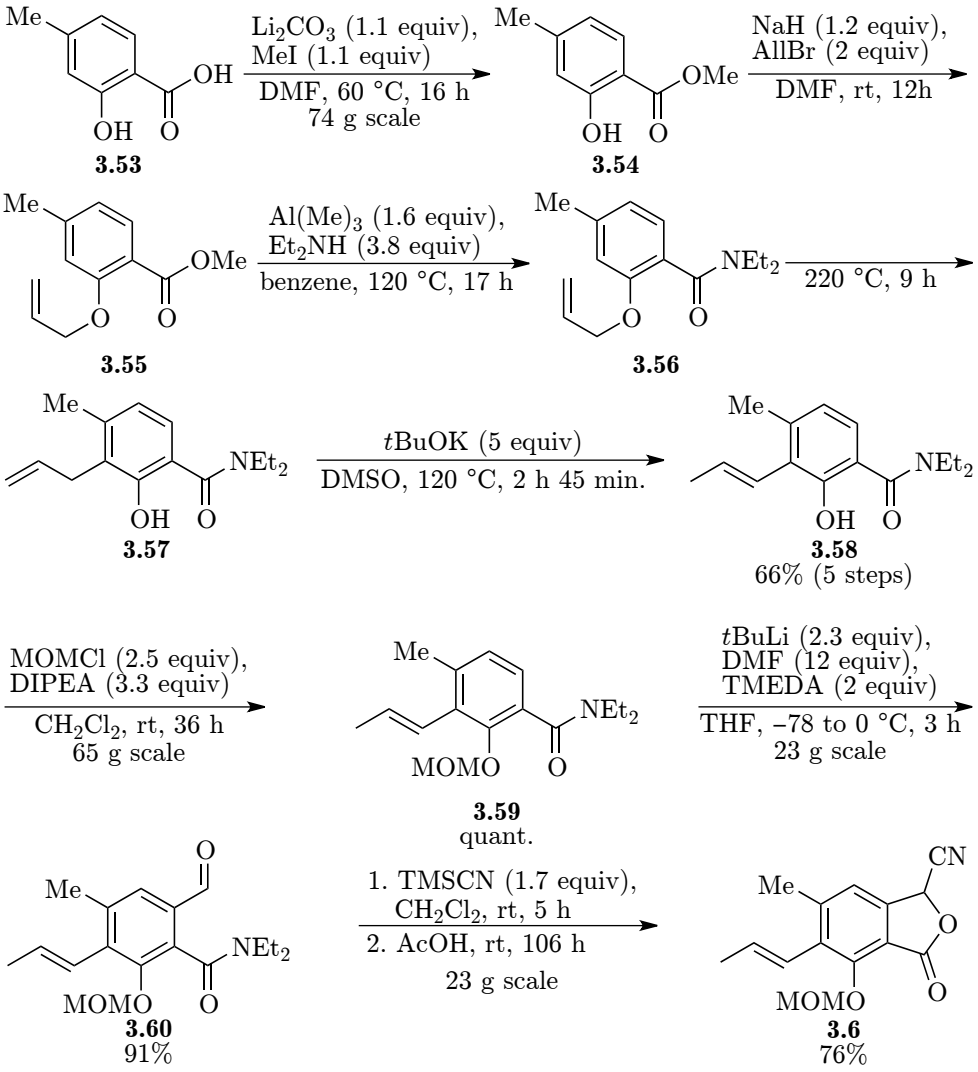


**Scheme 3.9:** Scale-up of cyanophthalide building block **3.6**.

KCN and 18-crown-6, on a 23 g scale, followed by exposure to AcOH provided cyanophthalide **3.6** in a yield of 76%.

## 3.4 Development of Route to TBS Ether Cyanophthalide Building Block 3.61

Due to low yields in the allylic oxidation of **3.12**, cf. scheme 3.2, primarily caused by low chemoselectivity resulting in oxidation of the benzylic methyl group when subjected to common allylic oxidation methods, investigations into a new strategy where the allylic alcohol was installed before the Hauser-Kraus was commenced, cf. scheme 3.10. Thus, a strategy for the synthesis of TBS ether cyanophthalide **3.61** was needed.

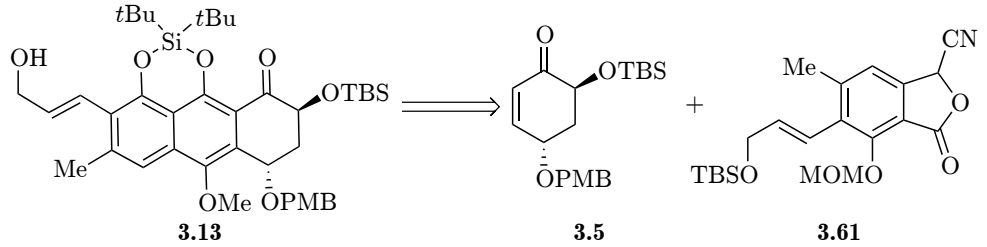


**Scheme 3.10:** Retrosynthetic analysis for the the Hauser-Kraus annulation of allylic alcohol **3.13**.

### 3.4.1 Attempts at synthesis of TBS ether cyanophthalide 3.61 via an isomerization/oxidation approach

The first attempted strategy relied on a isomerization/oxidation strategy inspired by a recent paper by the Jiang group, where they report the palladium-catalyzed transformation of terminal olefins into allylic aldehydes [175]. Thus phenol **3.57** was MOM-protected in a yield of 94%, cf. scheme 3.11. With

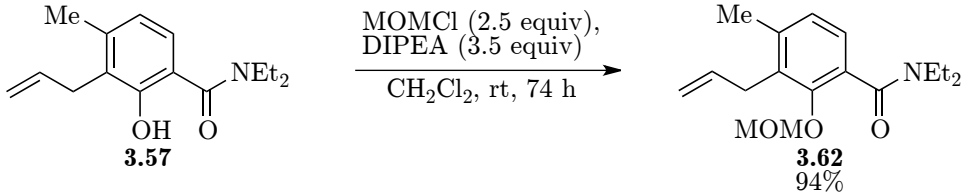


**Scheme 3.11:** MOM-protection of phenol **3.57**.

MOM ether **3.62** in hand the formation of allylic aldehyde **3.63** with DDQ, $H_2O$ and catalytic amounts of $PdCl_2$, as reported by Jiang, was attempted, cf. scheme 3.12. However, neither at rt nor at 50 °C was the desired al-

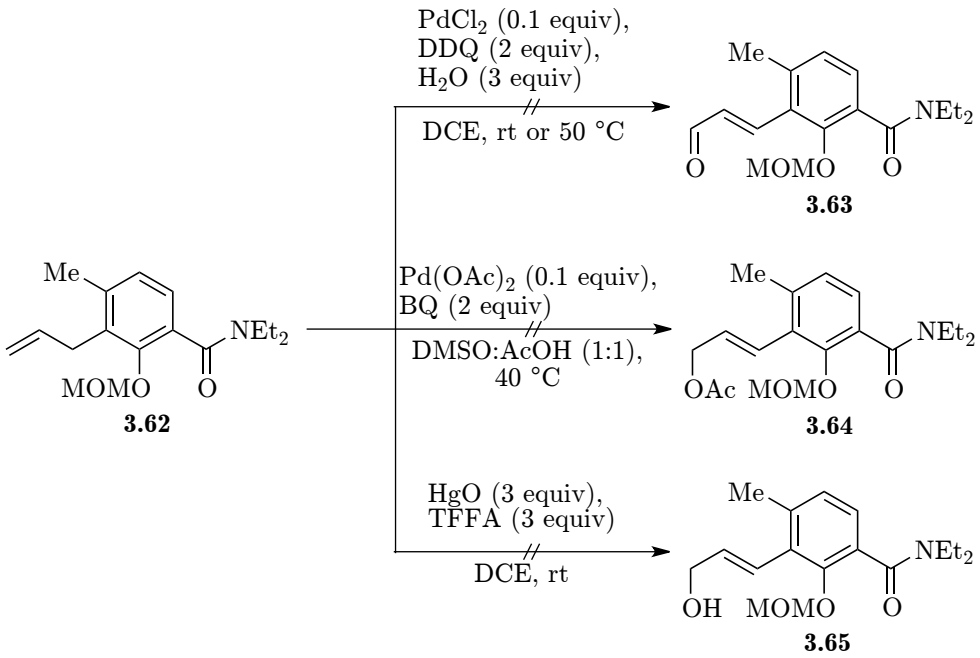


**Scheme 3.12:** Attempted isomerization/oxidation of MOM ether **3.62**.

lylic aldehyde **3.63** observed. When cyanophthalide **3.6** was subjected to the same conditions complete decomposition of starting material was observed, cf. scheme 3.13. Upon exposure to the same conditions, MOM ether **3.59** led to allylic alcohol **3.65**, however only in a very low yield (<10%), cf. scheme 3.13.

Another report by the White group detailed the formation of allylic acetates from terminal olefins effected by $Pd(OAc)_2$ and BQ, cf. scheme 3.12. However, none of the desired allylic acetate **3.64** was isolated. The last attempt at an isomerization/oxidation was a HgO mediated installation of an allylic alcohol.[5] The allylic alcohol **3.65** was however not observed.

As no successful conditions for an oxidative installment of the allylic alcohol had been found this strategy was abandoned.

### 3.4.2 Synthesis of TBS ether cyanophthalide 3.61 via a Stille cross-coupling approach

A new strategy comprising a Stille cross-coupling [176–178] was outlined, cf. scheme 3.14. Thus, TBS ether cyanophthalide **3.61** would originate from stannane **3.67** and iodocyanophthalide **3.68**, which could be accessed from cyanophthalide **3.69** by MOM-protection and iodination. Cyanophthalide **3.69** could ultimately be synthesized from 4-methylsalicylic acid **3.53** by

[5]These reaction conditions was based on prior experience within the group.

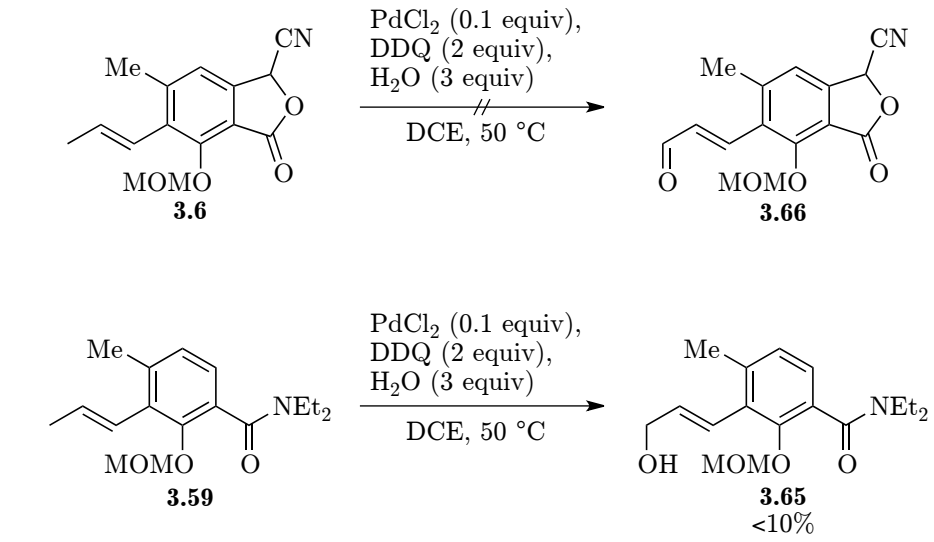


**Scheme 3.13:** Attempted allylic oxidation of MOM ethers **3.6** and **3.59**.

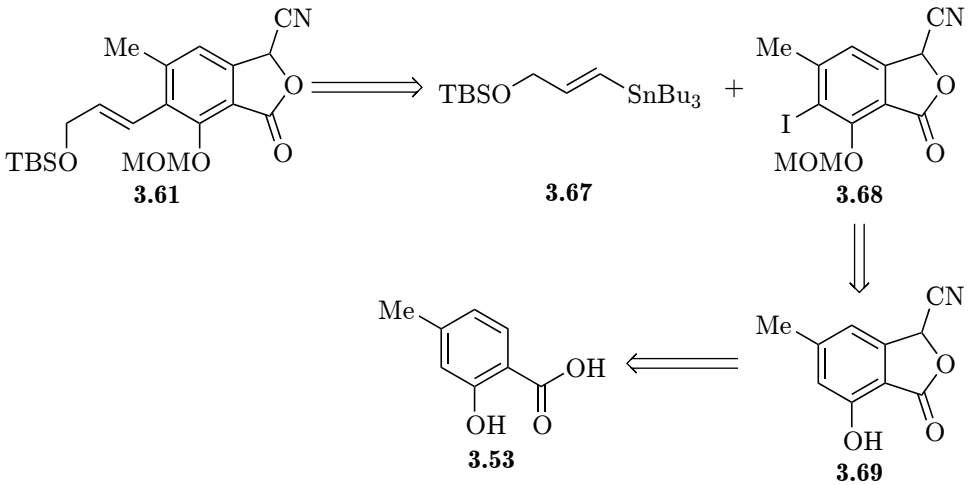


**Scheme 3.14:** Retrosynthetic analysis for TBS ether cyanophthalide **3.61** with a Stille cross-coupling as the key step.

a known procedure[6] [179]. In connection with an earlier synthetic strategy for the total synthesis of trioxacarcin DC-45-A2 **3.1** in the Nicolaou group, the iodination had been attempted before cyanophthalide formation, cf. scheme 3.15. However, all attempts at iodination of either ester **3.54** or

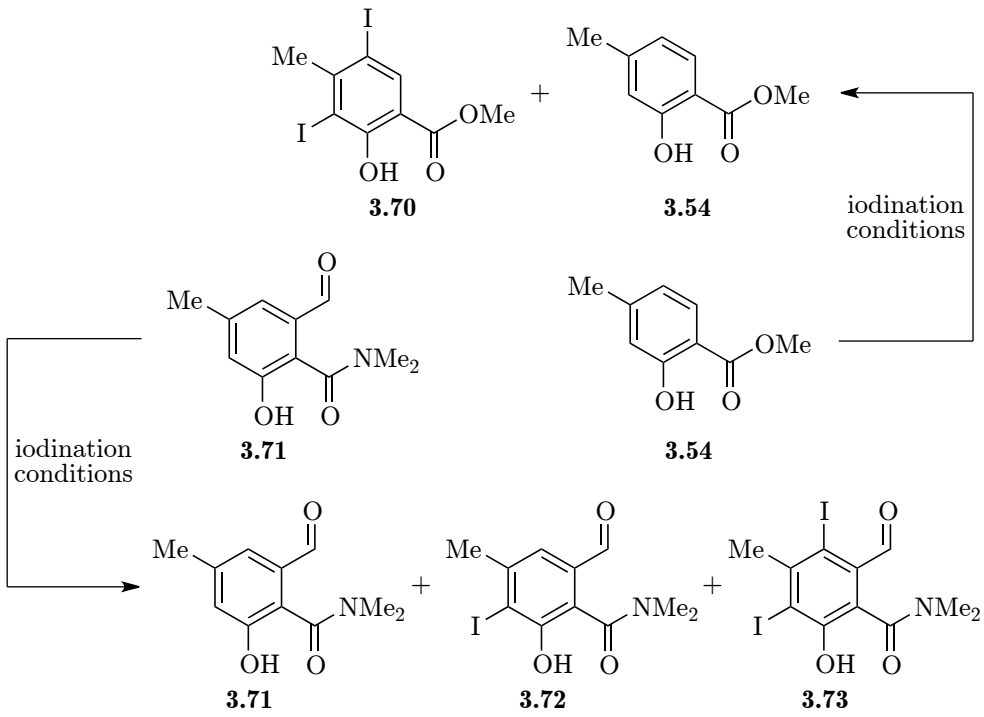


**Scheme 3.15:** Unsuccessful attempts at monoiodination of ester **3.54** and aldehyde **3.71**.

aldehyde **3.71** led to inseparable mixtures of the starting materials, mono- and diiodinated products. Thus, it was decided to install the iodide moiety after cyanophthalide formation.

Cyanophthalide **3.69** was MOM-protected in a yield of 86%, cf. scheme 3.16. With MOM cyanophthalide **3.74** in hand the next step was the iodination leading to iodocyanophthalide **3.68**. The desired iodocyanophthalide was not observed when MOM cyanophthalide **3.74** was exposed to either NIS or $I_2$, cf. scheme 3.17. Subjection of non MOM-protected cyanophthalide **3.69** to $I_2$ with either NMM or DIPEA as base did not provide the desired monoiodinated product either, cf. scheme 3.18. Exposure of cyanophthalide **3.69** to NIS did, however, lead to formation of monoiodinated cyanophthalide **3.75**. The purification of iodocyanophthalide **3.75** proved to be very difficult and thus a one-pot iodination and MOM-protection procedure was employed resulting in a less difficult purification, cf. scheme 3.19. The iodocyanophthalide

[6]Cyanophthalide **3.69** was available in the group.

Synthesis of TBS ether cyanophthalide **3.61** via a Stille cross-coupling approach

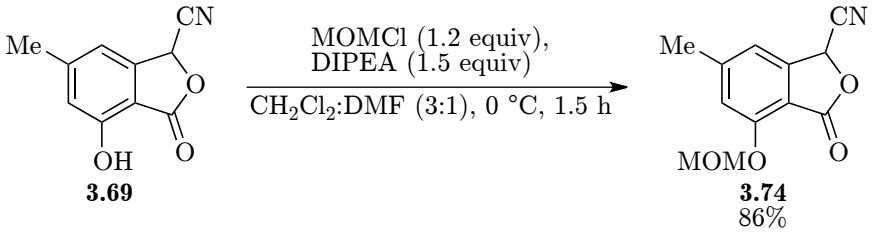


**Scheme 3.16:** MOM-protection of cyanophthalide **3.69**.

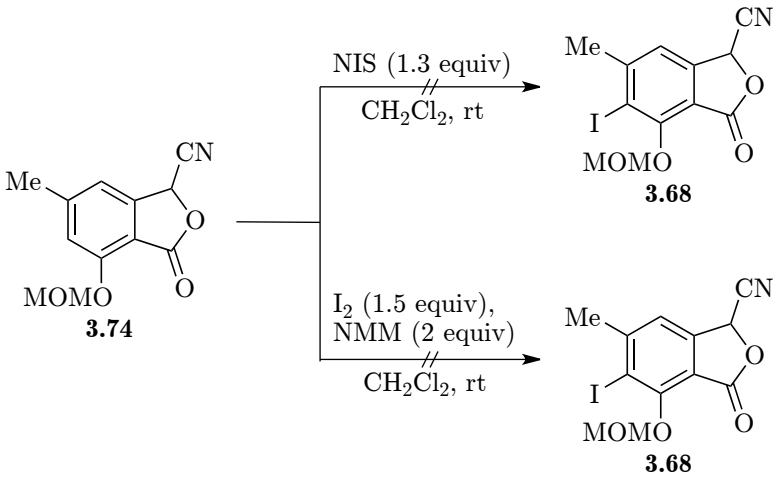


**Scheme 3.17:** Attempts at iodination of MOM cyanophthalide **3.74**.

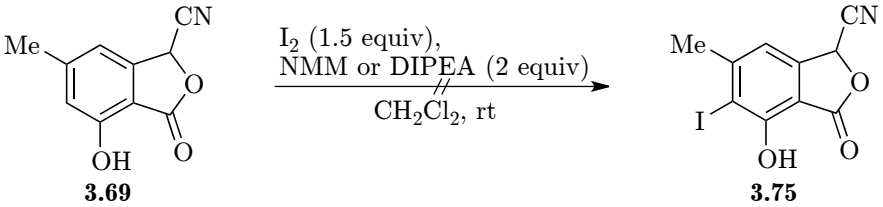


**Scheme 3.18:** Attempts at iodination of cyanophthalide **3.69** with $I_2$.

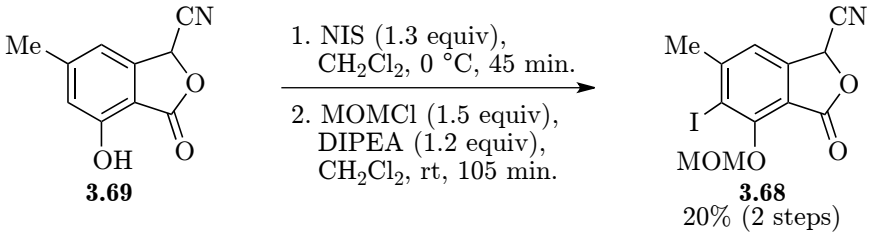


**Scheme 3.19:** One-pot iodination and MOM-protection of cyanophthalide **3.69**.

**3.68** was isolated in a yield of 20% over two steps with the diiodinated product being a major side product. Due to time constraints this result was not optimized any further.

With iodocyanophthalide **3.68** in hand all that remained for the successful synthesis of TBS ether cyanophthalide **3.61** was the stannane **3.67** and the final Stille cross-coupling between the two building blocks. Konoike reported that stannane **3.67** could be accessed from TBS-protected propargyl alcohol **3.76** by hydrostannylation with AIBN and $Bu_3SnH$ in refluxing benzene for 20 min. in a yield of 85%. This result was however not reproducible, with the reported conditions leading to a nearly inseparable mixture of the *trans* and *cis* isomers more akin to what Corey reported when subjecting non TBS-protected propargyl alcohol to the same conditions [180]. It was found that prolonged reaction times favored the *trans* isomer and after 16 h in refluxing benzene the stannane **3.67** was isolated in a yield of 38% with minor amounts of the *cis* isomer present, cf. scheme 3.20.

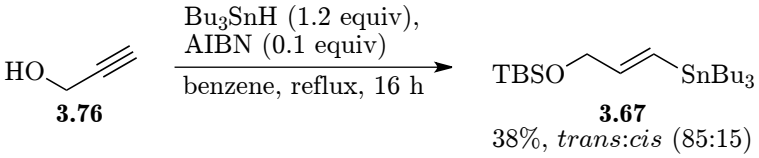


**3.76** **3.67**
38%, *trans*:*cis* (85:15)

**Scheme 3.20:** Hydrostannylation of TBS-protected propargyl alcohol **3.76**.

Everything was now set up for the final Stille cross-coupling leading to TBS ether cyanophthalide **3.61**. Initially, iodocyanophthalide **3.68** and stannane **3.67** was subjected to cross-coupling in toluene at rt catalyzed by $Pd(PPh_3)_4$, cf. scheme 3.21, however, no formation of the desired product **3.61** was observed. Changing the solvent to refluxing benzene did not lead to product formation either, but the use of refluxing toluene rewardingly led to the formation of the desired TBS ether cyanophthalide **3.61** in a moderate yield of 42%.[7]

## 3.5 Total Synthesis

The rest of the total synthesis was finished by the other members of the trioxacarcin team in the Nicolaou lab [145]. Commencing with a Hauser-Kraus annulation of building blocks **3.5** and **3.68** followed by methylation provided the core structure **3.77**, cf. scheme 3.22. MOM-deprotection followed by bis-

[7]Due to a hot plate malfunction the reaction was kept running longer than intended and slight decomposition of the product was observed when the reaction was stopped. Thus the yield would likely have been higher if the reaction had been stopped earlier. Since the reaction was performed during the last days of the external stay in the Nicolaou group there was no time left to run the reaction again.

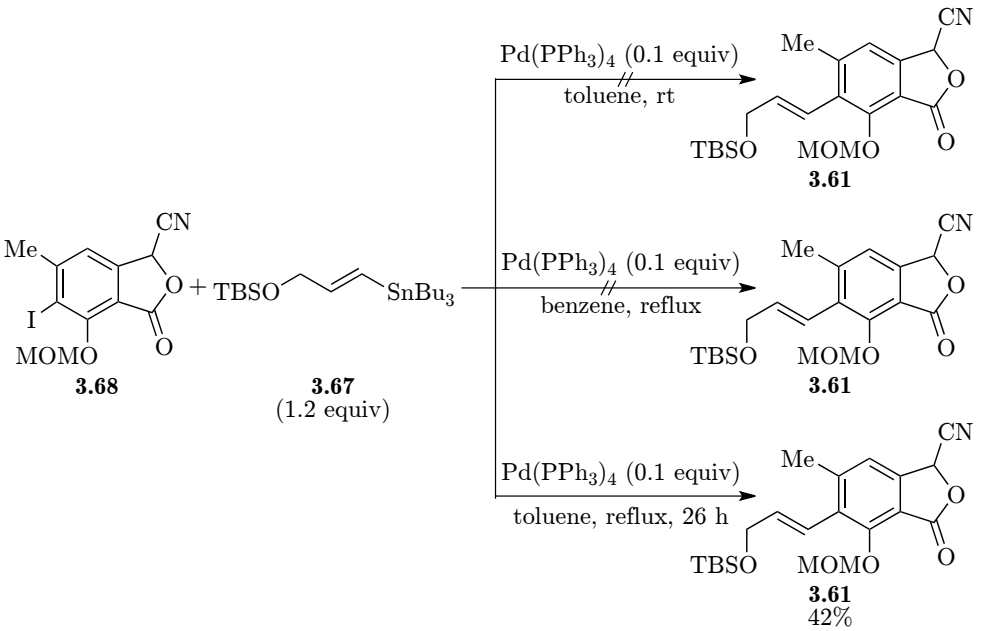


**Scheme 3.21:** Stille cross-coupling of iodocyanophthalide **3.68** and stannane **3.67**.

silylation led to iodide **3.78**, which was then subjected to Stille cross-coupling[8] with stannane **3.68** followed by a TEMPO oxidation leading to allylic aldehyde **3.79**. An enantioselective Jørgensen epoxidation [181], a Baylis-Hilman reaction [182,183] and a TMS protection provided the key cyclization precursor **3.82**.

Everything was now set for the key epoxide rearrangement leading to the bicyclic polyoxygenated system. Cyclization precursor **3.82** was exposed to $BF_3 \cdot OEt_2$ leading to formation of the desired product in a satisfying yield of 54%, cf. scheme 3.23.

TMS deprotection followed by a three step epoxidation sequence, comprised of dihydroxylation, tosylation and elimination, afforded epoxide **3.84**, which after TEMPO-mediated oxidation and silyl-deprotection underwent cyclization to form the tricyclic polyoxygenated system in **3.11**. Final removal of the PMB and TBS protection groups provided the coveted trioxacarcin DC-45-A2 **3.1**.

## 3.6 Conclusion

The total synthesis of trioxacarcin DC-45-A2 by the Nicolaou group employed distinct features comprising, among others, a Stille cross-coupling, a Baylis-

[8] In the final total synthesis the Stille cross-coupling was performed after the Hauser-Kraus annulation instead of before as outlined in §3.4.2.

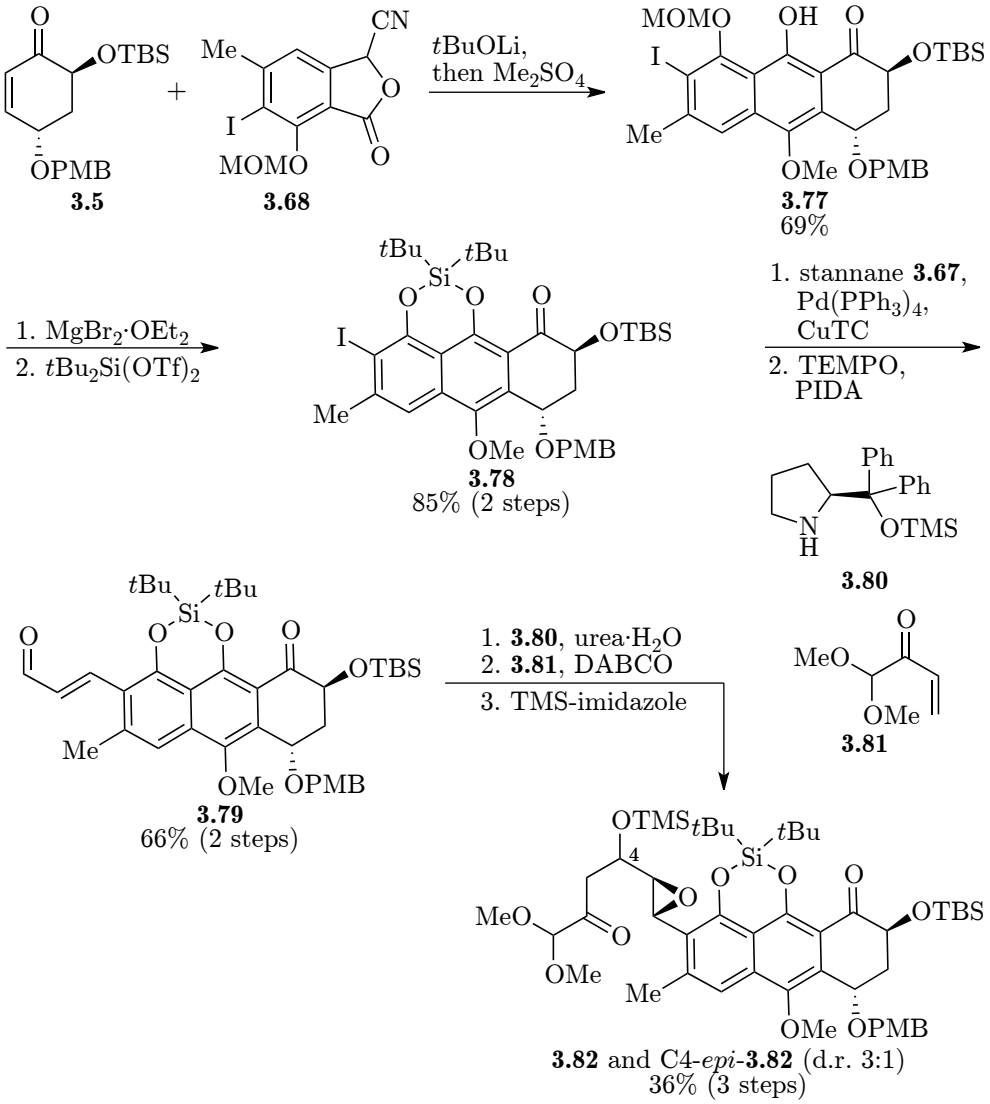


**Scheme 3.22:** Total synthesis of trioxacarcin DA-45-A2 **3.1** by Nicolaou. Synthesis of key cyclization precursor **3.82**

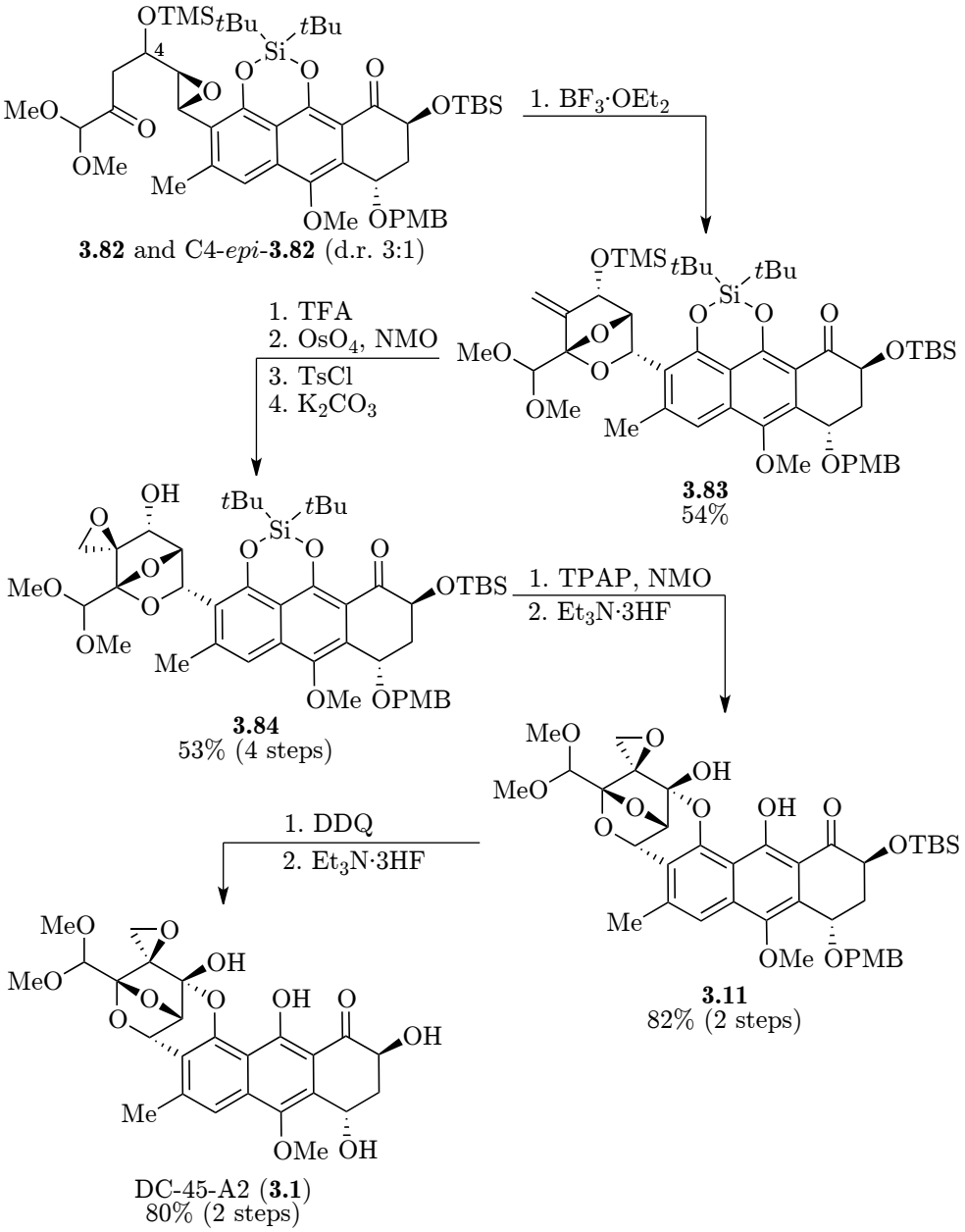


**Scheme 3.23:** Total synthesis of trioxacarcin DA-45-A2 **3.1** by Nicolaou. Key step and end game.

Hilman reaction and an improved strategy for the formation of tricyclic polyoxygenated system present in trioxacarcin DC-45-A2. Myers' key step, a rhodium mediated 1,3-dipolar cycloaddition, featured poor diastereoselectivity and a low yield of 28% whereas the epoxide rearrangement utilized by the Nicolaou group showed better diastereoselectivity and afforded **3.83** in a yield of 54%.

Nicolaou's synthesis furthermore included a new route for cyclohexenone **3.5** that, upon optimization, featured distinct and high yielding steps and thus provided superior access to this key building block in terms of overall yield, step count and scalability.

Overall, the synthetic strategy developed by Nicolaou was an improvement in terms of diastereoselectivity and yield of the key step and provided improved access to the key building block cyclohexenone **3.5** thus easing the throughput of material.

## 3.7 Experimental

### 3.7.1 General methods

Reagents were purchased at the highest commercial quality and used without further purification, unless otherwise noted. All reactions were carried out under an argon atmosphere with dry solvent under anhydrous conditions, unless otherwise noted. Dry solvents were obtained by passing commercially available pre-dried, oxygen-free formulations through activated alumina columns. Yields refer to chromatographically and spectroscopically ($^1$H NMR) homogeneous material, unless otherwise stated.

Reactions were monitored by thin-layer chromatography (TLC) carried out on 0.25 mm E. Merck silica gel plates (60F254) using UV light as visualizing agent or an aqueous solution of phosphomolybdic acid and cerium sulfate or a basic aqueous solution of potassium permanganate and heat as developing agents. Acros Organics silica gel (60, particle size 0.035–0.070 mm) was used for flash column chromatography.

NMR spectra were recorded on a Bruker Avance III HD 600 MHz instrument equipped with a 5 mm DCH cryoprobe. The chemical shifts ($\delta$) are reported in parts per million (ppm) and the coupling constants ($J$) in Hz. For spectra recorded in DMSO-$d_6$, signal positions were measured relative to the signal for DMSO ($\delta$ 2.50 ppm for $^1$H NMR and $\delta$ 39.43 ppm for $^{13}$C NMR). For spectra recorded in $CDCl_3$, signal positions were measured relative to the signal for $CHCl_3$ ($\delta$ 7.26 ppm for $^1$H NMR and $\delta$ 77.0 ppm for $^{13}$C NMR).

Infrared (IR) spectra were recorded on a Perkinâ^'Elmer 100 FT-IR spectrometer. High-resolution mass spectra (HRMS) were recorded on an Ion Trap-Time of Flight Mass Spectrometer (Shimadzu, Columbia, MD) operated with an ESI source interface and a VG ZAB-ZSE mass spectrometer using MALDI (matrix-assisted laser-desorption ionization) or ESI (electrospray ionization).

Optical rotations were recorded on a Schmidt+Haensch Polartronic M100 polarimeter at 589.44nm using 100mm cells and the solvent and concentration indicated.

### 3.7.2 Synthesis of cyclohexenone building block 3.5

**Diol 3.47**. 1,4-cyclohexadiene **3.46** (51.18 g, 638.7 mmol) was dissolved in acetone (1.5 L) and $NMO \cdot H_2O$ (86.34 g, 638.8 mmol) and $OsO_4$ (4% (w/v) aq. solution, 82.0 mL, 12.9 mmol) were added. The reaction mixture was stirred at rt for 24 h. $Na_2SO_3$ (50 g) and $MgSO_4$ (200 g) was then added and the mixture was stirred for 1 h at rt whereupon it was filtered through a short pad of silica gel, rinsed with EtOAc and concentrated *in vacuo* to give the title compound as a black solid (44.71 g, 61%). $R_f = 0.22$ (EtOAc); $^1$H NMR ($CDCl_3$, 600 MHz) $\delta$ 5.58 (t, $J$ = 1.8 Hz, 2H), 3.94 (t, $J$ = 6.0 Hz, 2H), 2.36

(dd, $J = 16.2, 6.0$ Hz, 2H), 2.25 (dd, $J = 16.2, 6.0$ Hz, 2H), 2.20 (br s, 1H), 2.17 (br s, 1H). $^1$H NMR spectroscopic data were consistent with those in the literature [171].

**Bis-TBS ether 3.48**. Diol **3.47** (15.65 g, 137.1 mmol) was dissolved in $CH_2Cl_2$ (350 mL) and imidazole (46.68 g, 685.7 mmol) and TBSCl (62.11 g, 412.1 mmol) were added. The reaction mixture was stirred at rt for 40 h and was then washed with water (2 × 200 mL) whereupon the combined aqueous layers were extracted with $CH_2Cl_2$ (5 × 200 mL). The combined organic phases were then dried over $MgSO_4$ and the solvent was removed *in vacuo*. The residue was then purified by flash column chromatography on silica gel (hexanes) to give the title compound as a colorless oil (34.09g, 73%). $R_f = 0.39$ (EtOAc:hexanes (1:100)); $^1$H NMR ($CDCl_3$, 600 MHz) $\delta$ 5.50 (t, $J = 1.8$ Hz, 2H), 3.84 (t, $J = 5.4$ Hz, 2H), 2.21 (dd, $J = 16.2, 6.6$ Hz, 2H), 2.13 (dd, $J = 16.2, 5.4$ Hz, 2H), 0.88 (s, 18H), 0.06 (s, 6H), 0.05 (s, 6H). $^1$H NMR spectroscopic data were consistent with those in the literature [168].

**Epoxide 3.49**. Bis-TBS ether **3.48** (34.09 g, 99.48 mmol) was dissolved in cyclohexane (1.1 L) and $NaHCO_3$ (16.72 g, 199.0 mmol) and then *m*CPBA (41.70g, ca. 30% water content, 169.1mmol) in portions. The reaction mixture was stirred at rt for 24 h. Then the reaction was quenched with 10% $Na_2SO_3$ (aq) (800 mL) and water (300 mL). The layers were separated and the aqueous layer was extracted with $CH_2Cl_2$ (5 × 200 mL). The combined organic phases were then dried over $MgSO_4$ and the solvent was removed *in vacuo*. The residue was then purified by flash column chromatography on silica gel (EtOAc:hexanes (1:50)) to give the title compound as a colorless oil (30.43 g, 85%). $R_f = 0.34$ (EtOAc:hexanes (1:30)); $^1$H NMR ($CDCl_3$, 600 MHz) $\delta$ 3.67 (t, $J = 5.1$ Hz, 2H), 3.15 (s, 2H), 2.07–1.99 (m, 4H), 0.89 (s, 18H), 0.05 (s, 6H), 0.04 (s, 6H). $^1$H NMR spectroscopic data were consistent with those in the literature [168].

**Allylic alcohol 3.51**. Chiral amine **3.50** (3 × 4.568 g, 3 × 20.92 mmol) was dissolved in THF (3 × 15 mL) in three flasks and the solutions were cooled to 0 °C. *n*BuLi (2.5 M in hexanes, 3 × 8.37 mL, 3 × 20.9 mmol) was added dropwise over 5 min. After 55 min. the reaction mixtures was cooled to −10 °C and solutions of epoxide **3.49** (3 × 3.752 g, 3 × 10.46 mmol) in THF (3 × 15 mL) were added dropwise over 10 min. The reactions mixtures were allowed to warm to rt and stirred at this temperature overnight (18 h). The reaction mixtures were then quenched with sat. $NH_4Cl$ (3 × 10 mL) and combined. The resulting mixture was extracted with $Et_2O$ (3 × 120 mL) and the combined organic phases were washed with 2% HCl (aq) (3 × 120 mL), sat. $NaHCO_3$ (aq) (3 × 120 mL) and brine (80 mL), dried over $MgSO_4$ and the solvent was removed *in vacuo*. The residue was then purified by flash column chromatography on silica gel (EtOAc:hexanes (1.5:8.5)) to give the title compound as a white solid (10.64g, 95%, 89% *ee* by Mosher ester analysis [184]). $R_f = 0.31$ (EtOAc:hexanes (1:4)); $^1$H NMR ($CDCl_3$, 600 MHz) $\delta$ 5.74 (dd, $J = 10.1, 2.9$ Hz, 1H), 5.65 (dd, $J = 10.1, 3.3$ Hz, 1H), 4.47–4.42 (m, 1H),

4.15–4.12 (m, 1H), 4.09–4.05 (m, 1H), 2.27 (ddd, $J = 13.2, 8.0, 5.3$ Hz, 1H), 1.57 (ddd, $J = 13.2, 6.3, 2.1$ Hz, 1H), 1.44 (s, 1H), 0.90 (s, 9H), 0.89 (s, 9H), 0.08 (s, 3H), 0.08 (s, 3H), 0.08 (s, 3H), 0.07 (s, 3H). $^1$H NMR spectroscopic data were consistent with those in the literature [168].

**PMB-ether diol 3.52**. Allylic alcohol **3.51** (12.90 g, 35.97 mmol) and $TrBF_4$ (0.5946 g, 1.801 mmol) were dissolved in THF (380 mL) and then freshly prepared PMBTCA (25.41 g, 89.93 mmol) was added dropwise. The reaction mixture was stirred at rt for 2 h 40 min. whereupon TBAF (1 M in THF, 252 mL, 252 mmol) was added and the reaction mixture was heated to reflux for 12 h. The reaction mixture was concentrated on silica gel (400 g) *in vacuo* and purified by flash column chromatography on silica gel (acetone:pentane (1:3)→(2:3)) to give the title compound as an orange solid (8.67 g, 96%). $R_f = 0.39$ (acetone:pentane (2:3)); $^1$H NMR ($CDCl_3$, 600 MHz) $\delta$ 7.26 (d, $J = 8.2$ Hz, 2H), 6.87 (d, $J = 8.3$ Hz, 2H), 5.97 (dd, $J = 10.2, 2.0$ Hz, 1H), 5.78 (dd, $J = 10.1, 2.7$Hz, 1H), 4.53 (d, $J = 11.3$Hz, 1H), 4.49 (d, $J = 11.3$Hz, 1H), 4.22–4.11 (m, 3H), 3.80 (s, 3H), 2.26 (s, 2H), 2.19 (ddd, $J = 13.3, 8.0, 5.0$ Hz, 1H), 1.82 (ddd, $J = 13.3, 6.0, 2.3$Hz, 1H); $^{13}$C NMR ($CDCl_3$, 150MHz) $\delta$ 159.2, 130.6, 130.4, 129.4, 129.3, 113.8, 70.9, 70.4, 67.4, 66.7, 55.3, 32.7; IR (neat) cm$^{-1}$: 3373, 3031, 2931, 2837, 1611, 1512, 1388, 1301, 1244, 1172, 1063, 1031, 823; HRMS (ESI-TOF) calcd for $C_{14}H_{18}NaO_4^+$ $[M + Na]^+$ 273.1097, found 273.1086; $[\alpha]_D^{25} = -135.3$ ($c = 1.0$, $CHCl_3$); m.p.: 84–85 °C.

**Hydroxyenone 3.39**. PMB-ether diol **3.52** (14.88 g, 59.45 mmol) was dispersed in $CH_2Cl_2$ and the resulting mixture was cooled to 0 °C whereupon $p$TsOH · $H_2O$ was added (33.93 g, 178.4 mmol). Then a solution of TEMPO (27.87 g, 178.4 mmol) in $CH_2Cl_2$ (40 mL was added dropwise over 15–20 min. at 0 °C. The reaction mixture was stirred at 0 °C for 70 min. whereupon sat. $NaHCO_3$ (aq) (500 mL) was added. The layers were separated and the organic phase was washed with sat. $NaHCO_3$ (aq) (500 mL). The combined aqueous phases were then extracted with $CH_2Cl_2$ (2 × 500 mL), dried over $MgSO_4$ and the solvent was removed *in vacuo*. The residue was then purified by flash column chromatography on silica gel (EtOAc:hexanes (1:3)) to give the title compound as an orange oil (9.47 g, 64%). $R_f = 0.40$ (EtOAc:hexanes (1:1)); $^1$H NMR ($CDCl_3$, 600 MHz) $\delta$ 7.28 (d, $J = 8.4$ Hz, 2H), 6.92–6.87 (m, 3H), 6.10 (d, $J = 10.0$ Hz, 1H), 4.68–4.61 (m, 2H), 4.53 (d, $J = 11.3$ Hz, 1H), 4.26–4.22 (m, 1H), 3.81 (s, 3H), 3.38 (s, 1H), 2.71–2.64 (m, 1H), 1.95 (td, $J = 13.0, 3.9$ Hz, 1H). $^1$H NMR spectroscopic data were consistent with those in the literature [158, 160].

**Cyclohexenone 3.5**. Hydroxyenone **3.39** (9.410 g, 37.90 mmol) was dissolved in DMF (190 mL) and the resulting mixture was cooled to 0 °C whereupon imidazole (7.745 g, 113.8 mmol) and TBSCl (10.29 g, 68.27 mmol) were added. The reaction mixture was stirred at 0 °C for 1.5 h. Brine (300 mL), water (300 mL) and EtOAc (400 mL) were added and the layers were separated. The combined organic phases were washed with water (2 × 400 mL). The combined aqueous phases were then extracted with EtOAc (2 × 400 mL). The

combined organic phases were dried over $Na_2SO_4$ and the solvent was removed *in vacuo*. The residue was then purified by flash column chromatography on silica gel (EtOAc:hexanes (1:4)) to give the title compound as a colorless oil (11.62 g, 85%). $R_f = 0.55$ (EtOAc:hexanes (1:4)); $^1$H NMR ($CDCl_3$, 600 MHz) $\delta$ 7.28 (d, $J = 8.5$ Hz, 2H), 6.90 (d, $J = 8.6$ Hz, 2H), 6.88–6.86 (m, 1H), 5.95 (d, $J = 10.2$ Hz, 1H), 4.60 (d, $J = 11.4$ Hz, 1H), 4.55 (d, $J = 11.4$ Hz, 1H), 4.39–4.34 (m, 2H), 3.81 (s, 3H), 2.32–2.19 (m, 2H), 0.88 (s, 9H), 0.10 (s, 3H), 0.09 (s, 3H). $^1$H NMR spectroscopic data were consistent with those in the literature [158, 160].

### 3.7.3 Synthesis of cyanophthalide building block 3.6

**Ester 3.54**. 4-methylsalicylic acid **3.53** (74.09 g, 487.0 mmol) was suspended in DMF (650 mL) at rt and then $Li_2CO_3$ (39.58 g, 535.7 mmol) and MeI (33.36 mL, 535.9 mmol). The reaction mixture was then heated to 60 °C and stirred for 16 h. Then ice water was added (650 mL) and the resulting mixture was extracted with EtOAc ($2 \times 1$ L). Then the combined organic phases were washed with water $2 \times 650$ mL) and brine (650 mL), dried over $Na_2SO_4$ and the solvent was removed *in vacuo*. The residue was then used directly in the next reaction without purification. $R_f = 0.14$ (EtOAc:hexanes (2:98)). The $R_f$-value was consistent with that in the literature [151].

**Allylic ether 3.55**. NaH (60% dispersion in mineral oil, 23.41g, 584.3mmol) was suspended in DMF (500 mL) at 0 °C and then allyl bromide (85.0 mL, 982 mmol) was added. Then a solution of the crude ester **3.54** (487.0 mmol) in DMF (250 mL) was added and the resulting mixture was stirred at 0 °C for 10 min. whereupon the reaction mixture was allowed to warm to rt. The reaction mixture was stirred at rt for 12 h.Then ice water was added (750 mL) and the resulting mixture was extracted with $Et_2O$ ($3 \times 750$ mL). Then the combined organic phases were washed with water ($3 \times 500$ mL) and brine (500 mL), dried over $Na_2SO_4$ and the solvent was removed *in vacuo*. The residue was then used directly in the next reaction without purification. $R_f = 0.17$ (EtOAc:hexanes (1:9)). The $R_f$-value was consistent with that in the literature [151].

**Amide 3.56**. $Et_2NH$ (192.0 mL, 1857 mmol) was dissolved in benzene (300 mL) and cooled to 0 °C whereupon $AlMe_3$ (2.0 M in toluene, 399.0 mL, 798.0 mmol) was added. The resulting mixture was stirred at 0 °C for 20 min. and was then allowed to warm to rt. Allylic ether **3.55** (487.0 mmol) was then added dropwise over 25 min. and the reaction mixture was heated to 120 °C and stirred for 17 h. The reaction mixture was then allowed to cool to rt and was then poured into a mixture of ice water (1.5 L) and 12 M HCl (aq) (30 mL) and the layers were separated. The aqueous phase was then extracted with EtOAc ($3 \times 1$ L). The combined organic phases were washed with water (1 L), sat. $NH_4Cl$ (aq) (500 mL) and brine (500 mL), dried over $Na_2SO_4$ and the solvent was removed *in vacuo*. The residue was then used directly in the next

reaction without purification. $R_f$ = 0.08 (EtOAc:hexanes (1:4)); $^1$H NMR ($CDCl_3$, 600 MHz) $\delta$ 7.08 (d, $J$ = 7.6 Hz, 1H), 6.77 (d, $J$ = 7.6 Hz, 1H), 6.68 (s, 1H), 6.03–5.93 (m, 1H), 5.37 (d, $J$ = 17.3 Hz, 1H), 5.22 (d, $J$ = 10.6 Hz, 1H), 4.52 (s, 2H), 3.71 (s, 1H), 3.38 (s, 1H), 3.21–3.10 (m, 2H), 2.33 (s, 3H), 1.22 (t, $J$ = 7.1 Hz, 3H), 1.01 (t, $J$ = 7.1 Hz, 3H). $^1$H NMR spectroscopic data were consistent with those in the literature [151].

**Phenol 3.57**. Amide **3.56** (487.0 mmol) was heated neat to 220 °C and stirred for 9h whereupon it was allowed to cool to rt. The residue was then used directly in the next reaction without purification. $R_f$ = 0.40 (EtOAc:hexanes (4:21)); $^1$H NMR ($CDCl_3$, 600 MHz) $\delta$ 10.14 (s, 1H), 7.06 (d, $J$ = 8.0 Hz, 1H), 6.66 (d, $J$ = 8.0 Hz, 1H), 5.97–5.93 (m, 1H), 5.02–4.97 (m, 2H), 3.52 (q, $J$ = 7.1 Hz, 4H), 3.48–3.45 (m, 2H), 2.29 (s, 3H), 1.27 (t, $J$ = 7.1 Hz, 6H). $^1$H NMR spectroscopic data were consistent with those in the literature [151].

**Phenol 3.58**. Phenol **3.57** (487.0 mmol) was dissolved in DMSO (500 mL) at rt and then *t*BuOK (273.4 g, 2437 mmol) was added. The reaction mixture was heated to 120 °C and stirred for 2 h 45 min. The reaction mixture was then allowed to cool to rt, diluted with water (450 mL) and acidified to pH 1 with 6 M HCl (aq) (350 mL). The mixture was extracted with EtOAc (2 × 750 mL). The combined organic phases were washed with water (5 × 750 mL) and brine (750 mL), dried over $Na_2SO_4$ and the solvent was removed *in vacuo*. The residue was then purified by flash column chromatography on silica gel (EtOAc:hexanes (1:9)) to give the title compound as a yellow oil (79.28 g, 66% over five steps). $R_f$ = 0.18 (EtOAc:hexanes (1:4)); $^1$H NMR ($CDCl_3$, 600 MHz) $\delta$ 9.94 (s, 1H), 7.01 (d, $J$ = 7.9 Hz, 1H), 6.66 (d, $J$ = 8.0 Hz, 1H), 6.44–6.38 (m, 1H), 6.23 (dq, $J$ = 16.0, 6.5 Hz, 1H), 3.49 (q, $J$ = 7.1 Hz, 4H), 2.32 (s, 3H), 1.94 (dd, $J$ = 6.5, 1.7 Hz, 3H), 1.25 (t, $J$ = 7.1 Hz, 6H). $^1$H NMR spectroscopic data were consistent with those in the literature [151].

**MOM ether 3.59**. Phenol **3.58** (65.13 g, 263.3 mmol) was dissolved in $CH_2Cl_2$ (600 mL) and cooled to 0 °C whereupon DIPEA (150 mL, 861 mmol) and MOMCl (50.0 mL, 658 mmol) were added and the resulting mixture was stirred at 0°C for 20 min. The reaction mixture was then allowed to warm to rt and was then stirred for 36 h. Then water (1.1 L) was added and mixture was extracted with $CH_2Cl_2$ (3 × 1.1 L). The combined organic phases were washed with brine (1.1 L), dried over $Na_2SO_4$ and the solvent was removed *in vacuo*. The residue was then purified by flash column chromatography on silica gel (EtOAc:hexanes (1:1)) to give the title compound as a yellow oil (76.73 g, quant.). $R_f$ = 0.20 (EtOAc:hexanes (1:3)); $^1$H NMR ($CDCl_3$, 600 MHz) $\delta$ 6.99–6.93 (m, 2H), 6.40 (d, $J$ = 16.3 Hz, 1H), 6.05 (dq, $J$ = 16.0, 6.5 Hz, 1H), 5.01–4.90 (m, 2H), 3.67 (s, 1H), 3.48 (s, 3H), 3.42 (s, 1H), 3.23 (d, $J$ = 5.4 Hz, 1H), 3.14 (s, 1H), 2.31 (s, 3H), 1.91 (dd, $J$ = 6.6, 1.3 Hz, 3H), 1.23 (t, $J$ = 7.1 Hz, 3H), 1.04 (t, $J$ = 7.1 Hz, 3H). $^1$H NMR spectroscopic data were consistent with those in the literature [151].

**Aldehyde 3.60**. TMEDA (23.8 mL, 159 mmol) was dissolved in THF (200 mL) and cooled to −78 °C and then *t*BuLi (1.7 M in pentane, 105 mL,

179 mmol) was added slowly. The reaction mixture was stirred at −78 °C for 20 min. whereupon a solution of MOM ether **3.59** (22.99 g, 78.90 mmol) in THF (250 mL). The reaction mixture was then stirred for 50 min. and then DMF (73.0 mL, 947 mmol) was added. After 1 h the reaction mixture was allowed to warm to rt and was then stirred for 2 h. Water (200 mL) was added and after 20 min. the mixture was partially concentrated *in vacuo* to remove volatiles. The aqueous phase was then extracted with EtOAc (2 × 500 mL). The combined organic phases were washed with water (3 × 500 mL), dried over $Na_2SO_4$ and the solvent was removed *in vacuo*. The residue was then purified by flash column chromatography on silica gel (EtOAc:hexanes (3.5:6.5)) to give the title compound as a yellow oil (22.84 g, 91%). $R_f = 0.20$ (EtOAc:hexanes (3.5:6.5)); $^1$H NMR ($CDCl_3$, 600 MHz) $\delta$ 9.90 (s, 1H), 7.54 (s, 1H), 6.47–6.41 (m, 1H), 6.23 (dq, $J = 16.1, 6.6$ Hz, 1H), 5.02 (d, $J = 5.1$Hz, 1H), 4.96 (d, $J = 5.1$ Hz, 1H), 3.70–3.55 (m, 2H), 3.51 (s, 3H), 3.18–3.09 (m, 2H), 2.39 (s, 3H), 1.95 (dd, $J = 6.6, 1.7$ Hz, 3H), 1.30 (t, $J = 7.1$ Hz, 3H), 1.04 (t, $J = 7.2$ Hz, 3H). $^1$H NMR spectroscopic data were consistent with those in the literature [151].

**Cyanophthalide 3.6**. Aldehyde **3.60** (22.79 g, 71.35 mmol) was dissolved in $CH_2Cl_2$ and cooled to 0°C and then TMSCN (15.0mL, 120mmol) was added. The reaction mixture was stirred at 0 °C for 10 min. whereupon it was allowed to warm to rt. The reaction mixture was then stirred for 1 h and then KCN (0.012 g, 0.18 mmol) and 18-crown-6 (0.012 g, 0.045 mmol) were added. The reaction mixture was then stirred at rt for 5 h and the solvent was removed *in vacuo*. The residue was dissolved in AcOH (146 mL) and stirred at rt for 106 h whereupon the solvent was removed *in vacuo*. Sat. $NaHCO_3$ (aq) (1 L) was added and the aqueous phase was then extracted with EtOAc (3 × 500 mL). The combined organic phases were washed with water (1L), dried over $Na_2SO_4$ and the solvent was removed *in vacuo*. The residue was then purified by flash column chromatography on silica gel (EtOAc:hexanes (1:7)) to give the title compound as a yellow oil (14.90 g, 76%). $R_f = 0.32$ (EtOAc:hexanes (1:3)). The $R_f$-value was consistent with that in the literature [151].

### 3.7.4 Synthesis of TBS ether cyanophthalide building block 3.61

**MOM ether 3.62**. Phenol **3.57** (1.029 g, 4.160 mmol) was dissolved in $CH_2Cl_2$ (15 mL) and cooled to 0 °C whereupon DIPEA (2.50 mL, 14.4 mmol) and MOMCl (0.800 mL, 10.5 mmol) were added and the resulting mixture was stirred at 0 °C for 20 min. The reaction mixture was then allowed to warm to rt and was then stirred for 74 h. Then water (25 mL) was added and mixture was extracted with $CH_2Cl_2$ (3 × 25 mL). The combined organic phases were washed with brine (25 mL), dried over $Na_2SO_4$ and the solvent was removed *in vacuo*. The residue was then purified by flash column chromatography on silica gel (EtOAc:hexanes (3:7)) to give the title compound as a yellow oil

(1.135 g, 94%). $R_f = 0.20$ (EtOAc:hexanes (3:7)); $^1$H NMR ($CDCl_3$, 600 MHz) $\delta$ 7.02 (d, $J = 7.7$ Hz, 1H), 6.96 (d, $J = 7.7$ Hz, 1H), 5.98–5.90 (m, 1H), 5.02 (d, $J = 1.7$ Hz, 1H), 5.00 (s, 2H), 4.87 (dd, $J = 17.2, 1.8$ Hz, 1H), 3.69 (s, 1H), 3.52–3.48 (m, 5H), 3.40 (s, 1H), 3.17 (s, 1H), 3.13 (s, 1H), 2.29 (s, 3H), 1.24 (t, $J = 7.1$ Hz, 3H), 1.03 (t, $J = 7.1$ Hz, 3H); $^{13}$C NMR ($CDCl_3$, 150 MHz) $\delta$ 169.5, 151.5, 136.1, 132.1, 129.5, 126.5, 125.5, 115.2, 100.5, 57.6, 43.2, 39.2, 31.0, 19.7, 14.0, 13.0.

**MOM cyanophthalide 3.74**. Cyanophthalide **3.69** (0.100g, 0.529mmol) was dissolved in $CH_2Cl_2$:DMF (3:1) (1mL) and then cooled to 0°C. A solution of DIPEA (0.139 mL, 0.798 mmol) and MOMCl (0.049 mL, 0.65 mmol) in $CH_2Cl_2$ (0.250 mL) was added dropwise and the resulting mixture was stirred at 0 °C for 1.5 h. Then sat. $NH_4Cl$ (aq) (25 mL) was added and mixture was extracted with $CH_2Cl_2$ (3 × 15 mL). The combined organic phases were washed with water (20 mL), dried over $Na_2SO_4$ and the solvent was removed *in vacuo*. The residue was then purified by flash column chromatography on silica gel (EtOAc:hexanes (3.5:6.5)) to give the title compound as a yellow oil (0.106 g, 86%). $R_f = 0.55$ (EtOAc:hexanes (1:1)); $^1$H NMR ($CDCl_3$, 600 MHz) $\delta$ 7.14 (s, 1H), 7.06 (s, 1H), 5.93 (s, 1H), 5.36 (s, 2H), 3.54 (s, 3H), 2.51 (s, 3H); $^{13}$C NMR ($CDCl_3$, 150 MHz) $\delta$ 165.3, 156.7, 150.1, 144.3, 117.7, 116.1, 114.3, 110.3, 94.9, 64.8, 56.9, 22.7.

**Iodocyanophthalide 3.68**. Cyanophthalide **3.69** (0.600 g, 3.17 mmol) was dissolved in $CH_2Cl_2$ (60 mL) and cooled to 0 °C whereupon NIS (0.928 g, 4.12 mmol) was added. The reaction mixture was stirred at 0 °C for 45 min. and then 10% $Na_2S_2O_3$ (aq) (50 mL) was added. The layers were separated and the aqueous phase was extracted with $CH_2Cl_2$ (2 × 50 mL). The combined organic phases were washed with water (50 mL), dried over $Na_2SO_4$ and the solvent was removed *in vacuo*. The residue was then dissolved in $CH_2Cl_2$ (60 mL) and cooled to 0 °C whereupon DIPEA (0.660 mL, 3.79 mmol) and MOMCl (0.360 mL, 4.74 mmol) were added and the resulting mixture was then allowed to warm to rt and was then stirred for 105 min. Then sat. $NH_4Cl$ (aq) (50 mL) was added and the layers was separated whereupon the aqueous phase was extracted with $CH_2Cl_2$ (2 × 50 mL). The combined organic phases were washed with water (50 mL), dried over $Na_2SO_4$ and the solvent was removed *in vacuo*. The residue was then purified by flash column chromatography on silica gel (EtOAc:hexanes (1:7)) to give the title compound as a yellow solid (0.230 g, 20%). $R_f = 0.20$ (EtOAc:hexanes (1:3)); $^1$H NMR ($CDCl_3$, 600 MHz) $\delta$ 7.29 (s, 1H), 5.93 (s, 1H), 5.54 (d, J = 6.2 Hz, 1H), 5.50 (d, J = 6.2 Hz, 1H), 3.68 (s, 3H), 2.67 (s, 3H); $^{13}$C NMR ($CDCl_3$, 150 MHz) $\delta$ 164.3, 156.4, 153.3, 143.4, 118.1, 113.5, 112.2, 102.5, 101.6, 64.7, 59.0, 30.5. HRMS (ESI-TOF) calcd for $C_{12}H_9INO_4^-$ $[M-H]^-$ 357.9582, found 357.9572; m.p.: 117–118 °C.

**Stannane 3.67**. TBS ether[9] **3.76** (3.00 g, 17.6 mmol) was dissolved in benzene (90 mL) and then $Bu_3SnH$ (4.20 mL, 21.5 mmol) and AIBN (0.289 g,

[9]Prepared according to [185].

1.76mmol) were added. The resulting mixture was heated to reflux and stirred for 16 h. The solvent was removed *in vacuo* and the residue was then purified by flash column chromatography on silica gel (EtOAc:hexanes (0:100)→(1:99)) to give the title compound as a colorless oil (3.11 g, 38%, *trans*:*cis* (85:15)). $R_f$ = 0.15 (hexanes); $^1$H NMR ($CDCl_3$, 600 MHz) $\delta$ 6.17 (d, $J$ = 19.4 Hz, 1H), 6.05 (dt, $J$ = 19.0, 4.1 Hz, 1H), 4.22–4.18 (m, 2H), 1.55–1.46 (m, 6H), 1.34–1.27 (m, 6H), 0.92 (s, 9H), 0.90–0.82 (m, 15H), 0.07 (s, 6H). $^1$H NMR spectroscopic data were consistent with those in the literature [185].

**Allylic TBS ether 3.61**. A flask was charged with iodocyanophthalide **3.68** (0.060 g, 0.17 mmol) and $Pd(PPh_3)_4$ (0.019 g, 0.016 mmol). Then a solution of stannane **3.67** (0.093g, 0.20mmol) in toluene (3.4mL) and the resulting mixture was heated to reflux. The reaction mixture was stirred at reflux for 26 h whereupon the solvent was removed *in vacuo*. The residue was then purified by flash column chromatography on silica gel (EtOAc:$CH_2Cl_2$:hexanes (1:1:8)) to give the title compound as a colorless oil (0.029 g, 42%). $R_f$ = 0.27 (EtOAc:hexanes (1:3)); $^1$H NMR ($CDCl_3$, 600 MHz) $\delta$ 7.21 (s, 1H), 6.63 (d, $J$ = 16.1 Hz, 1H), 6.30 (dt, $J$ = 16.1, 4.0 Hz, 1H), 5.94 (s, 1H), 5.33–5.28 (m, 2H), 4.40 (d, $J$ = 1.9 Hz, 2H), 3.53 (s, 3H), 2.48 (s, 3H), 0.95 (s, 9H), 0.12 (s, 6H); $^{13}$C NMR ($CDCl_3$, 150 MHz) $\delta$ 165.8, 154.8, 144.0, 141.3, 137.8, 134.2, 120.9, 119.3, 114.2, 113.6, 101.1, 64.8, 63.6, 58.2, 26.0, 22.3, 18.5, −5.2; HRMS (ESI-TOF) calcd for $C_{21}H_{29}NNaO_5Si^+$ $[M + Na]^+$ 426.1707, found 426.1695.

Chapter 4

# Synthesis of Poly-fused Heterocycles

Poly-fused heterocycles are found in a wide variety of natural products and have rich biological activities [186–191], cf. figure 4.1.

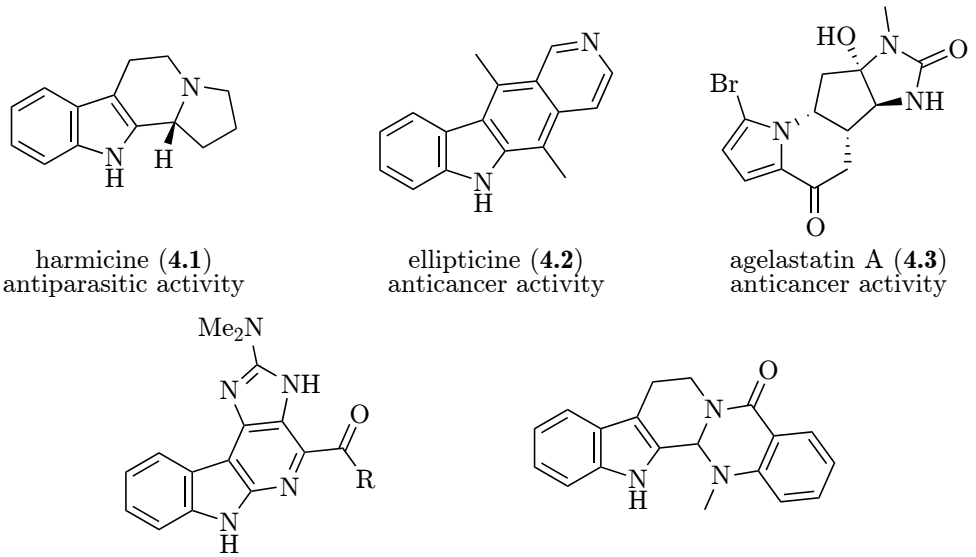


**Figure 4.1:** Poly-fused heterocycles with interesting biological activities.

To match the increasing scientific and pharmaceutical demand for biologically active compounds, efficient synthetic approaches for the construction of these heterocyclic skeletons are desirable.

Along these lines, we set out to develop an efficient strategy for the construction of structurally diverse poly-fused heterocycles.

## 4.1 Synthetic Strategy

To allow for a high degree of diversity, a strategy relying on a tandem aldol condensation/conjugate addition to form the core scaffold, was chosen. The strategy furthermore permitted variation around the core poly-fused scaffold, also called *appendage* diversity [192, 193], by employing building blocks in a convergent manner.

Thus, it was envisioned that a $\beta$-keto esters with an internal nucleophile attached (**4.7**) upon reaction with a hydrazine in a Knorr-like fashion [194] would lead to pyrazolone **4.8**, cf. scheme 4.1. An aldol condensation be-

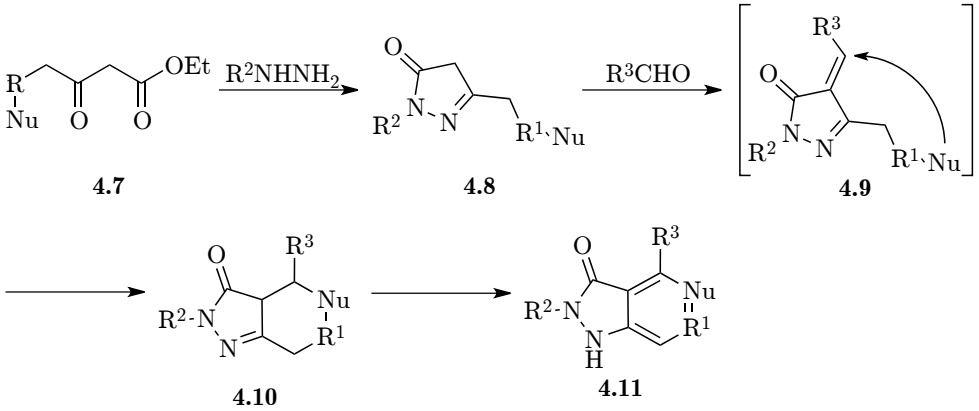


**Scheme 4.1:** Synthetic strategy for the synthesis of poly-fused heterocycles.

tween pyrazolone **4.8** and an aldehyde would then provide the intermediate $\alpha$,$\beta$-unsaturated carbonyl **4.9** [195, 196], now ready to undergo an internal conjugate addition leading to poly-fused heterocycle **4.10** [197]. This intermediate would upon final oxidation lead to the desired poly-fused heterocycle **4.11**.

## 4.2 Synthesis of $\beta$-Keto Esters

An efficient method for the preparation of $\beta$-keto esters with internal nucleophilic moieties was needed as these were not easily available commercially. Thus the corresponding substituted acetic acid derivatives **4.12a**–**c** were activated with CDI and then treated with the magnesium enolate of ethyl hydrogen malonate [198], cf. table 4.1. This provided the $\beta$-keto esters **4.13a** (R = 2,3-dimethoxyphenyl), **4.13b** (R = 2,4-dimethoxyphenyl) and **4.13c**

**Table 4.1:** Synthesis of $\beta$-keto ester building blocks from the corresponding substituted acetic acid derivatives.

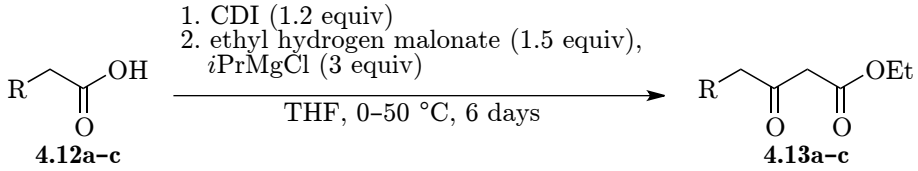


**4.12a–c** **4.13a–c**

| Entry | Acid | R | Product, yield (%)[a] |
|---|---|---|---|
| 1 | **4.12a** | 2,3-dimethoxyphenyl | **4.13a**, 83 |
| 2 | **4.12b** | 2,4-dimethoxyphenyl | **4.13b**, 72 |
| 3 | **4.12c** | 3-indole | **4.13c**, 87 |

[a] Isolated yield after flash column chromatography.

(R = 3-indole) in good yields (72–87%). It was furthermore found that increasing the amount of ethyl hydrogen malonate and *i*PrMgCl (to 2.25 equiv and 4.5 equiv respectively) sped up the reaction (leading to full conversion overnight) and that the potassium salt of the $\beta$-dicarbonyl (e.g. methyl potassium malonate) could be used instead of the acid, if needed.

## 4.3 Synthesis of Pyrazolols

With the $\beta$-keto esters **4.13a–c** in hand, the next step was the pyrazolone formation leading to **4.8**, cf. scheme 4.1. To save the more precious $\beta$-keto esters **4.13a–c** a solvent screen was performed[1] with a model substrate (ethyl acetoacetate **4.14**) and 4-chlorophenylhydrazine **4.15**, cf. table 4.2.

As can be seen from table 4.2, EtOH, AcOH, DMF, EtOAc and MeCN all led to similar results, with DMF proving slightly superior in terms of minimizing side products. However when $\beta$-keto ester **4.13c** was mixed with 4-chlorophenylhydrazine **4.15** in DMF at 60 °C a complex reaction mixture resulted, cf. scheme 4.2. When EtOH was used as solvent a cleaner conversion was observed but the desired product was only isolated in a unsatisfactory yield of 16%, cf. scheme 4.3. It was found that the desired pyrazolone was present as its pyrazolol tautomer **4.17c**, which proved to be a general trend for these compounds [199, 200]. The low yield obtained was also ascribed to the product being very difficult to purify due to solubility issues. Addition of $Et_3N$ slightly improved the yield to 25% cf. table 4.3. The pyrazolols **4.17a** (R = 2,3-dimethoxyphenyl) and **4.17b** (R = 2,4-dimethoxyphenyl) were isolated in somewhat higher yields of 42% and 39% respectively due to an easier purification process, cf. table 4.3. Due to time constraints the pyrazolol formation was not optimized further.

[1] This solvent screen was carried out by PhD student Kim Mortensen.

**Table 4.2:** Screen of solvents and reaction temperature for pyrazolone formation.

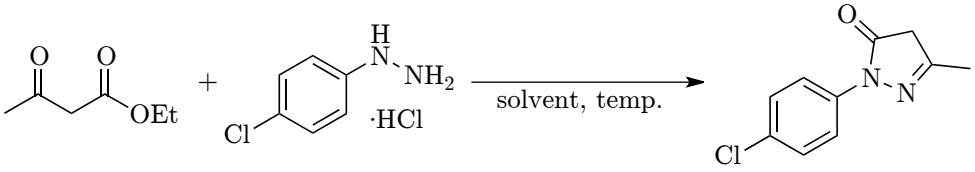


**4.14** **4.15** **4.16**

| Entry | Solvent | Temp. (°C) | Ratio **4.16**:side products[a] |
|---|---|---|---|
| 1 | EtOH | 80 | 68:32 |
| 2 | EtOH | 60 | 80:20 |
| 3 | AcOH | 120 | 81:19 |
| 4 | DMF | 60 | 90:10 |
| 5 | EtOAc | 60 | 80:20 |
| 6 | toluene | 60 | 0:100 |
| 7 | heptane | 60 | 0:100 |
| 8 | THF | 60 | complex mixture |
| 9 | MeCN | 60 | 83:17 |
| 10 | $CH_2Cl_2$ | 40 | complex mixture |

[a] As indicated by LCMS.

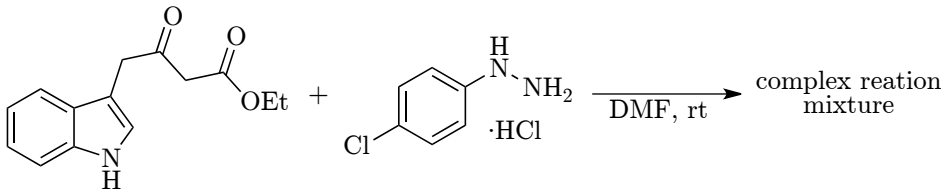


**4.13c** **4.15**

**Scheme 4.2:** Reaction between $\beta$-keto ester **4.13c** and 4-chlorophenylhydrazine **4.15** in DMF.

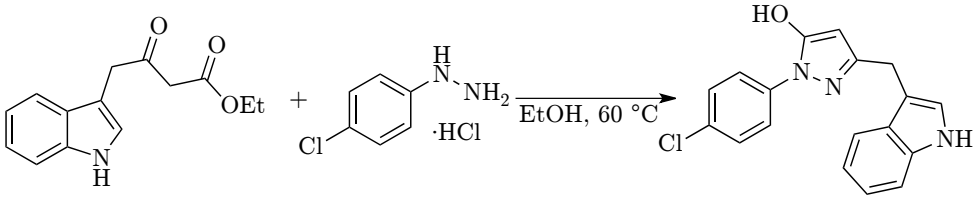


**4.13c** **4.15** **4.17c** 16%

**Scheme 4.3:** Reaction between $\beta$-keto ester **4.13c** and 4-chlorophenylhydrazine **4.15** in EtOH.

**Table 4.3:** Synthesis of pyrazolol building blocks from the corresponding $\beta$-keto esters.

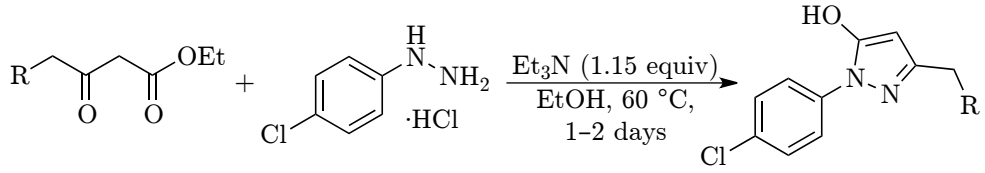


**4.13a–c** **4.15** **4.17a–c**

| Entry | $\beta$-keto ester | R | Product, yield (%)[a] |
|---|---|---|---|
| 1 | **4.13a** | 2,3-dimethoxyphenyl | **4.17a**, 42 |
| 2 | **4.13b** | 2,4-dimethoxyphenyl | **4.17b**, 39 |
| 3 | **4.13c** | 3-indole | **4.17c**, 25 |

[a] Isolated yield after flash column chromatography.

## 4.4 Tandem Aldol Condensation/Conjugate Addition and Oxidation

Everything was now set up to attempt the key tandem aldol condensation/conjugate addition. Thus pyrazolol **4.17a** was subjected to $BF_3{\cdot}OEt_2$ in EtOH, cf. table 4.4. However, none of the desired tetrahydroindazolone **4.18** was isolated

**Table 4.4:** Attempted tandem aldol condensation/conjugate addition of pyrazolol **4.17a**.

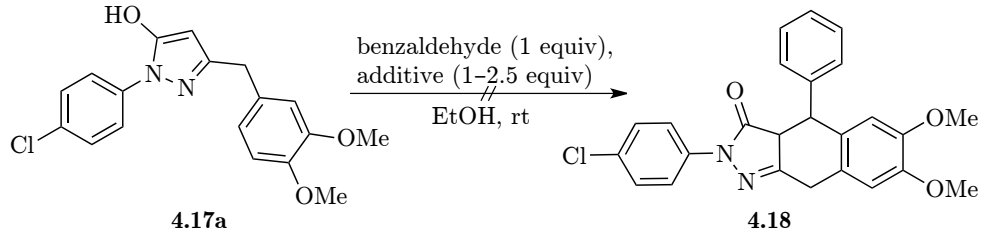


**4.17a** **4.18**

| Entry | Additive | Equiv |
|---|---|---|
| 1 | $BF_3 \cdot OEt_2$ | 1 |
| 2 | $p$TsOH $\cdot$ $H_2O$ | 2.5 |
| 3 | TMSTOf | 1 |

and complete conversion to the di-pyrazolone **4.19** was oberserved [201–205], cf. figure 4.2. The same was observed when subjecting **4.17a** to $p$TsOH $\cdot$ $H_2O$ or TMSTOf, cf. table 4.4.

As the electronic properties of the internal nucleophile in pyrazolol **4.17b** was considered more optimal due to superior positioning of the two methoxy groups, the tandem aldol condensation/conjugate addition was attempted on

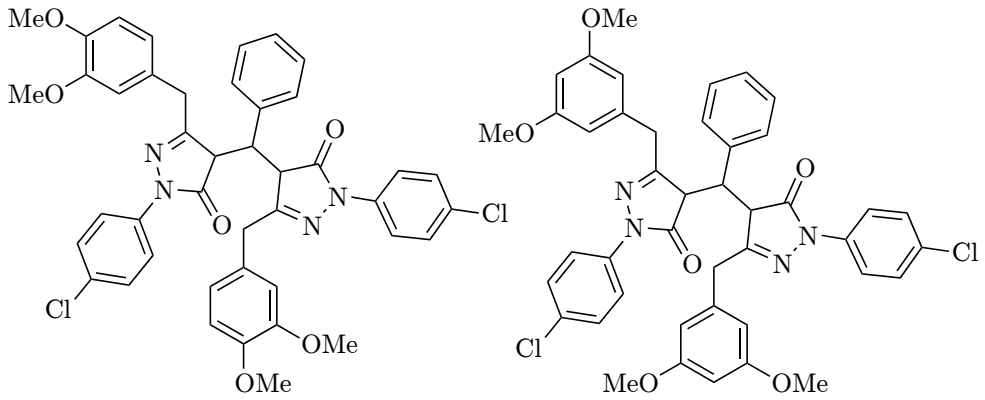


**Figure 4.2:** Side products formed in the tandem aldol condensation/conjugate addition reaction.

this substrate instead, cf. table 4.5. Upon subjection to $BF_3 \cdot OEt_2$ the desired product **4.21** and the di-pyrazolone **4.20**, cf. figure 4.2, were formed in a ratio of 12:88 (table 4.5, entry 1). The use of $p$TsOH $\cdot$ $H_2O$ further improved this ratio (table 4.5, entry 2) and increasing the amount of $p$TsOH $\cdot$ $H_2O$ led to further improvement (table 4.5, entries 4 and 6). The use of sub-stoichiometric amounts of benzaldehyde slightly improved the ratio (table 4.5, entry 3) whereas an excess of benzaldehyde led to increased formation of the side product **4.20** (table 4.5, entry 5). The use of TMSOTf led to even further improvement of the ratio between the desired product **4.21** and the side product **4.20** and the same trend was observed when varying the amount of benzaldehyde as for $p$TsOH $\cdot$ $H_2O$ (table 4.5, entries 7–9). Again, increasing the amount of TMSOTf improved the ratio with the use of 8 equiv leading to a ratio of 93:7 (table 4.5, entries 10–12).

Using the optimized conditions for the tandem aldol condensation/conjugate addition, pyrazolol **4.17b** was subjected to TMSTOf (8 equiv) furnishing the tetrahydroindazolone **4.21** in a good yield of 72%, cf. scheme 4.4. When pyrazolol **4.17c** was subjected to the same reaction conditions a mixture of what appeared to be different tautomeric forms of the desired product, with **4.22** as the major component, was obtained in a yield of 41% cf. scheme 4.4. Just as for the indole containing pyrazolol **4.17c**, cf. §4.3, the product mixture was very difficult to purify and it was not possible to separate the different tautomeric forms. The tautomeric mixture was furthermore difficult to analyze by NMR.

The final oxidation could now be attempted. However when tetrahydroindazolones **4.21** and **4.22** were subjected to DDQ, decomposition of starting materials was observed and none of the desired products were isolated, cf. scheme 4.5. Due to time constraints, no further attempts towards the oxida-

**Table 4.5:** Screen of reaction conditions for the tandem aldol condensation/conjugate addition of pyrazolol **4.17b**.

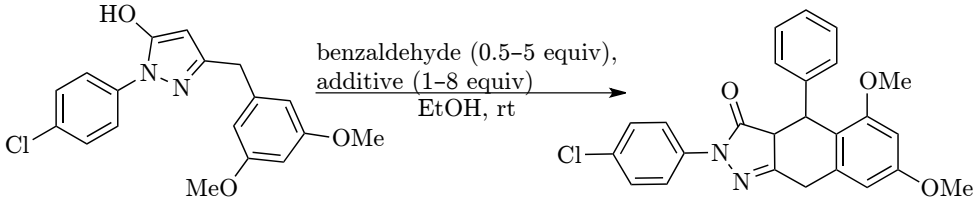


**4.17b** **4.21**

| Entry | Additive | Additive equiv | Benzaldehyde equiv | Ratio **4.21**:**4.20**[a] |
|---|---|---|---|---|
| 1 | $BF_3 \cdot OEt_2$ | 1 | 1 | 12:88 |
| 2 | $p$TsOH $\cdot H_2O$ | 1 | 1 | 19:81 |
| 3 | $p$TsOH $\cdot H_2O$ | 2.5 | 0.5 | 56:44 |
| 4 | $p$TsOH $\cdot H_2O$ | 2.5 | 1 | 50:50 |
| 5 | $p$TsOH $\cdot H_2O$ | 2.5 | 5 | 19:81 |
| 6 | $p$TsOH $\cdot H_2O$ | 5 | 1 | 66:34 |
| 7 | TMSOTf | 1 | 0.5 | 57:43 |
| 8 | TMSOTf | 1 | 1 | 46:54 |
| 9 | TMSOTf | 1 | 5 | 21:79 |
| 10 | TMSOTf | 2 | 1 | 76:24 |
| 11 | TMSOTf | 4 | 1 | 89:11 |
| 12 | TMSOTf | 8 | 1 | 93:7 |

[a] As indicated by LCMS.

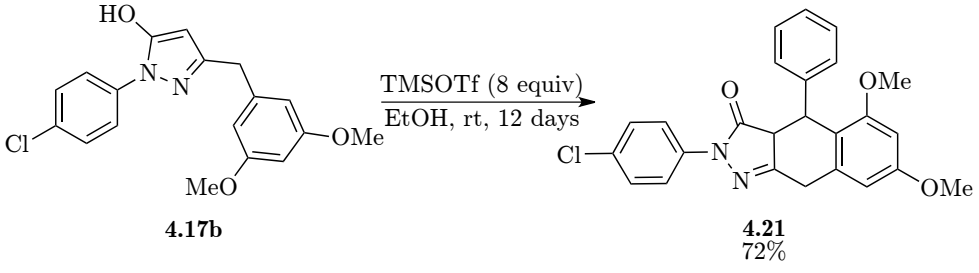


**4.17b** **4.21**
72%

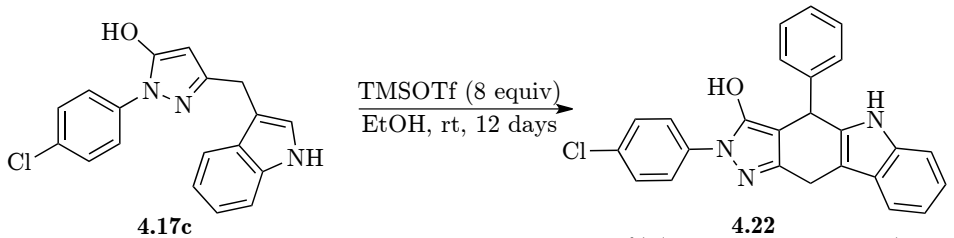


**4.17c** **4.22**
41% (mixture of tautomers)

**Scheme 4.4:** Tandem aldol condensation/conjugate addition of pyrazolol **4.17b** and **4.17c**.

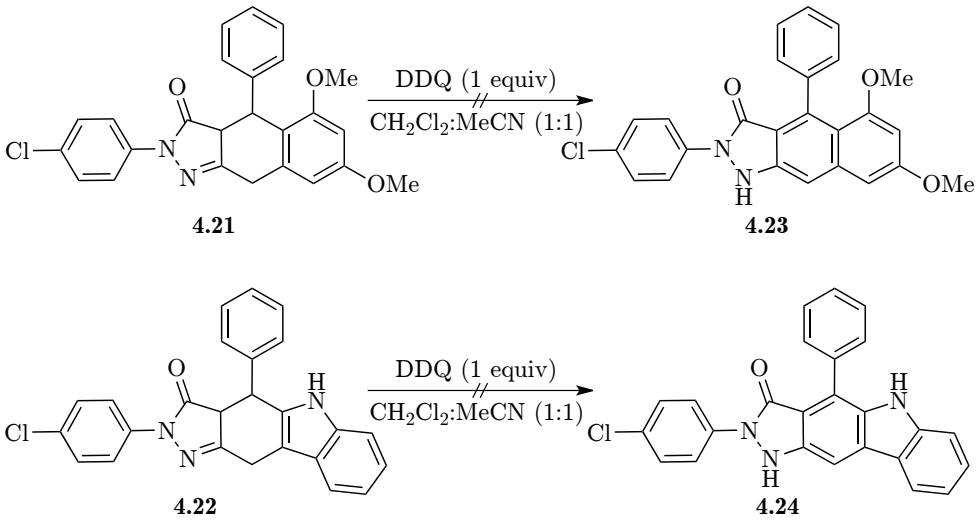


**4.21** **4.23** **4.22** **4.24**

**Scheme 4.5:** Attempts at oxidation of tetrahydroindazolones **4.21** and **4.22**.

tion of **4.21** and **4.22** were made.

## 4.5 Conclusion

Three $\beta$-keto esters were synthesized in good yields. These were furthermore transformed into the pyrazolols **4.17a**–**c**. This transformation was in all cases rather low yielding and further optimization would improve the overall synthetic scheme.

The key aldol condensation/conjugate addition was optimized and led to the synthesis of tetrahydroindazolones **4.21** and **4.22** in yields of 72% and 41%, respectively. Tetrahydroindazolone **4.22** was however present as what appeared to be a mixture of tautomers, which were difficult to purify, resulting in a lower yield. One attempt at the final oxidation of tetrahydroindazolones **4.21** and **4.22** was made, which was unsuccessful and further investigation into this step is needed.

## 4.6 Experimental

### 4.6.1 General methods

Reagents were purchased at the highest commercial quality and used without further purification, unless otherwise noted. All reactions were carried out under an argon atmosphere with dry solvent under anhydrous conditions, unless otherwise noted. Dry solvents were obtained by passing commercially available pre-dried, oxygen-free formulations through activated alumina columns. Yields refer to chromatographically and spectroscopically ($^1$H NMR) homogeneous material, unless otherwise stated.

Reactions were monitored by thin-layer chromatography (TLC) carried out on Merck aluminium sheets covered with silica (C60) using UV light as visualizing agent or an aqueous solution of phosphomolybdic acid and cerium sulfate or a basic aqueous solution of potassium permanganate and heat as developing agents. Matrex silica gel (60, particle size 0.035–0.070 mm) was used for flash column chromatography.

NMR spectra were recorded on a Bruker Ascend 400 MHz instrument equipped with a Prodigy cryoprobe. The chemical shifts ($\delta$) are reported in parts per million (ppm) and the coupling constants ($J$) in Hz. For spectra recorded in DMSO-$d_6$, signal positions were measured relative to the signal for DMSO ($\delta$ 2.50 ppm for $^1$H NMR and $\delta$ 39.43 ppm for $^{13}$C NMR). For spectra recorded in $CDCl_3$, signal positions were measured relative to the signal for $CHCl_3$ ($\delta$ 7.26 ppm for $^1$H NMR and $\delta$ 77.0 ppm for $^{13}$C NMR).

Infrared (IR) spectra were recorded on a Bruker Alpha FT-IR spectrometer. Analytical RP-UPLC-MS (ESI) analysis was performed on a Waters AQUITY RP-UPLC system equipped with a diode array detector using an AQUITY UPLC BEH C18 column ($d$ 1.7 mm, 2.1 × 50 mm; column temp: 65 °C; flow: 0.6 mL/min.). Eluents A (0.1% $HCO_2H$ in $H_2O$) and B (0.1% $HCO_2H$ in MeCN) were used in a linear gradient (5% B to 100% B) in a total run time of 2.6 min. The LC system was coupled to a SQD mass spectrometer. Analytical LC-HRMS (ESI) analysis was performed on an Agilent 1100 RP-LC system equipped with a diode array detector using a Phenomenex Luna C18 column ($d$ 3 mm, 2.1 × 50 mm; column temp: 40 °C; flow: 0.4 mL/min.). Eluents A (0.1% $HCO_2H$ in $H_2O$) and B (0.1% $HCO_2H$ in MeCN) were used in a linear gradient (20% B to 100% B) in a total run time of 15 min. The LC system was coupled to a Micromass LCT orthogonal time-of- flight mass spectrometer equipped with a Lock Mass probe operating in positive electrospray mode.

### 4.6.2 Synthesis of β-keto esters

**β-keto ester 4.13a**. Acid **4.12a** (1.000 g, 5.097 mmol) was dissolved in THF (37 mL) at rt. CDI (0.992 g, 6.12 mmol) was added and the resulting

mixture was stirred overnight (flask **A**). Ethyl hydrogen malonate (0.905 mL, 7.67 mmol) was dissolved in THF (27 mL) and stirred at 0 °C for 30 min. (flask **B**). Isopropyl magnesium chloride (2.0 M in THF, 7.65 mL, 15.3 mmol) was added and after 30 min. the temperature of the reaction mixture was adjusted to rt. After 1 h the temperature of the reaction mixture was adjusted to 50 °C and stirred for 30 min. whereupon it was cannulated in to the solution in flask **A**. The resulting mixture was stirred at rt for 6 days whereupon cold 1 M HCl (aq) (200 mL) was added. The resulting mixture was extracted with EtOAc (3 × 200 mL) and the combined organic phases were washed with water (2 × 300 mL) and brine (600 mL), dried over $MgSO_4$ and the solvent was removed *in vacuo*. The residue was then purified by flash column chromatography on silica gel (EtOAc:hexanes (3:7)) to give the title compound as a yellow oil (1.126 g, 83%). $R_f$ = 0.41 (EtOAc:hexanes (1:1)); $^1$H NMR (DMSO, 400 MHz) $\delta$ 6.89 (d, $J$ = 8.2 Hz, 1H), 6.79 (d, $J$ = 1.7 Hz, 1H), 6.71 (dd, $J$ = 8.2, 1.7 Hz, 1H), 4.07 (q, $J$ = 7.1 Hz, 2H), 3.76 (s, 2H), 3.73 (s, 6H), 3.62 (s, 2H), 1.17 (t, $J$ = 7.1 Hz, 3H); $^{13}$C NMR (DMSO, 101 MHz) $\delta$ 201.5, 167.2, 148.6, 147.76, 126.3, 121.8, 113.5, 111.8, 60.5, 55.5, 55.40, 48.5, 48.23, 14.0; IR (neat) cm$^{-1}$: 2969, 2938, 2907, 2837, 1740, 1713, 1514, 1259, 1236, 1140, 1024; HRMS (ESI) calcd for $C_{14}H_{19}O_5^+$ $[M + H]^+$ 267.1227, found 267.1226.

***β*-keto ester 4.13b**. Acid **4.12b** (0.250 g, 1.27 mmol) was dissolved in THF (9 mL) at rt. CDI (0.248 g, 1.53 mmol) was added and the resulting mixture was stirred overnight (flask **A**). Ethyl hydrogen malonate (0.225 mL, 1.91 mmol) was dissolved in THF (7 mL) and stirred at 0 °C for 30 min. (flask **B**). Isopropyl magnesium chloride (2.0 M in THF, 1.91 mL, 3.82 mmol) was added and after 30 min. the temperature of the reaction mixture was adjusted to rt. After 1 h the temperature of the reaction mixture was adjusted to 50 °C and stirred for 30 min. whereupon it was cannulated in to the solution in flask **A**. The resulting mixture was stirred at rt for 6 days whereupon cold 1 M HCl (aq) (50 mL) was added. The resulting mixture was extracted with EtOAc (3 × 50 mL) and the combined organic phases were washed with water (2 × 75 mL) and brine (75 mL), dried over $MgSO_4$ and the solvent was removed *in vacuo*. The residue was then purified by flash column chromatography on silica gel (EtOAc:hexanes (3:7)) to give the title compound as a yellow oil (0.244 g, 72%). $R_f$ = 0.51 (EtOAc:hexanes (1:1)); $^1$H NMR (DMSO, 400 MHz) $\delta$ 6.41–6.38 (m, 1H), 6.37–6.35 (m, 2H), 4.08 (q, $J$ = 7.1 Hz, 2H), 3.77 (s, 2H), 3.72 (s, 6H), 3.63 (s, 2H), 1.17 (t, $J$ = 7.1 Hz, 3H); $^{13}$C NMR (DMSO, 101 MHz) $\delta$ 201.0, 167.1, 160.4, 136.1, 107.8, 98.6, 60.5, 55.1, 54.9, 49.1, 48.4, 14.0; IR (neat) cm$^{-1}$: 2979, 2941, 2906, 2839, 1740, 1716, 1594, 1461, 1430, 1316, 1203, 1148, 1061, 1028, 834; HRMS (ESI) calcd for $C_{14}H_{19}O_5^+$ $[M + H]^+$ 267.1227, found 267.1228.

***β*-keto ester 4.13c**. Acid **4.12c** (0.500 g, 2.85 mmol) was dissolved in THF (20 mL) at rt. CDI (0.555 g, 3.42 mmol) was added and the resulting mixture was stirred overnight (flask **A**). Ethyl hydrogen malonate (0.505 mL,

4.28 mmol) was dissolved in THF (15 mL) and stirred at 0 °C for 30 min. (flask **B**). Isopropyl magnesium chloride (2.0 M in THF, 4.30 mL, 8.55 mmol) was added and after 30 min. the temperature of the reaction mixture was adjusted to rt. After 1 h the temperature of the reaction mixture was adjusted to 50 °C and stirred for 30 min. whereupon it was cannulated in to the solution in flask **A**. The resulting mixture was stirred at rt for 6 days whereupon cold 1 M HCl (aq) (100 mL) was added. The resulting mixture was extracted with EtOAc (3 × 100 mL) and the combined organic phases were washed with water (2 × 150 mL) and brine (150 mL), dried over $Na_2SO_4$ and the solvent was removed *in vacuo*. The residue was then purified by flash column chromatography on silica gel (EtOAc:hexanes (3.5:6.5)) to give the title compound as a brown oil (0.611 g, 87%). $R_f = 0.38$ (EtOAc:hexanes (1:1)); $^1$H NMR ($CDCl_3$, 400 MHz) $\delta$ 8.38 (s, 1H), 7.53 (d, $J$ = 7.9 Hz, 1H), 7.36 (d, $J$ = 8.1 Hz, 1H), 7.24–7.17 (m, 1H), 7.16–7.08 (m, 2H), 4.13 (q, $J$ = 7.1 Hz, 2H), 3.94 (s, 2H), 3.48 (s, 2H), 1.22 (t, $J$ = 7.1 Hz, 3H); $^{13}$C NMR ($CDCl_3$, 101 MHz) $\delta$ 201.8, 167.7, 136.3, 127.2, 123.8, 122.5, 120.0, 118.6, 111.5, 107.5, 61.5, 47.8, 40.2, 14.1; IR (neat) cm$^{-1}$: 3391, 2982, 1709, 1458, 1409, 1369, 1315, 1195, 1150, 1026, 742; HRMS (ESI) calcd for $C_{14}H_{16}NO_3^+$ $[M + H]^+$ 246.1125, found 246.1124.

### 4.6.3 Synthesis of pyrazolols

**Pyrazolol 4.17a**. $\beta$-keto ester **4.13a** (0.400 g, 1.50 mmol) was dissolved in EtOH (7.5 mL) and then 4-chlorophenylhydrazine hydrochloride **4.15** (0.269 g, 1.50 mmol) and $Et_3N$ (0.240 mL, 1.72 mmol) were added. The reaction mixture was stirred at 60 °C for 2 days whereupon water was added (30 mL). The resulting mixture was extracted with EtOAc (3 × 30 mL) and the combined organic phases were washed with water (2 × 45 mL) and brine (45 mL), dried over $Na_2SO_4$ and the solvent was removed *in vacuo*. The residue was then purified by flash column chromatography on silica gel (acetone:toluene (5:95)) to give the title compound as a yellow amorphous solid (0.217 g, 42%). $R_f$ = 0.39 (EtOAc:hexanes (1:1)); $^1$H NMR (DMSO, 400 MHz) $\delta$ 11.70 (s, 1H), 7.77 (d, $J$ = 8.8 Hz, 2H), 7.48 (d, $J$ = 8.9 Hz, 2H), 6.92–6.83 (m, 2H), 6.77 (d, $J$ = 8.0 Hz, 1H), 5.31 (s, 1H), 3.72 (s, 6H), 3.71 (s, 2H); $^{13}$C NMR (DMSO, 100 MHz) $\delta$ 153.3, 152.2, 148.6, 147.2, 137.9, 132.1, 129.0, 128.8, 121.9, 120.5, 112.6, 111.9, 87.2, 55.5, 55.5, 34.5; IR (neat) cm$^{-1}$: 2929, 1605, 1589, 1488, 1452, 1321, 1198, 1141, 1091, 1050, 825, 695; MS (ESI) calcd for $C_{18}H_{18}ClN_2O_3^+$ $[M + H]^+$ 345.1, found 345.1.

**Pyrazolol 4.17b**. $\beta$-keto ester **4.13b** (0.100 g, 0.376 mmol) was dissolved in EtOH (2.0 mL) and then 4-chlorophenylhydrazine hydrochloride **4.15** (0.067 g, 0.37 mmol) and $Et_3N$ (0.060 mL, 0.43 mmol) were added. The reaction mixture was stirred at 60 °C for 2 days whereupon water was added (10 mL). The resulting mixture was extracted with EtOAc (3 × 10 mL) and the combined organic phases were washed with water (2 × 20 mL) and brine (20 mL), dried over $Na_2SO_4$ and the solvent was removed *in vacuo*. The residue was

then purified by flash column chromatography on silica gel (MeOH:$CH_2Cl_2$ (0.4:99.6)) to give the title compound as a yellow amorphous solid (0.050 g, 39%). $R_f$ = 0.56 (MeOH:$CH_2Cl_2$ (2:98)); $^1$H NMR (DMSO, 400 MHz) $\delta$ 11.71 (s, 1H), 7.77 (d, $J$ = 8.9 Hz, 2H), 7.48 (d, $J$ = 8.9 Hz, 2H), 6.46–6.43 (m, 2H), 6.34 (s, 1H), 5.35 (s, 1H), 3.72 (s, 2H), 3.71 (s, 6H); $^{13}$C NMR (DMSO, 101 MHz) $\delta$ 160.4, 153.2, 151.6, 141.9, 137.8, 129.1, 128.8, 121.9, 106.8, 97.8, 87.3, 55.1, 35.1; IR (neat) cm$^{-1}$: 2932, 2834, 1588, 1492, 1316, 1291, 1200, 1155, 1139, 1066, 833; HRMS (ESI) calcd for $C_{18}H_{18}ClN_2O_3^+$ $[M+H]^+$ 345.1006, found 345.1001.

**Pyrazolol 4.17c**. $\beta$-keto ester **4.13c** (1.000g, 4.077mmol) was dissolved in EtOH (20 mL) and then 4-chlorophenylhydrazine hydrochloride **4.15** (0.723 g, 4.08mmol) and $Et_3N$ (0.655mL, 4.70mmol) were added. The reaction mixture was stirred at 60 °C for 18 h 30 min. whereupon water was added (70 mL). The resulting mixture was extracted with EtOAc (3 × 70 mL) and the combined organic phases were washed with water (2 × 140 mL) and brine (140 mL), dried over $Na_2SO_4$ and the solvent was removed *in vacuo*. The residue was then purified by flash column chromatography on silica gel (MeOH:$CH_2Cl_2$ (0.5:99.5)) to give the title compound as a brown amorphous solid (0.333 g, 25%). $R_f$ = 0.48 (MeOH:$CH_2Cl_2$ (2:98)); $^1$H NMR (DMSO, 400 MHz) $\delta$ 11.61 (s, 1H), 10.83 (s, 1H), 7.78 (d, $J$ = 8.8 Hz, 2H), 7.53 (d, $J$ = 7.9 Hz, 1H), 7.47 (s, 2H), 7.34 (d, $J$ = 8.1 Hz, 1H), 7.20 (s, 1H), 7.06 (t, $J$ = 7.4 Hz, 1H), 6.96 (t, $J$ = 7.4 Hz, 1H), 5.29 (s, 1H), 3.90 (s, 2H); $^{13}$C NMR (DMSO, 101 MHz)[2] $\delta$ 153.1, 152.6, 138.0, 136.3, 128.8, 127.1, 123.1, 121.8, 120.9, 118.6, 118.3, 112.1, 111.4, 87.2, 25.0; IR (neat) cm$^{-1}$: 3234, 3108, 3057, 1694, 1490, 1355, 1322, 1088, 827, 743; HRMS (ESI) calcd for $C_{18}H_{15}ClN_3O^+$ $[M+H]^+$ 324.0898, found 324.0900.

### 4.6.4 Synthesis of tetrahydroindazolones

**Tetrahydroindazolone 4.21**. Pyrazolol **4.17b** (0.201g, 0.583mmol) was dissolved in EtOH (12mL) and then benzaldehyde (0.059mL, 0.58mmol) and TMSOTf (0.845mL, 4.67mmol) were added. The reaction mixture was stirred at rt for 12days whereupon the solvent was removed *in vacuo*. The residue was then purified by flash column chromatography on silica gel (EtOAc:$CH_2Cl_2$:heptane (1:1:2)) to give the title compound as a yellow amorphous solid (0.181 g, 72%). $R_f$ = 0.38 (EtOAc:heptane (1:1)); $^1$H NMR (DMSO, 400 MHz) $\delta$ 7.80–7.74 (m, 2H), 7.50–7.44 (m, 2H), 7.20–7.12 (m, 4H), 7.09–7.03 (m, 1H), 6.60 (d, $J$ = 2.2 Hz, 1H), 6.44 (d, $J$ = 2.2 Hz, 1H), 5.25 (s, 1H), 4.08 (d, $J$ = 20.2 Hz, 1H), 3.84 (d, $J$ = 19.8 Hz, 1H), 3.77 (s, 3H), 3.71 (s, 1H), 3.68 (s, 3H); $^{13}$C NMR (DMSO, 101 MHz) $\delta$ 160.4, 158.9, 157.7, 149.1, 145.5, 137.2, 135.4, 128.8, 128.5, 127.4, 125.6, 120.6, 119.5, 105.2, 97.1, 55.5, 55.2, 35.3, 35.0, 28.3; IR (neat) cm$^{-1}$: 2929, 2835, 1605, 1589, 1488, 1452, 1321, 1299, 1198, 1141,

[2]Signal from the carbon atom directly attached to chlorine could not be observed.

1091, 825, 695; HRMS (ESI) calcd for $C_{25}H_{22}ClN_2O_3^+$ $[M+H]^+$ 433.1313, found 433.1315.

# References


[1] Merrifield, R. B., *J. Am. Chem. Soc.* **1963**, 85 (14), 2149–2154.

[2] Hermkens, P. H. H.; Ottenheijm, H. C. J.; Rees, D., *Tetrahedron* **1996**, 52 (13), 4527–4554.

[3] Hermkens, P. H. H.; Ottenheijm, H. C. J.; Rees, D. C., *Tetrahedron* **1997**, 53 (16), 5643–5678.

[4] Booth, S.; Hermkens, P. H. H.; Ottenheijm, H. C. J.; Rees, D. C., *Tetrahedron* **1998**, 54 (51), 15385–15443.

[5] Testero, S. A.; Mata, E. G., *J. Comb. Chem.* **2008**, 10 (4), 487–97.

[6] Andres, C. J.; Denhart, D. J.; Deshpande, M. S.; Gillman, K. W., *Mol. Divers.* **1999**, 2 (4), 191–210.

[7] Dolle, R. E.; Nelson, K. H., *J. Comb. Chem.* **1999**, 1 (4), 235–282.

[8] Taylor, S. J.; Morken, J. P., *Science* **1998**, 280 (5361), 267–270.

[9] Vaino, A. R.; Janda, K. D., *J. Comb. Chem.* **2000**, 2 (6), 579–596.

[10] Atherton, E.; Clive, D. L.; Sheppard, R. C., *J. Am. Chem. Soc.* **1975**, 97 (22), 6584–6585.

[11] Atherton, E.; Gait, M. J.; Sheppard, R. C.; Williams, B. J., *Bioorg. Chem.* **1979**, 8 (3), 351–370.

[12] Zalipsky, S.; Chang, J. L.; Albericio, F.; Barany, G., *React. Polym.* **1994**, 22 (3), 243–258.

[13] Bayer, E., *Angew. Chem. Int. Ed.* **1991**, 30 (2), 113–129.

[14] Meldal, M., *Tetrahedron Lett.* **1992**, 33 (21), 3077–3080.

[15] Renil, M.; Meldal, M., *Tetrahedron Lett.* **1995**, 36 (26), 4647–4650.

[16] Auzanneau, F. I.; Meldal, M.; Bock, K., *J. Peptide Sci.* **1995**, 1 (1), 31–44.

[17] Renil, M.; Meldal, M., *Tetrahedron Lett.* **1996**, 37 (34), 6185–6188.

[18] Buchardt, J.; Meldal, M., *Tetrahedron Lett.* **1998**, 39 (47), 8695–8698.

[19] García-Martín, F.; Quintanar-Audelo, M.; García-Ramos, Y.; Cruz, L. J.; Gravel, C.; Furic, R.; Côté, S.; Tulla-Puche, J.; Albericio, F., *J. Comb. Chem.* **2006**, 8 (2), 213–220.

[20] Guillier, F.; Orain, D.; Bradley, M., *Chem. Rev.* **2000**, 100 (6), 2091–2157.

[21] Pietta, P. G.; Cavallo, P. F.; Takahashi, K.; Marshall, G. R., *J. Org. Chem.* **1974**, 39 (1), 44–48.

[22] Matsueda, G. R.; Stewart, J. M., *Peptides* **1981**, 2 (1), 45–50.

[23] Fréchet, J. M. J.; Haque, K. E., *Tetrahedron Lett.* **1975**, 16 (35), 3055–3056.

[24] Fréchet, J. M. J.; Nuyens, L. J., *Can. J. Chem.* **1976**, 54 (6), 926–934.

[25] Fyles, T. M.; Leznoff, C. C., *Can. J. Chem.* **1976**, 54 (6), 935–942.

[26] DeGrado, W. F.; Kaiser, E. T., *J. Org. Chem.* **1980**, 45 (7), 1295–1300.

[27] DeGrado, W. F.; Kaiser, E. T., *J. Org. Chem.* **1982**, 47 (17), 3258–3261.

[28] Rink, H., *Tetrahedron Lett.* **1987**, 28 (33), 3787–3790.

[29] Kenner, G. W.; McDermott, J. R.; Sheppard, R. C., *J. Chem. Soc., Chem. Commun.* **1971**, (12), 636–637.

[30] Holmes, C. P.; Jones, D. G., *J. Org. Chem.* **1995**, 60 (8), 2318–2319.

[31] El-Faham, A.; Albericio, F., *Chem. Rev.* **2011**, 111 (11), 6557–6602.

[32] Goodman, M.; Levine, L., *J. Am. Chem. Soc.* **1964**, 86 (14), 2918–2922.

[33] Antonovics, I.; Young, G. T., *Chem. Commun.* **1965**, (17), 398–399.

[34] Antonovics, I.; Young, G. T., *J. Chem. Soc. C* **1967**, 595–601.

[35] Carpino, L. A., *J. Am. Chem. Soc.* **1993**, 115 (13), 4397–4398.

[36] Castro, B.; Dormoy, J. R.; Evin, G.; Selve, C., *Tetrahedron Lett.* **1975**, 16 (14), 1219–1222.

[37] Coste, J.; Le-Nguyen, D.; Castro, B., *Tetrahedron Lett.* **1990**, 31 (2), 205–208.

[38] Coste, J.; Frérot, E.; Jouin, P.; Castro, B., *Tetrahedron Lett.* **1991**, 32 (17), 1967–1970.

[39] Frérot, E.; Coste, J.; Pantaloni, A.; Dufour, M.-N.; Jouin, P., *Tetrahedron* **1991**, 47 (2), 259–270.

[40] Dourtoglou, V.; Ziegler, J.-C.; Gross, B., *Tetrahedron Lett.* **1978**, 19 (15), 1269–1272.

[41] Knorr, R.; Trzeciak, A.; Bannwarth, W.; Gillessen, D., *Tetrahedron Lett.* **1989**, 30 (15), 1927–1930.

[42] Abdelmoty, I.; Albericio, F.; Carpino, L. A.; Foxman, B. M.; Kates, S. A., *Lett. Pept. Sci.* **1994**, 1 (2), 57–67.

[43] Falb, E.; Yechezkel, T.; Salitra, Y.; Gilon, C., *J. Pept. Res.* **1999**, 53 (5), 507–517.

[44] Kisfaludy, L.; Schön, I.; Szirtes, T.; Nyéki, O.; Löw, M., *Tetrahedron Lett.* **1974**, 15 (19), 1785–1786.

[45] Kisfaludy, L.; Schön, I., *Synthesis* **1983**, 1983 (04), 325–327.

[46] Blankemeyer-Menge, B.; Nimtz, M.; Frank, R., *Tetrahedron Lett.* **1990**, 31 (12), 1701–1704.

[47] Anderson, G. W.; McGregor, A. C., *J. Am. Chem. Soc.* **1957**, 79 (23), 6180–6183.

[48] Carpino, L. A.; Han, G. Y., *J. Am. Chem. Soc.* **1970**, 92 (19), 5748–5749.

[49] Atherton, E.; Fox, H.; Harkiss, D.; Logan, C. J.; Sheppard, R. C.; Williams, B. J., *J. Chem. Soc., Chem. Commun.* **1978**, (13), 537–539.

[50] Bergmann, M.; Zervas, L., *Chem. Ber.* **1932**, 65 (7), 1192–1201.

[51] Zervas, L.; Theodoropoulos, D. M., *J. Am. Chem. Soc.* **1956**, 78 (7), 1359–1363.

[52] Barlos, K.; Papaioannou, D.; Theodoropoulos, D., *J. Org. Chem.* **1982**, 47 (7), 1324–1326.

[53] Sieber, P.; Riniker, B., *Tetrahedron Lett.* **1987**, 28 (48), 6031–6034.

[54] Loffet, A.; Zhang, H. X., *Int. J. Pept. Protein Res.* **2009**, 42 (4), 346–351.

[55] Bycroft, B. W.; Chan, W. C.; Chhabra, S. R.; Hone, N. D., *J. Chem. Soc., Chem. Commun.* **1993**, 53 (9), 778–778.

[56] Bloomberg, G. B.; Askin, D.; Gargaro, A. R.; Tanner, M. J. A., *Tetrahedron Lett.* **1993**, 34 (29), 4709–4712.

[57] Dumy, P.; Eggleston, I. M.; Cervigni, S.; Sila, U.; Sun, X.; Mutter, M., *Tetrahedron Lett.* **1995**, 36 (8), 1255–1258.

[58] Barany, G.; Merrifield, R. B., *J. Am. Chem. Soc.* **1977**, 99 (22), 7363–7365.

[59] Barany, G.; Albericio, F., *J. Am. Chem. Soc.* **1985**, 107 (17), 4936–4942.

[60] Planas, M.; Bardají, E.; Jensen, K. J.; Barany, G., *J. Org. Chem.* **1999**, 64 (20), 7281–7289.

[61] Klán, P.; Šolomek, T.; Bochet, C. G.; Blanc, A.; Givens, R.; Rubina, M.; Popik, V.; Kostikov, A.; Wirz, J., *Chem. Rev.* **2013**, 113 (1), 119–191.

[62] Bamford, C. H.; Norrish, R. G. W., *J. Chem. Soc.* **1935**, 1504–1511.

[63] Dunkin, I. R.; Gębicki, J.; Kiszka, M.; Sanín-Leira, D., *J. Chem. Soc., Perkin Trans. 2* **2001**, 8, 1414–1425.

[64] Hellrung, B.; Kamdzhilov, Y.; Schwörer, M.; Wirz, J., *J. Am. Chem. Soc.* **2005**, 127 (25), 8934–5.

[65] Il'ichev, Y. V.; Wirz, J., *J. Phys. Chem. A* **2000**, 104 (33), 7856–7870.

[66] Walker, J. W.; Reid, G. P.; McCray, J. A.; Trentham, D. R., *J. Am. Chem. Soc.* **1988**, 110 (21), 7170–7177.

[67] Rich, D. H.; Gurwara, S. K., *J. Chem. Soc., Chem. Commun.* **1973**, (17), 610–611.

[68] Rich, D. H.; Gurwara, S. K., *J. Am. Chem. Soc.* **1975**, 97 (6), 1575–1579.

[69] Voss, C.; Dimarchi, R.; Whitney, D. B.; Tjoeng, F. S.; Merrifield, R. B.; Tam, J. P., *Int. J. Pept. Protein Res.* **1983**, 22 (2), 204–213.

[70] Tam, J. P.; Tjoeng, F. S.; Merrifield, R. B., *J. Am. Chem. Soc.* **1980**, 102 (19), 6117–6127.

[71] Giralt, E.; Albericio, F.; Pedroso, E.; Granier, C.; van Rietschoten, J., *Tetrahedron* **1982**, 38 (9), 1193–1201.

[72] Giralt, E.; Eritja, R.; Pedroso, E.; Granier, C.; Rietschoten, J. V., *Tetrahedron* **1986**, 42 (2), 691–698.

[73] Lloyd-Williams, P.; Gairi, M.; Albericio, F.; Giralt, E., *Tetrahedron* **1991**, 47 (47), 9867–9880.

[74] Baldwin, J. J.; Burbaum, J. J.; Henderson, I.; Ohlmeyer, M. H. J., *J. Am. Chem. Soc.* **1995**, 117 (20), 5588–5589.

[75] Greenberg, M. M., *Tetrahedron Lett.* **1993**, 34 (2), 251–254.

[76] Matray, T. J.; Greenberg, M. M., *J. Am. Chem. Soc.* **1994**, 116 (15), 6931–6932.

[77] Greenberg, M. M.; Gilmore, J. L., *J. Org. Chem.* **1994**, 59 (4), 746–753.

[78] Zehavi, U.; Sadeh, S.; Herchman, M., *Carbohydr. Res.* **1983**, 124 (1), 23–34.

[79] Nicolaou, K. C.; Winssinger, N.; Pastor, J.; DeRoose, F., *J. Am. Chem. Soc.* **1997**, 119 (2), 449–450.

[80] Nicolaou, K. C.; Watanabe, N.; Li, J.; Pastor, J.; Winssinger, N., *Angew. Chem. Int. Ed.* **1998**, 37 (11), 1559–1561.

[81] Kantchev, E. A.; Parquette, J. R., *Synlett* **2005**, (10), 1567–1570.

[82] Rich, D. H.; Gurwara, S. K., *Tetrahedron Lett.* **1975**, 16 (5), 301–304.

[83] Ajayaghosh, A.; Pillai, V. N. R., *J. Org. Chem.* **1990**, 55 (9), 2826–2829.

[84] Renil, M.; Pillai, V. N. R., *Tetrahedron Lett.* **1994**, 35 (22), 3809–3812.

[85] Kumar, K. S.; Pillai, V. N. R., *Tetrahedron* **1999**, 55 (34), 10437–10446.

[86] Hintersteiner, M.; Ambrus, G.; Bednenko, J.; Schmied, M.; Knox, A. J. S.; Meisner, N.-C.; Gstach, H.; Seifert, J.-M.; Singer, E. L.; Gerace, L.; Auer, M., *ACS Chem. Biol.* **2010**, 5 (10), 967–979.

[87] Eller, S.; Collot, M.; Yin, J.; Hahm, H. S.; Seeberger, P. H., *Angew. Chem. Int. Ed.* **2013**, 52 (22), 5858–5861.

[88] Calin, O.; Eller, S.; Seeberger, P. H., *Angew. Chem. Int. Ed.* **2013**, 52 (22), 5862–5865.

[89] Weishaupt, M. W.; Matthies, S.; Seeberger, P. H., *Chem. Eur. J.* **2013**, 19 (37), 12497–12503.

[90] Ajayaghosh, A.; Pillai, V. N. R., *Tetrahedron* **1988**, 44 (21), 6661–6666.

[91] Ajayaghosh, A.; Pillai, V. N. R., *J. Org. Chem.* **1987**, 52 (26), 5714–5717.

[92] Ajayaghosh, A.; Pillai, V. N. R., *Tetrahedron Lett.* **1995**, 36 (5), 777–780.

[93] Brown, B. B.; Wagner, D. S.; Geysen, H. M., *Mol. Div.* **1995**, 1 (1), 4–12.

[94] Sternson, S. M.; Schreiber, S. L., *Tetrahedron Lett.* **1998**, 39 (41), 7451–7454.

[95] Rodebaugh, R.; Fraser-Reid, B.; Geysen, H. M., *Tetrahedron Lett.* **1997**, 38 (44), 7653–7656.

[96] Zehavi, U.; Patchornik, A., *J. Am. Chem. Soc.* **1973**, 95 (17), 5673–5677.

[97] Yoo, D. J.; Greenberg, M. M., *J. Org. Chem.* **1995**, 60 (11), 3358–3364.

[98] Venkatesan, H.; Greenberg, M. M., *J. Org. Chem.* **1996**, 61 (2), 525–529.

[99] Poijärvi, P.; Heinonen, P.; Virta, P.; Lönnberg, H., *Bioconjugate Chem.* **2005**, 16 (6), 1564–1571.

[100] Holmes, C. P., *J. Org. Chem.* **1997**, 62 (8), 2370–2380.

[101] Whitehouse, D. L.; Savinov, S. N.; Austin, D. J., *Tetrahedron Lett.* **1997**, 38 (45), 7851–7852.

[102] McKeown, S. C.; Watson, S. P.; Carr, R. A. E.; Marshall, P., *Tetrahedron Lett.* **1999**, 40 (12), 2407–2410.

[103] Gea, A.; Farcy, N.; Roqué i Rossell, N.; Martins, J. C.; Clercq, P. J. D.; Madder, A., *Eur. J. Org. Chem.* **2006**, 2006 (18), 4135–4146.

[104] Lin, Q.; Blackwell, H. E., *Chem. Commun.* **2006**, 17 (27), 2884–2886.

[105] Gennari, C.; Longari, C.; Ressel, S.; Salom, B.; Piarulli, U.; Ceccarelli, S.; Mielgo, A., *Eur. J. Org. Chem.* **1998**, 1998 (11), 2437–2449.

[106] Ruhland, B.; Bhandari, A.; Gordon, E. M.; Gallop, M. A., *J. Am. Chem. Soc.* **1996**, 118 (1), 253–254.

[107] Minkwitz, R.; Meldal, M., *QSAR Comb. Sci.* **2005**, 24 (3), 343–353.

[108] Qvortrup, K.; Nielsen, T. E., *Chem. Commun.* **2011**, 47 (11), 3278–3280.

[109] Qvortrup, K.; Komnatnyy, V. V.; Nielsen, T. E., *Org. Lett.* **2014**, 16 (18), 4782–4785.

[110] Kim, J.; Kyeong, S.; Shin, D.-S.; Yeo, S.; Yim, J.; Lee, Y.-S., *Synlett* **2013**, 24 (06), 733–736.

[111] Lam, K. S.; Salmon, S. E.; Hersh, E. M.; Hruby, V. J.; Kazmierski, W. M.; Knapp, R. J., *Nature* **1991**, 354 (6348), 82–84.

[112] Lam, K. S.; Lebl, M.; Krchnák, V., *Chem. Rev.* **1997**, 97 (2), 411–448.

[113] Salmon, S. E.; Lam, K. S.; Lebl, M.; Kandola, A.; Khattri, P. S.; Wade, S.; Pátek, M.; Kocis, P.; Krchnák, V.; Thorpe, D., *Proc. Natl. Acad. Sci. U.S.A.* **1993**, 90 (24), 11708–11712.

[114] Maillard, N.; Darbre, T.; Reymond, J. L., *J. Comb. Chem.* **2009**, 11 (4), 667–675.

[115] Maillard, N.; Biswas, R.; Darbre, T.; Reymond, J. L., *ACS. Comb. Sci.* **2011**, 13 (3), 310–320.

[116] Nitz, M.; Franz, K. J.; Maglathlin, R. L.; Imperiali, B., *ChemBioChem* **2003**, 4 (4), 272–276.

[117] Upert, G.; Merten, C. A.; Wennemers, H., *Chem. Commun.* **2010**, 46 (13), 2209–2211.

[118] Silen, J. L.; Lu, A. T.; Solas, D. W.; Gore, M. A.; Maclean, D.; Shah, N. H.; Coffin, J. M.; Bhinderwala, N. S.; Wang, Y.; Tsutsui, K. T.; Look, G. C.; Campbell, D. A.; Hale, R. L.; Navre, M.; Deluca-Flaherty, C., *Antimicrob. Agents Chemother.* **1998**, 42 (6), 1447–1453.

[119] Lebl, M.; Pátek, M.; Kocis, P.; Krchnák, V.; Hruby, V. J.; Salmon, S. E.; Lam, K. S., *Int. J. Pept. Protein Res.* **1993**, 41 (2), 201–203.

[120] Clemons, P. A.; Koehler, A. N.; Wagner, B. K.; Sprigings, T. G.; Spring, D. R.; King, R. W.; Schreiber, S. L.; Foley, M. A., *Chem. Biol.* **2001**, 8 (12), 1183–1195.

[121] Salmon, S. E.; Liu-Stevens, R.; Zhao, Y.; Lebl, M.; Krchñák, V.; Wertman, K.; Sepetov, N.; Lam, K. S., *Mol. Divers.* **1996**, 2 (1–2), 57–63.

[122] Fluxà, V. S.; Maillard, N.; Page, M. G. P.; Reymond, J.-L., *Chem. Commun.* **2011**, 47 (5), 1434–1436.

[123] Marco, A. D.; Gaetani, M.; Scarpinato, B., *Cancer Chemother. Rep.* **1969**, 53 (1), 33–37.

[124] Abdella, B. R. J.; Fisher, J., *Environ. Health. Perspect.* **2013**, 64, 3–18.

[125] Minotti, G.; Menna, P.; Salvatorelli, E.; Cairo, G.; Gianni, L., *Pharmacol. Rev.* **2004**, 56 (2), 185–229.

[126] Gewirtz, D. A., *Biochem. Pharmacol.* **1999**, 57 (7), 727–741.

[127] Mross, K., *Eur. J. Cancer* **1991**, 27 (12), 1542–1544.

[128] Hortobágyi, G. N., *Drugs* **1997**, 54, 1–7.

[129] Hande, K. R., *Biochim. Biophys. Acta* **1998**, 1400 (1–3), 173–184.

[130] Burke, P. J.; Koch, T. H., *J. Med. Chem.* **2004**, 47 (5), 1193–1206.

[131] Weiss, R. B., *Semin. Oncol.* **1992**, 19 (6), 670–686.

[132] de Jong, J.; Klein, I.; Bast, A.; der Vijgh van, *Cancer Chemother. Pharmacol.* **1992**, 31 (2), 156–160.

[133] Masquelier, M.; Baurain, R.; Trouet, A., *J. Med. Chem.* **1980**, 23 (11), 1166–1170.

[134] Nagy, A.; Armatis, P.; Schally, A. V., *Proc. Natl. Acad. Sci. U.S.A.* **1996**, 93 (6), 2464–2469.

[135] Post, G. C.; Barthel, B. L.; Burkhart, D. J.; Hagadorn, J. R.; Koch, T. H., *J. Med. Chem.* **2005**, 48 (24), 7648–7657.

[136] Schmid, B.; Chung, D.-E.; Warnecke, A.; Fichtner, I.; Kratz, F., *Bioconjugate Chem.* **2007**, 18 (3), 702–716.

[137] Gupta, P. K.; Lam, F. C.; Hung, C. T., *Drug. Dev. Ind. Pharm.* **1988**, 14 (12), 1657–1671.

[138] Beijnen, J. H.; Potman, R. P.; van Ooijen, R. D.; Driebergen, R. J.; Voskuilen, M. C. H.; Renema, J.; Underberg, W. J. M., *Int. J. Pharm.* **1987**, 34 (3), 247–257.

[139] Beijnen, J. H.; van der Houwen, O. A. G. J.; Underberg, W. J. M., *Int. J. Pharm.* **1986**, 32 (2-3), 123–131.

[140] Kaushik, D.; Bansal, G., *J. Pharm. Anal.* **2015**, 5 (5), 285–295.

[141] Wassermann, K.; Bundgaard, H., *Int. J. Pharm.* **1983**, 14 (1), 73–78.

[142] Thern, B.; Rudolph, J.; Jung, G., *Tetrahedron Lett.* **2002**, 43 (28), 5013–5016.

[143] Chen, Q.; Sowa, D. A.; Gabathuler, R., *Synth. Commun.* **2003**, 33 (14), 2391–2400.

[144] Nicolaou, K. C.; Vourloumis, D.; Winssinger, N.; Baran, P. S., *Angew. Chem. Int. Ed.* **2000**, 39 (1), 44–122.

[145] Nicolaou, K. C.; Cai, Q.; Qin, B.; Petersen, M. T.; Mikkelsen, R. J. T.; Heretsch, P., *Angew. Chem. Int. Ed.* **2015**, 54 (10), 3074–3078.

[146] Tomita, F.; Tamaoki, T.; Morimoto, M.; Fujimoto, K., *J. Antibiot.* **1981**, 34 (12), 1519–1524.

[147] Tamaoki, T.; Shirahata, K.; Iida, T.; Tomita, F., *J. Antibiot.* **1981**, 34 (12), 1525–1530.

[148] Maskey, R. P.; Helmke, E.; Kayser, O.; Fiebig, H. H.; Maier, A.; Busche, A.; Laatsch, H., *J. Antibiot.* **2004**, 57 (12), 771–779.

[149] Pfoh, R.; Laatsch, H.; Sheldrick, G. M., *Nucleic Acids Res.* **2008**, 36 (10), 3508–3514.

[150] Maskey, R. P.; Sevvana, M.; Usón, I.; Helmke, E.; Laatsch, H., *Angew. Chem. Int. Ed.* **2004**, 43 (10), 1281–1283.

[151] Švenda, J.; Hill, N.; Myers, A. G., *Proc. Natl. Acad. Sci. U.S.A.* **2011**, 108 (17), 6709–6714.

[152] Smaltz, D. J.; Švenda, J.; Myers, A. G., *Org. Lett.* **2012**, 14 (7), 1812–1815.

[153] Magauer, T.; Myers, A. G., *Org. Lett.* **2011**, 13 (20), 5584–5587.

[154] Magauer, T.; Smaltz, D. J.; Myers, A. G., *Nat. Chem.* **2014**, 25 (3), 886–893.

[155] Hauser, F. M.; Rhee, R. P., *J. Org. Chem.* **1978**, 43 (1), 178–180.

[156] Kraus, G. A.; Sugimoto, H., *Tetrahedron Lett.* **1978**, 19 (26), 2263–2266.

[157] Mal, D.; Pahari, P., *Chem. Rev.* **2007**, 107 (5), 1892–1918.

[158] Myers, A. G.; Hill, N. E.; Švenda, J.; Yu, R. T.; Smaltz, D. J.; Maguer, T. **2011**, WO 2011119549.

[159] Urakawa, Y.; Sugimoto, T.; Sato, H.; Ueda, M., *Tetrahedron Lett.* **2004**, 45 (30), 5885–5888.

[160] Kato, N.; Inada, M.; Sato, H.; Miyatake, R.; Kumagai, T.; Ueda, M., *Tetrahedron* **2006**, 62 (31), 7307–7318.

[161] Collum, D. B.; McDonald III, J. H.; Still, W. C., *J. Am. Chem. Soc.* **1980**, 102 (6), 2118–2120.

[162] Schinzer, D.; Bauer, A.; Schieber, J., *Chem. Eur. J.* **1999**, 5 (9), 2492–2500.

[163] Lim, S. M.; Hill, N.; Myers, A. G., *J. Am. Chem. Soc.* **2009**, 131 (16), 5763–5765.

[164] Trost, B. M.; Romero, A. G., *J. Org. Chem.* **1986**, 51 (2), 2332–2342.

[165] Audia, J. E.; Boisvert, L.; Patten, A. D.; Villalobos, A.; Danishefsky, S. J., *J. Org. Chem.* **1989**, 54 (15), 3738–3740.

[166] Rubottom, G. M.; Vazquez, M. A.; Pelegrina, D. R., *Tetrahedron Lett.* **1974**, 15 (49–50), 4319–4322.

[167] Ferrier, R. J., *J. Chem. Soc., Perkin. Trans. 1* **1979**, 1455–1458.

[168] O'Brien, P.; Poumellec, P., *J. Chem. Soc., Perkin Trans.1* **1998**, 2435–2442.

[169] Sousa, S. E. D.; O'Brien, P.; Pilgram, C. D., *Tetrahedron* **2002**, 58 (23), 4643–4654.

[170] VanRheenen, V.; Kelly, R. C.; Cha, D. Y., *Tetrahedron Lett.* **1976**, 17 (23), 1973–1976.

[171] Maras, A.; Secen, H.; Sutbeyaz, Y.; Balci, M., *J. Org. Chem.* **1998**, 63 (97), 2039–2041.

[172] Woodward, R. B.; Brutcher, F. V., *J. Am. Chem. Soc.* **1958**, 80 (1), 209–211.

[173] Banwell, M. G.; Bridges, V. S.; Dupuche, J. R.; Richards, S. L.; Walter, J. M., *J. Org. Chem.* **1994**, 59 (21), 6338–6343.

[174] Claisen, L., *Ber. Dtsch. Chem. Ges.* **1912**, 45 (3), 3157–3166.

[175] Chen, H.; Jiang, H.; Cai, C.; Dong, J.; Fu, W., *Org. Lett.* **2011**, 13 (5), 992–994.

[176] Milstein, D.; Stille, J. K., *J. Am. Chem. Soc.* **1978**, 100 (11), 3636–3638.

[177] Milstein, D.; Stille, J. K., *J. Am. Chem. Soc.* **1979**, 101 (1), 4992–4998.

[178] Stille, J. K., *Angew. Chem. Int. Ed.* **1986**, 25 (6), 508–524.

[179] Nicolaou, K. C.; Yee, H. L.; Piper, J. L.; Papageorgiou, C. D., *J. Am. Chem. Soc.* **2007**, 129 (13), 4001–4013.

[180] Bansal, R.; Cooper, G. F.; Corey, E. J., *J. Org. Chem.* **1991**, 56 (3), 1329–1332.

[181] Marigo, M.; Franzén, J.; Poulsen, T. B.; Zhuang, W.; Jørgensen, K. A., *J. Am. Chem. Soc.* **2005**, 127 (19), 6964–6965.

[182] Baylis, A. B.; Hillman, M. E. D. **1972**, DE 2155113 A1.

[183] Basavaiah, D.; Reddy, B. S.; Badsara, S. S., *Chem. Rev.* **2010**, 110 (9), 5447–5674.

[184] Hoye, T. R.; Jeffrey, C. S.; Shao, F., *Nat. Protoc.* **2007**, 2 (10), 2451–2458.

[185] Araki, Y.; Konoike, T., *J. Org. Chem.* **1997**, 62 (97), 5299–5309.

[186] Kam, T.-S.; Sim, K.-M., *Phytochemistry* **1998**, 47 (1), 145–147.

[187] Miller, C. M.; McCarthy, F. O., *RSC Adv.* **2012**, 2 (24), 8883–8918.

[188] Mason, C. K.; McFarlane, S.; Johnston, P. G.; Crowe, P.; Erwin, P. J.; Domostoj, M. M.; Campbell, F. C.; Manaviazar, S.; Hale, K. J.; El-Tanani, M., *Mol. Cancer Ther.* **2008**, 7 (3), 548–558.

[189] D'Ambrosio, M.; Guerriero, A.; Pietra, F.; Ripamonti, M.; Debitus, C.; Waikedre, J., *Helv. Chim. Acta.* **1996**, 79 (3), 727–735.

[190] Moquin-Pattey, C.; Guyot, M., *Tetrahedron* **1989**, 45 (11), 3445–3450.

[191] Kobayashi, Y.; Nakano, Y.; Kizaki, M.; Hoshikuma, K.; Yokoo, Y.; Kamiya, T., *Planta Med.* **2001**, 67 (7), 628–633.

[192] Galloway, W. R. J. D.; Bender, A.; Welch, M.; Spring, D. R., *Chem. Commun.* **2009**, (18), 2446–2462.

[193] Isidro-Llobet, A.; Murillo, T.; Bello, P.; Cilibrizzi, A.; Hodgkinson, J. T.; Galloway, W. R. J. D.; Bender, A.; Welch, M.; Spring, D. R., *Proc. Natl. Acad. Sci. U.S.A.* **2011**, 108 (17), 6793–6798.

[194] Knorr, L., *Ber. Dtsch. Chem. Ges.* **1883**, 16 (2), 2597–2599.

[195] Deb, M. L.; Bhuyan, P. J., *Tetrahedron Lett.* **2005**, 46 (38), 6453–6456.

[196] Tripathy, R.; Reiboldt, A.; Messina, P. A.; Iqbal, M.; Singh, J.; Bacon, E. R.; Angeles, T. S.; Yang, S. X.; Albom, M. S.; Robinson, C.; Chang, H.; Ruggeri, B. A.; Mallam, J. P., *Bioorg. Med. Chem. Lett.* **2006**, 16 (8), 2158–2162.

[197] Hamama, W. S.; Hammouda, M.; Afsah, E. M., *J. Prakt. Chem.* **1987**, 329 (1), 62–66.

[198] Moyer, M. P.; Feldman, P. L.; Rapoport, H., *J. Org. Chem.* **1985**, 50 (12), 5223–5230.

[199] Holzer, W.; Kautsch, C.; Laggner, C.; Claramunt, R. M.; Pérez-Torralba, M.; Alkorta, I.; Elguero, J., *Tetrahedron* **2004**, 60 (32), 6791–6805.

[200] Metwally, M. A.; Bondock, S. A.; Abdou, M. M., *Int. J. Modern Org. Chem.* **2012**, 1 (1), 19–54.

[201] Stefan, S. L., *Monatsh. Chem.* **1994**, 125 (8–9), 859–867.

[202] Singh, D.; Singh, D., *J. Chem. Eng. Data* **1984**, 29 (3), 355–356.

[203] Pavlov, P. T.; Goleneva, A. F.; Lesnov, A. E.; Prokhorova, T. S., *Pharm. Chem. J.* **1998**, 32 (7), 370–372.

[204] Breuer, E.; Melumad, D.; Sarel, S., *Eur. J. Med. Chem.* **1983**, 18 (6), 481–485.

[205] Buzykin, B. I.; Lonshchakova, T. I., *B. Acad. Sci. USSR CH+* **1971**, 20 (10), 2224–2226.

# Appendices

Appendix A

# RP-HPLC-UV Chromatograms for Solid-Phase Products

## A.1 RP-HPLC-UV Chromatogram for Gly-DOX 2.32

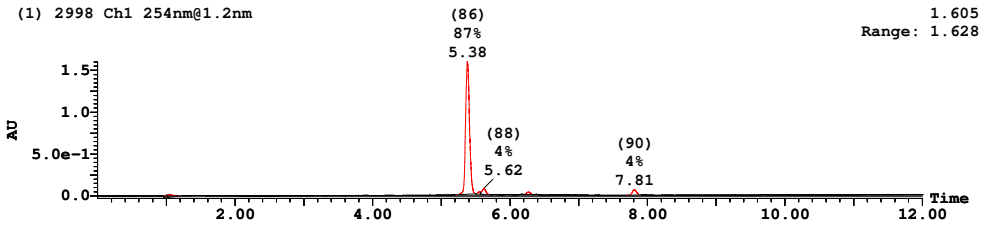


## A.2 RP-HPLC-UV Chromatogram for Leu-DOX 2.38a

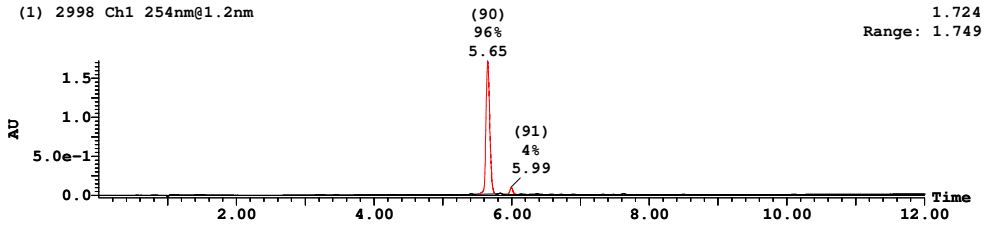

## A.3 RP-HPLC-UV Chromatogram for Ala-DOX 2.38b

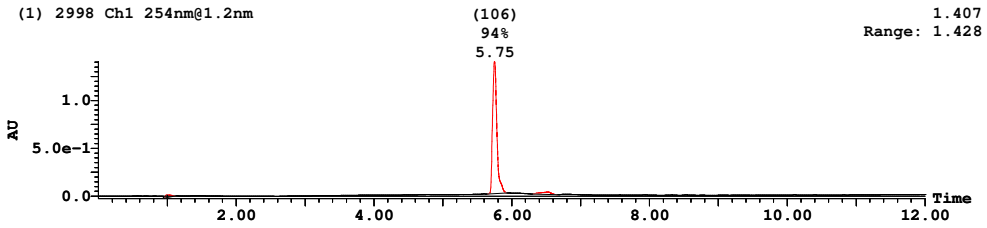


## A.4 RP-HPLC-UV Chromatogram for Phe-DOX 2.38c

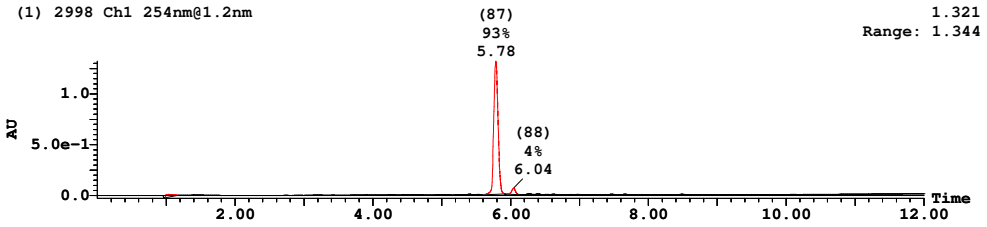


## A.5 RP-HPLC-UV Chromatogram for Ala-Gly-Gly-DOX tripeptide 2.43

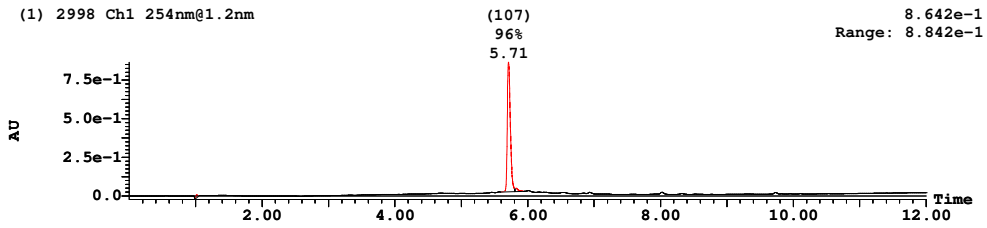


## A.6 RP-HPLC-UV Chromatogram for DOX amide 2.51

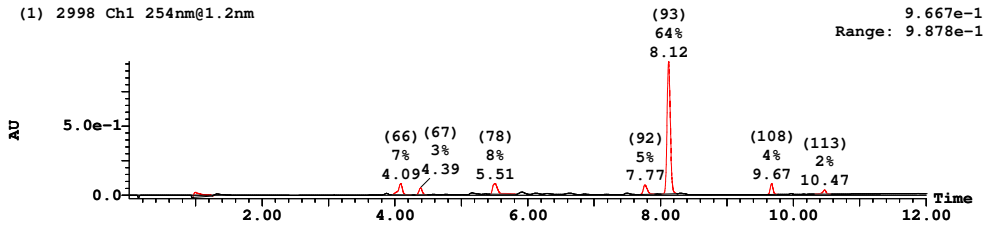

## A.7 RP-HPLC-UV Chromatogram for Ala-DOX amide 2.52

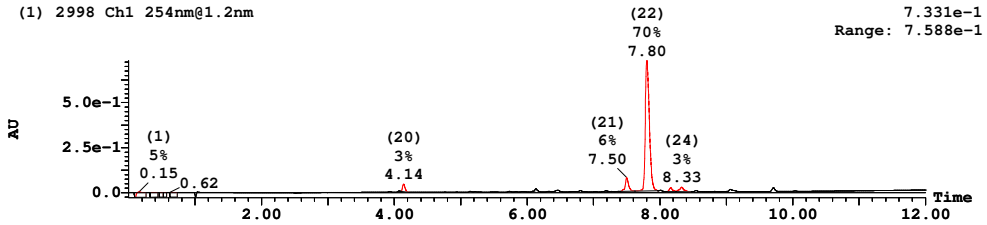


## A.8 RP-HPLC-UV Chromatogram for DOX dipeptide 2.55

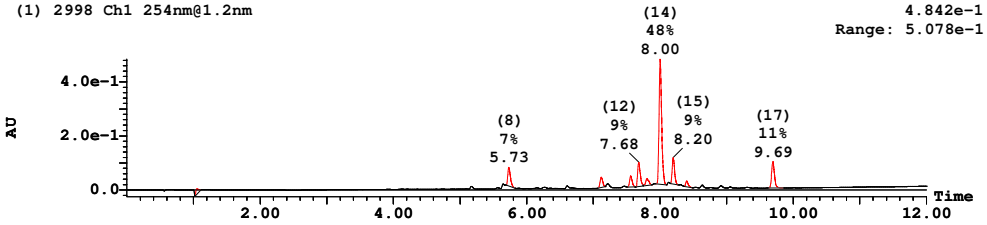

Appendix B

# Paper: Total Synthesis of Trioxacarcin DC-45-A2

Natural Product Synthesis

DOI: 10.1002/anie.201410369

# Total Synthesis of Trioxacarcin DC-45-A2**

*K. C. Nicolaou,* Quan Cai, Bo Qin, Mette T. Petersen, Remi J. T. Mikkelsen, and Philipp Heretsch*

*Dedicated to Professor Stephen Hanessian on the occasion of his 80th birthday*

***Abstract:*** *An enantioselective total synthesis of trioxacarcin DC-45-A2 (**1**) featuring a novel Lewis acid-induced cascade rearrangement of epoxyketone **6** to forge the polyoxygenated 2,7-dioxabicyclo[2.2.1]heptane core of the molecule is described.*

Trioxacarcin DC-45-A2 (**1**, Figure 1)[1] is a naturally occurring antitumor antibiotic that serves as a biosynthetic precursor to a variety of other biologically active members of the family, including the highly potent DC-45-A1 (**2**), trioxacarcin A (**3**), and LL-D49194α1 (**4**) (Figure 1).[1] Possessing a highly oxygenated and complex architecture, trioxacarcin DC-45-A2 (**1**) presents an appealing synthetic challenge and provides opportunities for method and strategy development, chemical biology, and drug discovery efforts.[2] Recent synthetic studies have culminated in a total synthesis of this target molecule and a number of its congeners.[3] In this Communication, we report an enantioselective and distinctively different approach to the total synthesis of the parent trioxacarcin DC-45-A2 (**1**) that could be applied to the synthesis of all other members of the class and their designed analogues.

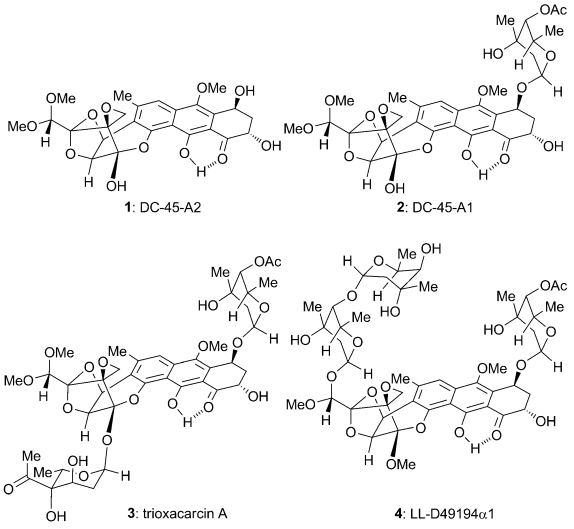


***Figure 1.*** Molecular structures of trioxacarcins DC-45-A2 (**1**), DC-45-A1 (**2**), A (**3**), and LL-D49194α1 (**4**).

The polyoxygenated 2,7-dioxabicyclo[2.2.1]heptane system of the trioxacarcins is a most intriguing structural motif requiring special attention with regard to strategy and experimentation for its construction. Figure 2 presents our designed strategy toward DC-45-A2 (**1**) in retrosynthetic format. Thus, disconnection of the hemiacetal moiety of **1** followed by functional group transformations led to advanced precursor **5**, whose conversion to the target molecule could be envisioned through sequential and selective deprotection/oxidations. Dismantling of the bicyclo-[2.2.1]heptane system within **5** through an epoxyketone rearrangement[4] revealed epoxyketone **6** as a precursor, whose origin could be traced back to key building blocks **7**–**10** through the disconnections indicated in Figure 2 [that is, a) Hauser–Kraus annulation; b) Stille reaction; c) asymmetric Jørgensen epoxidation; and d) Baylis–Hillman reaction]. The key epoxyketone rearrangement (**6**→**5**, Figure 2) was presumed to be inducible in a stereo- and regioselective manner through the action of a suitable monodentate Lewis acid that would involve inversion of configuration at C6, as indicated in Figure 2 (see arrows on structure **6**).

The required cyclohexenone **10** was prepared enantioselectively from cyclohexadiene **11**, as summarized in Scheme 1. Thus, **11** was subjected to Upjohn dihydroxylation ($OsO_4$ cat., NMO, 50% yield) and the resulting diol **12** was silylated to afford bis-TBS ether **13** (TBSCl, 92% yield). Epoxidation of the latter (*m*CPBA, 89% yield) led selectively to epoxide **14**, whose regioselective opening with (−)-norephedrine-derived amine **15** in the presence of *n*BuLi furnished allylic alcohol **16** in 94% yield and 89% *ee*.[5] Protection of this alcohol with 4-methoxybenzyl-2,2,2-trichloroacetimidate (PMBTCA) followed by TBAF-induced desilylation led to PMB-ether diol **17** in 84% yield. Selective oxidation of the allylic alcohol of

[*] Prof. Dr. K. C. Nicolaou, Dr. Q. Cai, Dr. B. Qin, M. T. Petersen, R. J. T. Mikkelsen, Dr. P. Heretsch
Department of Chemistry, BioScience Research Collaborative
Rice University
6100 Main Street, Houston, TX 77005 (USA)
E-mail: kcn@rice.edu

[**] K.C.N. acknowledges financial support from the Cancer Prevention & Research Institute of Texas (CPRIT), the Welch Foundation, fellowships to Q.C. and B.Q. from Chongqing University, to M.T.P. and R.J.T.M. from the Danish Agency for Science, Technology and Innovation (The Frants Alling Scholarship), and to P.H. from Deutsche Akademie der Naturforscher Leopoldina. Part of the initial work of this project was carried out at The Scripps Research Institute (TSRI). M.T.P. participated at TSRI only; K.C.N., Q.C., and P.H. participated at both TSRI and Rice University; B.Q. and R.J.T.M. participated at Rice University only.

Supporting information for this article is available on the WWW under http://dx.doi.org/10.1002/anie.201410369.

  

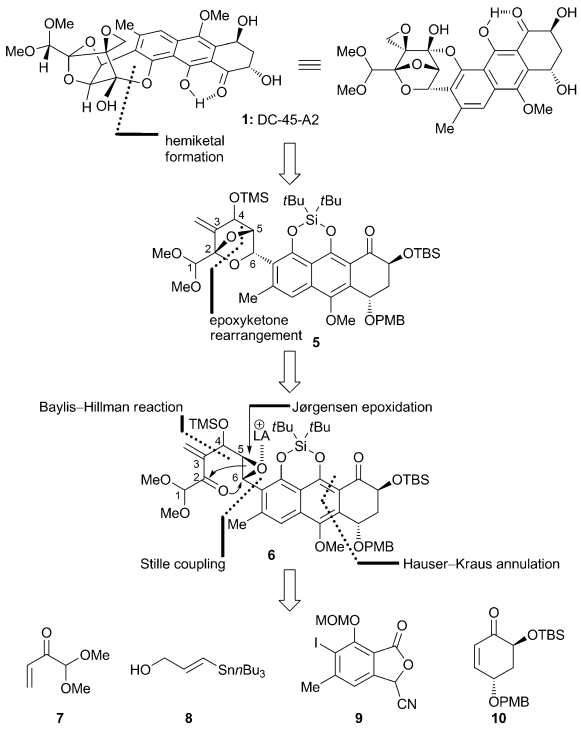


***Figure 2.*** Retrosynthetic analysis of trioxacarcin DC-45-A2 (**1**). MOM = methoxymethyl, PMB = *para*-methoxybenzyl, TBS = *tert*-butyldimethylsilyl, TMS = trimethylsilyl.

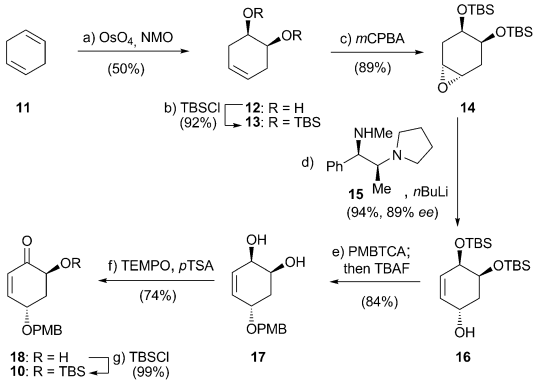


***Scheme 1.*** Synthesis of key building block **10**. Reagents and conditions: a) $OsO_4$ (4% w/v aq. solution, 0.02 equiv), NMO (1.0 equiv), acetone, 25 °C, 72 h, 50%; b) TBSCl (2.4 equiv), imidazole (5.0 equiv), $CH_2Cl_2$, 25 °C, 48 h, 92%; c) *m*CPBA (1.4 equiv), $NaHCO_3$ (2.0 equiv), cyclohexane, 25 °C, 17 h, 89%; d) **15** (2.0 equiv), *n*BuLi (2.0 equiv), THF, 0→25 °C, 18 h, 94%, 89% *ee*; e) PMBTCA (2.5 equiv), $TrBF_4$ (0.05 equiv), THF, 25 °C, 1 h; then TBAF (7.0 equiv), THF, 66 °C, 4 h, 84%; f) TEMPO (3.0 equiv), *p*TSA (3.0 equiv), $CH_2Cl_2$, 0 °C, 45 min, 74%; g) TBSCl (1.8 equiv), imidazole (3.0 equiv), $CH_2Cl_2$, 25 °C, 1.5 h, 99%. *m*CPBA = *meta*-chloroperoxybenzoic acid, NMO = *N*-methylmorpholine-*N*-oxide, PMBTCA = *para*-methoxybenzyl-2,2,2-trichloroacetimidate, *p*TSA = *para*-toluenesulfonic acid, TBAF = tetra-*n*-butylammonium fluoride, TEMPO = 2,2,6,6-tetramethyl-1-piperidinyloxy, THF = tetrahydrofuran, $TrBF_4$ = trityltetrafluoroborate.

the latter (TEMPO, *p*TSA, 74% yield)[6] furnished hydroxyenone **18**, whose silylation (TBSCl, 99% yield) led to the targeted key building block enone **10**.

Enone **10** was coupled with the easily accessible iodocyanophthalide derivative **9** through a Hauser–Kraus annulation,[7] and the product was elaborated to intermediate **21** as shown in Scheme 2. Thus, iodocyanophthalide **9** [prepared

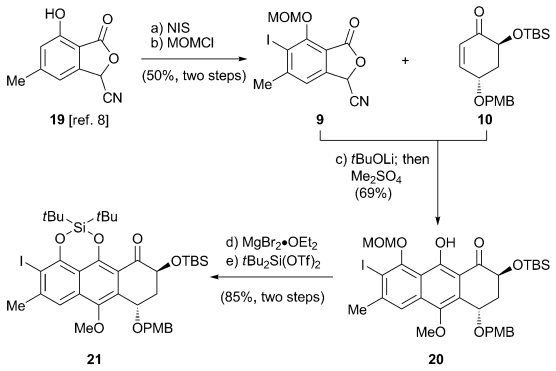


***Scheme 2.*** Synthesis of key building block **21**. Reagents and conditions: a) NIS (1.4 equiv), DCE, −10 °C, 6 h; b) MOMCl (1.3 equiv), DIPEA (3.0 equiv), $CH_2Cl_2$, 25 °C, 6 h, 50% over two steps; c) **9** (1.0 equiv), **10** (1.0 equiv), *t*BuOLi (3.0 equiv), THF, −78 °C, 0.5 h; then $Me_2SO_4$ (10 equiv), 0 °C, 5 h, 69%; d) $MgBr_2{\cdot}OEt_2$ (3.0 equiv), THF, 0 °C, 15 min; e) $tBu_2Si(OTf)_2$ (1.2 equiv), 2,6-lutidine (2.5 equiv), DMF, 0 °C, 0.5 h, 85% over two steps. DCE = 1,2-dichloroethane, DIPEA = *N*,*N*-diisopropylethylamine, DMF = *N*,*N*-dimethylformamide, NIS = *N*-iodosuccinimide.

from the known cyanophthalide **19**[8] by sequential iodination (NIS) and MOM protection (MOMCl, DIPEA, 50% overall yield)] was reacted with enone **10** in the presence of *t*BuOLi (−78 °C)[3,8] and the resulting *p*-dihydroquinone derivative was selectively methylated with $Me_2SO_4$ to afford tricyclic system **20** in 69% overall yield. Removal of the MOM group from the latter intermediate with $MgBr_2{\cdot}OEt_2$,[9] followed by treatment with $tBu_2Si(OTf)_2$ and 2,6-lutidine then gave silylated product **21** in 85% overall yield.

Intermediate **21** was advanced to the key cyclization precursor **6**, as summarized in Scheme 3. Thus, Stille coupling of aryl iodide **21** with stannane **8**[10] proceeded in the presence of CuTC and catalytic amounts of $Pd(PPh_3)_4$[11] to afford allylic alcohol **22** (74% yield), whose oxidation with TEMPO and PIDA gave aldehyde **23** (89% yield). Jørgensen asymmetric epoxidation of α,β-unsaturated aldehyde **23** (**24** cat., urea·$H_2O_2$)[12] led to epoxyaldehyde **25**, which was subjected without purification to Baylis–Hillman reaction with enone **7**[13] (DABCO, 4-nitrophenol) to give labile hydroxyepoxide **26**. The latter was immediately protected with *N*-trimethylsilylimidazole (TMS-imid) to furnish the targeted precursor **6** (+C4-*epi*-**6**, d.r. ca. 3:1) in 36% yield over the three steps.

With the penultimate bis-cyclization precursor **6** in hand, the stage was now set for the coveted cascade ring closures to forge the targeted 2,7-dioxabicyclo[2.2.1]heptane system of the growing molecule. To this end, and as shown in Scheme 4,

  

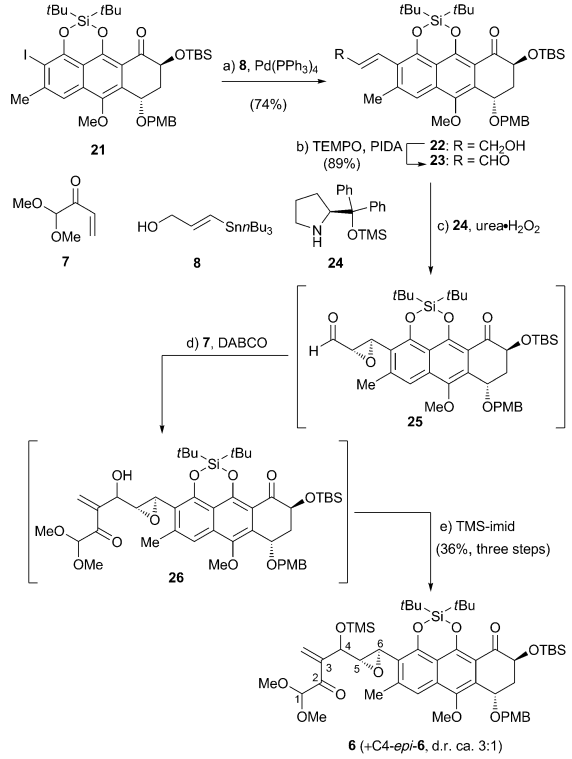


*Scheme 3.* Synthesis of bis-cyclization precursor epoxyketone **6**. Reagents and conditions: a) $Pd(PPh_3)_4$ (0.2 equiv), **8** (3.0 equiv), CuTC (1.2 equiv), DMF/THF 1:1, 85 °C, 12 h, 74%; b) TEMPO (0.1 equiv), PIDA (1.3 equiv), $CH_2Cl_2$, 25 °C, 4 h, 89%; c) **24** (0.2 equiv), urea·$H_2O_2$ (7.0 equiv), $CHCl_3/H_2O$ 20:1, 25 °C, 7 h; d) **7** (10 equiv), DABCO (0.5 equiv), 4-nitrophenol (0.5 equiv), THF, 25 °C, 12 h; e) TMS-imid (1.0 equiv), $CH_2Cl_2$, 25 °C, 0.5 h, 36% over three steps, d.r. ca. 3:1 at C4. CuTC = copper(I)-thiophene-2-carboxylate, DABCO = 1,4-diazabicyclo[2.2.2]octane, PIDA = iodobenzene diacetate, TMS-imid = *N*-trimethylsilylimidazole.

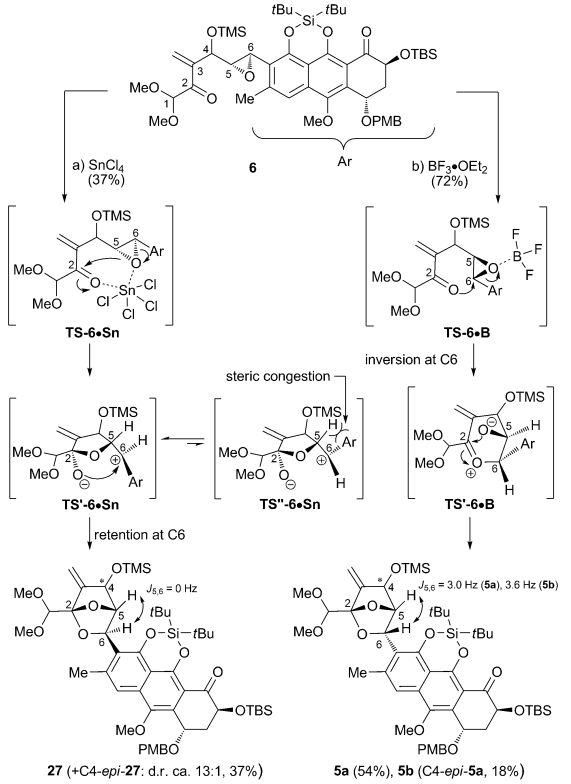


*Scheme 4.* Bis-cyclization of precursor epoxyketone **6**. Reagents and conditions: a) $SnCl_4$ (0.05 equiv), $CH_2Cl_2$, −78 °C, 1 h, d.r. ca. 13:1 at C4, 37%; b) $BF_3$·$OEt_2$ (0.3 equiv), $CH_2Cl_2$, −78 °C, 3 h, 54% (**5a**), 18% (**5b**).

epoxyketone **6** (ca. 3:1 mixture of C4-diastereoisomers) was reacted with catalytic amounts of $BF_3$·$OEt_2$ (monodentate Lewis acid) in $CH_2Cl_2$ at −78 °C, furnishing the desired product as a mixture of C4-diastereoisomers (d.r. ca. 3:1) (**5a**, C4-α-diastereoisomer, 54% yield; **5b**, C4-β-diastereoisomer, 18% yield). The assignments of the C4 and C6 configurations of diastereoisomers **5a** and **5b** were based on their H4, H5, H6 coupling constants (**5a**:[14] $J_{4,5} = 4.8$ Hz, $J_{5,6} = 3.0$ Hz; **5b**:[14] $J_{4,5} = 0$ Hz, $J_{5,6} = 3.6$ Hz).[15] Both compounds were obtained as single diastereoisomers at C6 (inverted configuration). The reaction is presumed to proceed through transition states **TS-6·B** and **TS′-6·B** as shown in Scheme 4. In contrast, reaction of substrate **6** with catalytic amounts of bidentate Lewis acid $SnCl_4$ in $CH_2Cl_2$ at −78 °C led to the opposite diastereoisomers at C6 ($J_{5,6} = 0$ Hz), **27** (+C4-*epi*-**27**) (37% yield, d.r. ca. 13:1). This reaction is presumed to proceed through transition states **TS-6·Sn** and **TS′-6·Sn**, the latter being favored over its more sterically congested alternative conformer **TS″-6·Sn** that would have led to inversion of configuration at C6 (see Scheme 4). These results support our originally proposed monodentate Lewis acid-catalyzed epoxyketone rearrangement upon which the strategy for the construction of the dioxabicyclo[2.2.1]heptane structural motif possessing the desired configurations was based.

Having succeeded in building the most challenging structural domain of the targeted molecule, we proceeded to complete the remaining tasks of the synthesis that included installation of the epoxide moiety, oxidation at C4, and deprotection. Thus, advanced intermediate **5a** (major diastereoisomer) was converted to the targeted natural product (**1**) as shown in Scheme 5. Selective cleavage of the TMS-ether of **5a** gave allylic alcohol **28** (TFA, 65% yield) and recovered **5a** (24% yield). Due to difficulties in obtaining the desired epoxide **29** from **28** through *m*CPBA or *t*BuOOH/VO(acac)$_2$ epoxidations, we resorted to a three-step process involving diastereoselective Upjohn dihydroxylation of the olefinic bond within **28** ($OsO_4$ cat., NMO) followed by selective monotosylation of the resulting triol (TsCl, $Et_3N$, DMAP cat.) and epoxide formation ($K_2CO_3$, MeOH, 82% overall yield). TPAP-catalyzed oxidation of hydroxyepoxide **29** led to ketoepoxide **30** (93% yield), which could be sequentially and selectively deprotected to afford trioxacarcin derivatives **31** ($Et_3N$·3HF, 3.0 equiv, 15 min, 88% yield) and **32** (DDQ, 93% yield). Finally, trioxacarcin DC-45-A2 (**1**) was liberated

  

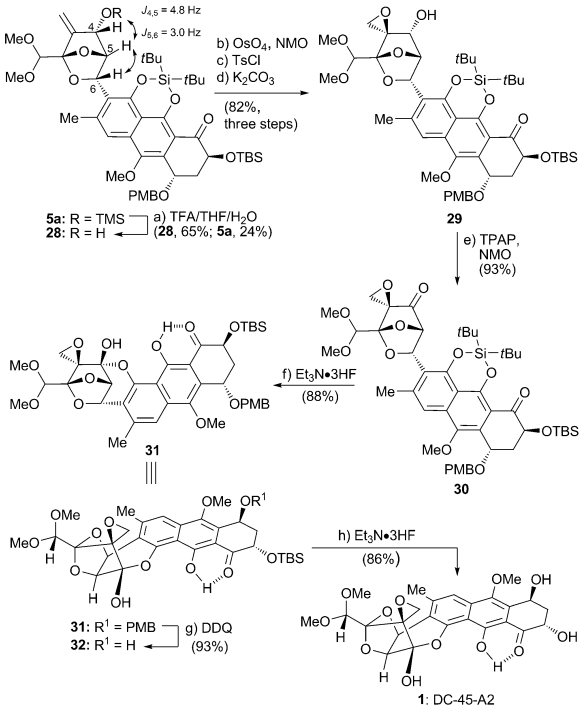


***Scheme 5.*** Completion of the total synthesis of trioxacarcin DC-45-A2 (**1**). Reagents and conditions: a) TFA (0.1 M, 10 equiv), THF/$H_2O$ 5:1, 25 °C, 6 h, 65% and recovered **5a**, 24%; b) $OsO_4$ (4% w/v, aq. solution, 0.2 equiv), NMO (0.48 M aq. solution, 4.0 equiv), acetone, 25 °C, 12 h; c) TsCl (5.0 equiv), $Et_3N$ (10 equiv), DMAP (0.2 equiv), $CH_2Cl_2$, 0→25 °C, 5 h; d) $K_2CO_3$ (2.0 equiv), MeOH, 0 °C, 3 h, 82% over three steps; e) TPAP (0.2 equiv), NMO·$H_2O$ (3.0 equiv), $CH_2Cl_2$, 0 °C, 2 h, 93%; f) $Et_3N{\cdot}3HF$ (3.0 equiv), $CH_3CN$, 25 °C, 15 min, 88%; g) DDQ (2.0 equiv), $CH_2Cl_2/H_2O$ 10:1, 25 °C, 1 h, 93%; h) $Et_3N{\cdot}3HF$ (20 equiv), $CH_3CN$, 25 °C, 13 h, 86%. DDQ = 2,3-dichloro-5,6-dicyano-1,4-benzoquinone, DMAP = *N*,*N*-dimethyl-4-aminopyridine, TFA = trifluoroacetic acid, TPAP = tetra-*n*-propylammonium perruthenate, Ts = 4-toluenesulfonyl.

from its TBS-ether **32** by exposure to $Et_3N{\cdot}3HF$ (excess, 13 h, 86% yield). Synthetic **1** exhibited identical physical properties (i.e., $^1H$ and $^{13}C$ NMR and mass spectra) to those reported in the literature.[1e,3a]

The total synthesis described herein provides rapid access to the parent trioxacarcin DC-45-A2 (**1**) and could be deployed to reach all other members of the trioxacarcin family of compounds. Furthermore, the developed synthetic strategy and technologies could be applied to the construction of designed analogues for structure activity relationship studies and drug discovery efforts. Of particular interest is the design and synthesis of potent trioxacarcins equipped with handles that could be employed to attach them onto specific antibodies to construct antibody drug conjugates (ADCs) for targeted chemotherapy purposes. These objectives are currently being pursued.

Received: October 22, 2014
Published online: January 12, 2015

**Keywords:** antitumor agents · cascade reactions · natural products · total synthesis · trioxacarcins

[1] a) F. Tomita, T. Tamaoki, *J. Antibiot.* **1981**, *34*, 1519–1524; b) T. Tamaoki, K. Shirahata, T. Iida, F. Tomita, *J. Antibiot.* **1981**, *34*, 1525–1530; c) W. M. Maiese, D. P. Labeda, J. Korshalla, N. Kuck, A. A. Fantini, M. J. Wildey, J. Thomas, M. Greenstein, *J. Antibiot.* **1990**, *43*, 253–258; d) R. P. Maskey, E. Helmke, O. Kayser, H. H. Fiebig, A. Maier, A. Busche, H. Laatsch, *J. Antibiot.* **2004**, *57*, 771–779; e) K. Shirahata, T. Kaisha, US patent 4,459,291, **1984**.

[2] a) J. Cassidy, M. A. Graham, W. Ten Bokkel Huinink, C. McDaniel, A. Setanoians, E. M. Rankin, D. J. Kerr, S. B. Kaye, *Cancer Chemother. Pharmacol.* **1993**, *31*, 395–400; b) D. Sun, M. Hansen, J. J. Clement, L. H. Hurley, *Biochemistry* **1993**, *32*, 8068–8074; c) C. K. Smith, G. J. Davies, E. J. Dodson, M. H. Moore, *Biochemistry* **1995**, *34*, 415–425; d) R. P. Maskey, M. Sewana, I. Usón, E. Helmke, H. Laatsch, *Angew. Chem. Int. Ed.* **2004**, *43*, 1281–1283; *Angew. Chem.* **2004**, *116*, 1301–1303; e) A. Fitzner, H. Frauendorf, H. Laatsch, U. Diederichsen, *Anal. Bioanal. Chem.* **2008**, *390*, 1139–1147; f) R. Pfoh, H. Laatsch, G. M. Sheldrick, *Nucleic Acids Res.* **2008**, *36*, 3508–3514.

[3] a) J. Švenda, N. Hills, A. G. Myers, *Proc. Natl. Acad. Sci. USA* **2011**, *108*, 6709–6714; b) T. Magauer, D. J. Smaltz, A. G. Myers, *Nat. Chem.* **2013**, *5*, 886–893.

[4] a) Y. Gaoni, *J. Chem. Soc. C* **1968**, 2925–2934; b) H. H. Wasserman, E. H. Barber, *J. Am. Chem. Soc.* **1969**, *91*, 3674–3675; c) H. H. Wasserman, S. Wolff, T. Oku, *Tetrahedron Lett.* **1986**, *27*, 4909–4912; d) H. H. Wasserman, T. Oku, *Tetrahedron Lett.* **1986**, *27*, 4913–4916; e) H. H. Wasserman, M. Thyes, S. Wolff, V. Rusiecki, *Tetrahedron Lett.* **1988**, *29*, 4973–4976; f) H. H. Wasserman, V. Rusiecki, *Tetrahedron Lett.* **1988**, *29*, 4977–4980; g) Y. Naruse, T. Esaki, H. Yamamoto, *Tetrahedron* **1988**, *44*, 4747–4756; h) Y. Naruse, T. Esaki, H. Yamamoto, *Tetrahedron Lett.* **1988**, *29*, 1417–1420; i) D. A. Evans, R. P. Polniaszek, K. M. DeVries, D. E. Guinn, D. J. Mathre, *J. Am. Chem. Soc.* **1991**, *113*, 7613–7630.

[5] a) A. Maraş, H. Seçen, Y. Sütbeyaz, M. Balcı, *J. Org. Chem.* **1998**, *63*, 2039–2041; b) P. O'Brien, P. Poumellec, *J. Chem. Soc. Perkin Trans. 1* **1998**, 2435–2441; c) B. Colman, S. E. de Sousa, P. O'Brien, T. D. Towers, W. Watson, *Tetrahedron: Asymmetry* **1999**, *10*, 4175–4182; d) S. E. de Sousa, P. O'Brien, C. D. Pilgram, *Tetrahedron* **2002**, *58*, 4643–4654.

[6] M. G. Banwell, V. S. Bridges, J. R. Dupuche, S. L. Richards, J. M. Walter, *J. Org. Chem.* **1994**, *59*, 6338–6343.

[7] a) F. M. Hauser, R. P. Rhee, *J. Org. Chem.* **1978**, *43*, 178–180; b) G. A. Kraus, H. Sugimoto, *Tetrahedron Lett.* **1978**, *19*, 2263–2266; For selected examples of the application of the Hauser–Kraus annulation in total synthesis, see: c) J. A. Wendt, P. J. Gauvreau, R. D. Bach, *J. Am. Chem. Soc.* **1994**, *116*, 9921–9926; d) T. Matsumoto, H. Yamaguchi, M. Tanabe, Y. Yasui, K. Suzuki, *Tetrahedron Lett.* **2000**, *41*, 8393–8396; e) K. C. Nicolaou, Y. H. Lim, J. L. Piper, C. D. Papageorgiou, *J. Am. Chem. Soc.* **2007**, *129*, 4001–4013; f) K. C. Nicolaou, H. Zhang, J. S. Chen, J. J. Crawford, L. Pasunoori, *Angew. Chem. Int. Ed.* **2007**, *46*, 4704–4707; *Angew. Chem.* **2007**, *119*, 4788–4791; g) O. Andrey, J. Sperry, U. S. Larsen, M. A. Brimble, *Tetrahedron* **2008**, *64*, 3912–3927; For a review, see: h) D. Mal, P. Pahari, *Chem. Rev.* **2007**, *107*, 1892–1918.

[8] K. C. Nicolaou, J. Becker, Y. H. Lim, A. Lemire, T. Neunauer, A. Montero, *J. Am. Chem. Soc.* **2009**, *131*, 14812–14826.

[9] X. Yang, B. Fu, B. Yu, *J. Am. Chem. Soc.* **2009**, *131*, 12433–12435.

[10] R. A. Pilli, C. K. Z. de Andrade, C. R. O. Souto, A. J. de Meijere, *J. Org. Chem.* **1998**, *63*, 7811–7819.

  

[11] K. K. Pulukuri, T. K. Chakraborty, *Org. Lett.* **2012**, *14*, 2858 – 2861.
[12] M. Marigo, J. Franzén, T. B. Poulsen, W. Zhuang, K. A. Jørgensen, *J. Am. Chem. Soc.* **2005**, *127*, 6964 – 6965.
[13] M. L. Edwards, P. J. Cox, S. Amendola, S. D. Deprets, T. A. Gillespy, A. Timothy, C. D. Christopher, A. D. Morley, C. J. Gardner, B. Pedgrift, H. Bouchard, D. Babin, L. Gauzy, A. Le Brun, T. N. Majid, J. C. Reader, L. J. Payne, N. M. Khan, M. Cherry, WO 2003035065, **2003**.
[14] See Supporting Information for the structures of **5a**, **5b** and the coupling constants (*J*) of their H4, H5, H6.
[15] a) A. Padwa, R. L. Chinn, S. F. Hornbuckle, Z. J. Zhang, *J. Org. Chem.* **1991**, *56*, 3271 – 3278; b) K. Kraehenbuehl, P. Vogel, *Tetrahedron Lett.* **1995**, *36*, 8595 – 8598; c) K. Kraehenbuehl, S. Picasso, P. Vogel, *Helv. Chim. Acta* **1998**, *81*, 1439 – 1479; d) S. Muthusamy, S. A. Babu, C. Gunanathan, B. Ganguly, E. Suresh, P. Dastidar, *J. Org. Chem.* **2002**, *67*, 8019 – 8033.

  

Appendix C

# Paper Draft: Photolabile Linkers for Solid-Phase Organic Synthesis

# Photolabile Linkers for Solid-Phase Organic Synthesis

Remi J. T. Mikkelsen[†], Katrine Qvortrup[†], and Thomas E. Nielsen*[,†,‡]

[†]Department of Chemistry, Technical University of Denmark, DK-2800 Kgs. Lyngby, Denmark.

[‡]Singapore Centre on Environmental Life Sciences Engineering, Nanyang Technological University, Singapore 637551, Singapore.

* Corresponding author. E-mail: ten@kemi.dtu.dk.

## Contents



## 1 Introduction

Originally developed by Merrifield for the synthesis of peptides [1], solid phase organic chemistry is an attractive synthetic technique that offers unique advantages over conventional

solution phase chemistry, both in terms of purification and experimental simplicity. Since its introduction half a century ago, many laboratories have focused on the development of technologies and chemistry suitable for solid phase organic synthesis, which has resulted in a remarkable outburst of chemical transformations that can be applied for the routine synthesis of organic molecules on solid support [2, 3, 4, 5, 6]. This has led to the application of solid phase synthesis in the generation of combinatorial libraries both in academia and industry, ultimately leading to the identification of new drugs and catalysts [7, 8].

The use of solid supports in organic synthesis relies on two interconnected requirements. One must be able to link the substrate to the solid phase while retaining the ability to selectively cleave off some or all of the product from the solid support during synthesis for the analysis of reactions and ultimately to release the target molecule of interest. Furthermore, a strategy must exist for the chemical protection of reactive groups, allowing for selective protection and deprotection during synthesis.

In solid phase organic synthesis the desired molecule is bound through a linker inserted between the solid support and the molecule in question. Often harsh cleavage conditions such as strong acids/bases or nucleophiles, are needed, which can pose compatibility problems with acid- and base-labile compounds as well as commonly used protecting groups. Furthermore, the range of chemical transformations available for the synthesis of compounds is restricted by the cleavage conditions of the linker so premature cleavage is avoided. Thus, to provide a further dimension for the introduction of chemical diversity, linkers relying on other cleavage principles are needed.

Photolysis offers a method of cleavage, which is fully orthogonal to conventional chemical methods. Photolabile linkers are particularly interesting since they do not need acidic, basic or metal-assisted activation for cleavage. Indeed photochemical substrate release often occurs without additional reagents and under mild conditions that renders the process environmentally friendly and especially appealing in the context of green chemistry. The mild conditions are, furthermore, attractive for direct applications in biological screening where contamination with cleavage reagents is undesired. Additionally, recent advances in LED lighting have significantly increased the ease with which photochemical transformations can be achieved, a fact we suspect will lead to increased interest in photochemical substrate activation.

Below follows an overview of the most commonly used photolabile linkers in solid phase organic synthesis.

# 2 Photolabile Linkers

## 2.1 *o*-nitrobenzyloxy linkers

The first account of a photolabile linker was the *o*-nitrobenzyloxy based linker pioneered by Rich and Gurwara in 1973 [9]. The resin was contructed with a Friedel-Crafts-type chloromthylation of the aromtaic rings of polymer **1**, cf. scheme 1. A nitration, as described by Merrifield [1], set up the resin for attachment of the first amino acid at the *C*-terminus affording **3**. After standard SPPS and photolysis the first peptide ever constructed on a photolabile linker was released in a yield of 62%.

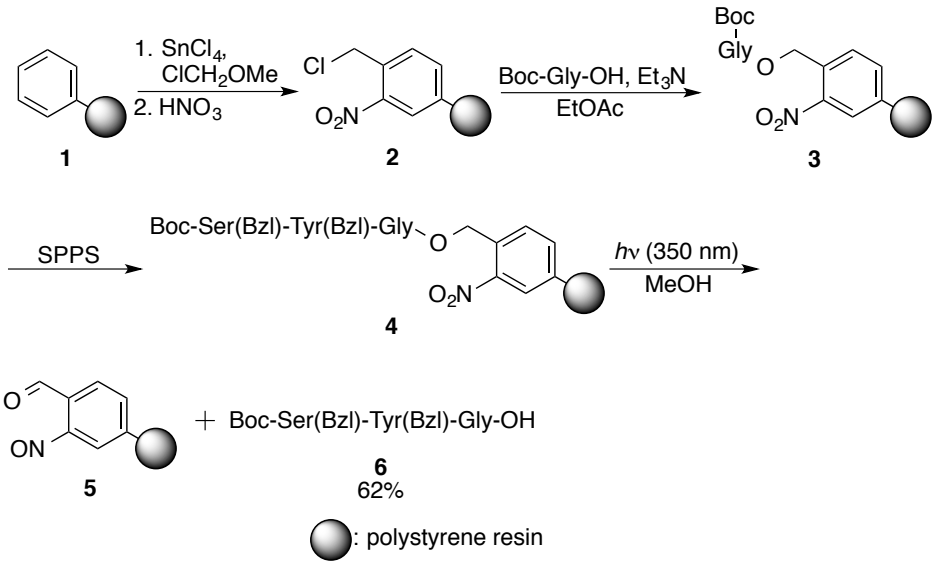


**Scheme 1**. Synthesis and use of the first photolabile linker based on the *o*-nitrobenzyloxy functional group.

However, it eventually became clear to Rich and Gurwara that this strategy was not appropriate for the synthesis of peptides incorporating more than four amino acids [10]. Over-nitration of the resin apparently caused reduced swelling of the resin in organic solvents due to enhanced polarity. Thus in attempt to find a solution to this limitation a new strategy was developed where the linker was prepared separately and then coupled to the resin [10], cf. scheme 2. The linker **8** was prepared and then coupled to the resin. The construct **9** was then set up for attachment of the first amino acid and following standard SPPS the decapeptide **11** was synthesized in 64% yield.

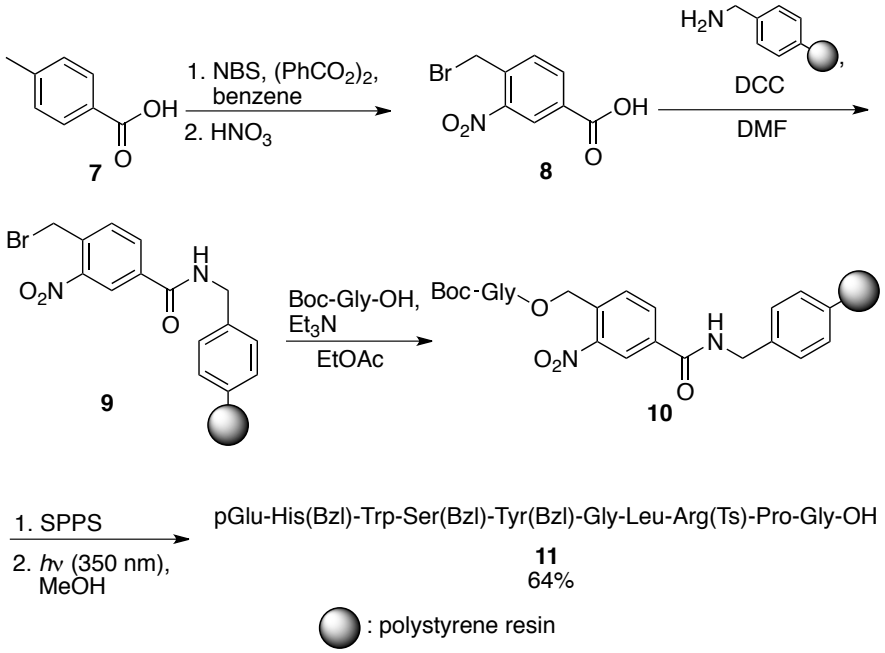


**Scheme 2**. Synthesis and use of *o*-nitrobenzyloxy linker prepared separately from resin.

The linker has been used by Merrifield for the preparation of multi detachable resins [11, 12] and by Barany and co-workers to achieve three dimensional orthogonal protection in solid phase organic synthesis [13]. The construct **9** was used in the synthesis of photolabile construct **12**, containing a *t*-butyl group and a dithiasuccinoyl group, both of which are photochemically inert and mutually orthogonal, cf. scheme 3.

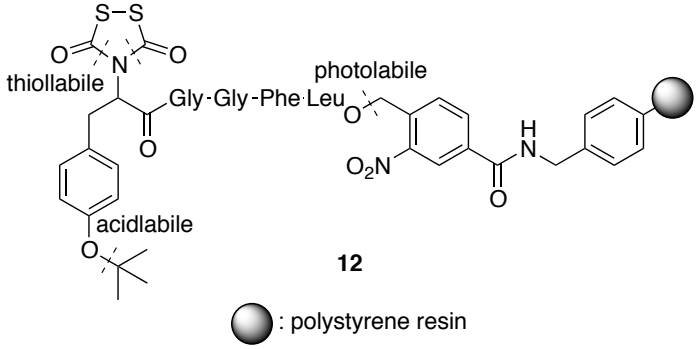


**Scheme 3**. Three-dimensional and orthogonal protection of a resin-bound peptide.

Different variations of the connection of the linker unit to the resin have been explored, e.g. adding a phenyl group in the benzyllic position [14, 15] or the use of a glycine unit as an internal standard [16].

The *o*-nitrobenzyloxy linker has also been used by Pillai in experiments combining the advantages of both solid-phase and solution-phase synthesis by incorporating a PEG unit in between the photolabile linker unit and the solid support [17].

In a study focusing on the synthesis of combinatorial ligand libraries with molecular libraries Ohlmeyer used the *o*-nitrobenzyloxy linker, which facilitated easy release of the synthesized ligands under conditions optimal for subsequent use in biological assays [18].

In 1993 Greenberg demonstrated the first application of *o*-nitrobenzyloxy linkers to oligonucleotide synthesis [19, 20, 21]. A DCC mediated coupling of succinatothymidine **13** to trichlorphenyl ester **14** followed by a coupling to the solid support (long chain alkyl amine controlled pore glass, LCAA-CPG) in the presence of HOBt led to the construct **15** which allowed for the synthesis of oligonucleotides, cf. scheme 4.

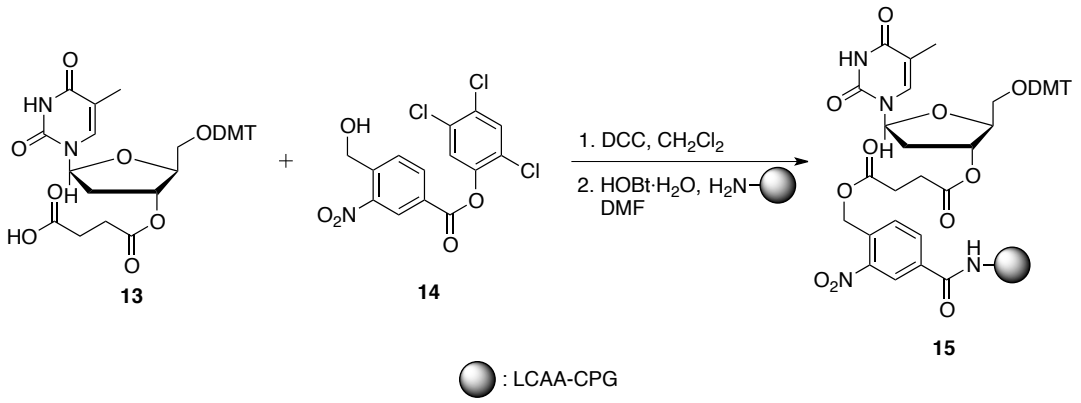


13 14 15

**Scheme 4**. Oligonucleotide synthesis on a photolabile linker.

Alcohol-containing groups can also be attached to a *o*-nitrobenzyloxy linker either through carbonates [22] or as ethers as shown by Merrifield [23] or as seen in the oligosaccharide synthesis by Zehavi and coworkers [24], cf. scheme 5. This linker was also used for solid-phase oligosaccharide synthesis by Nicolaou [25, 26] and Parquette [27].

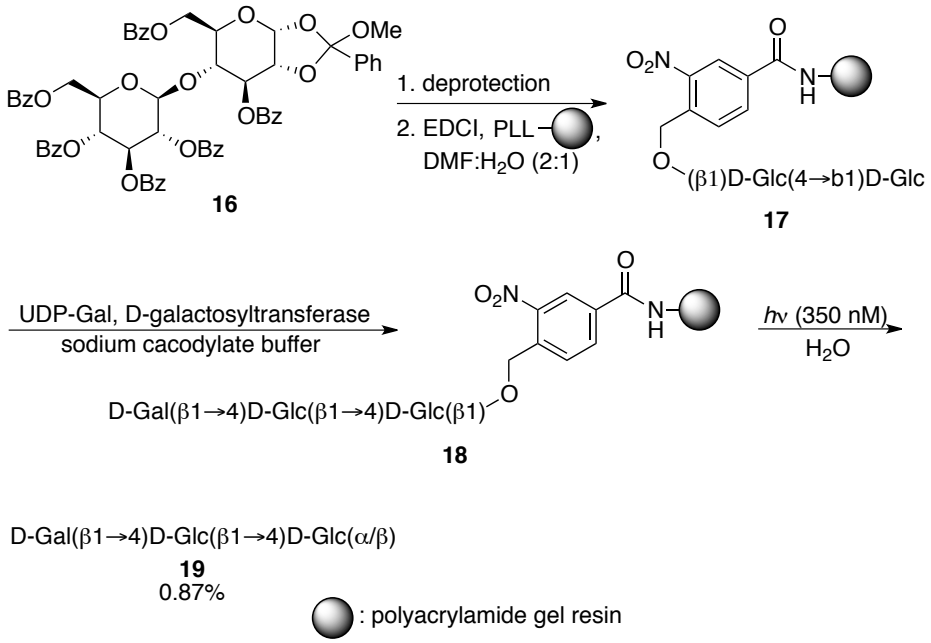


**Scheme 5**. Oligosaccharide synthesis utilizing a photolabile *o*-nitrobenzyloxy linker.

Amines can be attached through a carbamate function as shown by Armstrong in a Passerini reaction-based combinatorial library synthesis [28], cf. scheme 6.

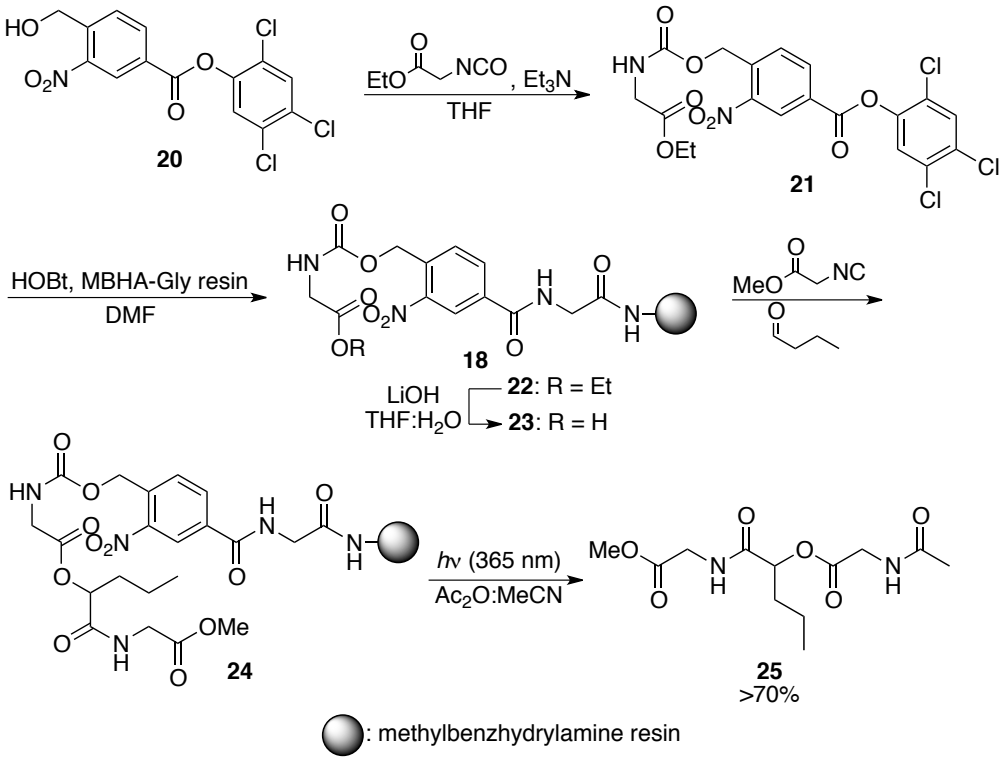


**Scheme 6**. Photolabile *o*-nitrobenzyloxy linker attached to an amine through a carbamate function.

Damha hypothesized that incorporating a tertiary carbon center would accelerate the photolysis times and thus developed a linker incorporating this feature [29]. Starting from **26** the linker **28** was synthesized in two steps and subsequently attached to the solid support, cf. scheme 7. With the construct **29** in hand Damha synthesized oligoribonucleotides and rewardingly found that that the target molecule could readily be cleaved from the linker in only 15 minutes at room temperature.

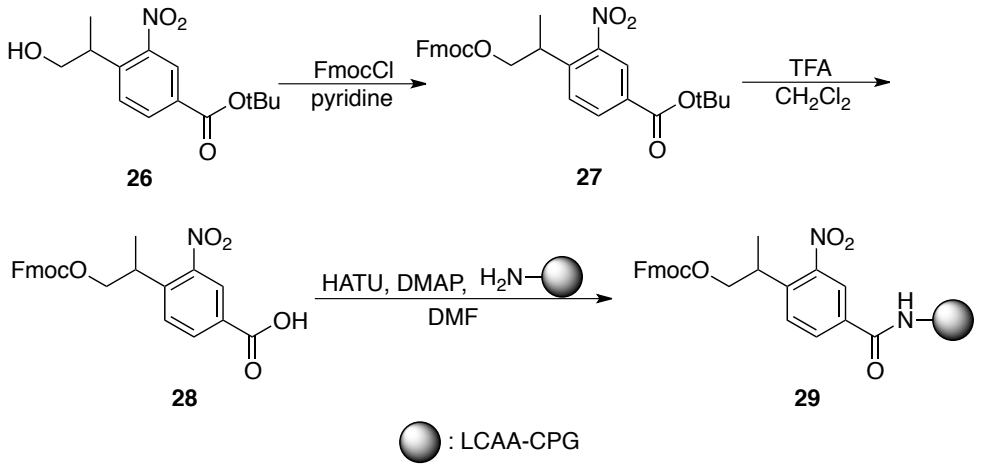


**Scheme 7**. Photolabile *o*-nitrobenzyloxy linker incorporating a tertiary carbon center.

## 2.2 *o*-nitrobenzylamino linkers

To take into account the fact that many biologically active peptides possess a terminal primary amide, Rich and Gurwara developed a variation of the *o*-nitrobenzyl-based linker that upon photolysis releases an amide [30], cf. scheme 8. Starting from *p*-toluic acid, initial bromination followed by nitration led to **8**. The bromide **8** was then aminated and immediately Boc-protected with Boc-azide furnishing **30**. After attachment to the resin and deprotection Boc-Val-OH was coupled. Photolysis provided Boc-Val-$NH_2$ (**33**) in quantitative yield. Furthermore it was shown that a decapeptide could be prepared and released in a yield of 65%. Other synthetic routes to **30** was suggested by Barany starting from 4-aminomethylbenzoic acid [31]. Pillai and co-workers documented the possibility of releasing secondary amides by substituting the linker precursor **8** (or the corresponding chloride) with a primary amine instead of ammonia [32, 33, 34]. An *o*-nitrobenzylamino linker was used by Gerace and Auer in their on-bead screening of a one-bead one-compound library in the search for nuclear import inhibitors [35].

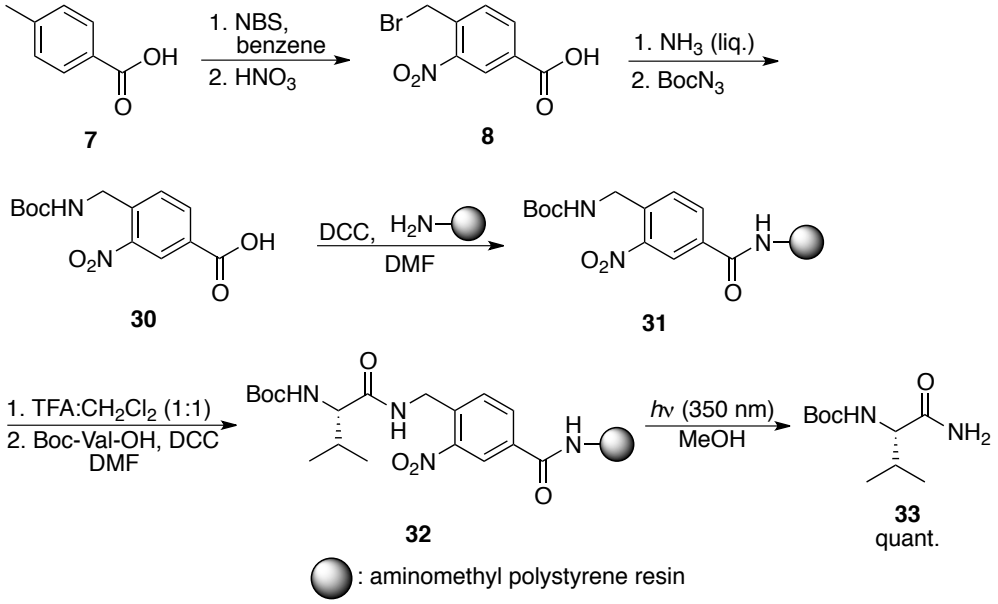


**Scheme 8**. Photolabile *o*-nitrobenzylamino linker releasing amides upon photolysis.

Recently Seeberger developed an approach for the automated synthesis of glucosaminoglycans utilizing an *o*-nitrobenzylamino linker [36]. Iterative cycles of coupling of carbohydrate building blocks **35** and **36** to the linker construct **34** yielded, in 16 steps, the hexasaccharide **38** in 13% yield after photoclevage in a continuous flow photoreactor, cf. scheme 9.

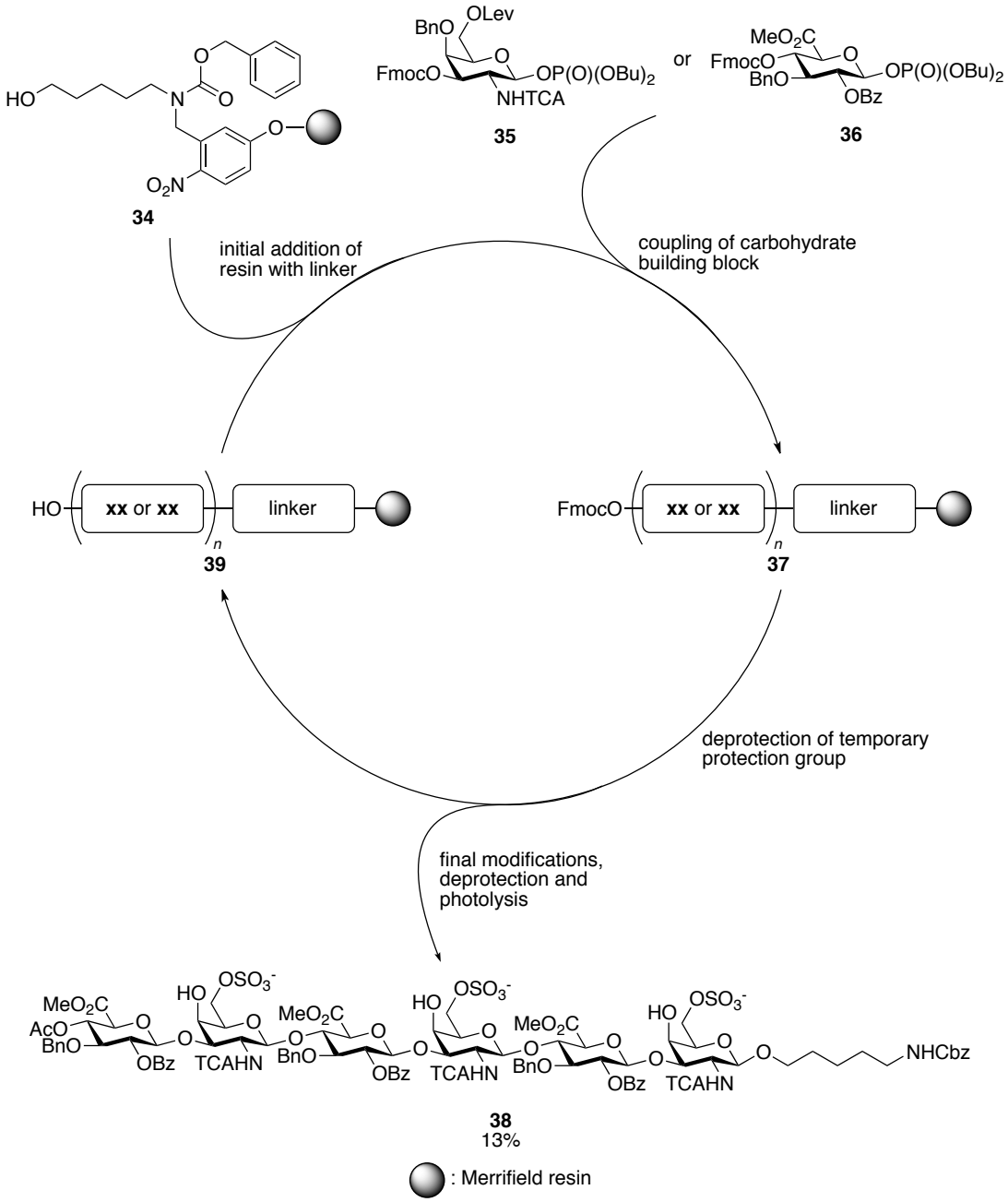


**Scheme 9**. Automated solid-phase synthesis of glucoseaminoglycans using an *o*-nitrobenzylamino linker.

The same linker was later used for the synthesis of a 30mer mannoside [37] and for the synthesis of β-(1,3)-glucans [38].

## 2.3 α-substituted *o*-nitrobenzyl linkers

The *o*-nitrobenzyl-based linkers presented so far have the disadvantage that the side product of their photolysis is an *o*-nitrosobenzaldehyde, a very reactive species that is prone to polymerization, generating a highly colored side product, which acts as an internal light filter. This has a detrimental effect on the photolytic cleavage of the desired compounds due to limited access of light to the reaction site [39].

To solve this issue Pillai documented the preparation of resin **41**, featuring a methyl group in the α-position [39], cf. scheme 10.

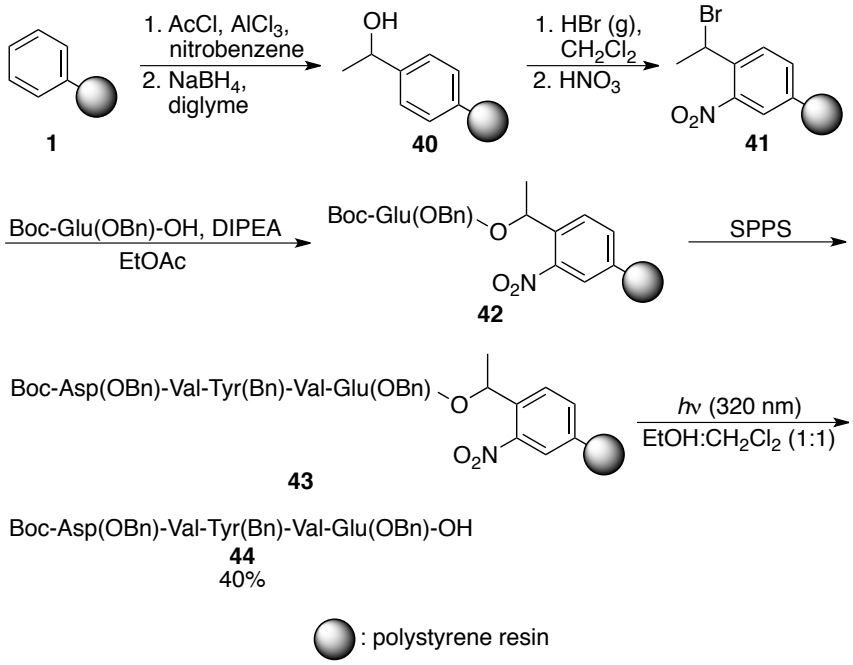


**Scheme 10**. Integral α-substituted nitrobenzyl-derived photolabile linker used for the synthesis of pentapeptide **44**.

The resin **1** was subjected to Friedel-Crafts acylation followed by reduction leading to the alcohol-functionalized resin **40**, which after substitution and nitration was transformed into the bromide functionalized integral linker **41**. This linker was used for the synthesis of pentapeptide **44** in a yield of 40%. This resin however suffered from the same problems as seen with Rich and Gurwara's original *o*-nitrobenzyloxy linker, cf. scheme 1, in that over-nitration degraded the swelling properties of the resin and prevented the synthesis of longer peptides.

A solution to this issue is to introduce the support itself in the α-position instead of a methyl group [40], cf. scheme 11. The resin **1** underwent Friedel-Crafts acylation followed by reduction leading to *o*-nitrobenzhydryl resin **46**. With this resin in hand Pillai synthesized both peptides **49** [40] and, after transformation to the amine-functionalized resin **47** [41], amidopeptides **48**. Peptides with up to 10 amino acids were synthesized in good yields.

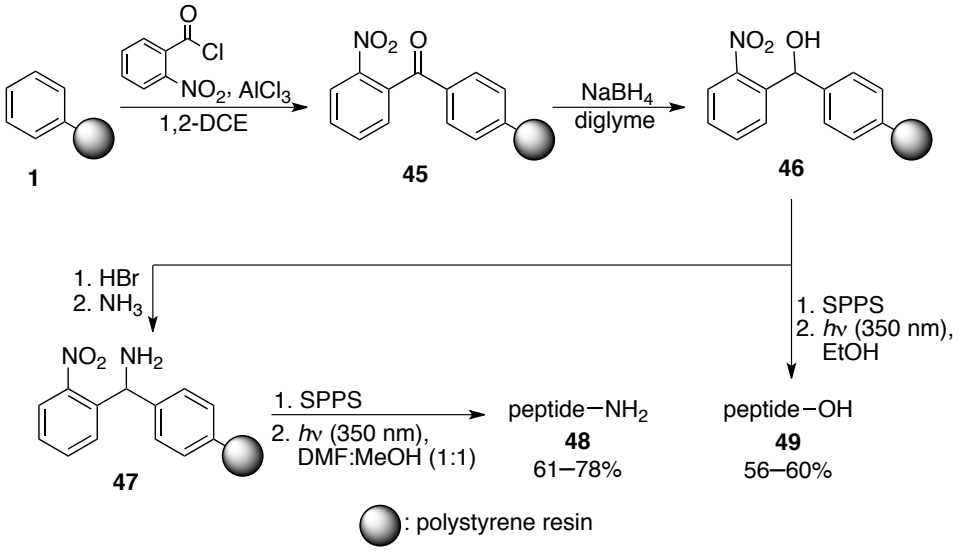


**Scheme 11**. *o*-nitrobenzhydryl resin providing access to both peptides and amidopeptides.

Another related linker is the 3-amino-3-(2-nitrophenyl)propionyl (ANP) linker **51** developed by Geysen and used for the synthesis of amidopeptides [42], cf. scheme 12. A more acid stable variant was proposed by Schreiber with two methyl groups in the α position of the amide [43]. An alcohol-based variant of linker **51** was used for oligosaccharide synthesis by Geysen [44]. It also incorporated a longer spacer between the support and the photosensitive part to avoid problems with β-elimination and lactonization of the alcohol [44].

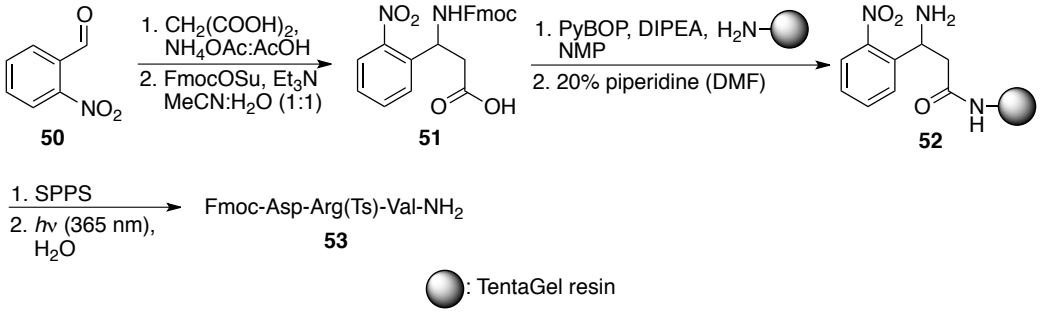


**Scheme 12**. Synthesis of photolabile ANP resin used for the synthesis of amidopeptide **53**.

An alternate route to similar linkers was designed by Harran allowing access to both hydroxyl- and amino-containing linker versions, **58** and **59**, both from the ketone **54** [45], cf. scheme 13.

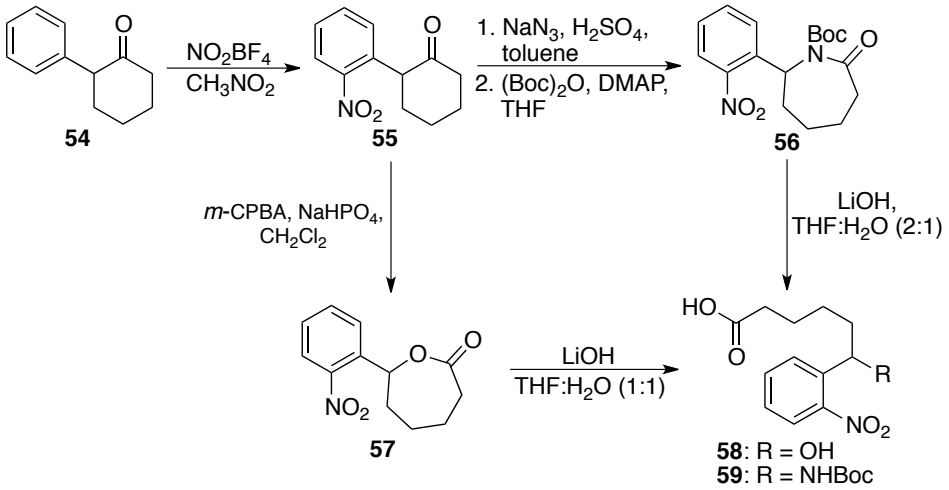


**Scheme 13**. Synthesis of photolabile ANP type linker.

## 2.4 *o*-nitroveratryl linkers

Initially introduced by Patchornik as a photolabile linker in 1973 [46], use of the *o*-nitroveratryl group (4,5-dimethoxy-2-nitrobenzyl) in photolabile linkers was popularized in the mid-1990s by Greenberg [47] and Holmes [48].

Greenberg utilized this type of linker to circumvent some of the issues observed with the original unsubstituted *o*-nitrobenzyl linker, namely long photolysis times and low yields of liberation [47]. The synthesis of linker **62** commenced from vanillin (**60**) which after etherification and nitration provided the aldehyde **61**, cf. scheme 14. After a few functional group interconversions the linker **62** was obtained [47].

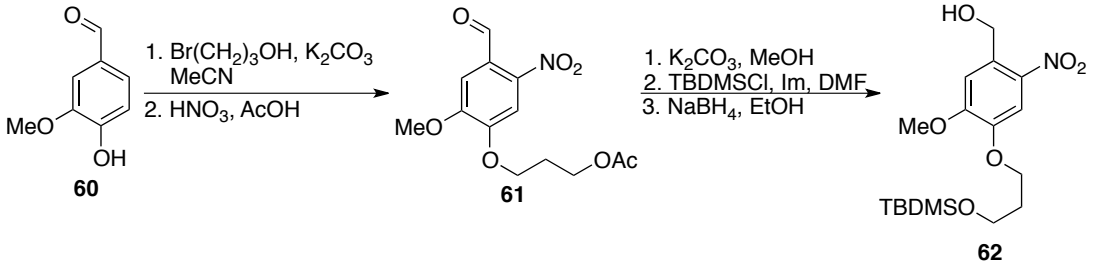


**Scheme 14**. Synthesis of photolabile *o*-nitroveratryl-based linker.

The linker **62** was then bound to a LCAA-CPG support in a few steps leading to the construct **65** which was then used for the synthesis of oligonucleotides in good yields [47], cf. scheme 15. Later it was shown that a more efficient photolysis could be achieved by linking the hydroxyl group of the nucleotide directly to the linker via a carbonate functionality [49]. This modified linker, also prepared from vanillin, was later used for oligonucleotide synthesis by other groups [50].

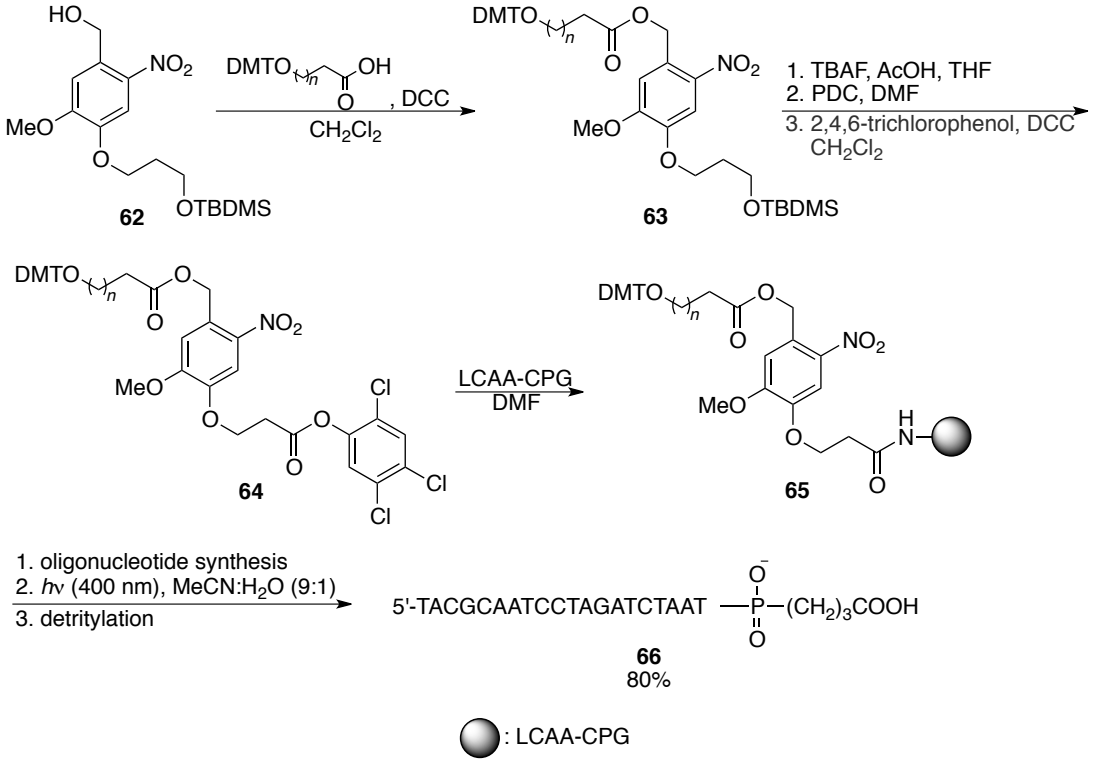


**Scheme 15**. Use of photolabile *o*-nitroveratryl-based linker for the synthesis of oligonucleotides.

Nearly simultaneously, Holmes introduced an *o*-nitroveratryl-based amine linker with a methyl group in the α-position [48]. This linker, producing amides upon photolysis, also solved the problem with formation of a reactive nitroso aldehyde upon photolysis as described earlier. The synthesis of the linker started from acetovanillone (**67**) and was a 7 step sequence providing linker **72**, which was then used for the synthesis of hexapeptide **74** in a yield of 70%, cf. scheme 16.

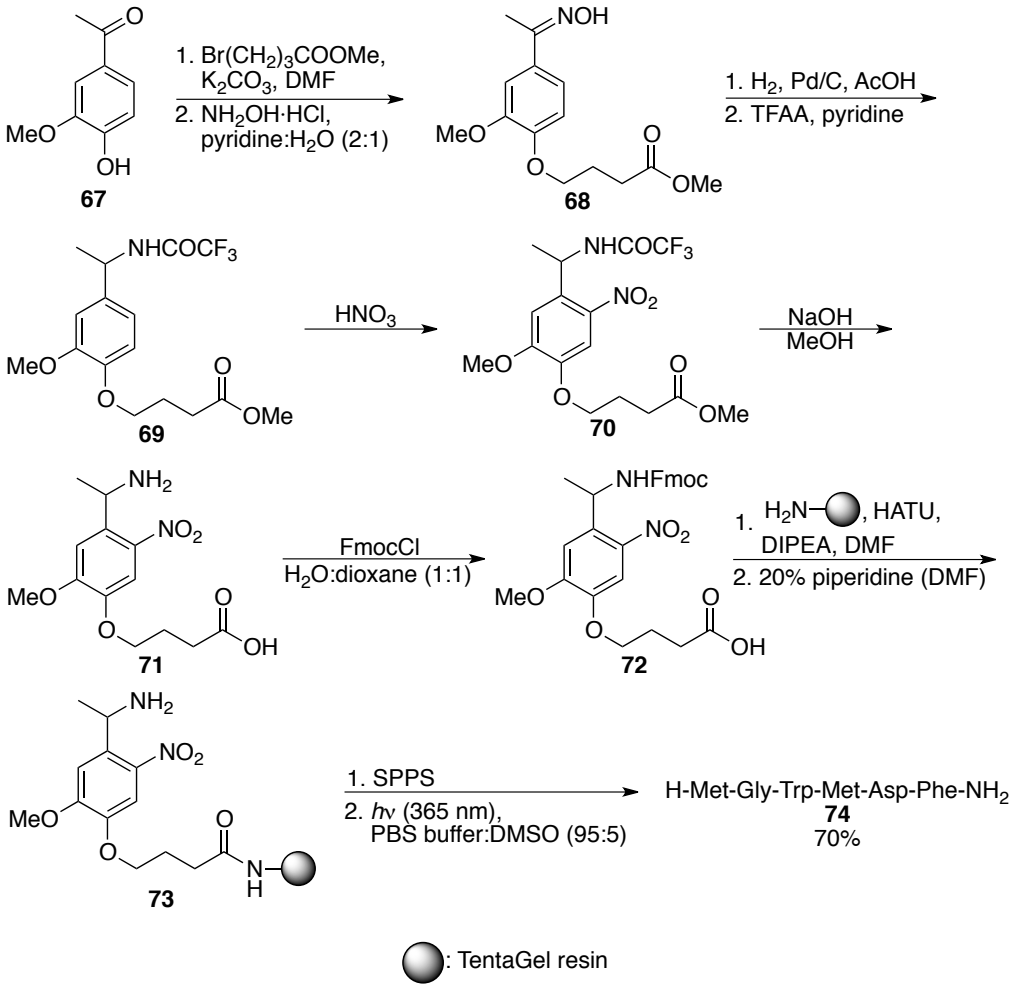


**Scheme 16**. Synthesis of photolabile amine-containing α-methylated nitroveratryl linker and its use for the synthesis of a hexapeptide.

In 1997, Holmes published a systematic study of the effect of nitroveratryl substituents on the photolysis efficiency [51]. It was shown that the rate of cleavage was 7 to 20 times higher when the *o*-nitrobenzyl ring was substituted with electron-donating alkoxy substituents. It was also shown that an alkyl group in the α-position to the amine increased the rate by a factor of 3. The length of the spacer chain also had an influence with a slightly increased rate for longer chains. It was concluded that both the alkoxy substituents on the aromatic ring and the alkyl group in the α-position were significantly beneficial for the photochemical reactivity.

Holmes also developed an alcohol-based version of the linker **72** [51], which was synthesized in a manner resembling that of the amine linker, cf. scheme 17.

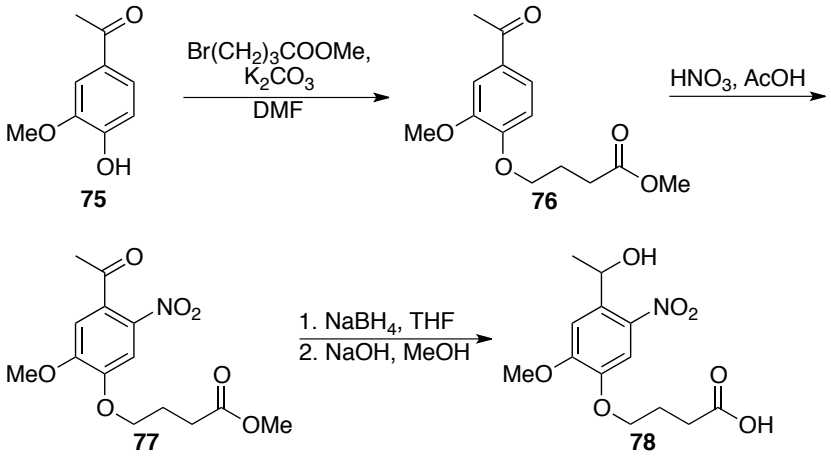


**Scheme 17**. Synthesis of photolabile alcohol-containing α-methylated nitroveratryl linker.

Alternate synthetic pathways for the ester **77** were developed by Teague [52].

The linkers **72** and **78** have been used for numerous applications and it has also been shown that this linker type could be coupled to a hydroxy based resin without effect on the efficiency of the photolytic cleavage [53]. An *o*-nitroveratryl linker was used by McKeown to develop methods for easing the analysis of solid phase synthesis reactions by mass spectroscopic techniques [54]. Another example is the use of linker **72** by Madder for the preparation of serine protease mimics [55]. Blackwell likewise used this linker for the synthesis of a diketopiperazine library using the Ugi multicomponent reaction [56], cf. scheme 18. The linker **72** was attached to the solid support and subsequent coupling of Fmoc-Phe(4-$NO_2$)-OH by standard methods led to the construct **80**. Subjection to Ugi conditions and subsequent methanolysis and photochemical release afforded diketopiperazines **82** in moderate to good purities.

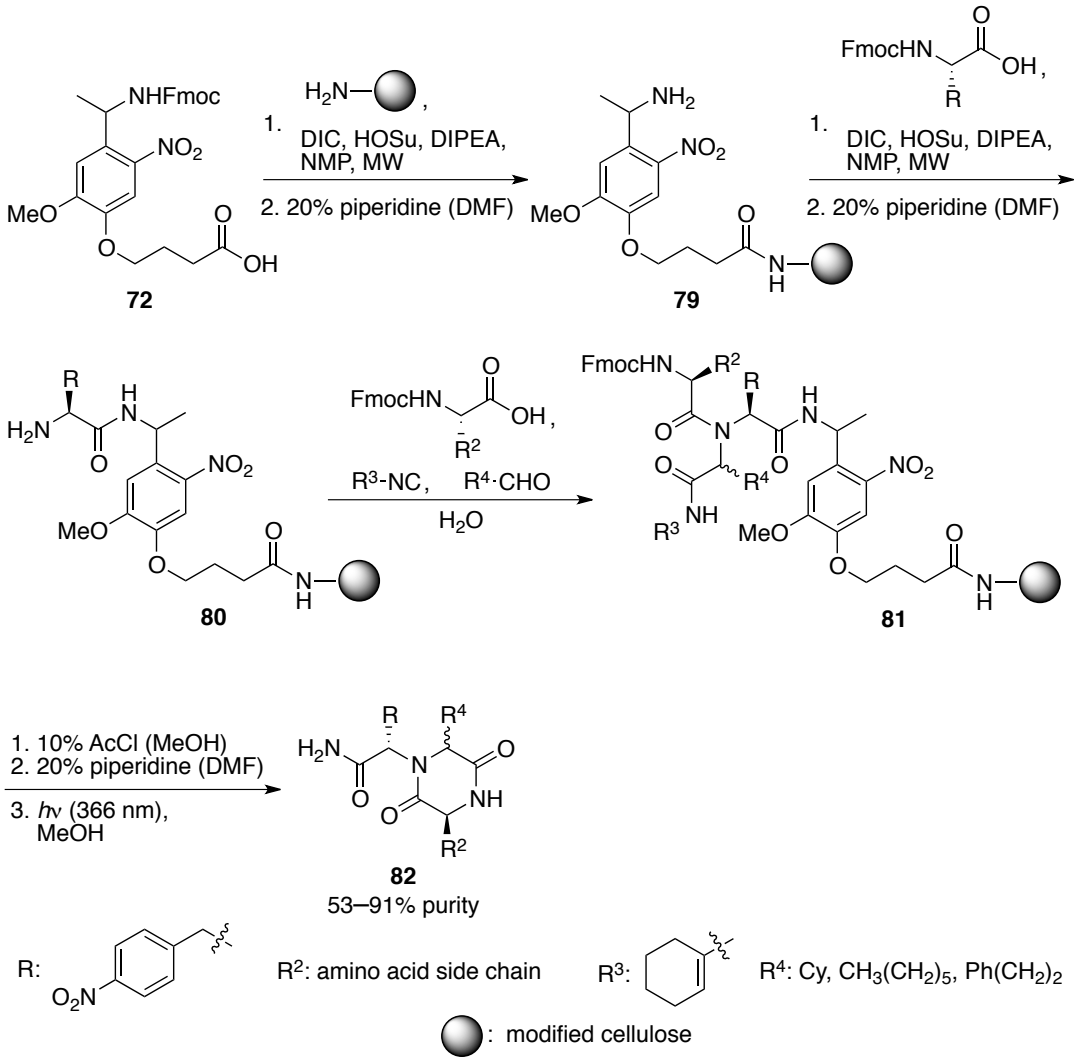


**Scheme 18**. *o*-nitroveratryl linker used in multicomponent reactions by Blackwell.

The linker **72** was again used by Gennari for the synthesis of combinatorial libraries of vinylogous sulfonamidopeptides [57]. Furthermore this study confirmed the trends Holmes had encountered [51] namely that *o*-nitroveratryl-based linkers are superior to *o*-nitrobenzyl linkers due to the beneficial effects of alkoxy-substituents and the presence of an α-methyl group.

Another example is the synthesis of 3,4-disubstituted β-lactams by Gallop [58], cf. scheme 19. The construct **83** was deprotected and condensed with an aldehyde producing imine **84** which then underwent a [2+2] cycloaddition with a ketene providing **85**. Final photolysis led to β-lactams **86** in good yields [58], cf. scheme 19.

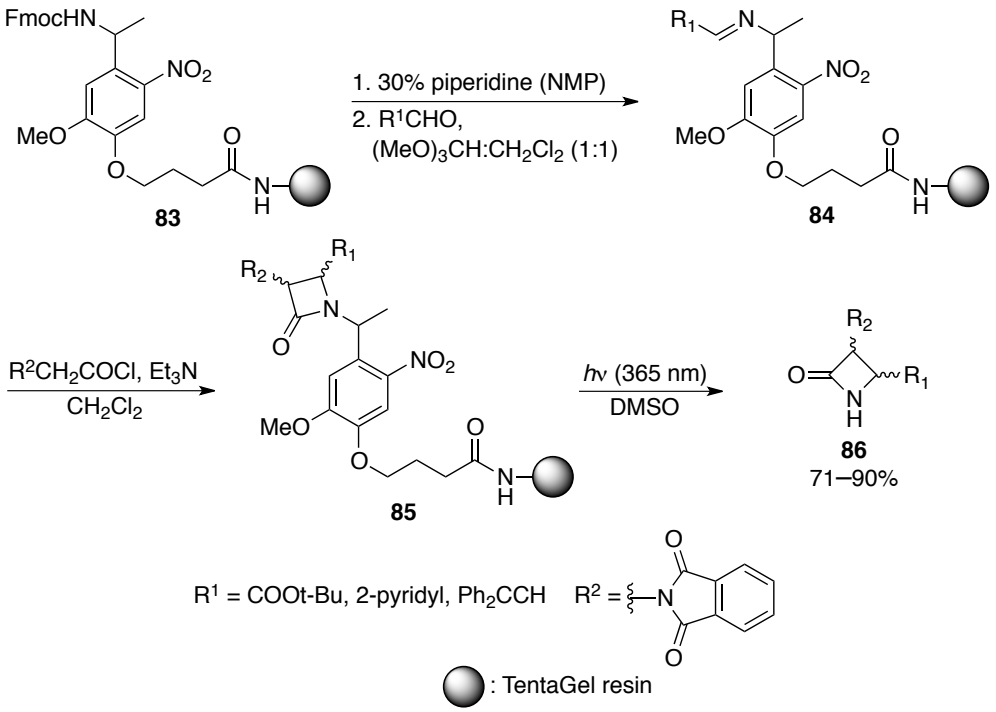


**Scheme 19**. α-methylated nitroveratryl linker used in the synthesis of β-lactams.

Meldal used an aldehyde linker, set up for reductive amination and closely related to **72**, for the synthesis of a small library of arylpiperazine melanocortin subtype-4 agonists [59]. Thus, the linker **87** was synthesized and attached to the solid support cf. scheme 20. Construct **88** was then subjected to reductive amination and subsequent acylation of the formed amine afforded **90**. Finally, two alkylation steps and photolytic cleavage provided arylpiperazines **93**.

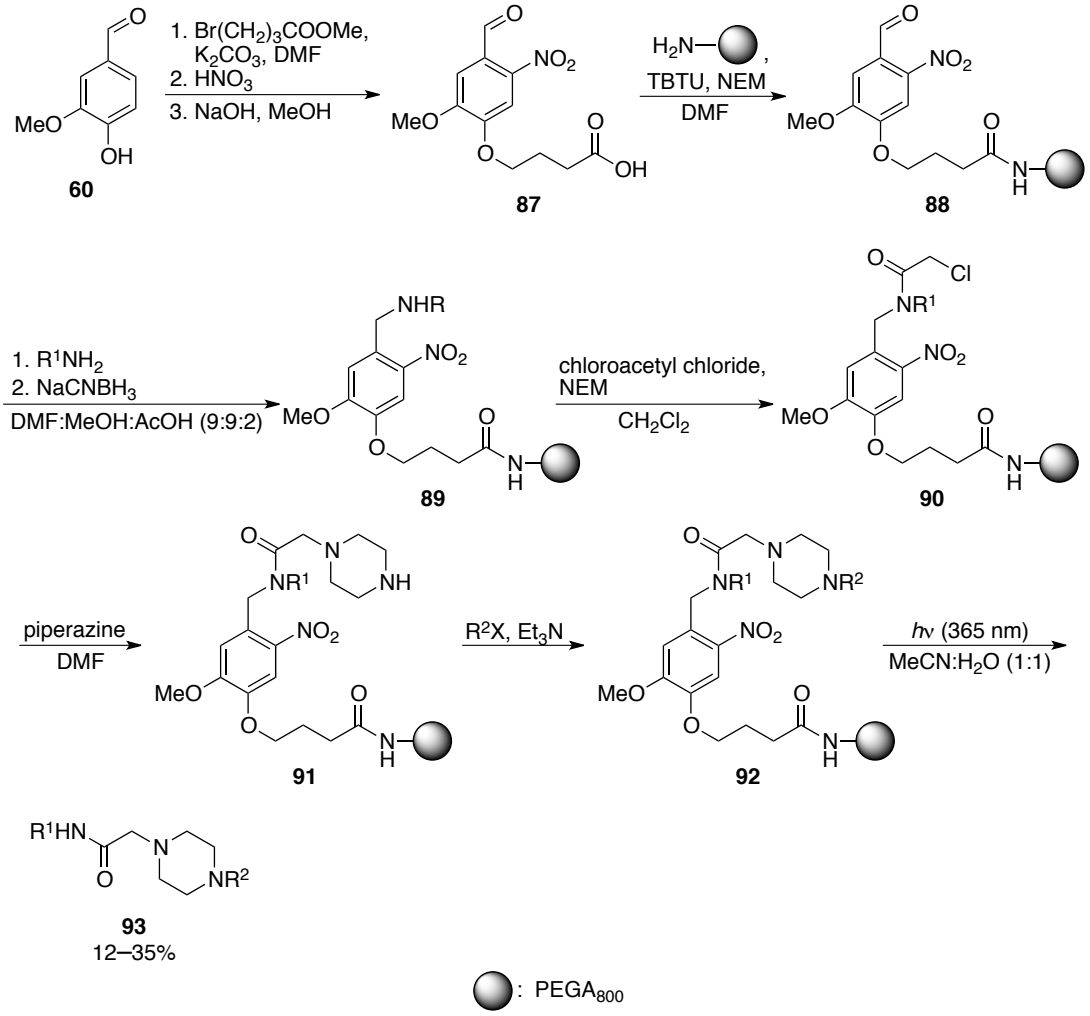


**Scheme 20**. Photolabile linker used for the synthesis of melanocortin subtype-4 agonists.

Recently, a new azido-linker based on the *o*-nitroveratryl group was introduced by Qvortrup and Nielsen for the synthesis of 1,2,3-trizoles [60], cf. scheme 21.

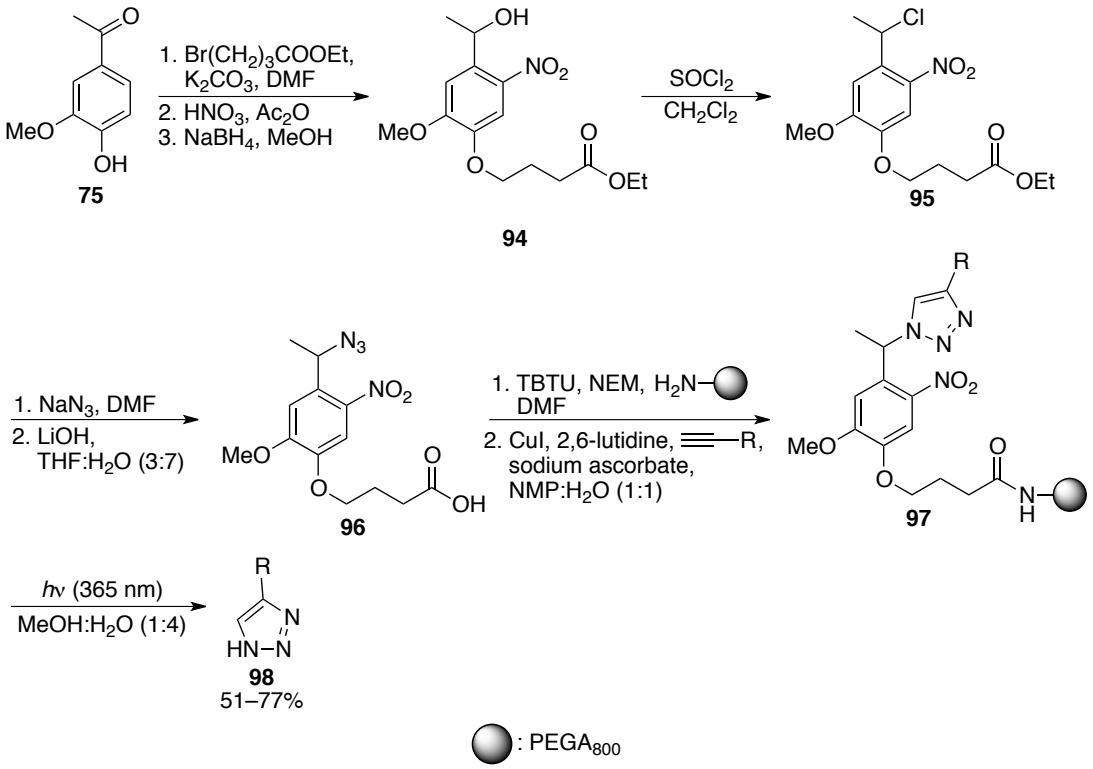


**75** **94** **95** **96** **97** **98** 51–77%

**Scheme 21**. Photolabile nitroveratryl-based azido-linker used for the synthesis of 1,2,3-triazoles.

The synthesis commenced from acetovanillone (**75**) and the alcohol **94** was synthesized in analogy to Holmes' alcohol linker, cf. scheme 17. The alcohol **94** was then subjected to $SOCl_2$ and after substitution with $NaN_3$ and final ester hydrolysis with LiOH the azido linker **96** was obtained. Attachment to the solid support and subsequent copper(I)-catalyzed azide–alkyne cycloaddition led to the construct **97**, which after photoytic cleavage provided 1,2,3-triazoles in good yields.

Later they introduced a hydrazine linker [61]. Starting from chloride **95** the linker **100** was synthesized in two steps and after attachment to the solid support, SPPS and photolytic cleavage provided peptide hydrazides in yields of 21–83%, cf. scheme 22.

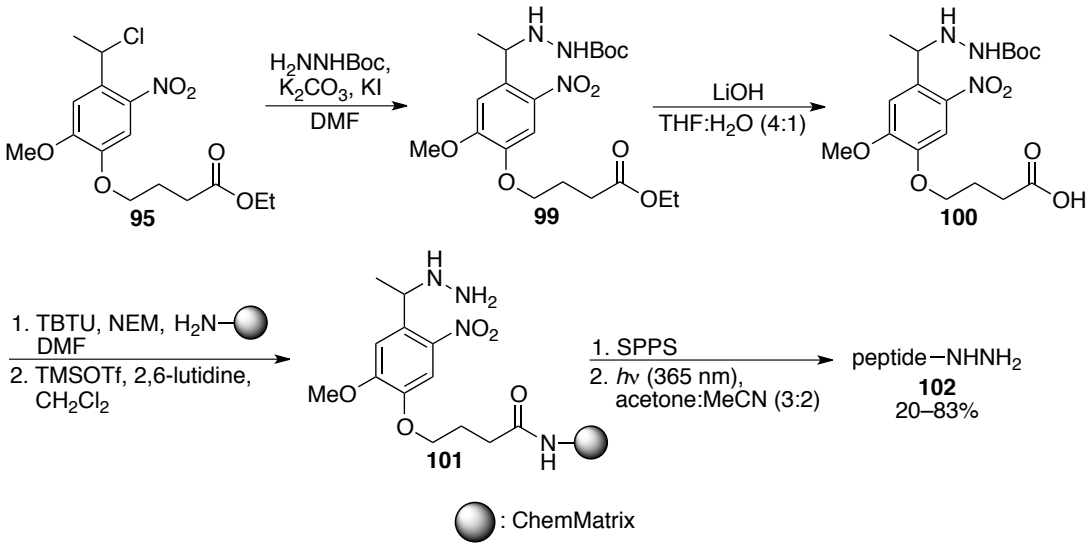


**Scheme 22**. Photolabile nitroveratryl-based linker used for the synthesis of peptide hydrazides.

The construct **101** could also be utilized for the solid-phase synthesis of dihydropyrano[2,3-c]pyrazoles [61].

Another recent example is the linker developed by Lee [62]. This linker has the tether to the solid support positioned in the α-position. Starting from veratraldehyde (**103**) the linker **108** was synthesized in six steps, cf. scheme 23.

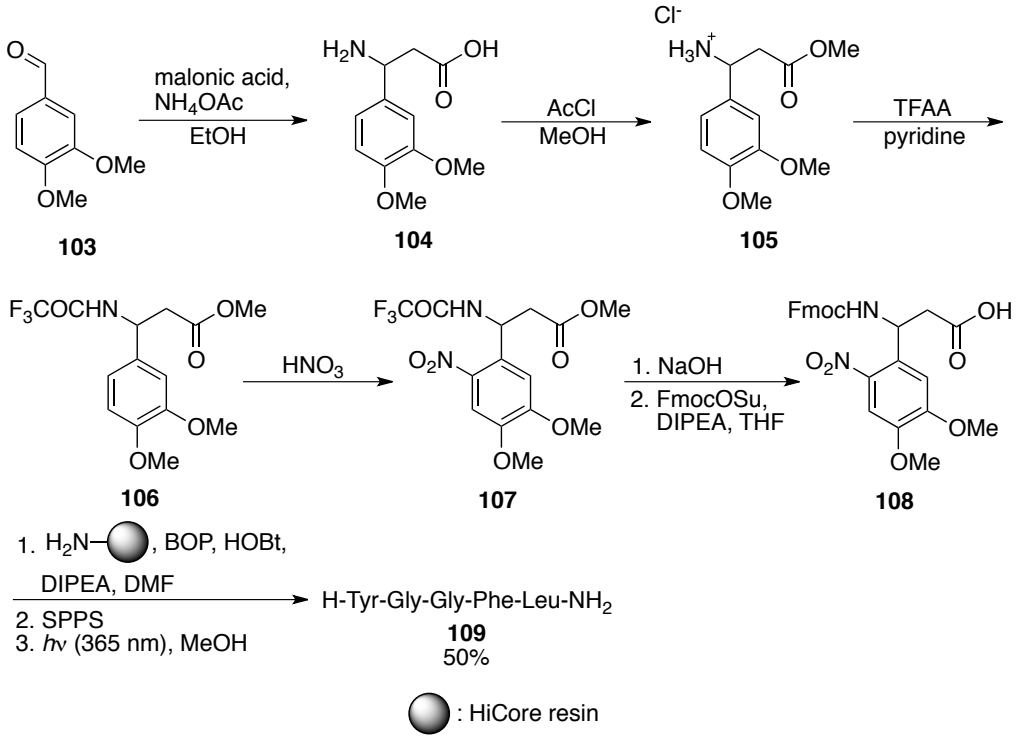


**Scheme 23**. Synthesis of Leu-enkephalin as an amide using photolabilie linker **108**.

After coupling to the solid support, standard SPPS and photolytic cleavage Leu-enkephaline (**109**) was liberated as an amide in a yield of 50%.

## 2.5 Phenacyl linkers

The Phenacyl group was introduced by Wang during the early exploration of photolabile linkers [63]. The resin **1** was subjected to Friedel-Crafts acylation and subsequently the first amino acid was coupled leading to the construct **111**, cf. scheme 24. Then standard SPPS followed and upon final photolysis the peptide **113** was released in 70% yield.

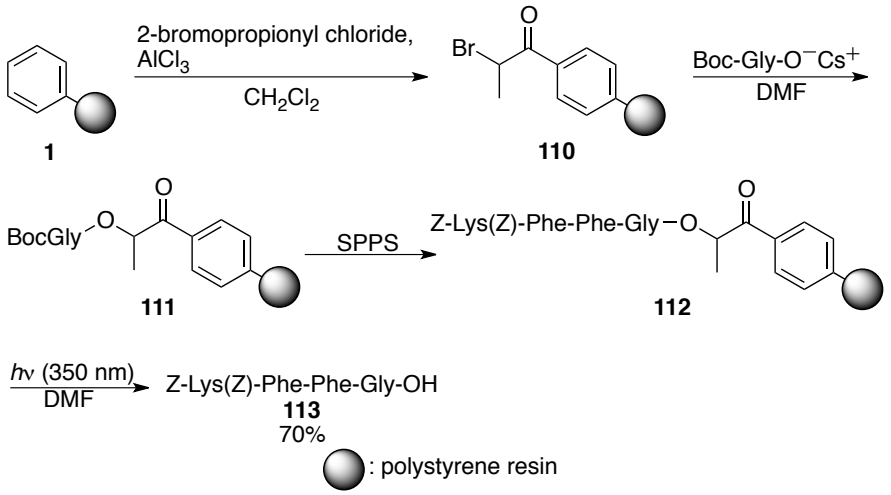


**Scheme 24**. Synthesis of phenacyl photolabile handle and its use in peptide synthesis.

A phenacyl linker was also used by Tam in multi detachable resins cleavable both under photolytic conditions and by base or nucleophiles [11, 12].

In 1982 Tjoeng developed a phenacyl linker system [64] which this time was a non-integral linker that could be coupled to the resin instead of direct derivatization of the resin as described by Wang. Initial esterification of phenylacetic acid (**114**) and subsequent Friedel-Crafts acylation led to the methyl ester **115** which upon simple ester hydrolysis led to the phenacyl linker **116**, cf. scheme 25. With **116** in hand, coupling of the first amino acid followed by standard SPPS led to the peptide **120** in 78% yield after photolytic cleavage [64].

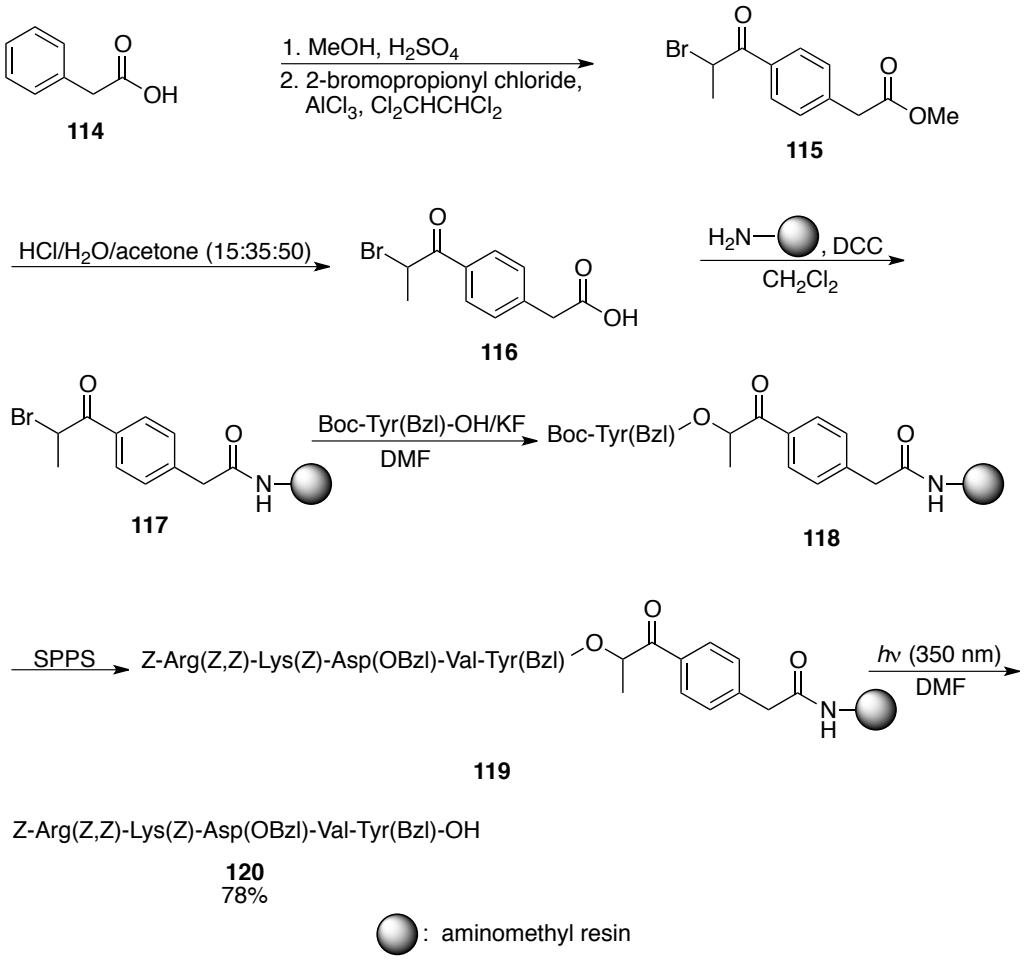


**Scheme 25**. Synthesis of phenacyl photolabile linker **116** and its use for the synthesis of thymopoietin II fragments.

## 2.6 *p*-alkoxyphenacyl linkers

Introduced by Mutter in 1985 [65], the *p*-alkoxyphenacyl linker is very similar to the phenacyl linker, but has an electron-releasing alkoxy substituent in the *para*-position making photolysis at 350 nm much more efficient. The synthesis started from methyl phenoxyacetate (**121**) which after Friedel-Crafts acylation and ester hydrolysis provided the bromide **122**, cf. scheme 26. Coupling to the resin followed by attachment of the first amino acid either in the presence of KF or as its cesium salt led to **124**. Standard SPPS followed and final photolysis and deprotection led to the peptide **125** in 71% yield.

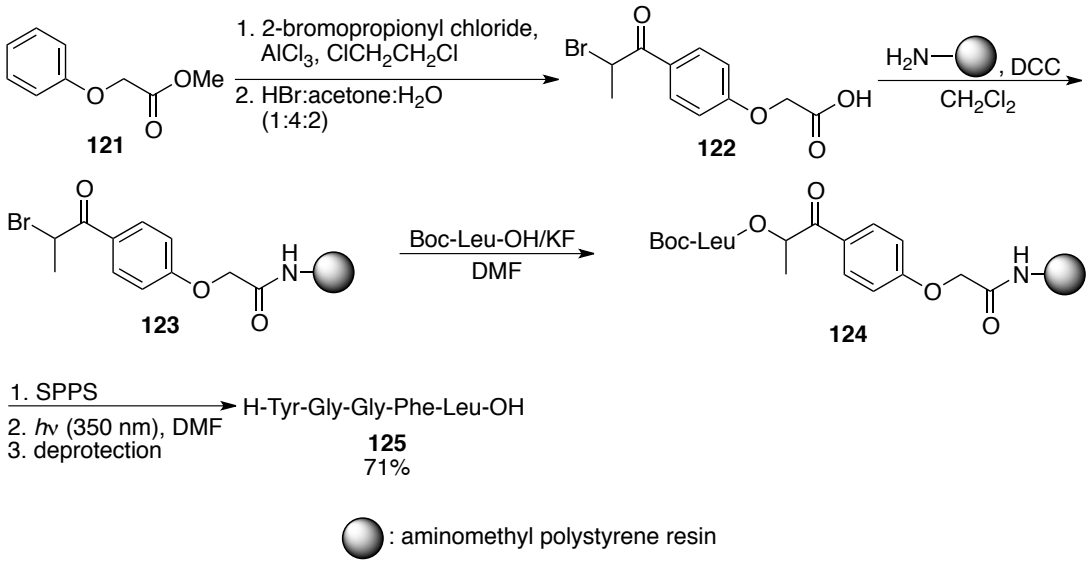


**Scheme 26**. Synthesis of *p*-alkoxyphenacyl photolabile linker and its use in peptide synthesis.

Gauthier used the same linker for the synthesis of octapeptides in good yield (>85%) in his synthesis of mammalian glucagon [66].

Belshaw developed a safety-catch photolabile linker based on the *p*-alkoxyphenacyl moiety [67]. The idea was to mask the photolability of the linker thus making the linker photostable and enabling the use of photolabile protecting groups in a light directed synthesis of oligonucleotides. The linker synthsis started from acetophenone **126**, cf. scheme 27. A Mitsunobu reaction led to **127** which after acetal formation and methyl oxidation provided the alcohol **128**. Protection with the photolabile NPPOC group followed by alcohol deprotection gave **129**, which was then prepared for attachment to the solid support by treatment with 2-cyanoethyl diisopropylchlorophosporamidite resulting in the linker **130**. **130** was then attached to the solid support and iterative cycles of photolytic deprotection and coupling of nucleotides bearing a photolabile protecting group furnished construct **132**. Mild acidic hydrolysis then activated the linker for photolytic cleavage and final photolysis provided the DNA chain **134**.

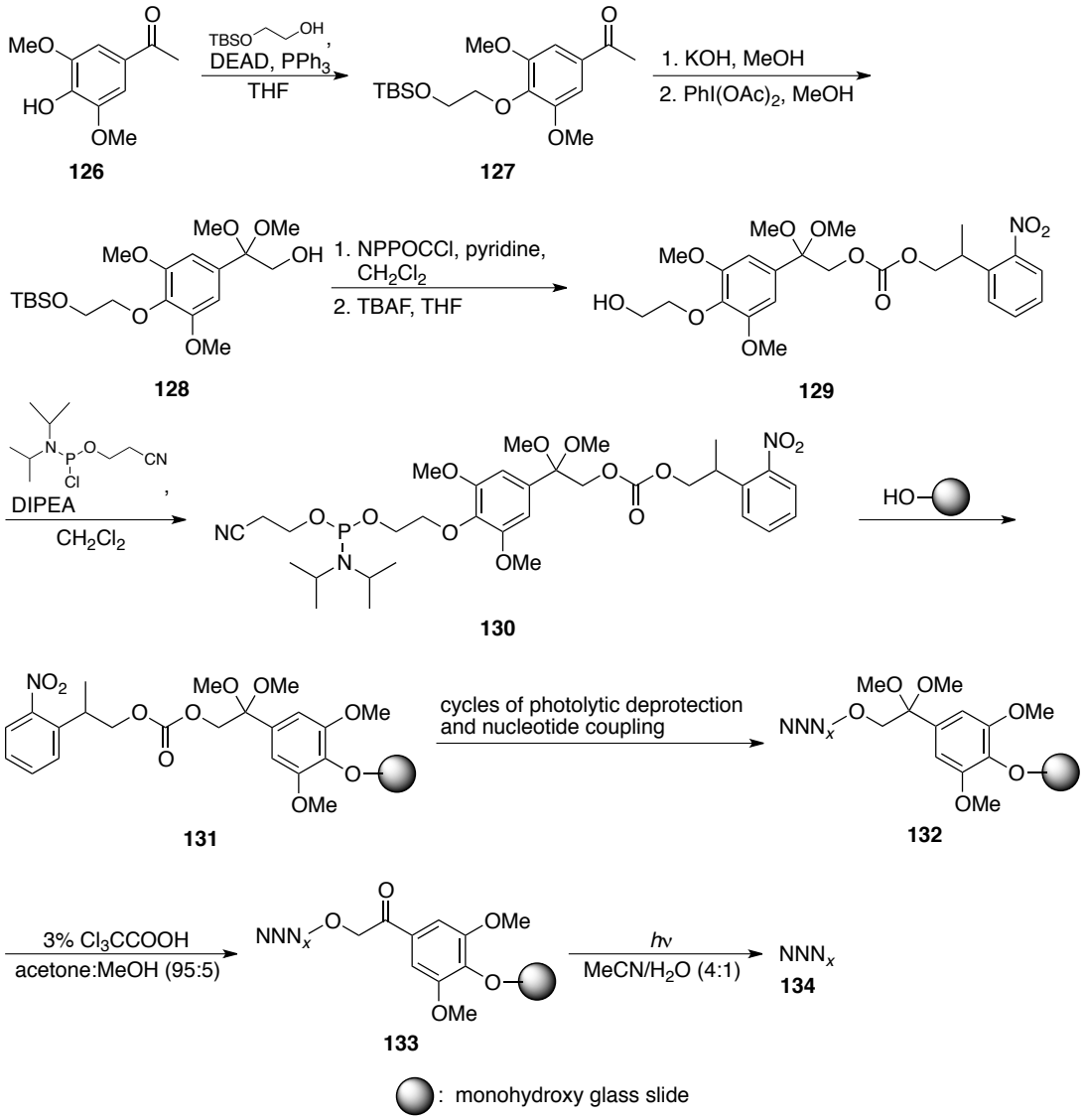


**Scheme 27**. Synthesis and use of safety-catch photolabile linker for light directed synthesis and release of oligonucleotides ($NNN_x$ = DNA chain).

Sucholeiki introduced a traceless thioether *p*-methoxyphenacyl linker for use in Stille cross-couplings [68, 69]. Methylation of **135** and subsequent Friedel-Crafts acylation and halogen exchange led to the chloride **138**, cf. scheme 28.

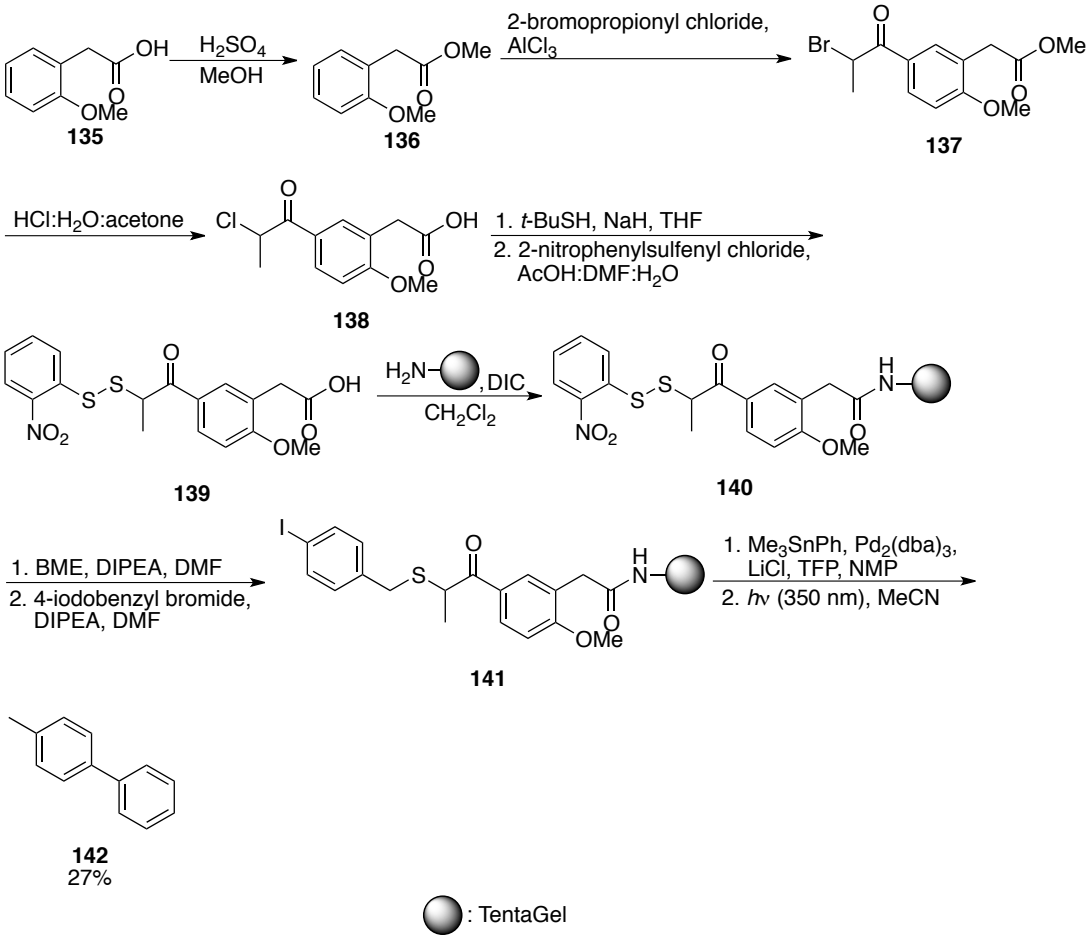


**135** **136** **137** **138** **139** **140** **141**

**142**
27%

**Scheme 28**. Synthesis and use of traceless thioether *p*-methoxyphenacyl linker in Stille couplings.

Substitution and disulfide formation then furnished the linker **139** which after attachment to the solid support and disulfide cleavage was reacted with 4-iodobenzyl bromide providing the construct **141** set up for Stille coupling. Stille coupling and subsequent photolysis finally led to the biaryl **142** in a yield of 27% with a C-H bond at the former attachment point.

## 2.7 Benzoin linkers

The benzoin safety-catch linker was first developed by Chan for the purpose of binding two molecules together in solution [70]. It was later exploited for solid phase synthesis by Balasubramanian [71, 72]. The synthesis started from 3-hydroxybenzaldehyde (**143**) which was coupled to the resin and then reacted with 2-phenyl-1,3-dithiane to form a dithioacetal that acted

as a masked ketone and the safety-catch trigger upon hydrolysis, cf. scheme 29. Fmoc-$\beta$-Ala-OH was then coupled to the resin providing **146** which after hydrolysis of the dithioacetal and subsequent photolysis released the amino acid **148** in excellent yield. Good to excellent yields (75–97%) were obtained using this strategy with other carboxylic acids.

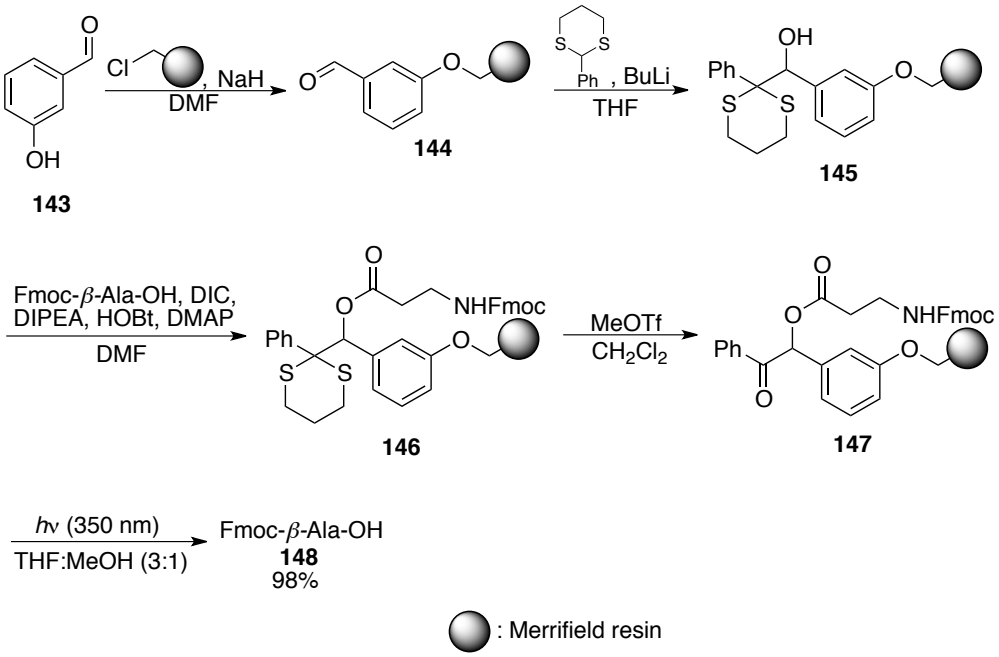


**Scheme 29**. Use of photolabile benzoin safety-catch linker in solid-phase synthesis.

Later Balasubramanian developed a second generation benzoin linker, this time as a non-integral linker system where the linker was prepared in solution and then coupled to the solid support [73]. The linker was prepared with a carboxylic acid as anchoring point to exploit the wide range of amine functionalized resins available and with a longer tether as this had been shown to be advantageous (cf. *o*-nitroveratryl linkers). The synthesis started from aldehyde **149** and a six step sequence led to the linker **155**, cf. scheme 30.

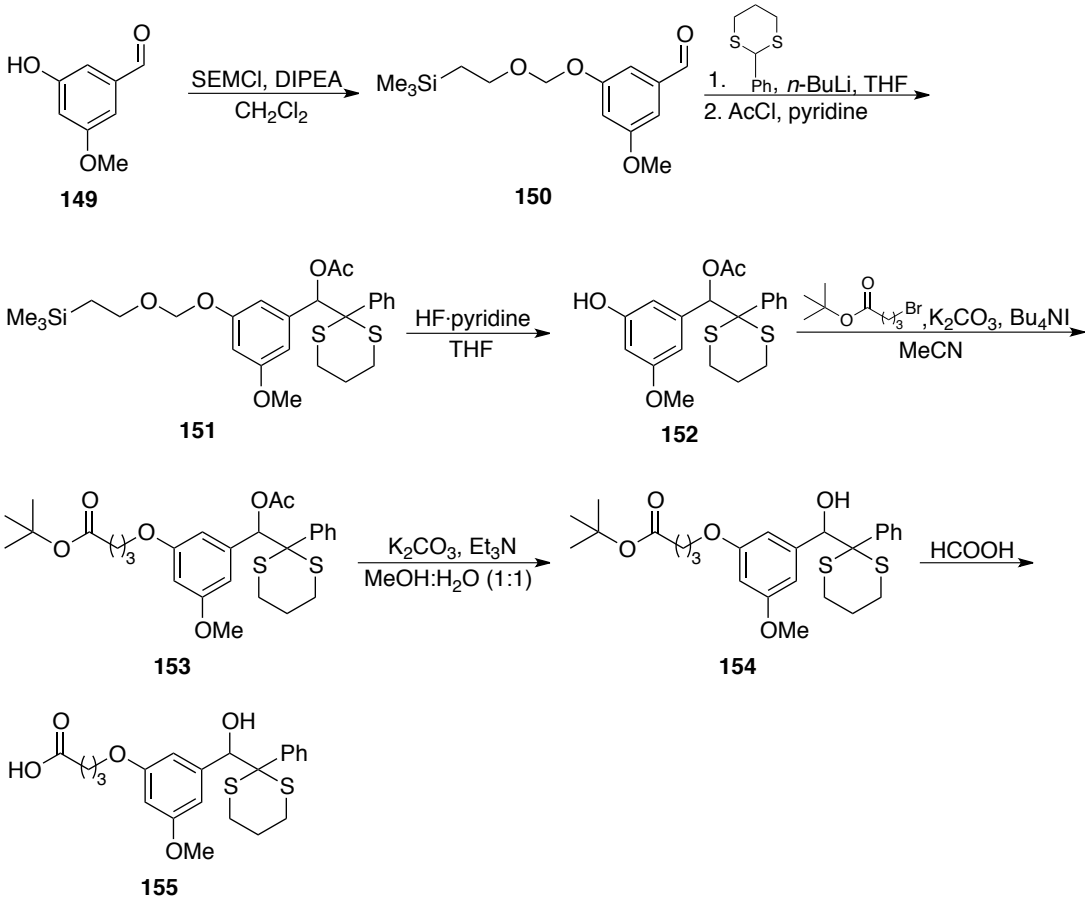


**Scheme 30**. Synthesis of photolabile benzoin linker with a carboxylic acid anchor.

To address the sometimes tricky dithioacetal removal Copley developed a new benzoin linker in which the carbonyl group is protected as a dimethyl ketal instead [74]. The dimethyl ketal protection is stable towards common solid phase esterification and amide bond formation techniques and can be easily removed with 3% TFA in under five minutes. The synthesis of the linker started from 3-formylbenzoic acid (**156**) and a four step sequence provided the dithioacetal **160**, cf. scheme 31. Finally the dithioacetal functionality was replaced with a dimethyl ketal leading to the linker **161**. Attachment to the solid support and subsequent standard SPPS followed by photolysis released the tetradecapeptide **162**.

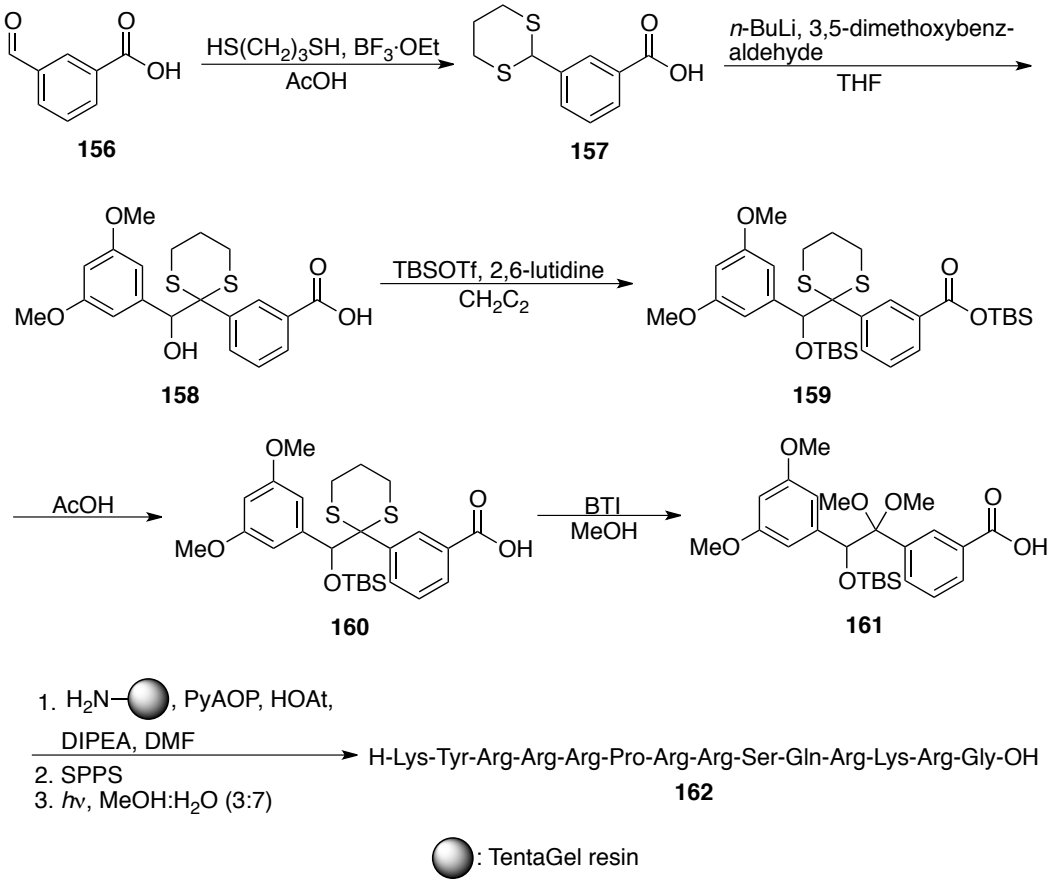


**Scheme 31**. Synthesis and use of photolabile dimethyl ketal benzoin linker for peptide synthesis.

## 2.8 Pivaloyl linkers

A new photolabile linker was developed by Giese based on the pivaloyl group [75]. The synthesis started from 1,3-dihydroxyacetone dimer (**163**) and a six step sequence gave the linker **168** in an overall yield of 40%, cf. scheme 32. The linker was then coupled to the solid support and after attachment of the first amino acid and then standard SPPS provided construct **171**, which finally upon photolysis, released the peptide **172**, in a yield of 86%.

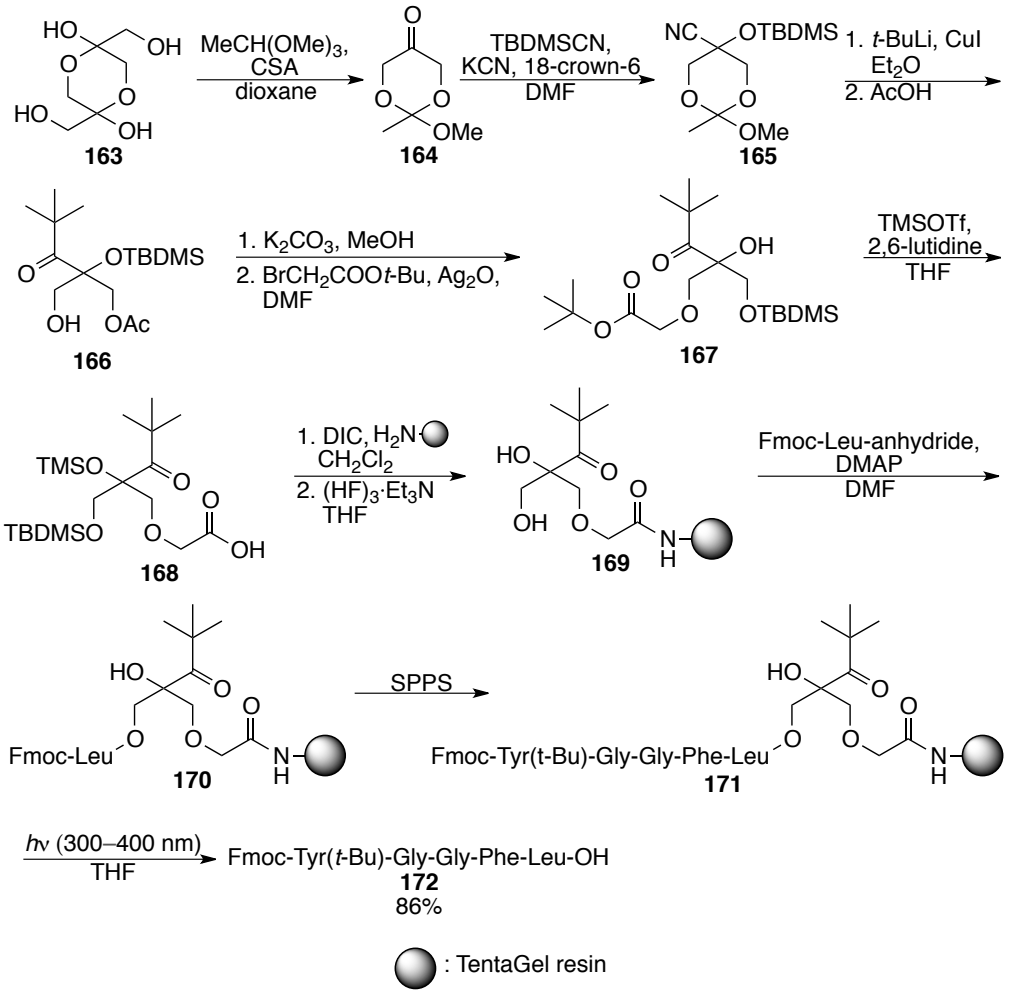


**Scheme 32**. Synthesis and use of pivaloyl-based photolabile linker.

The linker **168** also proved useful for the synthesis and release of compounds arising from Stille, Suzuki or epoxidation reactions [75]. Later a modified version able to release alcohols upon photolysis was proposed by Giese [76].

Bochet exploitet the fact that the pivaloyl linker used in his synthesis of Leu-Enkephalin is stable at longer wavelengths thus enabling the use of photolabile protection groups with a different chromatic lability [77]. The synthesis started with the coupling of NVOC-Leu-OH to the linker resin **173** under standard conditions, cf. scheme 33. Then four cycles of photolytic deprotection (at 360 nm) and amino acid coupling furnished construct **175**. Final deprotection and photolytic cleavage from the resin (at 305 nm) released Leu-enkephalin in a yield of 55%.

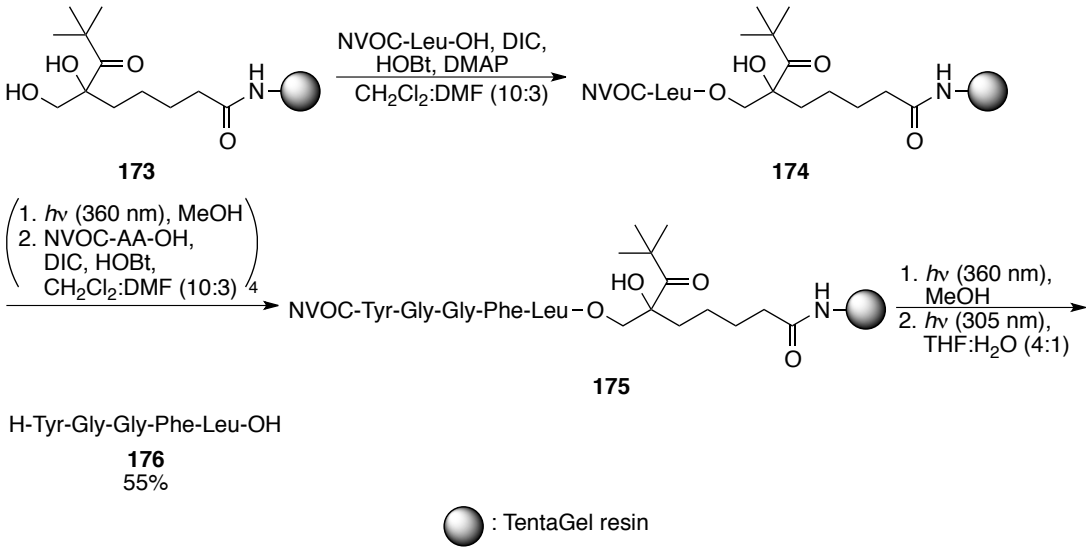


**Scheme 33**. Synthesis of Leu-Enkephalin utilizing both a photolabile linker and photolabile protection groups.

## 2.9 Other photolabile linkers

Routledge introduced a traceless photolabile linker based on thiohydroxamic acid [78]. Starting with the attachment of trityl protected 4-hydroxymercaptophenol **177** to the solid support, the linker construct **181** was prepared in four steps, cf. scheme 34.

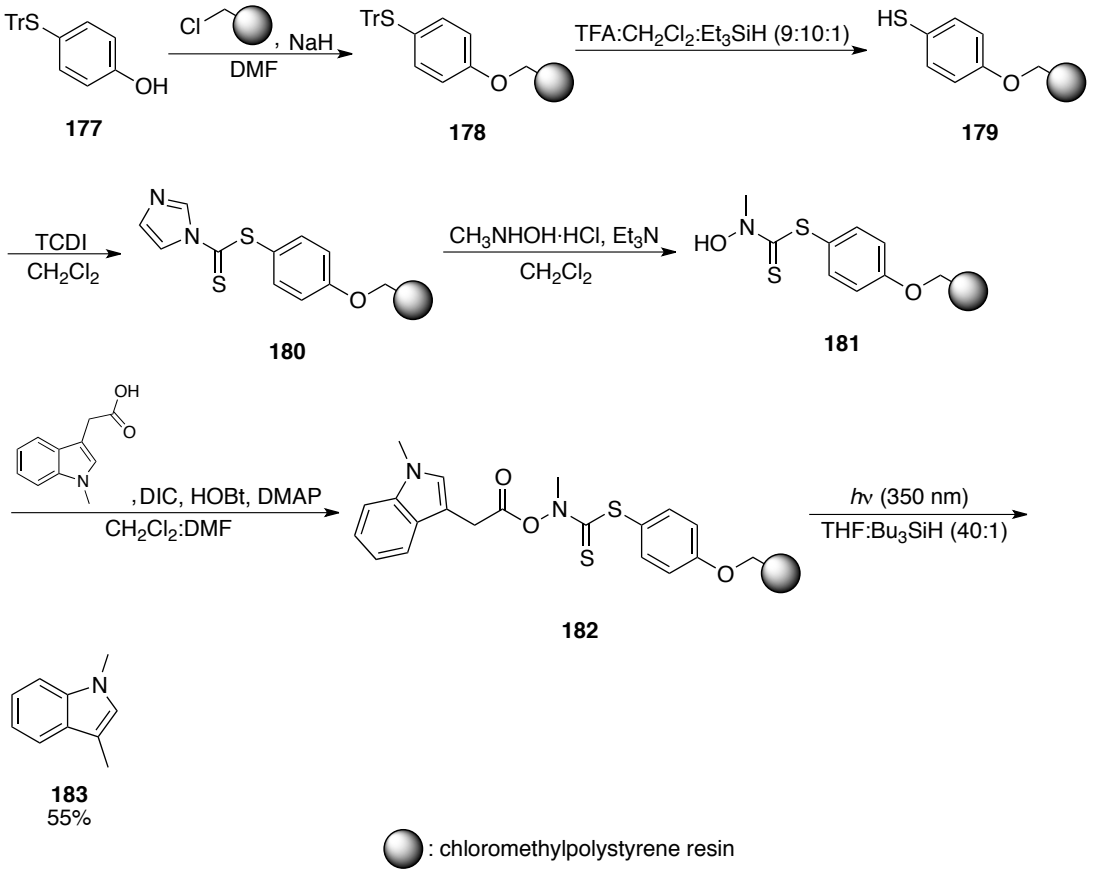


**Scheme 34**. Synthesis and use of traceless photolabile linker.

Then *N*-methylindole-3-acetic acid was attached and photolysis yielded 1,3-dimethylindole **183** in a yield of 55% with a C-H bond at the former attachment point to the solid support. This method does however haw a drawback in form of the need of a hydrogen donor, in this case a toxic tin species, to facilitate the release from the solid support whereas photolysis in other cases normally can be achieved under mild and neutral conditions.

Nicolaou introduced a photolabile linker exploiting the photochemical properties of the 5-bromo-7-nitroindoline group [79]. Photolytic release in the presence of amines provided amides and intramolecular trapping of an amine was also possible with this linker leading to heterocycles. The synthesis started from the indole **184**, cf. scheme 35.

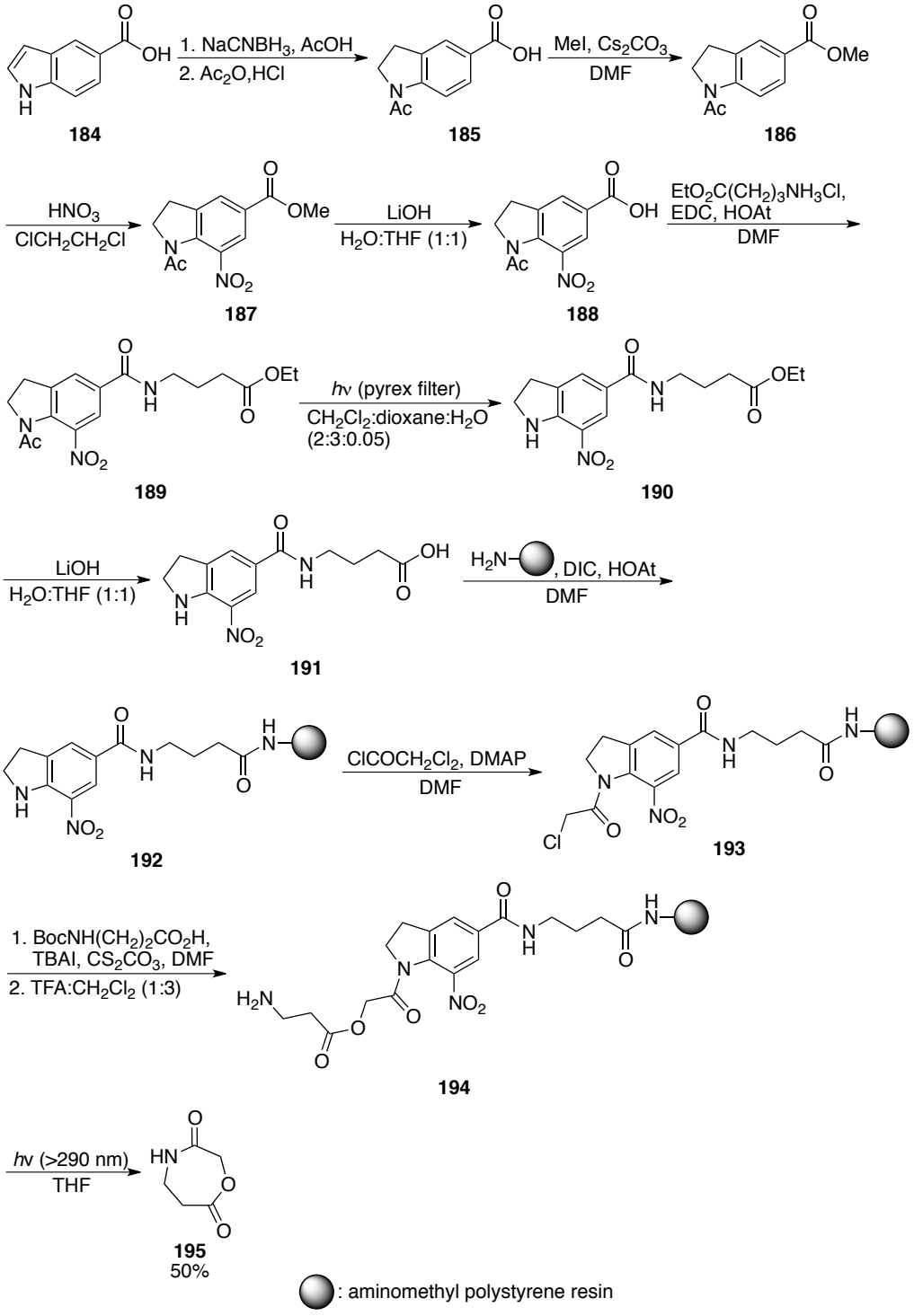


**Scheme 35**. Photolabile linker for the synthesis of heterocycles.

Reduction, acylation and methylation led to the methyl ester **186**. Nitration followed by ester hydrolysis and amide formation provided the amide **189**, which after photolytic removal of the acetyl group and ester hydrolysis furnished the linker **191**. Attachment to the solid support and further synthetic elaboration led to the costruct **194**, which upon photolytic cyclorelease provided the heterocycle **195** in a yield of 50%.

A triazene-based photolabile linker was developed by Enders [80]. 3-hydroxyaniline (**196**) was attached to Merrifiled resin and diazotation and reaction with a secondary amine (in this case piperazine) led to the triazene construct **199**, cf. scheme 36.

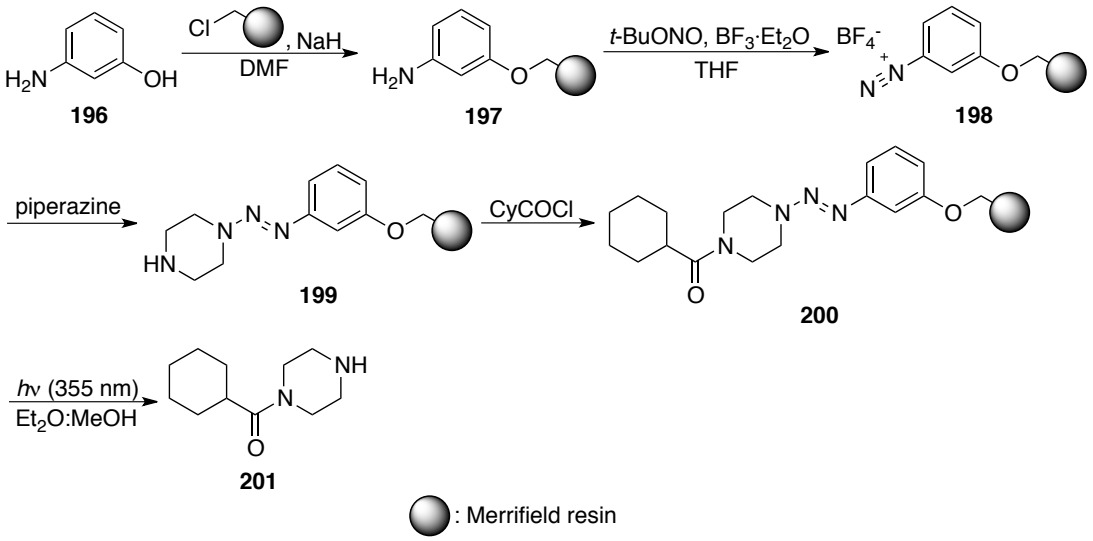


**Scheme 36**. Synthesis and use of triazene-based photolabile linker developed by Enders.

Acylation and photolytic release provided the tertiary amide **201**. Generally moderate yields and excellent purities were achieved.

# 3 Conclusions

Since the first photolabile linker was published more than 40 years ago a wide range of photolabile linkers have been developed providing an extensive toolkit for the synthesis of peptides, oligosaccharides, oligonucleotides and small molecules. Photolabile linkers provide an orthogonal method of cleavage compared to traditional linkers and even systems utilising groups with different chromatic lability thus enabling the simultaneous use of both photolabile protection groups and photolabile linkers that are completely orthogonal to each other have been developed. Furthermore photolabile linkers can commonly be cleaved under very mild

conditions a fact that among others have made them attractive for and widely used in chemical biology [81].

## References


[1]: Merrifield, R. B. *J. Am. Chem. Soc.* **1963**, *85*, 2149–2154.

[2]: Testero, S. A.; Mata, E. G. *J. Comb. Chem.* **2008**, *10*, 487–497.

[3]: Hermkens, P. H. H.; Ottenheijm, H. C. J.; Rees, D. *Tetrahedron* **1996**, *52*, 4527–4554.

[4]: Hermkens, P. H. H.; Ottenheijm, H. C. J.; Rees, D. C. *Tetrahedron* **1997**, *53*, 5643–5678.

[5]: Booth, S.; Hermkens, P. H. H.; Ottenheijm, H. C. J.; Rees, D. C. *Tetrahedron* **1998**, *54*, 15385–15443.

[6]: Hall, S. E *Mol. Divers.* **1999**, *4*, 131–142.

[7]: Dolle, R. E.; Nelson, K. H., Jr. *J. Comb. Chem.* **1999**, *1*, 235–282.

[8]: Taylor, S. J.; Morken, J. P. *Science* **1998**, *280*, 267–270.

[9]: Rich, D. H.; Gurwara, S. K. *J. Chem. Soc., Chem. Commun.* **1973**, 610–611.

[10]: Rich, D. H.; Gurwara, S. K. *J. Am. Chem. Soc.* **1975**, *97*, 1575–1579.

[11]: Tam, J. P.; Tjoeng, F. S.; Merrifield, R. B. *J. Am. Chem. Soc.* **1980**, *102*, 6117–6127.

[12]: Voss, C; Dimarchi, R; Whitney, D. B. ; Tjoeng, F. S.; Merrifield, R. B.; Tam, J. P. *Int. J. Pept. Protein Res.* **1983**, *22*, 204–213.

[13]: Barany, G.; Albericio, F. *J. Am. Chem. Soc.* **1985**, *107*, 4936–4942.

[14]: Giralt, E.; Albericio, F.; Pedroso, E.; Granier, C.; Van Rietschoten, J. *Tetrahedron* **1982**, *38*, 1193–1201.

[15]: Giralt, E.; Eritja, R.; Pedroso, E. *Tetrahedron* **1986**, *42*, 691–698.

[16]: Lloyd-Williams, P.; Gairi, M.; Albericio, F.; Giralt, E. *Tetrahedron* **1991**, *47*, 9867–9880.

[17]: Pillai, V. N. R.; Renil, M.; Haridasan, V. K. *Indian J. Chem., Sect. B* **1991**, *30B*, 205–212.

[18]: Baldwin, J. J.; Burbaum, J. J.; Henderson, I.; Ohlmeyer, M. H. J. *J. Am. Chem. Soc.* **1995**, *117*, 5588–5589.

[19]: Greenberg, M. M. *Tetrahedron Lett.* **1993**, *34*, 251–254.

[20]: Matray, T. J.; Greenberg, M. M. *J. Am. Chem. Soc.* **1994**, *116*, 6931–6932.

[21]: Greenberg, M. M.; Gilmore, J. L. *J. Org. Chem.* **1994**, *59*, 746–753.

[22]: Alsina, J.; Chiva, C.; Ortiz, M.; Francesc, R.; Giralt, E.; Albericio, F. *Tetrahedron Lett.* **1997**, *38*, 883–886.

[23]: Tam, J. P.; Dimarchi, R. D.; Merrifield, R. B. *Int. J. Pept. Protein Res.* **1980**, *16*, 412–425.

[24]: Zehavi, U.; Sadeh, S.; Herchman, M. *Carbohydr. Res.* **1983**, *124*, 23–34.

[25]: Nicolaou, K. C.; Winssinger, N.; Pastor, J.; DeRoose, F. *J. Am. Chem. Soc.* **1997**, *119*, 449–450.

[26]: Nicolaou, K. C.; Watanabe, N.; Li, J.; Pastor, J.; Winssinger, N. *Angew. Chem. Int. Ed.* **1998**, *37*, 1559–1561.

[27]: Kantchev, E. A. B.; Parquette, J. R. *Synlett* **2005**, 1567–1570.

[28]: Armstrong, R. W.; Combs, A. P.; Tempest, P. A.; Brown, S. D.; Keating, T. A. *Acc. Chem. Res.* **1996**, *29*, 123–131.

[29]: Johnsson, R; Lackey, J. G.; Bogojeski, J. J.; Damha, M. J. *Bioorg. Med. Chem. Lett.* **2011**, *21*, 3721–3725.

[30]: Rich, D. H.; Gurwara, S. K. *Tetrahedron Lett.* **1975**, *16*, 301–304.

[31]: Hammer, R. P.; Albericio, F.; Gera, L.; Barany, G. *Int. J. Pept. Protein Res.* **1990**, *36*, 31–45.

[32]: Ajayaghosh, A.; Pillai, V. N. R. *J. Org. Chem.* **1990**, *55*, 2826–2829.

[33]: Renil, M.; Pillai, V. N. R. *Tetrahedron Lett.* **1994**, *35*, 3809–3812.

[34]: Kumar, K. S.; Pillai, V. N. R. *Tetrahedron* **1999**, *55*, 10437–10446.

[35]: Hintersteiner, M.; Ambrus, G.; Bednenko, J.; Schmied, M.; Knox, A. J. S.; Meisner, N.-C.; Gstach, H.; Seifert, J.-M.; Singer, E. L.; Gerace, L.; Auer, M. *ACS Chem. Biol.* **2010**, *5*, 967–979.

[36]: Eller, S.; Collot, M.; Yin, J.; Hahm, H. S.; Seeberger, P. H. *Angew. Chem. Int. Ed.* **2013**, *52*, 5858–5861.

[37]: Calin, O; Eller, S.; Seeberger, P. H. *Angew. Chem. Int. Ed.* **2013**, *52*, 5862–5865.

[38]: Weishaupt, M. W.; Matthies, S.; Seeberger, P. H. *Chem. Eur. J.* **2013**, *19*, 12497–12503.

[39]: Ajayaghosh, A; Pillai, V. N. R. *Tetrahedron* **1988**, *44*, 6661–6666.

[40]: Ajayaghosh, A; Pillai, V. N. R. *J. Org. Chem.* **1987**, *52*, 5714–5717.

[41]: Ajayaghosh, A; Pillai, V. N. R. *Tetrahedron Lett.* **1995**, *36*, 777–780.

[42]: Brown, B. B.; Wagner, D. S.; Geysen, H. M. *Mol. Div.* **1995**, *1*, 4–12

[43]: Sternson, S. M.; Schreiber, S. L. *Tetrahedron Lett.* **1998**, *39*, 7451–7454.

[44]: Rodebaugh, R.; Fraser-Reid, B.; Geysen, H. M. *Tetrahedron Lett.* **1997**, *97*, 7653–7656.

[45]: Ryba, T. D.; Harran, P. G. *Org. Lett.* **2000**, *2*, 851–853.

[46]: Zehavi, U.; Patchornik, A. *J. Am. Chem. Soc.* **1973**, *95*, 5673–5677.

[47]: Yoo, D. J.; Greenberg, M. M. *J. Org. Chem.* **1995**, *60*, 3358–3364.

[48]: Holmes, C. P.; Jones, D. G.; *J. Org. Chem.* **1995**, *60*, 2318–2319.

[49]: Venkatesan, H.; Greenberg, M. M. *J. Org. Chem.* **1996**, *61*, 525–529.

[50]: Poijaervi, P.; Heinonen, P.; Virta, P.; Loennberg, H. *Bioconjugate Chem.* **2005**, *16*, 1564–1571.

[51]: Holmes, C. P. *J. Org. Chem.* **1997**, *62*, 2370–2380.

[52]: Teague, S. J. *Tetrahedron Lett.* **1996**, *37*, 5751–5754.

[53]: Whitehouse, D. L.; Savinov, S. N.; Austin, D. J. *Tetrahedron Lett.* **1997**, *38*, 7851–7852.

[54]: McKeown, S. C.; Watson, S. P.; Carr, R. A. E.; Marshall, P. *Tetrahedron Lett.* **1999**, *40*, 2407–2410.

[55]: Gea, A.; Farcy, N.; Roqué i Rossell, N.; Martins, J. C.; De Clercq, P. J.; Madder, A. *Eur. J. Org. Chem.* **2006**, 4135–4146.

[56]: Lin, Q.; Blackwell, H. E. *Chem. Commun.* **2006**, 2884–2886.

[57]: Gennari, C.; Longari, C.; Ressel, S.; Salom, B.; Piarulli, U.; Ceccarelli, S.; Mielgo, A. *Eur. J. Org. Chem.* **1998**, 2437–2449.

[58]: Ruhland, B.; Bhandari, A.; Gordon, E. M.; Gallop, M. A. *J. Am. Chem. Soc.* **1996**, *118*, 253–254.

[59]: Minkwitz, R.; Meldal, M. *QSAR Comb. Sci.* **2005**, *24*, 343–353.

[60]: Qvortrup, K; Nielsen, T. E. *Chem. Commun.* **2011**, *47*, 3278–3280.

[61]: Qvortrup, K; Komnatnyy, V. V; Nielsen, T. E. *Org. Lett.* **2014**, *16*, 4782–4785.

[62]: Kim, J.; Kyeong, S.; Shin, D.-S.; Yeo, S.; Yim, J.; Lee, Y.-S. *Synlett* **2013**, 733–736.

[63]: Wang, S.-S.; *J. Org. Chem.* **1976**, *41*, 3258–3261.

[64]: Tjoeng, F. S.; Heavner, G. A. *J. Org. Chem.* **1983**, *48*, 355–359.

[65]: Bellof, D.; Mutter, M. *Chimia* **1985**, *39*, 317–320.

[66]: Abraham, N. A.; Fazal, G.; Ferland, J. M.; Rakhit, S.; Gauthier, J. *Tetrahedron Lett.* **1991**, *32*, 577–580.

[67]: Flickinger, S. T.; Patel, M.; Binkowski, B. F. ; Lowe, A. M.; Li, M.-H.; Kim, C.; Cerrina, F.; Belshaw, P. J. *Org. Lett.* **2006**, *8*, 2357–2360.

[68]: Sucholeiki, I *Tetrahedron Lett.* **1994**, *35*, 7307–7310.

[69]: Forman, F. W.; Sucholeiki, I. *J. Org. Chem.* **1995**, *60*, 523–528.

[70]: Rock, R. S.; Chan, S. I. *J. Org. Chem.* **1996**, *61*, 1526–1529.

[71]: Routledge, A.; Abell, C.; Balasubramanian, S. *Tetrahedron Lett.* **1997**, *38*, 1227–1230.

[72]: Lee, H. B.; Balasubramanian, S. *J. Org. Chem*. **1999**, *64*, 3454–3460.

[73]: Cano, M.; Ladlow, M.; Balasubramanian, S. *J. Org. Chem.* **2002**, *67*, 129–135

[74]: Chumachenko, N.; Novikov, Y; Shoemaker, R. K.; Copley, S. D. *J. Org. Chem* **2011**, *76*, 9409–9416.

[75]: Peukert, S.; Giese, B. *J. Org. Chem.* **1998**, *63*, 9045–9051.

[76]: Glatthar, R. Giese, B. *Org. Lett.* **2000**, *2*, 2315–2317.

[77]: Kessler, M.; Glatthar, R.; Giese, B.; Bochet, C. G. *Org. Lett.* **2003**, *5*, 1179.

[78]: Horton, J. R.; Stamp, L. M.; Routledge, A. *Tetrahedron Lett.* **2000**, *41*, 9181–9184.

[79]: Nicolaou, K. C.; Safina, B. S.; Winssinger, N. *Synlett* **2001**, 900–903.

[80]: Enders, D. Rijksen, C.; Bremus-Köbberling, E.; Gillner, A.; Köbberling, J. *Tetrahedron Lett.* **2004**, *45*, 2839–2841.

[81]: (a) Fluxà, V. S.; Maillard, N.; Page, M. G. P.; Reymond, J.-L. *Chem. Commun.* **2011**, *47*, 1434–1436. (b) Shin, D.; Kim, Y.-G.; Kim, E.-M.; Kim, M.; Park, H.; Kim, J.-H.; Lee, B.-S.; Kim, B.; Lee, Y. *J. Comb. Chem.* **2008**, *10*, 20–23. (c) Guillena, G.; Halkes, K. M.; Rodríguez, G.; Batema, G. D.; van Koten, G.; Kamerling, J. P. *Org. Lett.* **2003**, *5*, 2021–2024. (d) Johannesson, P.; Erdélyi, M.; Lindeberg, G.; Frändberg, P.-A.; Nyberg, F.; Karlén, A.; Hallberg, A. *J. Med. Chem.* **2004**, *47*, 6009–6019. (e) Miyashita, M.; Otake, Y.; Oda, M.; Miyagawa, H. *J. Agric. Food Chem.* **2007**, *55*, 806–811. (f) Maillard, N.; Biswas, R.; Darbre, T.; Reymond, J.-L. *ACS Comb. Sci.* **2011**, *13*, 310–320. (g) Maillard, N.; Darbre, T.; Reymond, J.-L. *J. Comb. Chem.* **2009**, *11*, 667–675. (h) Tornøe, C. W.; Sanderson, S. J.; Mottram, J. C.; Coombs, G. H.; Meldal, M. *J. Comb. Chem.* **2004**, *6*, 312–324. (i) Usui, K.; Kikuchi, T.; Tomizaki, K.;

Kakiyama, T.; Mihara, H. *Chem. Commun.* **2013**, *49*, 6394–6396. (j) Zhou, G.; Khan, F.; Dai, Q.; Sylvester, J. E.; Kron, S. J. *Mol. BioSyst.* **2012**, *8*, 2395–2404. (k) Bodé, C. A; Bechet, T.; Prodhomme, E.; Gheysen, K.; Gregoir, P.; Martins, J. C.; Muller, C. P.; Madder, A. *Org. Biomol. Chem.* **2009**, *7*, 3391–3399. (l) Verzele, D.; Madder, A. *Eur. J. Org. Chem.* **2013**, 673–687. (m) Boeijen, A.; Liskamp, R. M. J. *Eur. J. Org. Chem.* **1999**, 2127–2135. (n) Jang, K.; Sato, K.; Mawatari, K.; Konno, T.; Ishihara, K.; Kitamori, T. *Biomaterials* **2009**, *30*, 1413–1420.